OFFICE OF CIVILIAN RADIOACTIVE WASTE MANAGEMENT
ANALYSIS/MODEL COVER SHEET

Complete Only Applicable Items

1. QA: QA

Page: 1 of: 174

2. ☒ Analysis — Check all that apply

Type of Analysis	☐ Engineering ☒ Performance Assessment ☐ Scientific
Intended Use of Analysis	☒ Input to Calculation ☒ Input to another Analysis or Model ☒ Input to Technical Document
Describe use:	See Section 1 and Section 6.2

3. ☒ Model — Check all that apply

Type of Model	☒ Conceptual Model ☒ Abstraction Model ☐ Mathematical Model ☐ System Model ☒ Process Model
Intended Use of Model	☒ Input to Calculation ☒ Input to another Model or Analysis ☒ Input to Technical Document
Describe use:	See Section 1 and Section 6.2

4. Title:

In-Drift Microbial Communities

5. Document Identifier (including Rev. No. and Change No., if applicable):

ANL-EBS-MD-000038 Rev 00 ICN 1

6. Total Attachments:

6

7. Attachment Numbers - No. of Pages in Each:

I-9, II-14, III-6, IV-4, V-3, VI-19

	Printed Name	Signature	Date
8. Originator	Darren M. Jolley		11/9/00
9. Checker(s)	James Schreiber	for E. J. Nowak	11/9/00
10. Lead/Supervisor	James Nowak	E J Nowak	11/9/00
11. Responsible Manager	Robert MacKinnon	for R. MacKinnon	Nov 9, 2000

12. Remarks:

The following controlled documents and associated TBV's will be superceded or closed out by the approval of this document:
B00000000-01717-0200-00171 Rev 00 — TBV 0369; B00000000-01717-0200-00167 Rev 00 — TBV 0372;
B00000000-01717-0200-00168 Rev 00 — TBV 0371; B00000000-01717-0200-00172 Rev 00 — TBV 0373.

The following DTN:s will be superceded by this ICN approval:
MO0003SPAMLU38.020, MO0003SPAMLD38.022, MO9909SPAMING1.002, MO0001SPAREA38.008, MO0001SPAAWP38.010, MO0001SPAREA38.008, and MO9911SPAAWC68.002.

OFFICE OF CIVILIAN RADIOACTIVE WASTE MANAGEMENT
ANALYSIS/MODEL REVISION RECORD

Complete Only Applicable Items

2. Analysis or Model Title:

In-Drift Microbial Communities

3. Document Identifier (including Rev. No. and Change No., if applicable):

ANL-EBS-MD-000038 Rev 00 ICN 1

4. Revision/Change No.	5. Description of Revision/Change
00	Initial Issue
00/1	ICN to insert data/information reported as TBD in Rev 00 so that the addition of SR calculations could be added. SR Calculations and results were added and include evaluations of no backfill design and backfill sensitivity option, potential biofilm development, colloid generation and CO_2 gas generation. Updates to the text were made to comply with the latest procedural changes to AP-3.10Q. Changes were made for updates on data qualification status of some input and close out of AP-3.14Q Input Transmittals. Some inputs were reclassified as assumptions to address data qualification issues. Corrections were also made because of both typographical and technical errors. All references in Section 8 were updated from DIRS to reflect most current status. Finally, general renumbering of sections, tables and figures occurred when new information was added.

CONTENTS

Page

FIGURES

Page

TABLES

Page

ACRONYMS

AMR	Analysis/Modeling Report
AP	Administrative Procedure
ASME	American Society of Mechanical Engineers
ASTM	American Society for Testing and Materials
AT	Altered Tuff
BWR	Boiling Water Reactor
CAM	Waste package Corrosion Allowance Material
CD	Carbon Deficient microbial growth media
CDF	Cumulative Distribution Function
CFR	Code of Federal Regulations
CNS	Calcium Naphthalene Sulfonate (superplasticizer)
CRM	Corrosion Resistant Material
CRWMS	Civilian Radioactive Waste Management System
CSCI	Computer Software Configuration Identifier
CSNF	Commercial Spent Nuclear Fuel
DC	Dilute Complete growth media
DHLW	Defense High Level Waste
DOC	Dissolved Organic Carbon
DOE	U. S. Department of Energy
DTN	Data Tracking Number
EBS	Engineered Barrier System
EBSO	Engineered Barrier System Operations
EDA	Enhanced Design Alternative
EMMA	Estimation of Maximum Microbiological Activity
ESF	Exploratory Studies Facility
FEP	Features, Events, and Processes
FFTF	Fast Flux Test Facility
FR	Federal Register
FW	Formula Weight
GFW	Gram Formula Weight
HLW	High Level Waste
IDGE	In-Drift Geochemical Environment
INEEL	Idaho National Engineering & Environmental Laboratory
INEL	Idaho National Engineering Laboratory (now INEEL)
IRSR	Issue Resolution Status Report
KTI	Key Technical Issues
LADS	License Application Design Selection

LLNL	Lawrence Livermore National Laboratories
M&O	Management and Operations
MIC	Microbial Induced Corrosion
ML	Material Lifetime
NFE	Near Field Environment
NFGE	Near Field Geochemical Environment
NRC	Nuclear Regulatory Commission
PA	Performance Assessment
PD	Phosphate Deficient microbial growth media
PWR	Pressurized Water Reactor
QA	Quality Assurance
QAP	Quality Assurance Procedure
QARD	Quality Assurance Requirements and Description
RH	Relative Humidity
RSDO	Repository Subsurface Design Organization
SQR	Software Qualification Report
SR	Site Recommendation
SR/LA	Site Recommendation/License Application
SZ	Saturated Zone
TBD	To Be Determined
TBV	To Be Verified
TDMS	Technical Data Management System
TH	Thermohydrologic
THC	Thermal-Hydrological-Chemical
TIC	YMP Technical Information Center
TMN	Topopah Spring Tuff Middle Non Lithophysal Unit
TSPA	Total System Performance Assessment
UT	Unaltered Tuff
UZ	Unsaturated Zone
VA	Viability Assessment
WP	Waste Package
WPO	Waste Package Operations
WWF	Welded Wire Fabric
YMC	Yucca Mountain Complete microbial growth medium
YMP	Yucca Mountain Project

1. PURPOSE

As directed by written work direction (CRWMS M&O 1999f), Performance Assessment (PA) developed a model for microbial communities in the engineered barrier system (EBS) as documented here. The purpose of this model is to assist Performance Assessment and its Engineered Barrier Performance Section in modeling the geochemical environment within a potential repository drift for TSPA-SR/LA, thus allowing PA to provide a more detailed and complete near-field geochemical model and to answer the key technical issues (KTI) raised in the NRC Issue Resolution Status Report (IRSR) for the Evolution of the Near Field Environment (NFE) Revision 2 (NRC 1999). This model and its predecessor (the in-drift microbial communities model as documented in Chapter 4 of the TSPA-VA Technical Basis Document, CRWMS M&O 1998a, see Section 6.1 below) was developed to respond to the applicable KTIs (See Section 4.2.1 below). Additionally, because of the previous development of the in-drift microbial communities model as documented in Chapter 4 of the TSPA-VA Technical Basis Document (CRWMS M&O 1998a), the M&O was effectively able to resolve a previous KTI concern regarding the effects of microbial processes on seepage and flow (NRC 1998).

This document supercedes the in-drift microbial communities model as documented in Chapter 4 of the TSPA-VA Technical Basis Document (CRWMS M&O 1998a). This document provides the conceptual framework of the revised in-drift microbial communities model to be used in subsequent performance assessment (PA) analyses.

This model has been developed to serve as a basis for the in-drift geochemical modeling work performed by PA and as an input to the EBS process model report (CRWMS M&O 2000j). However, portions of the conceptual model discussed within this report may also apply to near and far-field geomicrobiological processes and can have conceptual application within the unsaturated zone (UZ) and saturated zone (SZ) transport modeling efforts. This model reports the total biomass that can be produced from the degradation of EBS materials and inputs from the natural system using a comparative mass balance approach. The biomass produced is based on the lower of two calculated values, namely, 1) the total energy available via redox reactions utilized by microbial catalysis and 2) the number of microbes produced based on the yearly availability of nutrients (i.e. as a result of emplaced materials corrosion and flux from groundwater and gas into the drift) to the modeled system. From this calculated biomass several key abstraction analyses are made to determine bounds on CO_2 gas generation, biofilm production, and colloid generation. The outputs from these abstractions feed the microbially induced corrosion (MIC) portions of the waste package corrosion modeling for TSPA-SR/LA, feed in-drift gas flux modeling for SR/LA, and can serve as a source term for microbial colloids in the in-drift colloid modeling for SR/LA.

2. QUALITY ASSURANCE

The Quality Assurance (QA) program applies to the development of this model. The Performance Assessment Department responsible manager has evaluated the technical document development activity in accordance with QAP-2-0, *Conduct of Activities*. The QAP-2-0 activity evaluation, *Conduct of Performance Assessment* (CRWMS M&O 1999a), has determined that

the preparation and review of this technical document is subject to *Quality Assurance Requirements and Description* (QARD) DOE/RW-0333P (DOE 2000) requirements. Preparation of this analysis did not require the classification of items in accordance with QAP-2-3, *Classification of Permanent Items.* This activity is not a field activity. Therefore, an evaluation in accordance with NLP-2-0, *Determination of Importance Evaluations* was not required. With regard to the development of this model, the control of electronic management of data was evaluated in accordance with AP-SV.1Q, *Control of the Electronic Management of Data.* The evaluation (MacKinnon 2000) determined that current work processes and procedures are adequate for the control of electronic management of data for this activity.

3. COMPUTER SOFTWARE AND MODEL USAGE

3.1 COMPUTER SOFTWARE

The following software is used in this model:

- MING V1.0 (MING V1.0 CSCI 30018 V1.0 MI 30018-M04-001, CRWMS M&O 1998i) was obtained from the software configuration management (CM) organization. MING V1.0 is used within the range of validation as described in the users manual and qualification documentation (CRWMS M&O 1998d and 1998h) and is appropriate for use in this model as a tool for conducting model validation calculations and for estimating microbial growth within a repository drift through time. MING V1.0 was run on a Dell Power Edge personal computer (CRWMS M&O tag # 112370 located in the PA Department, Las Vegas, NV) using Windows NT 4.0 (build 1381, service pack 4) and Microsoft Access 97 (SR-2).

- Microsoft Excel 97, a commercially available standard spreadsheet software package. This software was used to tabulate and chart results.

- CorelDRAW 7, a commercially available graphics package. This software was used to create Figure 3 (see Section 6.3.3.1.3).

- SigmaPlot for Windows, Version 4.00, a commercially available graphics plotting software package. This software was used to chart results.

No other software codes or routines besides MING V1.0 were developed for use in this model. Three other pieces of software are mentioned in Section 6.4 of this report (EMMA, AREST-CT, and EQ3/6). These three pieces of software were not used to produce results or output for this model, therefore only the documentation for these codes is cited in Section 6.4.

3.2 MODELS

The previous model used for PA near-field geochemical environment analysis of microbial communities growth is documented in Chapter 4 of the TSPA-VA Technical Basis Document (CRWMS M&O 1998a). This new model is being developed to supercede the old microbial communities model discussed in the technical basis document. However the majority of the

conceptual model documentation presented in Section 6.3 below was originally documented in the technical basis document (CRWMS M&O 1998a). The soon to be superceded TSPA-VA near-field geochemical environment (NFGE) microbial communities model is only used in this document as a reference. The old model consists of the documentation found in Chapter 4 of the technical basis document (CRWMS M&O, 1998a) the use of MING V1.0 software [CSCI 30018 V1.0 as documented in CRWMS M&O 1998d, and 1998h] and the input and output files found in the following DTN: MO9807MWDEQ3/6.005.

Documented within the *Engineered Barrier System: Physical and Chemical Environment Model* document (CRWMS M&O 2000k) is the Microbial Effects Model. This conceptual model which was developed independent of and much later than the model documented in Section 6 below is used to corroborate and validate the conceptual model discussed in Section 6.3 below. There is no Model Warehouse DTN associated with the Microbial Effects Model.

4. INPUTS

Note: this document may be affected by technical product input information that requires confirmation. Any changes to the document or its conclusions that may occur, as a result of completing the confirmation activities will be reflected in subsequent revisions. The status of the input information quality may be confirmed by review of the Document Input Reference System database.

4.1 DATA AND PARAMETERS

For TSPA-Site Recommendation/License Application (SR/LA) analyses, requests were made by PA to the Waste Package Operations (WPO), Engineered Barrier System Operations (EBSO) and Repository Subsurface Design Organization (RSDO) to obtain the appropriate design information for the in-drift geochemical model analyses. Each organization responded using AP-3.14Q *Transmittal of Input* to provide the requested information (CRWMS M&O 1999e, CRWMS M&O 1999g, and CRWMS M&O 1999h). Because these inputs are not all qualified or accepted they are considered TBV inputs. However, these inputs do contain some qualified and/or accepted data (e.g. reference to American Society for Testing and Materials [ASTM] standards).

In addition to the AP-3.14Q *Transmittal of Input* information cited above and the listed technical design documents, the following tables (Tables 1 through 5) list the technical data management system (TDMS) data tracking numbers (DTN), accepted data, or developed data (within this document) which are used as input values to the modeling runs.

These inputs are considered appropriate for this model.

Table 1. Source Data/Input Information used in Parameter Derivation.

DTN/Source	Description	Location in Text
LA000000000086.002	Iron Mineral Types	Attachment I
LA000000000086.002	Maximum Mineral % In Repository Horizon Tuff	Attachment I
Sargent-Welch (1979)	Gram Formula Weights	Attachment I
CRWMS M&O (2000s)	Repository Drift Radius	Attachment I
GS960908312231.004	Bulk Density Of TMN	Attachment I
GS931208314211.047	Depth Of TMN Horizon	Attachment I
MO9909SPAMICRO.001	Microbial Volume	Attachment I
MO9909SPAMICRO.001	Microbial Water Content	Attachment I
LALH831342AQ96.002	Biomass In ESF	Attachment I
MO9909SPABMASS.000	Biomass In Rainier Mesa	Attachment I
Weast (1979)	Composition Of Air	Attachment I
MO9912SEPMKTDC.000	Composition Of Type K Cement	Attachment II
MO0004SPASMA05.004	Stainless Steel General Corrosion Distribution	Section 6.5.2.3
MO0003SPASUP02.003	Alloy 22 And Ti7 General Corrosion CDF	Section 6.5.2.3
SN9911T0811199.003	Aqueous Dissolution Rates For HLW Glass	Section 6.5.2.3
American Society of Metals (1987)	Corrosion Rates For Aluminum	Section 6.5.2.3
LL980704605924.035	Aqueous Corrosion Rates For Mild Carbon Steel	Section 6.5.2.3
LL980504105924.034	Aqueous Corrosion Rate For Neutronit A978	Section 6.5.2.3
CRWMS M&O (1999g)	Mass Of Steel Sets In Lithophysal Areas Per Meter Of Drift	Attachment II
CRWMS M&O (1999g)	Mass Of Steel Sets In Nonlithophysal Areas Per Meter Of Drift	Attachment II
CRWMS M&O (1999g)	Mass Of Rock Bolts In Nonlithophysal Areas Per Meter Of Drift	Attachment II
CRWMS M&O (1999g)	Mass Of Cement In Rock bolt Grout Per Meter Of Drift	Attachment II
CRWMS M&O (1999g)	Mass Of Steel Invert Per Meter Of Drift	Attachment II
CRWMS M&O (1999g)	Mass Of Gantry Rail Per Meter Of Drift	Attachment II
CRWMS M&O (1999g)	Mass Of Rail Fittings Per Meter Of Drift	Attachment II
CRWMS M&O (1999g)	Mass Of Conductor Bar Fittings Per Meter Of Drift	Attachment II

DTN/Source	Description	Location in Text
CRWMS M&O (1999g)	Mass Of Communications Cable Per Meter Of Drift	Attachment II
CRWMS M&O (1999g)	Composition Of Rock Bolt Grout	Attachment II
CRWMS M&O (1999g)	Composition Of Grout Admixtures	Attachment II
CRWMS M&O (1999g)	Composition Of Rail Fittings	Attachment II
CRWMS M&O (1999g)	Composition Of Wire Conductor	Attachment II
CRWMS M&O (1999g)	Composition Of Communications Cable	Attachment II
CRWMS M&O (1999g)	Composition Of Wire Mesh(WWF)	Attachment II
CRWMS M&O (1999g)	Mass Of WWF Per Meter Of Drift In Lithophysal Area	Attachment II
CRWMS M&O (1999g)	Mass Of WWF Per Meter Of Drift In Nonlithophysal Area	Attachment II
CRWMS M&O (2000d, 2000e, 2000g)	Waste Package Lengths For 21PWR, 44BWR, 5DHLW, And Naval SNF	Attachment III
CRWMS M&O (2000i)	Length Of Drip Shield Segment	Attachment III
CRWMS M&O (2000i)	Length Of Waste Package Pallet	Attachment III
CRWMS M&O (2000i)	Masses Of Materials In Drip Shield Design	Attachment III
CRWMS M&O (2000d, 2000e, 2000g)	Masses Of Materials In Waste Package Design	Attachment III
CRWMS M&O (2000i)	Masses Of Materials In Waste Package Pallet Design	Attachment III
CRWMS M&O (2000g)	Waste Package Outer Barrier Thickness	Section 6.5.2.3
CRWMS M&O (2000g)	Waste Package Inner Barrier Thickness	Section 6.5.2.3
CRWMS M&O (2000g)	Basket Plate (Neutronit) Thickness	Section 6.5.2.3
CRWMS M&O (2000g)	Basket Plate (Aluminum) Thickness	Section 6.5.2.3
CRWMS M&O (2000g)	Basket Guide Thickness	Section 6.5.2.3
CRWMS M&O (1999e)	Invert Material Thickness	Section 6.5.2.3
CRWMS M&O (1999e)	Gantry Rail Material Thickness	Section 6.5.2.3
CRWMS M&O (1999e)	Rail Fittings (Anchor Clips) Material Thickness	Section 6.5.2.3
CRWMS M&O (1999e)	WWF (Wire Mesh) Material Thickness	Section 6.5.2.3
CRWMS M&O (2000e)	Drip Shield Material Thickness	Section 6.5.2.3

DTN/Source	Description	Location in Text
CRWMS M&O (2000e)	Waste Package Pallet Steel Tube Material Thickness	Section 6.5.2.3
GS980908312322.008	Aqueous groundwater compositions for various wells at Yucca Mountain	Section 6.5.1.3
SN0001T0872799.006	Abstracted Percolation flux at the Drift Wall Through Time	Section 6.5.1.1
MO9912SPAPAI29.002	Abstracted Incoming Water Compositions Through Time	Section 6.5.1.3
SN0002T0872799.008	Abstracted Temperature/RH At Drift Wall Through Time	Section 6.5.1.2

Table 2. Parameter Listing and Status for TSPA-SR Calculations.

Input #	Parameter	Location in Text	Source
1	Material Lifetimes	Table 32	Section 6.5.2.3
2	Breakdown Codes	Table 33	Attachment II
3	Delta G Relationships For Redox Half Reactions	Table 18	DTN: MO9909SPAMING1.003
4	Atomic Mass	Table 19	Sargent-Welch (1979)
5	Temperature Cutoff	Table 23	Section 6.3.1.3
6	Humidity Cutoff	Table 23	Section 6.3.3.2.2
7	MING V1.0 Near-Field Porosity	Table 23	CRWMS M&O (1998h)
8	Gas Buttons	Table 23	Section 6.3.1.10
9	Energy Cut Off	Table 23	McKinley et al. (1997)
10	Reactant Compositions	Table V-2	Section 6.5.2.2 and Attachment V
11	Tunnel Length	Table 23	User Selected
12	Tunnel Diameter	Table 23	CRWMS M&O (2000s)
13	Layer Designator	Table 34	Section 6.5.2.5
14	Elemental Composition Of Type K Concrete	Table II-20	Attachment II
15	Elemental Composition Of Superplasticizer	Table II-22	Attachment II
16	Elemental Composition Of Rock Bolts	Table II-17	Attachment II: ASTM F 432-95
17	Elemental Composition Of Welded Wire Fabric	Table II-19	Attachment II
18	Elemental Composition Of Gantry Rail	Table II-18	Attachment II: ASTM A759-85
19	Elemental Composition Of Rail Fittings	Table II-23	Attachment II
20	Elemental Composition Of Steel Set Ground Support	Table II-16	Attachment II: ASTM A572/A572M-99a

Input #	Parameter	Location in Text	Source
21	Elemental Composition Of Conductor Bar Fittings	Table II-16	Attachment II: ASTM A572/A572M-99a
22	Elemental Composition Of Commo Cable	Table II-25	Attachment II
23	Masses Of Materials For A One Meter Repository Segment	Table II-26 and Table II-27	Attachment II
24	Composition Of PWR CNSF Waste Assembly	Table IV-4	Attachment IV
25	Composition Of BWR CNSF Waste Assembly	Table IV-5	Attachment IV
26	Composition Of DHLW Waste Glass	Table IV-3	DTN: SN9911T0811199.003
27	Composition Of Waste Package Supports (316L Stainless Steel and Alloy C-22)	Table III-8 Table III-10	Attachment III ASTM A276-91a ASME Section II B SB-575
28	Composition Of Drift Invert	Table II-16	Attachment II: ASTM A572/A572M-99a
29	Composition Of Waste Package Corrosion Resistant Material (CRM) (Alloy C-22)	Table III-10	Attachment III ASME Section II B SB-575
30	Composition Of Waste Package Structural Steel (316NG Stainless Steel)	Table III-9	Attachment III ASTM A276-91a
31	Composition Of Waste Package Thermal Shunts (Aluminum 6061)	Table III-11	Attachment III ASTM B 209M-92a
32	Composition Of Waste Package Absorber Plates (Neutronit A978)	Table III-13	Attachment III
33	Masses Of Materials For A One Lineal Meter Segment Of Design Waste Canisters	Table III-1 Table III-2 Table III-3 Table III-4	Attachment III
34	Abstracted Percolation Flux at the Drift Wall Through Time	Figure 8	Section 6.5.1.1
35	Abstracted Incoming Water Compositions Through Time	Table 22	Section 6.5.1.3
36	Abstracted Temperature/RH at WP Surface Through Time	Figure 6 and Figure 7	Section 6.5.1.2
37	Abstracted Cumulative Gas Flux Into The Drift Through Time	Table 8	Assumption 5.10
38	Elemental Composition of Silica Fume	Table II-21	Attachment II

Table 3. Referenced Data Used in Model Validation.

DTN	Description	Location in Text
MO0005EMMATEST.000	EMMA Test Case Results	Section 6.7.1

Table 4. Parameters and Status used in Ambient Validation Test Cases.

Parameter	Location in Text	Source
Infiltration Rates	Table 78	DTN: MO9807MWDEQ3/6.005
Cumulative Gas Flux	Table 7	DTN: MO9911SPACGF04.000
Material Lifetimes	Table 78	Assumption 5.5 MO9807MWDEQ3/6.005
J-13 Water Compositions	Table 77	DTN: MO9909SPA00J13.006 Assumption 5.11
Bulk Rock Compositions For Topopah Spring Tuff	Table 15	DTN: LL981209705924.059
Delta G Relationships For Redox Half Reactions	Table 18	DTN: MO9909SPAMING1.003
Atomic Mass	Table 19	Sargent-Welch (1979)
Temperature Cutoff	Table 23	Section 6.3.1.3
Humidity Cutoff	Table 23	Section 6.3.3.2.2
MING V1.0 Near-Field Porosity	Table 23	CRWMS M&O (1998h)
Gas Buttons	Table 23	Section 6.3.1.10
Energy Cut Off	Table 23	McKinley et al. (1997)
Reactant Compositions	Table 33	Section 6.5.2.4
Tunnel Length	Table 23	User Selected
Tunnel Diameter	Table 23	CRWMS M&O (1999e)
Layer Designator	Table 34	Section 6.5.2.5
RH	Section 6.7.2.1	Assumption 5.2

Table 5. Parameters and Status used in LLNL Validation Test Cases.

Parameter	Location in Text	Source
Flask Volume pH Of Growth Media Mass Of Crushed Tuff Temperature Of Growth Media Volume Of Growth Media In Flask	Table 83	LL000206105924.126
Growth Media Compositions	Table 84	LL980608505924.035
Bulk Rock Compositions For Topopah Spring Tuff	Table 15	LL981209705924.059
Delta G Relationships For Redox Half Reactions	Table 18	MO9909SPAMING1.003
Atomic Mass	Table 19	Sargent-Welch (1979)
Temperature Cutoff	Table 23	Section 6.3.1.3
Humidity Cutoff	Table 23	Section 6.3.3.2.2
MING V1.0 Near-Field Porosity	Table 23	CRWMS M&O (1998h)
Gas Buttons	Table 23	Section 6.3.1.10

Parameter	Location in Text	Source
Energy Cut Off	Table 23	McKinley et al. (1997)
Reactant Compositions	Table 33	Section 6.5.2.4
Layer Designator	Table 34	Section 6.5.2.5
RH	Section 6.6.3.2.1	Assumption 5.2
Tunnel Length	Table 23	Attachment I
Drift Diameter	Table 23	Attachment I

4.2 CRITERIA

Below is a summary of the applicable NRC review and acceptance criteria outlined in the issue resolution status report (IRSR). These acceptance criteria apply to model development for the following near-field environment (NFE) key technical issue (KTI) sub-issue effects: (a) coupled thermal-hydrologic-chemical processes on the waste package chemical environment, (b) coupled thermal-hydrologic-chemical processes on the chemical environment for radionuclide release, and (c) coupled thermal-hydrologic-chemical processes on radionuclide transport through engineered and natural barriers (NRC 1999).

Also, below is a listing of the applicable features, events and processes (FEP) that are associated with this document.

4.2.1 NRC IRSR Criteria

The exact wording below reflects only the criteria as presented in NRC (1999) Section 4.3.1. However, the wording is similar to those presented below in the other cited sections (i.e. 4.1.1, 4.2.1, 4.4.1, and 4.5.1) and can be used to obtain the general feel of each criteria. The exact wording of these sections can be found by referring to the appropriate section in the IRSR document (NRC 1999). A discussion is found in Section 7.5 below of the IRSR criteria and whether they were addressed in this model as documented in Section 6 of this document.

4.2.1.1 Data and Model Justification Acceptance Criteria

1. Available data relevant to both temporal and spatial variations in conditions affecting coupled THC effects on the chemical environment for radionuclide release were considered. [NRC (1999), Sections 4.1.1, 4.2.1, 4.3.1, 4.4.1, and 4.5.1]

2. DOE's evaluation of coupled THC processes properly considered site characteristics in establishing initial and boundary conditions for conceptual models and simulations of coupled processes that may affect the chemical environment for radionuclide release. [NRC (1999), Sections 4.1.1, 4.2.1, 4.3.1, 4.4.1, and 4.5.1]

3. Sufficient data were collected on the characteristics of the natural system and engineered materials, such as the type, quantity, and reactivity of materials, in establishing initial and boundary conditions for conceptual models and simulations of THC coupled processes that may affect the chemical environment for radionuclide release. [NRC (1999), Sections 4.1.1, 4.2.1, 4.3.1, 4.4.1, and 4.5.1]

4. A nutrient and energy inventory calculation should be used to determine the potential for microbial activity that could impact the waste package (WP) chemical environment. [NRC (1999), Sections 4.2.1, 4.3.1, and 4.4.1]

5. Should microbial activity be sufficient to allow microbial influenced corrosion (MIC) of the WP, then the time-history of temperature, humidity, and dripping should be used to constrain the probability for MIC. [NRC (1999), Sections 4.2.1, 4.3.1, and 4.4.1]

6. Sensitivity and uncertainty analyses (including consideration of alternative conceptual models) were used to determine whether additional new data are needed to better define ranges of input parameters. [NRC (1999), Sections 4.1.1, 4.2.1, 4.3.1, and 4.4.1]

7. If the testing program for coupled THC processes on the chemical environment for radionuclide release from the engineered barrier system is not complete at the time of license application, or if sensitivity and uncertainty analyses indicate that additional data are needed, DOE has identified specific plans to acquire the necessary information as part of the performance confirmation program. [NRC (1999), Sections 4.1.1, 4.2.1, 4.3.1, and 4.4.1]

4.2.1.2 Data Uncertainty and Verification Acceptance Criteria

1. Reasonable or conservative ranges of parameters or functional relations were used to determine effects of coupled THC processes on the chemical environment for radionuclide release. Parameter values, assumed ranges, probability distributions, and bounding assumptions are technically defensible and reasonably account for uncertainties. [NRC (1999), Sections 4.1.1, 4.2.1, 4.3.1, 4.4.1, and 4.5.1]

2. Uncertainty in data due to both temporal and spatial variations in conditions affecting coupled THC effects on the chemical environment for radionuclide release were considered. [NRC (1999), Sections 4.1.1, 4.2.1, 4.3.1, 4.4.1, and 4.5.1]

3. DOE's evaluation of coupled THC processes properly considered the uncertainties in the characteristics of the natural system and engineered materials, such as the type, quantity, and reactivity of materials, in establishing initial and boundary conditions for conceptual models and simulations of THC coupled processes that may affect the chemical environment for radionuclide release. [NRC (1999), Sections 4.1.1, 4.2.1, 4.3.1, 4.4.1, and 4.5.1]

4. The initial conditions, boundary conditions, and computational domain used in sensitivity analysis involving coupled THC effects on the chemical environment for radionuclide release were consistent with available data. [NRC (1999), Sections 4.1.1, 4.2.1, 4.3.1, 4.4.1, and 4.5.1]

5. DOE's performance confirmation program should assess whether the natural system and engineered materials are functioning as intended and anticipated with regard to coupled THC effects on the chemical environment for radionuclide release from the engineered barrier system (EBS). [NRC (1999), Sections 4.1.1, 4.2.1, 4.3.1, and 4.4.1]

4.2.1.3 Model Uncertainty Acceptance Criteria

1. Appropriate models, tests, and analyses were used that are sensitive to the THC couplings under consideration for both natural and engineered systems as described in the following examples. The effects of THC coupled processes that may occur in the natural setting or due to interactions with engineered materials or their alteration products include: (i) Thermohydrologic (TH) effects on gas and water chemistry; (ii) hydrothermally driven geochemical reactions, such as zeolitization of volcanic glass; (iii) dehydration of hydrous phases liberating moisture; (iv) effects of microbial processes; and (v) changes in water chemistry that may result from interactions between cementatious or WP, materials and groundwater, which, in turn, may affect the chemical environment for radionuclide release. [NRC (1999), Sections 4.1.1, 4.2.1, 4.3.1, and 4.4.1]

2. Alternative modeling approaches consistent with available data and current scientific understanding were investigated, and their results and limitations were appropriately considered. [NRC (1999), Sections 4.1.1, 4.2.1, 4.3.1, 4.4.1, and 4.5.1]

3. DOE provided a reasonable description of the mathematical models included in its analyses of coupled THC effects on the chemical environment for radionuclide release. The description should include a discussion of alternative modeling approaches not considered in its final analysis and the limitations and uncertainties of the chosen model. [NRC (1999), Sections 4.1.1, 4.2.1, 4.3.1, 4.4.1, and 4.5.1]

4.2.1.4 Model Verification Acceptance Criteria

1. The mathematical models for coupled THC effects on the chemical environment for radionuclide release are consistent with conceptual models based on inferences about the near-field environment, field data and natural alteration observed at the site, and expected engineered materials. [NRC (1999), Sections 4.1.1, 4.2.1, 4.3.1, 4.4.1, and 4.5.1]

2. DOE appropriately adopted accepted and well-documented procedures to construct and test the numerical models used to simulate coupled THC effects on the chemical environment for radionuclide release. [NRC (1999), Sections 4.1.1, 4.2.1, 4.3.1, 4.4.1, and 4.5.1]

3. Abstracted models for coupled THC effects on the chemical environment for radionuclide release are based on the same assumptions and approximations shown to be appropriate for closely analogous natural or experimental systems. Abstracted model results are verified through comparison to outputs of detailed process models and empirical observations. Abstracted model results are compared with different mathematical models to judge robustness of results. [NRC (1999), Sections 4.1.1, 4.2.1, 4.3.1, 4.4.1, and 4.5.1]

4.2.2 YMP Features Events and Processes (FEP)

Table 6 below gives a listing of Yucca Mountain Project FEPs (CRWMS M&O 2000h) that are discussed in this document. The YMP FEP # is part of the database search properties and is provided for convenience.

Table 6. A Listing of YMP FEPs that Pertain to Issues Discussed in this Document.

Number	YMP FEP #	FEP Name
1	2.1.09.06.00	Reduction-oxidation potential in waste and EBS
2	2.1.09.13.00	Complexation by organics in waste and EBS
3	2.1.09.18.00	Microbial colloid transport in the waste and EBS
4	2.1.10.01.00	Biological activity in waste and EBS
5	2.1.11.08.00	Thermal effects: chemical and microbiological changes in the waste and EBS
6	2.1.09.05.00	In-drift sorption

4.3 CODES AND STANDARDS

4.3.1 Codes

This AMR was prepared to comply with the DOE interim guidance (Dyer 1999) which directs the use of specified Subparts/Sections of the proposed NRC high-level waste rule, 10 CFR Part 63 (64 FR 8640). Subparts of this proposed rule that are applicable to data include Subpart B, Section 15 (Site Characterization) and Subpart E, Section 114 (Requirements For Performance Assessment). The subpart applicable to models is also outlined in Subpart E Section 114.

4.3.2 ASTM/ASME Standards

ASTM C 1174-97 Standard Practice for Prediction of the Long-Term Behavior of Materials, Including Waste Forms, Used in Engineered Barrier Systems (EBS) for Geological Disposal of High-Level Radioactive Waste was used as guidance in the preparation of this model.

The following ASTM/ASME Standards were used as a source for accepted chemical compositions of metals and alloys (see Section 8.2 for complete reference citations to these standards). Tables containing these compositions are found in Attachments II and III.

- ASME Section II B SB-575
- ASTM A240/A240M-97a
- ASTM A276-91a
- ASTM A516/A516M-90
- ASTM A572/A572M-99a
- ASTM A759-85
- ASTM B 209M-92a
- ASTM F432-95

The following ASTM standards were used as references to Type K cement and welded wire fabric, respectively.

- ASTM C845-96
- ASTM A185-97

5. ASSUMPTIONS

Assumptions used in each of the attachments are contained within the body of that attachment and are not duplicated here.

5.1 The unsaturated conditions within in the drift wall and in materials within the drift are in equilibrium with the relative humidity in the drift due to the capillary pressure of the unsaturated porous medium in the drift (used in Section 6.4.3.3 below).

This is a conservative bounding assumption as the capillary pressure in the rock and porous materials may not always allow the relative humidity (RH) in the atmosphere to be in equilibrium with the unsaturated conditions within the drift. This assumption is bounding in that it will allow microbial communities to develop under unsaturated conditions in the drift that might otherwise be prohibited due to the lack of water. This assumption allows for the use of Equation 2 (see Section 6.3.3.2.2) where RH becomes a surrogate for water activity (a_w).

5.2 MING V1.0 was designed to calculate microbial growth in both saturated conditions as well as unsaturated conditions. Modeling under these conditions requires the appropriate RH to be input. For saturated cases where the RH is 1, the input parameter value to be used will be 0.999, which approximates 100% RH (used in Sections 4.1, 6.7.2.1, and 6.7.3).

This will not cause any discrepancies, as the RH switch will be set at 0.90. Any value above this threshold whether saturated or unsaturated conditions will not make a difference in the calculation. Additionally, the relative humidity (RH) under ambient unsaturated conditions is calculated to be at 100% (see Figures 6 and 7 in Section 6.5.1.1).

5.3 304L stainless steel corrosion rates are assumed similar to 316L/NG stainless steel (used in Section 6.5.2.3).

No 304L specific rates are currently available. A similar assumption for using the 316L stainless steel rates as a surrogate for 304L rates has been used in the past in other modeling efforts (See DTN: SN9911T0811199.003) and is sufficient for this model.

5.4 Median material lifetimes for cement grout, silica fume, and superplasticizer of 10000 years was selected to represent a reasonable lifetime of cement. In addition, minimum and maximum material lifetimes were derived for these materials by taking a factor of five less and greater, respectively (used in Section 6.5.2.3).

No information is available on the material lifetimes of cement grout, superplasticizer or silica fume. Therefore, the 10,000-year median lifetime selected for the material lifetimes of cement grout, silica fume, and superplasticizer is based on TSPA-VA calculations. The TSPA-VA results show that the minimum duration for cement modified water compositions to be affected

by the cement and thus be a source of nutrients for microbial growth in the drift is around 10,000 years (CRWMS M&O 1998a, Section 4.7.2). This lifetime would then be a conservative value for the potential materials because the quantities of grout used in the SR design are significantly less than the VA design (CRWMS M&O 1998a).

5.5 Material lifetimes (minimum, median, and maximum) for the release of Fe^{2+} from biotite of 100,000, 1 million, and 10 million years were selected for use in model validation calculations (used in Section 6.7.2.1, Table 78).

The maximum release rate of Fe^{2+} from biotite was determined by assuming that hematite is not a syngenetic mineral (formed at the same time the volcanic tuff was deposited; Vaniman et al. 1996, Section 4.1.3.2) and that all hematite is thought to be an alteration product of biotite. This provides a conservative bound on the rate of oxidation of the iron minerals in the rock because some of the hematite in the rock could be syngenetic. Since the volcanic eruptions that emplaced the tuff at Yucca Mountain occurred at least 10 million years ago and there is approximately 1 percent of each mineral in the current system, a material lifetime of 10 million years for remaining 1 percent of biotite to alter was thought to represent a reasonable bound for the maximum lifetime. The median and minimum lifetimes were selected to be one and two orders of magnitude less than this. These faster rates will allow for the subsequently larger amounts of redox energy available for microbes to grow in the natural system.

5.6 J-13 water and TSw tuff serve as surrogates for the tuff and water at Rainier Mesa. (used in Sections 6.7.2.1, Table 77)

J-13 water and TSw tuff are similar to the water and rock compositions found at the Rainier Mesa natural analog site located in close proximity to Yucca Mountain. Some discussion on the similarity of fracture water from Rainier Mesa with J-13 water is documented in Section 6.3.2.1.2.1 and is reported in CRWMS M&O (1998a, Section 4.2.3.1.2). The similarity for the TSw tuff is demonstrated where Haldeman and Amy (1993) describe the ash fall tuff that was sampled in Rainier as being both vitric and zeolitic These terms are also used to describe the Topopah Spring and Calico Hills tuffs. The analog comparison of the sites is also referred to in CRWMS M&O (1998a, Section 4.2.3.1.2). Therefore, there should be no significant impact to the results due to the use of this assumption.

5.7 A surface area multiplication factor for glass waste of 30 is used to determine the surface area available for dissolution to account for cracks that form during glass cooling [used in Section 6.5.2.3].

This assumption was made because no actual measurements of surface area for cracked glass are reported in the TDMS. CRWMS M&O (1995) report a range between 10 and 30 for this factor. In order to account for the largest surface area available, the factor of 30 was selected.

5.8 The single corrosion rate value for Bohler A976 SD (Van Konynenburg et al. 1998) was used as a surrogate corrosion rate for Neutronit A978. This rate is found in the following DTN: LL980504105924.034 [used in Section 6.5.2.3].

The rationale for this assumption is that for Neutronit A978 there are no project documented corrosion rates available. However, a corrosion rate has been determined and documented for

two similar materials, Bohler A976 SD and Nutrosorb Plus. These materials, like Neutronit A978, are both borated stainless steels and have similar corrosion rates. (Van Konynenburg 1998). The use of the A976 SD material as a surrogate should capture the general impacts to microbial communities from the corrosion of the Neutronit A978.

5.9 Material lifetimes for the commo cable of 100, 1,000, and 10,000 were used [used in Section 6.5.2.3].

There are no rates available, therefore a two order of magnitude range of lifetimes was selected to bound the potential range of lifetimes. Because the mass of the commo cable (0.79 kg/m of drift) is small, lifetimes greater than the assumed values should not produce sufficient nutrients or energy to affect the overall results.

5.10 Because MING requires the cumulative flux of N_2, O_2 and CO_2 gas compositions entering the drift (Section 6.5.1.4), and the values for gas flux into the drift are not currently available to be abstracted from the *Drift-Scale Coupled Processes (DST and THC Seepage) Models* (CRWMS M&O 2000i), Table 7 below will be used to reflect the cumulative flux of gas into the drift. This table was generated using the discussion and references below. Because the calculations run for the validation of the Microbial Communities model show that gas sensitivity is not a large (Section 6.7.3.4.1), approximate values for the gas flux into the drift (see Table 7) should serve as a good surrogate and not greatly effect the results for the SR calculations. However, this assumption requires further confirmation because the values in Table 7 are based on the TSPA-VA thermal design. This assumption will be replaced upon the generation of the appropriate input in future updates to *Drift-Scale Coupled Processes (DST and THC Seepage) Models* (CRWMS M&O 2000i), the *Abstraction of the Drift-Scale Coupled Processes* (CRWMS M&O 2000b) and *In-Drift Gas Flux and Composition* (CRWMS M&O 2000l) [used in Section 6.5.1.4].

Previous calculations done for TSPA-VA (CRWMS M&O 1998a) established a data set (see Table 7 below) for use in ambient calculations where the TSPA-VA gas flux results that most closely applied to ambient conditions were the 100,000-year values. This instantaneous flux was then summed over time to create the input. In order to use these ambient results for the current SR calculations, the ambient values need to be modified to reflect the thermal load and temperature history of the SR design.

Table 7. Cumulative Gas Flux Values (kg/m^2) used in the Ambient Test Case Calculations

Year	CO_2	O_2	N_2
1	2.00E-5	4.64E-3	1.85E-2
50	1.00E-3	2.32E-1	9.25E-1
200	4.00E-3	9.28E-1	3.70E-0
3,000	6.00E-2	1.39E+1	5.55E+1
5,000	1.00E-1	2.32E+1	9.25E+1

Year	CO_2	O_2	N_2
27,560	5.55E-1	1.27E+2	5.10E+2
28,000	5.60E-1	1.30E+2	5.17E+2
50,000	1.00E-0	2.32E+2	9.25E+2
100,001	2.00E-0	4.64E+2	1.85E+3
1,000,000	2.00E+1	4.64E+3	1.85E+4

MO9911SPACGF04.000

Figure 1 below shows the general order of magnitude shift in yearly gas flux from the 100,001-year ambient values to the values during the thermal pulse (~0-1000 year timeframe). It appears that the O_2 and N_2 values change over this period by a factor of five and the CO_2 values change by a factor of three.

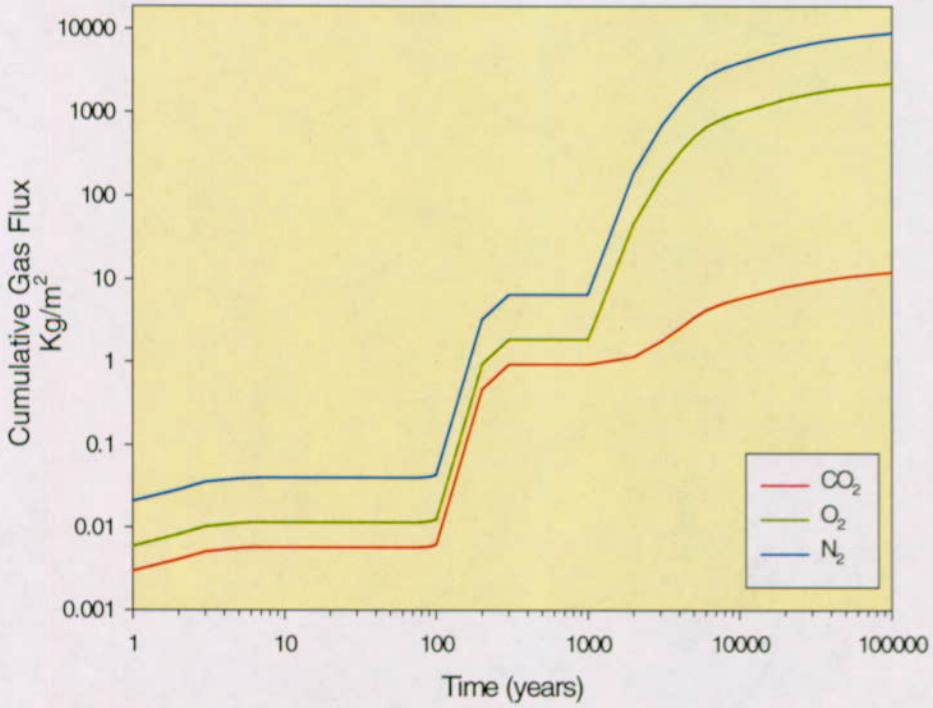

DTN: MO9807MWDEQ3/6.005

Figure 1. The Cumulative Fluxes of CO_2, O_2, and N_2 into the Drift to 100,000 Years used in TSPA-VA MING Calculations.

Table 8 below was created by cumulating the average yearly ambient flux (Year 1 from Table 7 above) for each of the three constituents and dividing by the factor of three or 5. This period lasts for approximately 3,700 years. This time was derived by looking at the high and average infiltration values for the TH abstractions (from 3 mm/yr to 60 mm/yr) as recorded in DTN SN0001T0872799.006 and taking the longest timeframe to have the RH return to 0.99%. Afterwards adding the cumulative flux for the remaining 96,300 years to the 3,700-year total completes the table. This will generally reflect a conservative time frame in which the air mass fraction will be perturbed by the high thermal flux and preclosure cooling and can potentially

alter the gas flux. This should be a reasonable approximation of the thermal effects on the gas composition in the drift through time.

Table 8. Cumulative Gas Flux Values (kg/m^2) used in TSPA-SR Calculations

Year	CO_2	O_2	N_2
1	6.6667E-06	9.2800E-04	3.7000E-03
3700	2.4667E-02	3.4336E+00	1.3690E+01
3701	2.4687E-02	3.4382E+00	1.3709E+01
10000	1.5069E-01	3.2670E+01	1.3026E+02
100000	1.9507E+00	4.5027E+02	1.7953E+03
1000000	1.9951E+01	4.6263E+03	1.8445E+04

5.11 A value of 1 ppm dissolved organic carbon (DOC) is used to represent the organic carbon available in the groundwater entering the drift [used in Section 6.5.1.3 and 6.7.2.1].

The rationale for this assumption is that values similar to this are present in the groundwater at Yucca Mountain (Harrar et al. 1990 and CRWMS M&O 1997b). CRWMS M&O (1997b, page 10) presents a discussion on the groundwater content of DOC where the mean and distribution of DOC in well J-13 compares to the mean and distribution in wells in the Death Valley region and other locations within the United States. The values for J-13 water reported in CRWMS M&O (1997b, page 10) report an average value for DOC of 0.96 ± 0.52 mg/l. This is equivalent to ~ 1 ppm DOC.

5.12 All calculated biomass is considered to be recycled by aerobic heterotrophs, which are able produce CO_2 from the metabolism of the calculated biomass. Due to the absence of large source of external organic carbon in the repository system, the primary source assumed available would be the utilization of existing microbial biomass as it died off. This assumption bounds the production of CO_2 gas for any given year, as all available organic matter is converted first to microbial growth (via calculations done in MING V1.0) then to the production of CO_2 gas via microbial respiration [used in Section 6.6.5.4].

The basis for this assumption is the ambient environment does contain aerobic heterotrophs (see Section 6.3.2.2), which are known to metabolize organic carbon and produce CO_2 gas as a byproduct. As long as there is sufficient oxygen to do this all of the available organic matter can be reduced to CO_2 by these types of organisms (Nealson and Stahl, 1997).

5.13 The glass mass and canister dimensions for the DHLW canisters received by the repository are assumed to be the same as the potential waste forms identified in DOE (1992). This information is shown on Tables 27 and IV-2 below. It is further assumed that the glass mass in pour canisters received from all locations will be similar to the values identified for Savannah River for the purposes of this model.

The rationale for this assumption is that while some variation in dimensions and mass is predicted by DOE (1992) for other locations, these variations are not expected to be large enough to be significant to this model [used in Section 6.5.2.3 and Attachment IV Section IV-5 below].

6. ANALYSIS/MODEL

6.1 PREVIOUS WORK

For TSPA-VA, a microbial communities model was developed to assess the possible magnitude of effects on the system's total chemistry by bounding the magnitude of development of microbial communities (CRWMS M&O 1998a). The TSPA-VA model was based on most of the concepts documented in Section 6.3, 6.4 and 6.6 below and was patterned after the models used in the Swiss and Canadian nuclear waste programs (McKinley and Grogan 1991, McKinley et al. 1997, and Stroes-Gascoyne 1989). The VA model used constraints on both the supply rate of nutrients and the limits on total energy available for microbial metabolism.

The constraints on the supply rates of the nutrients were used to build an idealized microbial composition, comprised of carbon, nitrogen, sulfur, and potassium in addition to the water components. The rates of supply of these constituents were input as constant release rates for each introduced material in the system by specifying the mass and composition of the material and its degradation lifetime. The other major constraint evaluated is the energy available for microbes to grow based on the pH corrected, standard state free energy released from oxidation/reduction reactions. Other constraints on microbial growth are temperature and RH thresholds in the model that limit the start of microbial activity until the boiling period is over. Although microbes could be sterilized out of the drifts during the highest temperature period, because they are present in the water-rock system they will return as water drips back into potential drifts. Microbes could also be sterilized in high radiation fields, but microbes would be reintroduced from the geosphere once the radiation field decays to lower levels. The TSPA-VA microbial communities model was not directly used in the TSPA-VA base case (CRWMS 1998a), but provided first-order limits on potential microbial effects.

The results of the TSPA-VA microbial communities model indicated that the TSPA-VA design would result in the growth of about 10-12 grams of microbial mass per year during the first 10,000 years of the repository (Figure 1). This mass is equivalent to approximately 0.6 parts per million. Based on this small mass of microbes being generated, effects to the bulk chemistry in the drift were determined to be negligible. However, the effects of the localized impacts such as biofilm development, colloid formation, and the production of inorganic acids, methane, organic byproducts, carbon dioxide, and other chemical species that could change the longevity of materials and the transport of radionuclides from the near field were not investigated.

Analyses of the TSPA-VA in-drift microbial communities model results indicated that

- The estimates of microbe masses growing in the potential repository system suggest that effects to the bulk in-drift geochemical environment would be negligible.
- Microbial influenced corrosion (MIC) and other localized microbial attack of materials from biofilm formation cannot be precluded.

- Consideration of microbes as colloids could be pursued in future work.
- There is some potential for additional ligands generated locally; however, the radionuclides would have to compete directly with many other available multivalent metals.

Therefore, the conceptual model documented below updates and enhances the concepts outlined in CRWMS M&O (1998a) and sets the stage for future investigation of the concerns listed above.

6.2 MODEL DESCRIPTION AND IMPORTANCE

This model supports the following post-closure safety case factors (none of which are principal factors): environments on the drip shield, environments on the waste package and drip shield, environments within the waste package, transport through the drift invert and colloid associated radionuclide transport. Therefore, this model is classified "Level 2" for importance purposes. This model also supports the resolution of FEPs outlined in Section 4.2.2 and is a direct feed to the EBS process model report (CRWMS M&O 2000j).

The in-drift microbial communities model is made up of the following parts; first, the conceptual model description as discussed in Section 6.3 below. Second, the use of MING V1.0 software as reported in the software documentation (CRWMS M&O 1998d and 1998h) and discussed in Section 6.4. Finally, the model inputs are derived and discussed in Sections 6.4.3.1, 6.5 and Attachments II to V. These three parts integrated together make up the model. Model results are presented in Section 6.6 and Attachment VI. Model validation parameter derivation, exercises, and results are discussed in Section 6.7 and are shown in Attachment I.

6.3 CONCEPTUAL MODEL

6.3.1 Environmental Limits on Microbial Activity

Included below is a summary describing the environmental conditions required to sustain and proliferate microbial life. The following citations were used as general references and are the basis for the majority of the text written in this section unless otherwise indicated: Amy and Haldeman (1997) is the fourth in a series of Chemical Rubber Company Volumes on The Microbiology of Extreme and Unusual Environments that compiles papers covering microbiology in the deep crust; Banfield and Nealson (1997) is the Mineralogical Society of America Reviews in Mineralogy Volume on geomicrobiology; and Pedersen and Karlsson (1995) is a Technical Report from the Swedish Program that assesses the potential importance of microorganisms to performance assessment of a radioactive waste disposal site.

6.3.1.1 Metabolism

Microbes act as catalysts in geochemical processes through their metabolism. The metabolic pathway that a given microorganism will use depends on the energy source (light or chemical) (Amy and Haldeman 1997; Banfield and Nealson 1997; Pedersen and Karlsson 1995). Thus, a microorganism is described as either a phototroph or chemotroph, respectively. Among the chemotrophs are those microorganisms that use organic carbon as an energy source (chemoorganotrophs) or those that use an inorganic energy source (chemolithotrophs). If an

organism uses organic carbon as its source of carbon, it is referred to as a heterotroph, while if it fixes all of its carbon from CO_2, it is an autotroph. Combinations of these metabolic pathways can give great versatility to organisms in nutrient-limited environments. The types of organisms that exist in the potential Yucca Mountain repository environment (see Section 6.3.2.2) should primarily follow the chemotrophic metabolic pathway.

Bacterial groups are known to use many redox pairs to derive their energy. If chemical kinetic constraints exist such that the rate of a given chemical reaction is sufficiently slow, bacteria can compete; thus, almost any redox couple that yields energy could be exploited (Amy and Haldeman 1997; Banfield and Nealson 1997; Pedersen and Karlsson 1995). The metabolic processes listed below usually define the types of redox processes and input of organic carbon that are available to provide energy and nutrients for growth. They are: aerobic respiration, nitrification and denitrification, methane oxidation, manganese and iron oxidation, sulfur oxidation, manganese and iron reduction, sulfate reduction, and methanogenesis (for a summary discussion on the metabolic processes listed above, see Kieft and Phelps 1997; Pedersen and Karlsson 1995; or Nealson and Stahl 1997). Table 9 gives a listing of possible redox half reaction associated with microbial catalysis. Microbes accumulate at redox interfaces because of the energy that is available to be harvested. Often the metabolic pathways listed above are used to describe the various types of organisms that are present in microbial ecology (i.e., a methanogen is a type of bacteria that uses the redox reactions specific to methanogenesis).

Additionally, research has demonstrated microbes that are involved in iron reduction can also reduce U(VI) to U(IV) and thus provide energy for their metabolic needs (Lovley et al. 1991, Lovley and Phillips 1992, Lovley et al. 1993, Francis et al. 1994, Abdelouas et al. 1998). This could play a potential role in the growth and sustainment of a microbial population within a high level radioactive waste repository where the majority of the waste emplaced would be spent nuclear fuel.

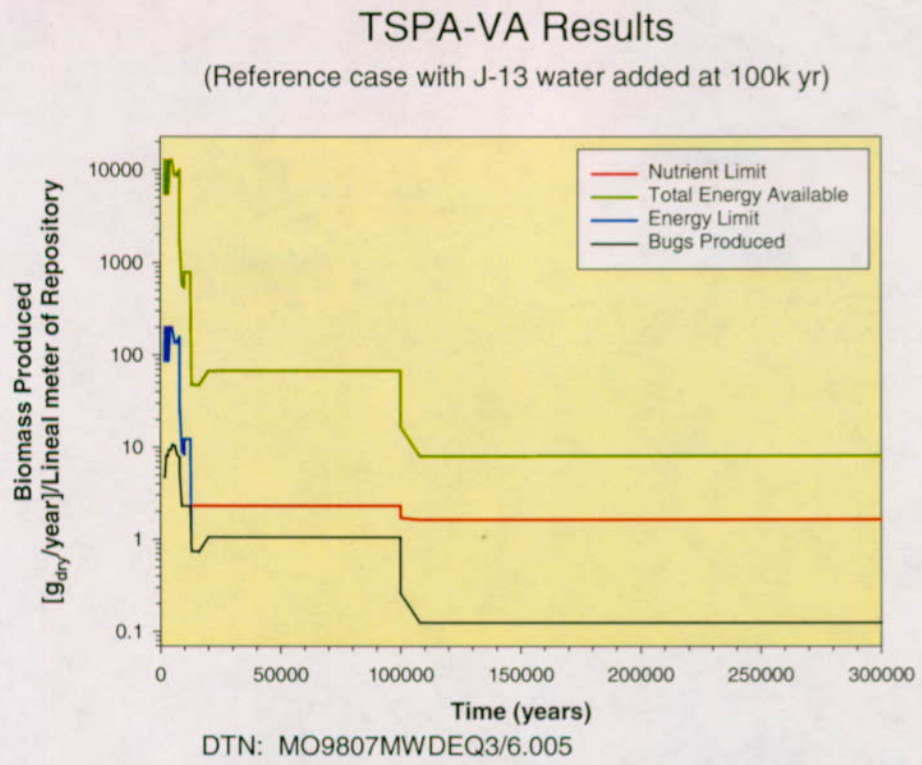

Figure 2. Results of TSPA-VA Model for Microbial Communities (see CRWMS M&O 1998a, Figure 4-85).

Table 9. Redox Half Reactions Associated with Microbial Catalysis.

Redox half reaction	Redox half reaction
Carbon	**Iron**
$CO_2 + H^+ + 2e^- = HCOO^-$	$Fe_2O_3 + 6H^+ + 6e^- = 2Fe + 3H_2O$
$CO_2 + 4H^+ + 4e^- = CH_2O + H_2O$	$Fe^{2+} + 2e^- = Fe$
$CO_2 + 6H^+ + 6e^- = CH_3OH + H_2O$	$Fe^{3+} + e^- = Fe^{2+}$
$HCOO^- + 3H^+ + 2e^- = CH_2O + H_2O$	$Fe_3O_4 + 8H^+ + 8e^- = 3Fe + 4H_2O$
$CO_2 + 8H^+ + 8e^- = CH_4 + 2H_2O$	$FeOOH + 3H^+ + e^- = Fe^{2+} + 2H_2O$
$CH_2O + 2H^+ + 2e^- = CH_3OH$	**Manganese**
$HCOO^- + 7H^+ + 6e^- = CH_4 + 2H_2O$	$MnO_2 + 4H^+ + 2e^- = Mn^{2+} + 2H_2O$
$CH_2O + 4H^+ + 4e^- = CH_4 + H_2O$	$Mn_3O_4 + 8H^+ + 2e^- = 3Mn^{2+} + 4H_2O$
$CH_3OH + 2H^+ + 2e^- = CH_4 + H_2O$	**Sulfur**
$CO_3^{2-} + 10H^+ + 8e^- = CH_4 + 3H_2O$	$S + H^+ + 2e^- = HS^-$
$CO_3^{2-} + 6H^+ + 4e^- = CH_2O + 2H_2O$	$S + 2H^+ + 2e^- = H_2S$
$CO_3^{2-} + 8H^+ + 6e^- = CH_3OH + 2H_2O$	$SO_4^{-2} + 9H^+ + 8e^- = HS^- + 4H_2O$
$CO_3^{2-} + 3H^+ + 2e^- = HCOO^- + H_2O$	$SO_4^{-2} + 10H^+ + 8e^- = H_2S + 4H_2O$
Nitrogen	$HSO_4^- + 7H^+ + 6e^- = S + 4H_2O$
$N_2 + 6H^+ + 6e^- = 2NH_3$	$SO_4^{-2} + 8H^+ + 6e^- = S + 4H_2O$
$N_2 + 8H^+ + 6e^- = 2NH_4^+$	$SO_2 + 4e^- + 4H^+ = S + 2H_2O$
$NO_2^- + 7H^+ + 6e^- = NH_3 + 2H_2O$	$SO_3^{2-} + 7H^+ + 6e^- = HS^- + 3H_2O$

Redox half reaction	Redox half reaction
$NO_3^- + 2H^+ + 2e^- = NO_2^- + H_2O$	$2SO_4^{-2} + 10H^+ + 8e^- = S_2O_3^{-2} + 5H_2O$
$NO_3^- + 10H^+ + 8e^- = NH_4^+ + 3H_2O$	**Hydrogen**
$NO_2^- + 8H^+ + 6e^- = NH_4^+ + 2H_2O$	$H^+ + e^- = 0.5H_2$
$NO_3^- + 6H^+ + 5e^- = 0.5N_2 + 3H_2O$	**Oxygen**
$2NO_2^- + 8H^+ + 6e^- = N_2 + 4H_2O$	$O_2 + 4H^+ + 4e^- = 2H_2O$
$NO_3^- + 9H^+ + 8e^- = NH_3 + 3H_2O$	

DTN: MO9909SPAMING1.003

6.3.1.2 Redox Conditions

Bacteria that are able to grow in the presence of molecular oxygen, either in gaseous or dissolved form, are termed aerobes, whereas those that can grow without oxygen are anaerobes (Amy and Haldeman 1997; Banfield and Nealson 1997; Pedersen and Karlsson 1995). Table 10 shows the terms used to describe the O_2 relations of bacteria. Thus, we see that different microbes can thrive at various redox conditions, including both the oxygenated environments that are at high redox potential and the reducing environments where the oxygen abundance is minimal.

6.3.1.3 Temperature

The temperature of the subsurface environment will greatly affect or limit the type of bacteria present, based on the optimum growth band of the microbe (Amy and Haldeman 1997; Banfield and Nealson 1997; Pedersen and Karlsson 1995). There are 5 temperature classifications of bacteria: psychrophiles, facultative psychrophiles, mesophiles, thermophiles, and hyperthermophiles. Table 11 shows the ranges of temperatures that are acceptable to the 5 classes of bacteria. Therefore, during elevated temperatures in the Yucca Mountain repository the microbial population would be dominated by thermophiles and hyperthermophiles; later, as the repository cooled, the repository would be dominated by mesophiles.

Table 10. Terms Used to Describe the O_2 Relations of Bacteria (Modified from Pedersen and Karlsson [1995]).

Group	O_2 Relation
Aerobes	
Obligate	O_2 is required
Facultative	O_2 is not required but growth is better with O_2
Microaerophilic	O_2 is required but at levels lower than atmospheric
Anaerobes	
Aerotolerant	O_2 is not required and growth is not better with O_2
Obligate (strict)	O_2 is harmful or lethal

Table 11. Bacterial Temperature Classes and Their Temperature Ranges. Data are taken from Pedersen and Karlsson (1995) and Horn and Meike (1995).

Temperature Class	Minima	Maxima	Optimum range
Psychrophiles	*	20°C	0 to 15°C
Facultative Psychrophiles	0°C	35°C	20 to 30°C
Mesophiles	15°C	45°C	20 to 45°C
Thermopiles	45°C	70°C	55 to 65°C
Hyperthermophiles	60°C	120°C	80 to 100°C

* No lower bound reported.

6.3.1.4 Radiation

Bacteria are much more resistant to radiation than are most humans (Amy and Haldeman 1997; Banfield and Nealson 1997; Pedersen and Karlsson 1995). The acute lethal dosage for many bacteria is approximately 5 to 1,000 krad (Pedersen and Karlsson 1995, p. 48-49). The medical sterilization threshold is about 2,500 krad, and the limit of microbial activity for some species indigenous to the ESF was found to be 200 krad (Pitonzo 1996). Therefore, levels of radiation in the drift thought to be present after waste emplacement at Yucca Mountain as reported by Van Konynenburg (1996) should be low enough to allow microbial growth and catalysis.

6.3.1.5 Hydrostatic Pressure

Although hydrostatic pressure is not thought to be a problem in the proposed Yucca Mountain repository, bacteria are able to withstand and flourish at the highest hydrostatic pressure on the planet (Amy and Haldeman 1997; Banfield and Nealson 1997; Pedersen and Karlsson 1995). Ordinary bacteria that have not been challenged by high hydrostatic pressure during their evolution are, nevertheless, remarkably tolerant to such pressure.

6.3.1.6 Water Activity

Water availability seems to be the most limiting condition for microbial growth (Amy and Haldeman 1997; Banfield and Nealson 1997; Pedersen and Karlsson 1995). Microbiologists normally use water activity (a_w) to quantify the amount of water available to bacteria. Water activity is normally defined by the ratio of the solution vapor pressure to the vapor pressure of pure water.

Most bacteria cannot exist when a_w falls below about 0.90 and have trouble thriving when a_w is less than 0.95. In order for bacteria to grow well, a_w needs to be around 0.98 (Pedersen and Karlsson 1995). Many fungi and yeast can thrive at lower a_w levels (on the order of 0.7 to 0.85; Pedersen and Karlsson 1995). Water activity in the potential repository will range from about 1 to values approaching zero because of the thermal perturbation.

6.3.1.7 Deep Vadose-Zone Microorganisms

By definition, vadose zones are unsaturated. However, this does not imply that the water found in the vadose zone limits the presence or growth of the microorganisms present. In fact, matric water potentials in most vadose zones are not sufficiently low to cause desiccation stress in microbes (Amy and Haldeman 1997; Banfield and Nealson 1997; Pedersen and Karlsson 1995). The microbes found in these unsaturated environments seem to be desiccation resistant (Kieft et al. 1993).

Work done in several vadose zones in arid and semiarid sites indicate that the total numbers of microbes that are considered ambient populations range from 10^4 to 10^7 cells/g dry wt. (Kieft et al. 1993). Kieft et al. (1993) also stated that in the various vadose systems, there are many populations that are growth limited, most by water or organic carbon, but some systems were growth limited by nitrogen or phosphorous.

6.3.1.8 Influence of pH

Bacteria grow over wide ranges of pH, but there are limits to their tolerance (Amy and Haldeman 1997; Banfield and Nealson 1997; Pedersen and Karlsson 1995). Bacteria frequently change the pH of their own habitat by producing acidic or basic metabolic waste products. Some bacteria create their own habitats by the formation of biofilms (see Section 6.3.1.14). Each species of microbe has a pH growth range and growth optimum. Table 12 below shows the types of microbes and their pH relationships. In certain areas of the Yucca Mountain repository where the pH is dominated by the cement phases, the repository is favorable to alkalophiles and extreme alkalophiles. In other areas of the repository where other materials would be present, such as iron from WPs, neutrophiles or acidophiles may thrive.

Table 12. pH Ranges of Differing Classes of Microbes. Data Taken from Pedersen and Karlsson (1995) and Horn and Meike (1995).

pH Class	pH Range
Acidophiles	1.0 to 5.5
Neutrophiles	5.5 to 8.5
Alkalophiles	8.5 to 11.5
Extreme Alkalophiles	>10.5

6.3.1.9 Salinity

Bacteria can be affected by changes in the osmotic concentration of their surroundings (Amy and Haldeman 1997; Banfield and Nealson 1997; Pedersen and Karlsson 1995). However, there are bacteria that have adapted to highly saline conditions and can grow in high levels of sodium chloride (2.8 to 6.8M; Pedersen and Karlsson 1995). Many bacteria are osmotolerant and thrive in saline solutions with concentrations up to 3M (Pedersen and Karlsson 1995).

6.3.1.10 Nutrition

About 95 percent of the microbial cell dry weight is made up of a few major elements: carbon, oxygen, hydrogen, nitrogen, sulfur, phosphorous, potassium, calcium, magnesium and iron (Amy and Haldeman 1997; Banfield and Nealson 1997; Pedersen and Karlsson 1995). Besides these macro-elements, there exists the requirement of several trace elements, namely, manganese, zinc, cobalt, molybdenum, nickel and copper. These trace elements are needed in such low concentrations that they are not thought to be the limiting factors in microbial growth. The requirements for carbon, hydrogen, and oxygen are normally satisfied together, because they are the chief constituents of the molecules that make up the carbon sources for microbes. One source for which this is not true is the autotroph utilization of CO_2 as its principal source of carbon as opposed to the heterotroph utilization of reduced organic carbon. However, the direct utilization of CO_2 is a very energy expensive process. It is far easier for most microbes to utilize the heterotrophic metabolic pathway. Heterotrophs show a great range of flexibility with respect to carbon sources. Some bacteria will degrade almost any reduced carbon source, whereas others will only catabolize a few select carbon compounds.

In order to grow, microbes need to be able to incorporate nitrogen, phosphorous, and sulfur (Amy and Haldeman 1997; Banfield and Nealson 1997; Pedersen and Karlsson 1995). Microbes usually employ inorganic sources of these elements. Nitrogen is often used by taking nitrate and reducing it to ammonia, which then can be incorporated via biosynthetic pathways. Some microbes are able to reduce and assimilate atmospheric nitrogen. However, this process is extremely sensitive to oxygen and requires a great deal of available energy. Almost all bacteria use inorganic phosphate as their phosphorous source and incorporate it directly. Most bacteria use sulfate as a source of sulfur and reduce it by assimilatory reduction. Sulfate is available in groundwater and is not usually a limiting nutrient, but quantities of phosphate and nitrogen can be small enough to limit the growth of microorganisms. However, in most conditions, the flux of energy will limit the amount of microbial growth possible. Table 13 shows the nutritional requirements for chemotrophs.

Table 13. Nutritional Requirements for Chemotrophic Organisms. Modified from Pedersen and Karlsson (1995).

Nutritional type	Carbon sources	Electron sources (reducing power)	Examples of organisms
Chemolithotrophic autotrophy	CO_2	NH_4^+, NO_2^-, Mn^{2+}, Fe^{2+}, H_2S, S, H_2	Ammonium, nitrite, manganese, iron, sulfur, and hydrogen oxidizing bacteria, methanogenic bacteria
Chemoorganotrophic heterotrophy	Organic compound	Organic compound	Most bacteria, fungi, animals

6.3.1.11 Starvation-Survival

Evidence that supports the concept that microbial populations can survive for millions of years in the subsurface has been recently presented (for a detailed explanation of starvation-survival, see Amy [1997] and Morita [1990]). The basic idea is termed starvation-survival and is defined as a state of metabolic arrest, which permits the organisms to survive for long periods without sufficient energy for growth and reproduction (Amy and Haldeman 1997; Banfield and Nealson

1997; Pedersen and Karlsson 1995). This state is the normal state of most microorganisms in nature. Cells exist at this starvation level until there are energy producing substrates present for growth and reproduction (Morita 1990). Following such a growth period, cells can then return to the starvation state when the metabolic substrates are depleted.

6.3.1.12 Size

The size of bacteria varies depending on the species and nutritional status. Growing (thriving) bacteria can be up to several μm long with a volume of several μm^3. The same species in a non-growing state (i.e., a low nutrient or starvation environment) may be as small as 0.2-0.3 μm and have a volume of not more than 0.05 μm^3. This small size is about the smallest possible size of a living organism because of the essential cellular functions that need to take place. This size would tend to be the smallest size involved in bacterial transport in a porous medium and defines the minimum pore size through which bacterial can be transported (Pedersen and Karlsson, 1995; Nealson and Stahl, 1997).

6.3.1.13 Movement in the Subsurface

Microorganisms tend to attach or sorb onto surfaces where they can obtain available redox energy. Once they become attached, microorganisms tend to form biofilms (see Section 6.3.1.14) and thus remain attached. At some point, biofilms grow and reach a steady state where attachment is balanced out by detachment and movement. Both water movement and gravitation are considered the chief mechanisms of transport in the subsurface. Over short distances hydrogeochemical (mineral surface coatings) and cell-associated biological factors (negative microbial surface charge) dominate the transport process. The presence of preferred flow paths can also influence the extent of the transport as well.

Often microbes are thought of as colloids, as they tend to show some of the same behaviors that abiotic colloidal particles do. The movement of microbes is often modeled using either a filtration or an advection-dispersion type model (see Mills [1997] for more detailed discussion on microbial transport).

6.3.1.14 Biofilm Production

After attachment to surfaces, microbes initiate production of slimy adhesive substances, generally exopolysaccharides. These extracellular polymers, which frequently extend from the cell to form a tangled matrix of fibers, provide structure to the microbial assemblage. This structure is normally termed a biofilm. Microorganisms within biofilms are capable of maintaining environments at biofilm/surface interfaces (both liquid/solid and gas liquid interfaces) that are radically different from the bulk in terms of pH, dissolved oxygen, and other organic and inorganic species. In some cases, these interfacial conditions could not be maintained in the bulk medium at room temperature near atmospheric pressure. As a consequence, microorganisms within biofilms produce minerals and mineral replacement reactions that are not predicted by thermodynamic arguments based on the chemistry of the bulk medium (Little et al., 1997). In other words, microbes can create the living conditions (biofilms) to which they are most suited and comfortable even if these conditions are not necessarily the same chemically as the bulk materials that serve as the substrate.

Biofilm accumulation is the result of the following microbial processes: attachment, growth, decay and detachment. Attachment is due to microbial transport and subsequent binding to surfaces. Growth (and biofilm decay) is due to cell division and is generally described by Monod kinetics:

$$\mu = \frac{\mu_{\max} S}{K_s} \qquad \text{(Eq. 1)}$$

where μ_{max} = maximum specific growth rate (t^{-1}), K_s = half saturation coefficient (mole L^{-3}), S = substrate concentration (mole L^{-3}) (Little et al. 1997). Detachment includes two processes: erosion and sloughing. Sloughing happens when large pieces of the biofilm are rapidly removed. Erosion is the continuous removal of individual cells or small groups.

6.3.2 The Ambient System

6.3.2.1 Ambient Environmental Conditions

Besides the presence of water and substrate, the other major necessity for microbial life is the presence in the environment of a few major nutritional elements: carbon, oxygen, hydrogen, nitrogen, sulfur, phosphorous, potassium, calcium, magnesium and iron (see Section 6.3.1.10 above). These elements are the chief building blocks of a microbe. These building blocks are present in the ambient environment in the gas, groundwater and strata that make up the Yucca Mountain site subsurface. The three components (gas, groundwater, and strata) are discussed below. Additionally, the ambient temperature and water activity in the subsurface is not extreme, nor are any of the other environmental limits discussed in Section 6.3.1 above (i.e. pH, salinity, nutrition, etc.) a concern.

6.3.2.1.1 Gas Compositions

As discussed in Section 6.3.1.10 autotrophic organisms can directly assimilate gases. The values of the gases O_2, N_2, and Ar in samples of pore gases from the UZ are all very close to their atmospheric values (CRWMS M&O 2000r, Section 5.3.8.2, p. 5.3-48). Measurements of gas compositions from various UZ boreholes demonstrate that UZ CO_2 gas concentrations are elevated above atmospheric CO_2 partial pressures (about 350 parts-per-million-by-volume [ppmv]) by about a factor of three (CRWMS M&O 2000r, Section 5.3.8.2, p. 5.3-48 to 5.3-49). The values of UZ pore-gas composition analyzed for the site indicate that the CO_2 content of pore gases tends to average about 1000 ppmv (CRWMS M&O 2000r, Section 5.3.8.2, p. 5.3-48 to 5.3-49). These elevated values could be the result of mixing of CO_2-rich gases generated in the soil zone with the rest of the gas volume of the mountain (CRWMS M&O 2000r, Section 5.3.8.2, p. 5.3-48).

6.3.2.1.2 Water Compositions

As discussed in Section 6.3.1.10 microorganisms can utilize nutrients that are found in groundwater. Analyses of the groundwater compositions at Yucca Mountain are described in

detail in the Site Description Document (CRWMS M&O 2000r, Section 5.3). The ambient water composition could either be defined by analyzed values of saturated-zone water (e.g., Well J-13), or from the analyses performed on pore water extracted from UZ rock samples.

6.3.2.1.2.1 Ambient SZ Water

Harrar et al. (1990) evaluated water from Well J-13 for use as a reference water composition and concluded that it could be used as such for the purpose of a reference case fluid. In addition, the saturated-zone fluids are similar compositionally to both the perched water (CRWMS M&O 2000r, Section 5.3.9.3, p. 5.3-55) and to that collected flowing from fractures at Rainier Mesa (Harrar et al. 1990, pp. 6.5 and 6.6, Table 6.1). At this time, it appears that a reasonable ambient water composition moving through fractures can be represented by the J-13 composition. The average composition of J-13 water from Harrar et al. (1990) is given in Table 14, together with averages for UZ fluids analyzed from boreholes UE-25 UZ-5 and UE-25 UZ-4 (Yang et al. 1988, 1990; Yang 1992).

In an analysis of the groundwater content of dissolved organic carbon (DOC, CRWMS M&O 1997b, Section 4.1), the DOC content of groundwaters from well J-13 and other wells in the Death Valley region show that the standard deviation of DOC falls between 1.48 ppm to 0.36 ppm with the average for J-13 well water at 0.96 ppm.

6.3.2.1.2.2 Ambient UZ Pore water

Analyzed water compositions from the UZ tuffaceous rocks (Yang et al. 1988, 1990; Peters et al. 1992; Yang 1992) indicate that they have pH values in the range of 6.4 to 7.5 and that some constituents (Ca^{2+}, K^{+}, Mg^{2+}, SO_4^{2-}, Cl^{-}, and dissolved silica) are more concentrated than found in samples from the SZ tuffaceous aquifer. However, the average HCO_3^{-} content measured in 83 water samples extracted from UZ nonwelded tuff was lower than that in the saturated-zone samples (Peters et al. 1992). Some of this variability may be caused by the extraction techniques used to remove water from unsaturated samples (Peters et al. 1992). No analyses of the dissolved organic content have been given in the studies of the UZ fluid compositions. Because of the intimate contact between the UZ fluids and the pore gases in the rock, these groundwaters are relatively oxidizing and the oxidation potentials are probably controlled primarily by atmospheric oxygen levels (CRWMS M&O 2000r, Section 5.3.8.2, p. 5.3-48). In the units above the Calico Hills, the pH of the water is thought to be dependent primarily on the carbon dioxide content of the gas, with some degree of Na^{+}-H^{+} ion exchange affecting the values (CRWMS M&O 2000r, Section 5.3.6.3.2, p. 5.3-23).

There are clearly differences between the J-13 (SZ) and UZ fluids, primarily higher Ca, Mg, Cl, and SO_4^{2-} in the UZ fluids (see Table 14 and discussion in CRWMS M&O 2000r, Sections 5.3.6 and 5.3.9). Whether these differences are meaningful, as well as which fluid composition most closely represents the ambient composition of fluid that moves through Yucca Mountain, is not currently completely understood. There may have been some alteration of UZ pore fluid chemistry from the extraction techniques, as discussed above. In addition, it was thought that the UZ-4 samples had lost water by evaporation, which may account for the generally higher values compared to UZ-5 analyses (Peters et al. 1992; Yang 1992). Because of low sample volumes, the UZ analyses are not as comprehensive as those for the SZ.

Table 14. Average Compositions for Saturated Zone Water Well (J-13) and for Unsaturated Zone Water (UZ-5 and UZ-4) (nr = not reported) (Table taken from CRWMS M&O 1998a, Table 4-2).

Constituent	Units	J-13 AVG	UE-25 UZ-5 AVG	UE-25 UZ-4 AVG
Ca	mg/l	12.9	45.2	99.2
Mg	mg/l	2.0	9.2	17.4
Na	mg/l	45.8	39.1	56.4
K	mg/l	5.0	8.6	14.2
SiO_2	mg/l	61.0	92.4	86.8
NO_3^-	mg/l	8.8	nr	nr
HCO_3^-	mg/l	128.9	nr	nr
Cl^-	mg/l	7.1	53.2	94.0
F^-	mg/l	2.2	nr	nr
SO_4^{2-}	mg/l	18.4	51.0	151.8
Li	µg/l	48.3	nr	nr
Fe	µg/l	~30	49.1	24.3
Mn	µg/l	~45	18.5	38.6
Sr	µg/l	~50	422.6	1196.5
Al	µg/l	~30	nr	nr
Zn	µg/l	nr	62.0	102.1
field Eh	mV	340.0	nr	nr
field O_2	mg/l	5.6	nr	nr
field pH	pH	7.4	7.0	7.5

6.3.2.1.3 Mineralogy of Strata

Microbial cells attach to and interact with associated mineral surfaces. Many nutrients that sustain microbial life are derived from the minerals and redox reactions at mineral surfaces provide metabolic energy. Even in nutrient poor environments such as tuff which contain mostly feldspars, existing microbial populations effectively scavenge the essential macronutrients necessary for survival by looking for inclusions of phosphorous based minerals such as apatite (Rogers et al. 1998). Bulk-rock compositions for Topopah Spring tuff are given below in Table 15.

By carefully looking at the information provided above for the three components (gas, water, and rock) of the ambient geochemical system, it is obvious that they contain the sufficient nutritional building blocks and provide enough energy to sustain microbial life.

Table 15. Bulk-rock Compositions for Topopah Spring Tuff.

Element	Unaltered Lower Vitrophyre Concentration wt%	Altered Lower Vitrophyre Concentration wt%
Si	72.2	69.6
Ti	0.07	0.10
Al	14.3	19.5
Fe^{3+}	0.78	1.07
Mn	0.05	0.06
Mg	0.45	1.33
Ca	0.69	3.73
Na	6.43	3.65
K	4.98	0.91
P	0.01	0.02

DTN: LL981209705924.059

6.3.2.2 Ambient Microbial Populations

As discussed above, the ambient environment has all of the requirements to sustain microbial activity at low levels in the host rock. In fact, microbial analyses conducted in the exploratory studies facility (ESF) have determined the existence of aerobic heterotrophs and autotrophs (Ringelberg et al. 1997). The organisms present include the following types: iron-oxidizing, sulfur oxidizing and nitrifying organisms. Cell counts for autotrophs range between 10 and 500 cells/g dry wt. and for the heterotrophs between 3.2×10^4 to 2×10^5 cells per gram of tuff. The samples were taken within a month of tunnel boring machine excavation, and sampling precautions were taken to ensure that there were no contamination problems from introduced microbes due to construction activities. Similar investigations were conducted on tuff samples taken from nearby Rainier Mesa and resulted in viable cell counts of about 10^4 per g of crushed tuff (Kieft et al. 1993).

Experiments were also conducted on microbes cultured from tuff collected from the ESF to determine which, if any, nutrients were the limiting factors in microbial growth (Kieft et al. 1997). The collected samples were thought to represent an uncontaminated ambient microbial population. The addition of both water and organic carbon to the cultured microbes caused substantial colony growth. From these experiments, the conclusion was that the potential for microbial growth is large, if nutrients and water are introduced into the environment.

6.3.3 Repository System Conditions and Constraints

Throughout the repository, microbes will use the nutrients and available energy from chemical oxidation and reduction reactions. The construction of the repository will add nutrients and available energy where microbes will be able grow beyond the ambient populations. Table 16 below represents the various materials that the VA design specified. These materials are similar to the materials that will be specified in the LA design. Thus, there will be an increase in nutrient and energy supply above that which the ambient system would provide to sustain its microbial populations.

In addition to the introduced materials, the emplacement of the high level waste will alter the repository environment due to the heating of the repository environment. This will change the ambient conditions, especially the temperature, water, and gas regimes that influence microbial growth.

6.3.3.1 Introduced Materials

As found in Table 16 below, there are three main categories of introduced materials that, as part of the waste package or as structural components, will potentially be abundant post-closure: steels/alloys, cementitious materials, and organic substances. This conceptual model's focus is on microbial interaction with the materials that potentially will be introduced into the drift environment containing some or all of these components. Figure 3 below shows the general locations of most of the major LADS design materials (CRWMS M&O, 1999c) within a repository drift.

6.3.3.1.2 Steels and Alloys

The alteration of metals/alloys in the ground support, waste packages and fuel rods/waste forms will produce metal-oxide and -hydroxide corrosion products within the drift and may form metal-silicate minerals. As the Fe, Mn, U, and other metals in the steel/alloys oxidize, they represent a sink for oxygen and could be a mechanism for generating locally reducing conditions if the oxygen flux into the potential drift is low enough. Such oxidation reactions represent a source of metabolic energy for microbial activity within the potential emplacement drifts. With the shear mass of these materials planned to be emplaced in the repository, abundant energy will be available for microbial catalysis. Additionally, the steels and alloys contain trace elements (i.e. carbon, sulfur, and phosphorous) that can be used for microbial growth.

6.3.3.1.3 Cementitious Materials

Cementitious materials are highly alkaline and have pHs ranging between 11 and 13 (CRWMS M&O 1998a, page 4-17 and Table 4-3). They require organic admixtures to assist in their workability in construction. They are also often high in sulfates and nitrates. In the case of concrete, steels are used as reinforcing agents. Essentially, because of their durability and longevity in the environment, cementitious materials could act as both a nutrient source and as an energy source.

The natural analog to alkaline groundwater is the natural springs in the Maqarin area in NW Jordan, where the groundwaters have pH values as high as 12.9. These springs contain diverse microbial populations, therefore the high alkalinity of the cementitious material and water in equilibrium with it will not preclude the growth of microorganisms (Pedersen 1999). The types of microorganisms residing in this environment would be alkalophiles and extreme alkalophiles (see Section 6.3.1.8, Table 12). Even the extreme alkaline pH environments will not preclude microbial colonization where biofilms have been known to form on concretes The biofilms create very low pH environments and can rapidly degrade the concrete (Diercks et al. 1991, Horn and Meike 1995).

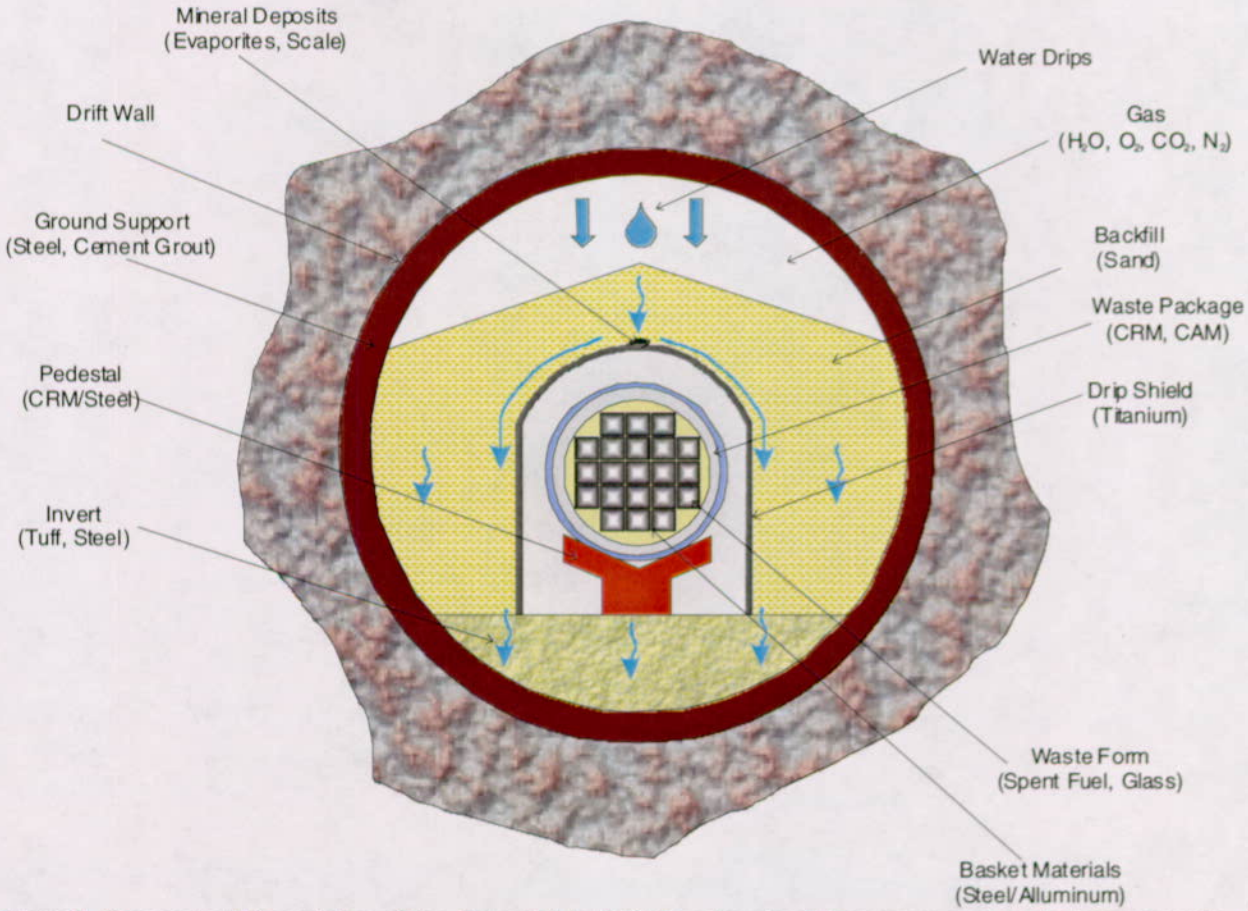

Figure 3. Conceptual Description of the Potential In-Drift Geochemical Processes and the Interaction with the Materials of the EDA II Design (CRWMS M&O 1999c, Rail and Gantry System not Depicted). For the No Backfill Design, this Figure would be Modified by the Removal of the Sand Backfill.

Table 16. Materials, Quantities and Compositions of the Various Design Materials and Waste Package Types. Values are Calculated or Documented in Attachments II, III and IV.

Material Name	Quantity kg/m (per WP)**	Element composition and Wt %						
		Fe	*Mn*	*C*	*P*	*S*	*N*	*Other*
304L Stainless Steel	651	65.045	2.0	0.03	0.045	0.03	0.10	Bal.
316L Stainless Steel	165	61.795	2.0	0.03	0.045	0.03	0.10	Bal.
316NG Stainless Steel	2178	61.805	2.0	0.02	0.045	0.03	0.10	Bal.
Alloy C-22	1651	6.0	0.5	0.015	0.02	0.02	-	Bal.
Aluminum 6061	65	0.7	0.15	-	-	-	-	Bal.
ASTM A572 Steel	587.2	97.48	1.65	0.23	0.04	0.05	-	Bal.
ASTM A759-85 Steel	133.9	97.59	1	0.82	0.04	0.5	-	Bal.
ASTM F432-95 Steel	48	99.022	-	0.79	0.058	0.13	-	Bal.
C Steel ASTM A516	1108	97.91	1.3	0.27	0.035	0.035	-	Bal.
Commo Cable	0.79	-	-	27	-	-	-	Bal.
CSNF Waste PWR	3145	1.85	0.05	0.01	0.01	-	0.01	Bal.
CSNF Waste BWR	2798	1.63	0.05	0.01	-	-	0.01	Bal.
DHLW Waste	2342	7.35	1.55	-	0.014	0.13	-	Bal.
Neutronit A978	400	66.66	-	0.04	-	-	-	Bal.
Rail Fittings	13.4	73.11	-	0.1725	0.03	0.0375	-	Bal.
Silica Fume	3.35	0.21		1.3		0.32		Bal.
Superplasticizer	0.67	-	-	16.12	-	4.28	-	Bal.
Ti Grade 7	670***	0.30	-	0.1	-	-	-	Bal.
Type K Cement	63.50	1.96	-	-	-	2.76	-	Bal.
WWF Steel	70	98.8	-	1.0	0.1	0.1	-	Bal.

Quantities generally represent PWR waste packages and a repository design representing the nonlythophasae host rock. Items like 304L, alloy C-22 and A572 are taken from the designs that apply or are summed from various tables found in the attachments. * Includes Ti grade 24.

6.3.3.1.4 Organic Substances

The introduction of organic substances into the drifts will promote microbial activity and may have an impact on performance through changes in the concentrations of organic acids and organic colloids which can increase WP corrosion, increase radionuclide solubility-limits and transport properties, and enhance silicate mineral dissolution (Choppin 1992; Minai et al. 1992; Bennett et al. 1993; Meike and Wittwer 1993). In addition, organic substances can take part in oxidation/reduction reactions and may therefore contribute to generation of locally reducing conditions, possibly reducing metal solubilities.

Depending on the amount of degradable organic carbon, heterotrophic bacteria will mineralize the organic carbon into inorganic nutrients and carbon dioxide. Under aerobic conditions the organic molecules are generally degraded completely into carbon dioxide. In anaerobic conditions the organic byproducts of one microbial community serves as a substrate for a different community. In these environments the organic carbon can be mineralized either to carbon dioxide by combined oxidative processes or to methane by oxidation-reduction processes, depending on the availability of inorganic electron acceptors in the system (Pedersen and Karlsson, 1995).

6.3.3.2 Thermal Perturbation

With the introduction of waste into the repository environment, there will be an increase in the temperature of the drifts and surrounding host rock. The four sections below describe the potential effects that this perturbation will have on microbial populations–whether they are indigenous species or introduced via construction.

6.3.3.2.1 Temperature

As discussed in Section 6.3.1.3 microorganisms are sensitive to the temperature of their environment. However, hypothermophiles can survive in high temperature regimes up to about 120°C (see Table 11). In the thermally perturbed environment, in-drift repository temperatures will likely rise above boiling for a substantial amount of time and could certainly be >120°C during some of that time. It would only be during this period of time (T>120°C) that the potential for microbial growth could be suspended. Otherwise, microbial growth is not limited by the temperature of the drift environment.

6.3.3.2.2 Water

Water entering the drift will have variable composition as a function of time as a result of the heating of the system driving processes such as boiling/condensation and reaction of both heated and condensate waters with minerals and gases in the fractures of the host rocks (Arthur and Murphy 1989; Glassley 1994; Murphy 1993; Wilder 1996; Lichtner and Seth 1996; Glassley 1997; Hardin 1998, Section 6.2.2). These reacted, or thermally perturbed, fluid compositions may flow down fracture pathways and enter potential emplacement drifts where they could undergo reaction with introduced materials or be boiled again and deposit mineral precipitates containing salts (Glassley 1994; Murphy and Pabalan 1994; Wilder 1996; Lichtner and Seth

1996). However, the different water compositions and water-rock reactions should have limited impact to microbial growth.

The real concern with the water is its availability. As discussed in Section 6.3.1.6, water activity is the limiting condition for microbial growth. Without water, microbes can not exist. Water activity in the unsaturated repository environment is then tied to the thermohydrology of the system. Thus, the elevated temperatures of the emplaced waste packages will tend to dry out the repository and dry up the atmosphere. If the porous medium in the near field and within the drift is in equilibrium with the atmosphere in the drift, then the water activity will be controlled by the relative humidity in the drift environment (see assumption 5.1). This allows us to relate the relative humidity in the atmosphere to the availability of moisture for microbial survival and growth by the following equation

$$a_w \approx \frac{RH}{100} \qquad \text{(Eq. 2)}$$

Where a_w is the water activity and RH is the relative humidity in the drift. If microbes do not thrive below an a_w of 0.90 then when the drift atmosphere falls below a RH of 90 there should be a suspension of microbial growth.

Because boiling of fluids will occur, mineral precipitates including salts will form in the region of boiling. Water undergoing boiling/evaporation or reacting with precipitated salts will become concentrated in a number of dissolved constituents either in close proximity to, or within, potential emplacement drifts (Hardin 1998, Section 6.2.2). However, unless the concentrations of the saline solutions are greater than 3M there should not be an impact from these fluids (see Section 6.3.1.9).

6.3.3.2.3 Gas

The thermally driven perturbations to the system will also affect the flux and composition of gas entering the potential emplacement drifts (Murphy 1991; Glassley 1994; Codell and Murphy 1992; Murphy and Pabalan 1994; Lichtner and Seth 1996; Wilder 1996; Glassley 1997; Hardin 1998, Section 5.7.1). One major process affecting the in-drift gas composition is the boiling of the pore water, which is expected to drive out most of the air component of the gas from the drift environment (CRWMS M&O 1998b). The changes in the air mass-fraction of the gas will drive changes in the redox system and pH in the environment. However there are no real limitations to microbial communities from this perturbation. Microbes can thrive in very different redox and pH environments as discussed in Sections 6.3.1.2 and 6.3.1.8.

6.3.3.2.4 Mineral Precipitation

The increased temperatures will vaporize much of the water in the near-field as an above-boiling zone forms in the very near-field (Glassley 1994). This transition will increase the capacity of the system to transport moisture as volatiles and will result in precipitation of all dissolved solids from boiling fluids in the near-field. Condensation of steam as water in cooler regions above the potential repository horizon will dissolve new material, which could be transported through fractures back down into the boiling zone with subsequent boiling and phase precipitation. This

refluxing could produce porosity and permeability changes that may impact the near-field hydrology (Glassley 1994; Hardin 1998, Section 5.6). However, mineral precipitation should not effect greatly the ability of microbes to thrive in the system.

6.3.4 Microbial Effects on EBS Performance

The EBS is one of the primary barriers to radionuclide release. The potential degradation of this barrier is of primary concern to the long term performance of the repository. A workshop conducted to examine the potential effects of microbial activity in the potential geologic repository at Yucca Mountain resulted in the following hypotheses (Horn and Meike 1995).

- Microbes can compromise the integrity of WPs (and other repository materials)
- Microbes can modify water chemistry outside the bounds predicted by abiotic chemical calculations
- Microbes can alter the rate of radionuclide transport from breached WPs.

In addition to these three potential effects of microbial populations on a radioactive waste disposal system, some additional concerns have been previously raised: degradation of concrete support structures (Perfettini et al. 1991), production of gas within a repository (Bachofen 1991), alteration of pH and redox conditions within a repository (Hersman 1997), and the disruption of surfaces, e.g. oxide surfaces on metals (West et al., 1985). These effects among others are depicted in Figure 4.

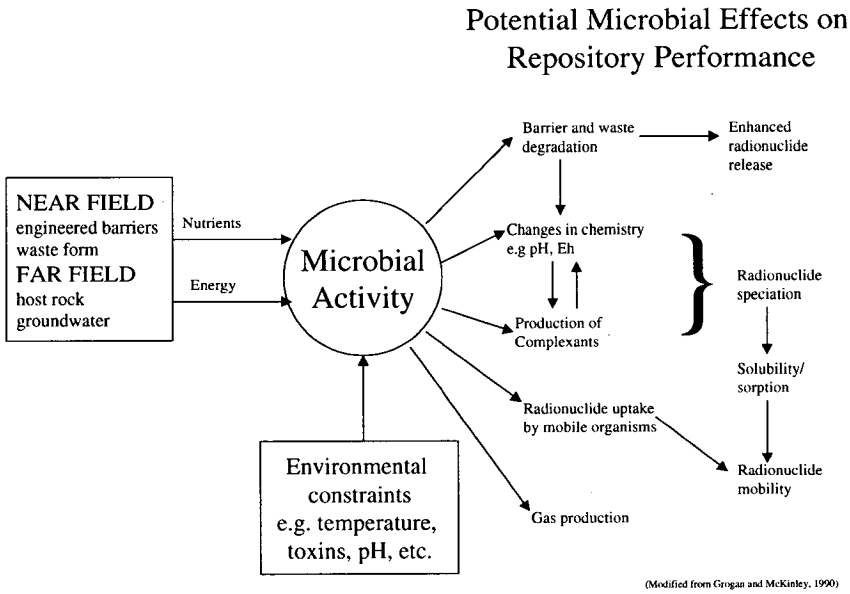

Figure 4. Simplified Flow Diagram of the Potential Effects of Microbial Activity on Repository Performance.

Figure 4 also depicts two major classifications of effects on the proposed repository due to the presence of microbial communities, that of impacts to EBS performance and effects on radionuclide transport. Because changes in aqueous chemistry, colloid generation and the production of complexants are integral to transport issues and in order to avoid duplicative discussion in this section, they will be discussed in Section 6.3.5 below.

6.3.4.1 Barrier and Waste Degradation

Perhaps the biggest impact to the proposed repository safety would be the premature degradation of the EBS. This event will cause the release of radionuclides into the transport environment at a much earlier time via degradation of the waste package/drip shield thus allowing entrance of drift seepage into the waste package, cladding, waste form, etc. As far as microbial communities are concerned, the direct way this would be accomplished is via MIC. However, there are other general impacts that would influence the in-drift geochemical environment and enhance the corrosion of metals, namely the changes to chemistry and the production of complexants. These areas are discussed in other sections of this report (see Section 6.3.5).

MIC generally manifests itself as localized corrosion via pitting on metal surfaces. This is usually a result of biofilm formation (see Section 6.3.1.14). Biofilms lead to the formation of electrochemical cells characterized by the physical separation of cathodic and anodic areas. This separation and the depletion of the cathodic reactant enhances the anodic dissolution of the area, promoting acidification as a result of the hydrolysis of the metal cations, increasing the concentration of the aggressive anions such as chloride, and fostering the oxidative dissolution of detrimental species from the metal (Geesey 1993). This in turn tends to increase the rate of anodic dissolution.

The localized environments in these areas are far more complex in the case of MIC than those present under abiotic conditions in crevices or beneath deposits. This complexity is the result of the multiple biochemical reactions associated with the generation of metabolic products through bacterial activities. With the possibility of MIC enhancing the degradation of all metals used in the construction of the repository drift and on the waste package and drip shield, MIC can influence the premature release of radionuclides from the repository. For a more detailed discussion of these processes, in both general and Yucca Mountain specific terms, the reader is referred to Geesey (1993) and Horn et al. (1998a and 1998b).

6.3.4.2 Gas Generation

Microbes do generate and consume various gases. All of these are found in the atmosphere and are members of the biogeochemical cycles of carbon, hydrogen, nitrogen, oxygen and sulfur (Bachofen 1991). The greatest potential for gas generation is the production of CO_2 via the aerobic respiration process. A bounding estimate for CO_2 gas generation is included in Section 6.6.5.4.

6.3.5 Potential Microbial Effects on Transport

Radionuclide transport is a performance issue that is continually being investigated. Thus, the effects of microbial populations are of concern to repository performance. Microbial processes affecting radionuclide transport are varied and significant (see Figure 5). The processes include,

but are not limited to, sorption/precipitation, complexation/ chelation, dissolution, oxidation/reduction reactions, and colloidal agglomeration. Additionally microorganisms create microenvironments of nutrient and chemical gradients that are capable of altering radionuclide solubilities. The basis for the majority of the information in this section was taken from Hersman (1997).

6.3.5.1 Microbial Sorption

Microorganisms can affect sorption/desorption reactions with the minerals on the surface of the matrix. Attached microbial populations occupy portions of the matrix surface area with cells and or exopolymers. Both have different sorption characteristics than the bare matrix. The outer cellular membranes of microbes have net negative charges and would tend to bind heavy metal cations. These cell walls have various surface functional groups such as carboxyl, phosphate and hydroxyl groups (Daughney et al. 1998, Fein et al. 1997). These are efficient metal building agents and are of importance in metal removal from solution (Hersman 1997). Therefore, with respect to sorption, microorganisms may decrease the amount of radionuclides in solution, thus reducing potential for transport as a dissolved species, yet increase potential for transport as a microbial colloid.

6.3.5.2 Complexation/Chelation

Microorganisms also perturb the geochemical speciation of metallic elements by releasing inorganic and organic chemicals into the surrounding extracellular environment (Stone 1997). These chemicals contain a variety of functional groups that complex strongly with metals. When a chemical attaches to a metal with two or more functional groups forming a ring structure, then this complexation is called chelation.

Two groups of microbial compound are considered complexing agents: by-products of microbial metabolism and degradation, and microbial exudates. The first group consists of simple organic compounds such as low molecular weight organic acids and alcohols and macromolecular humic and fulvic acids. The second group includes microbial exudates induced by metals ions. Iron-binding siderophores are produced in response to low iron concentrations and toxic-metal binding proteins.

6.3.5.2.1 By-products of Microbial Metabolism

Depending on the types of organic materials introduced into the repository drift and the environmental conditions there could be variable abundances of the small molecular weight complexing agents. Additionally, the large macromolecular humates are limited without the introduction of repository materials in the drift environment. The interactions with these materials can a) include altering adsorption, bioavailibility and toxicity, b) reduce Np(V), Pu(V), and Pu (VI), and solubilize ^{241}Am and Th (Hersman 1997).

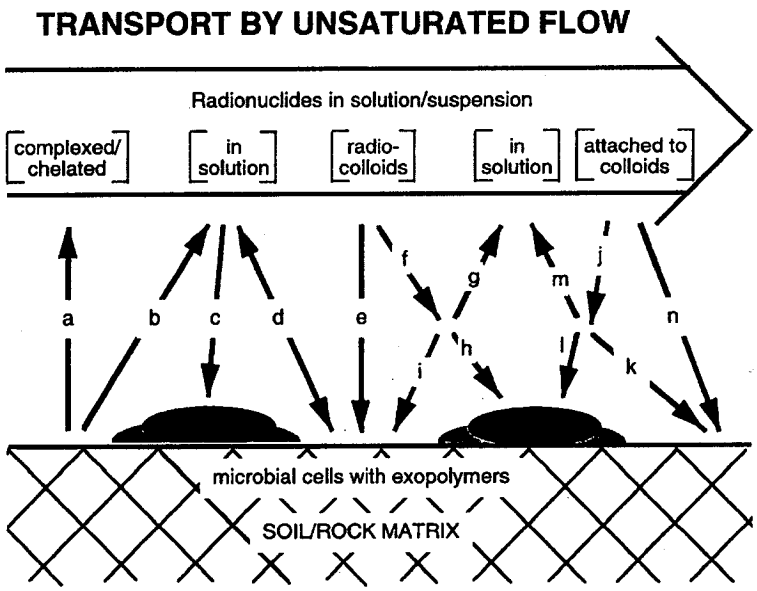

Note the following legend: (a) adsorbed radionuclides are complexed/chelated; (b) dissolution occurs; (c) radionuclides are sorbed by microorganisms; (d) various redox reactions result in solubilization or precipitation; (e and n) agglomeration of colloids; dissolution of (f) radiocolloids or (j) radionuclides attached to colloids, leading to (g and m) solubilization, (h and l) sorption, or (l and k) adsorption/precipitation. Figure taken from Hersman (1997).

Figure 5. Interactions Between Radionuclides in Solution/Suspension and Indigenous Microorganisms.

6.3.5.2.2 Microbial Exudates (Siderophores)

Microbes require Fe for DNA synthesis, electron transfer proteins, and nitrogen fixation. However, Fe suffers from extreme insolubility in aerobic environments at physiological pH. Aerobic and facultatively anaerobic microorganisms have developed a system where they can acquire Fe(III). This is done by the generation of siderophores. Siderophores are low molecular-mass, ferric-specific ligands that are induced at low iron concentration for the purpose of biological assimilation of Fe(III). The most common siderophores contain the hydroxamic acid functional group -R-CO-N(OH)-R', which forms a five membered chelate ring with Fe^{3+} (Hersman 1997). Because Fe(III) and Pu(IV) are similar in their charge/ionic radius ratio, Pu(IV) might serve as an analog to Fe(III) (Hersman et al. 1993). Complexation/chelation would increase the amount of radionuclides in solution, thus increasing their availability for transport.

6.3.5.3 Redox Reactions

The solubility of a radionuclide is generally related to its oxidation state. Therefore, if microorganisms affect the redox chemistry of radionuclides then they would also affect the solubility of radionuclides. The redox cycling of metals by microorganisms is the foundation of microbial growth as the redox cycles provide both nutrients and energy (see Sections 6.3.1.1, 6.3.1.2 and 6.3.1.10 above). Thus microorganisms are able both directly and indirectly to affect redox changes in metals. Direct effects are the oxidation of the metal as a source of energy and the use of a metal as a terminal electron acceptor, thus reducing the metal. The indirect effects

are the nonspecific oxidation of metals at the outer surface of the bacterial envelope and the reductions of secondary metals caused by the presence of a microbially reduced primary metal. Because the effect of redox on solubility varies with each radionuclide, the overall effect on total radionuclide solubility is unknown (Hersman 1997).

6.3.5.4 Biodegradation of Organic/Radionuclide Complexes

Hersman (1997) reports that complexed/chelated radionuclides may become subject to microbial degradation as the transport regime moves the complexed/chelated radionuclides into areas of the drift and unsaturated zone that have lower nutrient concentration. Low molecular weight organic acid, alcohols and siderophores could all serve as nutrients for indigenous microbial populations. The biodegradation could generally result in the precipitation of the released ion as water-insoluble hydroxide or salts and thus retard transport.

6.3.5.5 Dissolution

Due to similarities between Fe and Mn and radionuclides, evidence indicates that microorganisms will affect the dissolution rates of radionuclides (Hersman 1997). Microbially enhanced dissolution reactions will affect the stability of radionuclides in radiocolloids and radionuclides attached (either sorbed or precipitated) to natural colloidal particles, to the matrix surface, or to the surfaces of microorganisms. However, the overall results are difficult to predict (Hersman 1997). Radionuclides removed by dissolution would be available to be complexed or chelated by microbial metabolites, thus increasing the transport of radionuclides. However, radionuclides may precipitate onto surfaces or be reabsorbed. Also removal of the adsorbed/precipitated radionuclides from colloids or the dissolution of radionuclides, both of which have the potential to be mobile, can have a negative effect on transport rate.

6.3.5.6 Colloidal Agglomeration

In the presence of microorganisms colloidal movement through a rock matrix could be reduced because of an overall increase in the size of colloidal particle agglomerates (Hersman 1995). There are several general interactions between microorganisms and solid surfaces (including colloidal particles) and the affects of microbial adhesion on colloids. These interactions include attraction processes: adhesion, adsorption and flocculation.

6.3.5.6.1 Attraction of Bacteria to Solid Surfaces

Solid surfaces are potential sites for concentrating nutrients and for promoting microbial activity. Besides movement of water across a solid surface, there are many physico-chemical and biological attraction mechanisms at solid surfaces. These attraction mechanisms include chemotaxis, Brownian motion, electrostatic attraction, van der Waals interaction, electrical double layer effects, and cell surface hydrophobicity (for a more detailed discussion on these processes see Hersman 1995, page 2-4). Depending on the nature of the particulate matter, fabric organization, clay type, etc., the availability of the substrate may be either enhanced or reduced by the presence of particulates. If substrates were concentrated on the surface of clay minerals, this would enhance the colonization of microbes on those surfaces. These interactions can lead to the formation of multiple bacterial-colloidal particle agglomerates (Hersman 1997). In addition, Hersman (1995) indicates that clay colloids can be adsorbed onto the surfaces of microbes.

6.3.5.6.2 Adhesion

Adhesion of microorganisms is involved in fouling of man-made surfaces, in microbial influenced corrosion, and in syntrophic and other community interactions between microorganisms in natural habitats. Bacteria appear to adhere to surfaces by means of surface polymers, including cellular lipopolysaccharides, extracellular polymers and capsules, pili, fimbriae, and flagella. These materials are the same components that are used in biofilm production as described in Section 6.3.1.14. The composition and quantity of bacterial surface polymers vary considerably and are influenced by growth and environmental conditions (Hersman 1997).

6.3.5.6.3 Enhanced Flocculation

Hersman (1995) and Hersman (1997) discuss the processes that have been patented for the flocculation of clays. They include microbial polysaccharides and nucleoproteins. These processes have the potential to inhibit colloidal transport.

6.3.6 Conceptual Model Summary

In the repository environment, many different microbes could grow and provide a plethora of potential chemical processes that may affect the bulk chemistry within the emplacement drifts (Hardin 1998, Section 7). Large sources of potential nutrients for microbes are the materials used in the construction of the ground support. The waste-package materials represent reduced metals that can be oxidized to provide energy for microbes to thrive, and the waste forms themselves contain both nutrient and energy sources for microbes. This process conceptual model for microbial communities is meant to conceptualize the factors that limit the growth of microbes and to identify what are the potential chemical effects to the in-drift geochemical environment from the microbial community that would grow. Such growth would be a direct result of perturbing the ambient environment and adding potential nutrients (e.g., steel, concrete, and other repository materials) for bacterial catalysis and growth.

Microbes can thrive over a wide range of pH, under high hydrostatic pressures, in highly saline conditions, and in high radiation conditions that would normally be lethal to humans. Microbes live in nutrient starved environments and can be expected to continue to live even if the nutrient supply of introduced repository materials becomes exhausted. In these nutrient starved environments, some microbes even metabolize CO_2, N_2 and CH_4 directly from the gas phase via autotrophic behavior or methanogenic metabolic processes. Microbes will alter their environment by creating biofilms. Biofilms make it possible for anaerobic microbes to live in aerobic conditions by isolating them from the normal atmospheric conditions in which they would not survive. Biofilms also initiate pitting corrosion on metals via MIC. Therefore, all microbial influenced redox mineral transformations are possible in a Yucca Mountain repository. Microbes will adhere to mineral surfaces where they are able to utilize available nutrients and energy; otherwise, they can act as colloidal particles and move through the subsurface via advective-dispersive mechanisms.

Over time, the repository environment will have environmental conditions that will favor certain bacteria over others (i.e., thermophiles over mesophiles or acidophiles over neutrophiles).

However, with the exception of the period in time when the temperature of the repository is >120°C and the water activity is <0.90, microbes should be able to grow and produce their metabolic byproducts.

Microbes will either attach (accumulate) themselves to surfaces in the in-drift environment, thus affecting the chemical environment in the repository or they will be available to act as colloids, thus affecting radionuclide transport. Microbial processes affecting radionuclide transport are varied and significant. The processes include but are not limited to, sorption/precipitation, complexation/chelation, dissolution, oxidation/reduction reactions, and colloidal agglomeration. Additionally, microorganisms create microenvironments of nutrient and chemical gradients that are capable of altering radionuclide solubilities.

6.4 MING V1.0 SOFTWARE CODE

MING 1.0 [CSCI 30018 V1.0] has undergone a software verification and validation process (with the code having passed all its validation tests), as documented in CRWMS M&O (1998h), the finalized SQR (software qualification report, CSCI 30018 V1.0, 30018-2003). MING 1.0 is used in this report to evaluate potential impacts that the committed repository would have on microbial populations and their associated impacts to radionuclide release and facilitated transport. The MING code as discussed in Section 6.4.1 and 6.4.2 below, is based on the Swiss and Canadian models for estimating microbial production in potential repositories in the saturated-zone (McKinley et al., 1997; Stroes-Gascoyne, 1989; West et. al., 1989; Capon and Grogan, 1991; and Grogan and McKinley 1990).

The Swiss and Canadian models were enhanced for Yucca Mountain site-specific conditions (unsaturated zone, thermal perturbation, and specific design materials) and implemented in the MING code. Thus, MING accounts for growth thresholds based on (a) temperature (<120°C) and water activity (via relative humidity, where a_w=[RH/100] > 0.90), (b) flux of gas-phase constituents, (c) pH- and temperature-dependent redox couples, and (d) design-specific materials descriptions and degradation rates as discussed in Section 6.4.1 and 6.4.2 below.

MING uses the supply of constituents from design materials and constituent fluxes into the drift to perform two separate mass-balance calculations as a function of time. The first (nutrient limit) assesses the available nutrients (C, N, P and S) and calculates how many microbes can be produced based on a microbe stoichiometry of $C_{160}(H_{280}O_{80})N_{30}P_2S$. The second (energy limit) calculates the energy available from optimally combined redox couples (see Table 18 in Section 6.4.3.1 below for half reactions considered), for the temperature, and pH at that time. This optimization maximizes those reactions that produce >15kJ/mol (limit on useable energy, McKinley et al. 1997) using an iterative linear optimization technique. The final available energy value is converted to microbial mass at a rate of 1 kg of biomass for every 64 MJ of energy (Grogan and McKinley, 1990). These two values (nutrient limit and energy limit) are then compared and the smaller value represents the number of microbes that can be produced for that time. This code and the associated conceptual model for microbial activity (see Section 6.3) does not attempt to quantify the effects of individual microbial colonies or biofilms that may be present on repository materials, but attempts to quantify the overall global bulk effect of microbes on the in-drift geochemical environment (IDGE).

6.4.1 Code Development Concepts

The purpose for developing MING was to provide a tool to implement the applicable concepts in Section 6.3 to assess the microbial growth in a potential drift and the potential for microbial effects to bulk water compositions. MING can also provide a basis for discussing the other potential IDGE chemistry effects for the needs of performance assessment, given that microbial activity will occur in the proposed repository. The magnitude of such activity needs to be quantitatively analyzed. Three basic approaches are possible and have been previously documented in McKinley and Grogan (1991). They are as follows:

- Mass balance approach–the biomass will inherently be limited by the inventory and/or supply rate of some essential element (e.g., C, N, P, and S) which may represent a very significant constraint. If the biomass is very low, it may be possible to justify neglecting microbial processes in comparison with competing purely inorganic reactions.

- Thermodynamic approach–in addition to nutrients, constraints set by the available energy sources can be evaluated.

- Kinetic approach–the evolution of a population of organisms in a particular evolving chemical system is explicitly modeled using either empirical or mechanistically derived kinetic data.

The kinetic approach is mathematically possible and in fact, other near field geochemical model computer codes (EQ3/6, Wolery 1992; AREST-CT, Chen et al. 1995), used in PA analyses could potentially be modified and used to simulate the kinetic approach. However, it is not possible to obtain the required information about all the relevant microbial processes at the resolution that is required to interface directly with these codes at this point in time. Thus, we chose to use the more simplistic approaches, similar to those used by the Canadian High-Level Waste Repository program (Stroes-Gascoyne 1989) and the Swiss Low/Intermediate-Level Waste Repository program (Capon and Grogan 1991; McKinley and Grogan 1991; McKinley et al. 1997; and West et al. 1989, a natural analog study for the Swiss program) which use both mass balance and thermodynamics to quantify the impacts of microbial populations. Subsequently, these two approaches are used as the basis for the development of MING. In the first aspect of this, abiotic processes are used to determine the rate at which nutrients become available to microorganisms, which is used as the rate that the microorganisms convert those nutrients to the products (i.e., instantaneously in this mass balance approach). The second uses limiting guidelines of energy availability and the availability of all the required nutrients in the proper ratio to get the rate at which this occurs (thermodynamics approach).

Different design options can be examined by assessing various cases in which all of the available nutrients (derived from WP materials, ground support materials, gas flux, water flux, etc.) are converted into the appropriate products. All of the possible combinations of these parameter values will be used as input into MING in order to conduct sensitivity analyses of the various repository design options, temperatures, relative humidities, gas fluxes, and water chemistries, etc., that are derived from other TSPA and process level modeling efforts. The objective is to be as transparent (i.e. to integrate inputs and output so that all PA calculations and models are

consistent) as possible considering the multiple time dependent inputs. However, obtaining degradation rates of all the introduced materials in the near field (e.g. concrete, steel, polymers, etc.) is not a realistic goal at this time.

6.4.2 Software Development

The starting point for the MING software model development was based on documentation for the software routine titled Estimation of Maximum Microbiological Activity, also known as EMMA (Capon and Grogan 1991), and is also based on the documented approach to modeling the Swiss Low/Intermediate Level Waste Repository found in Grogan and McKinley (1990) and McKinley and Grogan (1991). MING contains the same basic modeling approach and structure of calculating the nutrient and energy limitations described in Grogan and McKinley (1990) and McKinley and Grogan (1991).

Early on, it was determined that EMMA would not be able to serve as the vehicle to do the calculations without some major modifications. Many of the concepts to which modifications to EMMA were derived are documented in the Near-Field Geochemical Environment Abstraction/Testing Workshop Results (CRWMS M&O 1997a). However, as programming developed, other requirements were added and the original concept was refined.

Essentially, there are two main components that were brought forward into MING from the Swiss modeling approach: (a) the numerical solution for the amount of energy available for microbial growth; and (b) the general method for calculating nutrient availability. However, smaller pieces of the approach were also maintained and used in MING (see Table 17 below) including the average empirical microbial formula [$C_{160}(H_{280}O_{80})N_{30}P_2S$] with a dry weight of 3998.1 g mol^{-1} (McKinley et al. 1997). This formula represents the ratio of elements needed to form a microbe (e.g., 160 carbon atoms for every sulfur atom). In addition, the implementation in MING also uses an average microbial water content of 99 percent and an average microbial volume of 1.5×10^{-13} ml (McKinley et al. 1997). Multiplying this latter value by the density of water (1 g/cm^3, Weast 1979) produces an average microbe mass of 1.5×10^{-13} g (see Attachment I).

Like the EMMA code, MING utilizes the same basic approach to thermodynamic modeling, where microbes use redox couples in order to supply the energy required to carry out their basic metabolic functions (i.e., aerobic respiration, nitrification and denitrification, methane oxidation, etc.). Because microbes tend to utilize specific, well-documented metabolic pathways (Amy and Haldeman 1997; Banfield and Nealson 1997; Pedersen and Karlsson 1995), a list of appropriate redox half reactions was derived (see Table 9, Section 6.3.1.1) based on the available nutrients in the system that will maximize energy production. MING uses the same values used by EMMA on the limits of usable energy available from a given full redox reaction, where 15 kJ per mole of electrons transferred is the lower limit of energy needed to create biomass (i.e. only those full reactions that produce >15kJ/mol are considered). The final available energy value is converted to microbial mass at a rate of 1 kg of biomass for every 64 MJ of energy limit on useable energy (Grogan and McKinley 1990, Appendix 3, p. AIII-1).

Table 17. Accepted Mass Balance Modeling Parameters used as Conversion Factors.

Parameter	Value
Microbial Composition	$C_{160}(H_{280}O_{80})N_{30}P_2S$
Average Water Content	99% by weight
Average Microbial Volume	1.5×10^{-13} ml

MO9909SPAMICRO.001

The EMMA model is based on a simplified thermodynamic system where the pH is fixed at 12; the temperature in the repository is set to 25° C; and the Gibbs free energies (ΔG) used to calculate the available energy for microbial production were fixed at standard temperature (25° C) and pressure (1 atmosphere). For example, any redox reaction can be written in the general form

$$A + ae^- + bH^+ = cB + dH_2O \qquad \text{(Eq. 3)}$$

for which a standard free energy of reaction ($\Delta G_r°$) can be specified. The $\Delta G_r°$ can be derived from standard free energies of formation ($\Delta G_f°$):

$$\Delta G_r^\circ = \sum \Delta G_f^\circ (\text{products}) - \sum \Delta G_f^\circ (\text{reactants}) \qquad \text{(Eq. 4)}$$

or from an equilibrium constant (K):

$$\Delta G_r^\circ = -RT \ln K \qquad \text{(Eq. 5)}$$

where R stands for the gas constant and T represents the absolute temperature. The calculations are made by combining independent half reactions and calculating the overall $\Delta G_r°$ for the reaction.

EMMA's simplified model is certainly not realistic in the sense that the repository environment will undergo temperature changes due to the hot WPs. For MING, in order to account for a chemically variable system, the time dependent temperatures, gas fluxes, and water chemistries need to be accounted for over the time frame of the calculations. With the incorporation of these variables, the calculations should end up being as transparent as possible with other calculations being derived from other TSPA abstractions.

6.4.3 Site-Specific Additions to the Software

Some of the features built into MING that extend its capabilities beyond those of EMMA are as follows:

- The addition of temperature dependencies on the ΔG calculations

- The stipulation that nutrient dependencies are calculated from the time dependent gas flux into the repository drift (to address autotrophic and aerobic behavior) as well as the presence of other repository materials

- The addition of time dependent water chemistries entering the drift

- The addition of pH dependence on the governing redox equations (EMMA used a single fixed pH value of 12 for all calculations)

- The ability to degrade one repository material before another becomes available (such is the case with a layered WP design where the CAM degrades well before the CRM)

- The addition of physical limitations to microbial growth as a result of temperature and RH

6.4.3.1 Corrections to ΔG_r° for pH and Temperature

It is important to note that within MING, only the standard-state free energies are used and these are not corrected for either Eh or the activity of dissolved species to derive the actual nonstandard-state free energies. By not calculating the nonstandard-state free energies, the calculation of available energy is not precise, but only represents a rough estimate of this value. Because the half-reactions are written as simple reduction reactions, the free energy of a full reaction constraint applies slightly more generally than purely standard-state conditions. It is actually constrained such that the ion activity ratios of the redox pairs are at isoactivities, which could be possible for ion activities different than unity (the standard-state conditions). For each full reaction, correcting for the actual pH brings the free energies of reaction further from the standard state values. However, using this simplified model should allow increased understanding of the complexity of the microbiological system and provide a mechanism to understand the bulk system at an approximate (order-of-magnitude) level.

Within a biofilm or an individual microbe, the pH (and speciation) can certainly be completely different than the bulk chemistry imposed by the in-drift or near-field environment. However, the bulk chemistry is the major influence on the types of nutrients and energy that can be provided for a given microbe or biofilm. Microenvironments do exist, however this model can not analyze those localized conditions. In order to gain the detail needed to correct ΔG_r° for the activity of dissolved species in the fluids and analyze microscale processes, a much greater effort must be made than is possible at this time. Only the first step in this process has currently been completed, which is to correct for the actual pH of the bulk system. To truly incorporate the localized system water chemistry effects, the effort would require iterative solution of changes to the activities of dissolved species for localized microbial processes. This iterative effort can be done, but would involve an enormous effort to collect the dissolved species data for the calculations

Because the temperature of the repository will not be fixed over time, a method to incorporate temperature effect on reaction free energies was derived in order to build into the MING results the transparency required to incorporate the thermohydrologic temperature histories provided from other modeling efforts (e.g., see Figure 6 below).

Regression analyses were performed on ΔG_r° values at various temperatures (0°, 25°, 50°, 60°, 75°, 100°, 125°, and 150°C) for a selected group of half reactions to define temperature dependent curves that could be incorporated into the energy calculations. The regression analyses are documented in CRWMS M&O (1998f) with the results shown on Table 18 below. The derived regression variables are used to calculate the temperature dependent ΔG_r° that is used in the derivation of the available energy for a given reaction. The temperature dependent regression variables are used in MING in the following way:

$$\Delta G_{r\,(\text{temp})}^{\circ} = B_0 + B_1 T + B_2 T^2 \qquad \text{(Eq. 6)}$$

where B_0, B_1 and B_2 are the second order regression coefficients. Thus, both the effects of variable pH and temperature (°C) are accounted for in the calculations.

6.4.3.2 Nutrient Supply

As documented in the microbial modeling approach for the Swiss Low/Intermediate-Level Repository (Grogan and McKinley 1990), MING only considers the major elements essential for cell growth (C, N, S, and P). Other nutrients will be considered freely available (i.e., Na, K, Ca, and Cl) except for water.

The mass balance calculations conducted in MING consider three sources of nutrient supply: first, the time dependent flux of groundwater into the repository; second, the degradation of repository materials including the multilayered effects of WPs (see Section 6.3.3.1 for a description of materials considered), and third, the time-dependent flux of gases (CO_2, N_2, O_2, and perhaps CH_4) into the repository. The nutrient limits will be calculated by determining the appropriate ratio (relative molar concentration) of material (determined by available nutrient flux) needed to create the typical organism having a stoichiometry of $C_{160}(H_{280}O_{80})N_{30}P_2S$.

6.4.3.3 Temperature and RH Effects on Microbial Growth

The availability of water for microbial growth in the UZ at Yucca Mountain will be dependent on the thermohydrological conditions within the repository. In order to account for periods where there is not enough moisture to allow microbial growth (a_w <0.90, see Section 6.3.3.2.2) the relationship between RH and a_w, is assumed (see Equation 2, Section 6.3.3.2.2, and assumption 5.1) and used to allow for the unsaturated conditions in the repository.

Temperature will also affect the ability of a microbe to reproduce. The temperature dependency of microbial activity is set by the temperature within the repository environment where microbes are not allowed to reproduce and grow above temperatures of 120°C.

6.4.4 Other Code Features

MING is designed to consider all of the committed (not intended to be removed before permanent closure) materials that are included in the current repository and WP designs, as well as the potential to evaluate any alternate design options that are relevant to microbial behavior. Section 6.3.3.1 above lists the various design materials, quantities, and compositions that are to be emplaced in the repository and are evaluated herein. For example, in MING, a committed

material (e.g., steel sets, drip shield, etc.) is broken down into its individual chemical composition and allowed to enter the nutrients available in a time step based on a fractional corrosion rate (1/estimated material lifetime) for that given material.

In calculating nutrient availability, MING also will allow a sequential introduction of committed materials. This means that a sequential layered model of the WP can be defined, where the CRM and other internal WP materials are not allowed to mutually degrade and be released into the nutrient stream until the drip shield is completely used up.

Another tool that MING can utilize is a "special reactant" flag where the intermediate breakdown products (other than the basic chemical composition) can be identified. Potential items that fall into this area are substances such as organic admixtures, which are common components of cement mixtures and tend to be resistant to biodegradation. These items can then have their releasable compositional quantities split among the several associated species that are included in the redox model.

MING is also designed to incorporate variable gas flux calculations and incoming water chemistries and provide these inputs to both the nutrient and energy calculations.

6.4.4.1 MING Parameter Inputs

The use and format of the MING input needs are documented with in the MING V.1.0 code and associated users manual (CSCI 30018 V1.0, CRWMS M&O 1998d) Any case specific inputs will be documented in Section 6.5 for each modeling case presented. However, four general types of inputs are needed for a MING model run. They are as follows:

6.4.4.1.1 Fixed Inputs

The most important of these is the redox reaction table and the associated temperature-dependent coefficients for each selected half reaction (see Table 18). Also included is Table 19 below, which is needed in the code to do various calculations but remains a fixed value.

Table 18 represents the redox half reactions and associated temperature dependant coefficients as described above that have been selected to represent generalized microbial catalysis reactions. They include selected half reactions that cover the following known microbial metabolic pathways: aerobic respiration, nitrification and denitrification, methane oxidation, manganese and iron oxidation, sulfur oxidation, manganese and iron reduction, sulfate reduction, and methanogenesis. The thermodynamic data used to derive this table are documented in CRWMS M&O (1998f).

6.4.4.1.2 Environmental Inputs

These include time-dependent temperature and RH values, time-dependent water chemistries (includes pH and infiltration rates) and time-dependent gas fluxes (includes CO_2, O_2, and N_2). These results are provided from other modeling efforts (TH calculations, NFGE THC incoming water, IDGE in-drift gas, seepage flux into the drift).

6.4.4.1.3 Design materials

These inputs include the proper formatting and documenting of quantities and elemental compositions of all the repository and WP design materials that may be placed into the repository. This also includes designation of expected material lifetimes and the designation of breakdown codes and specifying of material reactants necessary for utilization of the redox half reactions that are used to calculate the model energetics.

Table 18. Temperature Dependant ΔG Relationships for Selected Redox Half Reactions used in MING V1.0 (CRWMS M&O 1998f).

Redox half reaction		$\Delta Gr°$ (cal/mol) vs. T(°C)				$\Delta Gr°$ (kJ/mol) vs. T(°C)		
Carbon	RXN #	B0	B1	B2	r^2	B0	B1	B2
CO2 + H+ + 2e- = HCOO-	C1	9688.3396	27.9163	0.02913	0.9999	40.5554	0.1169	0.0001
CO2 + 4H+ + 4e- = CH2O + H2O	C2	18992.513	-5.888	-0.0623	0.9999	79.5027	-0.0246	-0.0003
CO2 + 6H+ + 6e- = CH3OH + H2O	C3	-4582.1156	5.4553	-0.0696	0.9996	-19.1807	0.0228	-0.0003
HCOO- + 3H+ + 2e- = CH2O + H2O	C4	-8475.1508	-7.7987	-0.0291	0.9999	-35.4770	-0.0326	-0.0001
CO2 + 8H+ + 8e- = CH4 + 2H2O	C5	-27359.7546	2.1845	-0.1187	0.9995	-114.5279	0.0091	-0.0005
CH2O + 2H+ + 2e- = CH3OH	C6	152221.87	-63.2114	-0.0798	0.9969	637.2007	-0.2646	-0.0003
HCOO- + 7H+ + 6e- = CH4 + 2H2O	C7	-37048.093	-25.7317	-0.1478	0.9998	-155.0833	-0.1077	-0.0006
CH2O + 4H+ + 4e- = CH4 + H2O	C8	126179.023	-100.3702	-7.35E-03	0.9988	528.1854	-0.4201	0.0000
CH3OH + 2H+ + 2e- = CH4 + H2O	C9	-22777.761	-3.2642	-0.0491	0.9998	-95.3477	-0.0137	-0.0002
CO32- + 10H+ + 8e- = CH4 + 3H2O	C10	-53532.1136	-95.1347	-0.1906	0.9999	-224.0854	-0.3982	-0.0008
CO32- + 6H+ + 4e- = CH2O + 2H2O	C11	-21683.8211	-50.6762	-0.1471	0.9999	-90.7685	-0.2121	-0.0006
CO32- + 8H+ + 6e- = CH3OH + 2H2O	C12	197588.961	-0.6827	-0.1204	0.9986	827.1074	-0.0029	-0.0005
CO32- + 3H+ + 2e- = HCOO- + H2O	C13	-13213.1388	-43.613	-0.10746	0.9999	-55.3102	-0.1826	-0.0004
Nitrogen								
N2 + 6H+ + 6e- = 2NH3	N1	-16395.0184	-28.7196	9.55E-03	0.9998	-68.6295	-0.1202	0.0000
N2 + 8H+ + 6e- = 2NH4+	N2	-41509.2762	-32.7202	0.0324	0.9996	-173.7578	-0.1370	0.0001
NO2- + 7H+ + 6e- = NH3 + 2H2O	N3	-111389.762	-24.6314	-0.1072	0.9999	-466.2775	-0.1031	-0.0004
NO3- + 2H+ + 2e- = NO2- + H2O	N4	-37615.91	-10.1959	-0.0169	0.9999	-157.4602	-0.0427	-0.0001
NO3- + 10H+ + 8e- = NH4+ + 3H2O	N5	-161590.028	-35.9487	-0.1181	0.9999	-676.4159	-0.1505	-0.0005
NO2- + 8H+ + 6e- = NH4+ + 2H2O	N6	-123974.113	-25.7531	-0.1011	0.9999	-518.9556	-0.1078	-0.0004
NO3- 6H+ + 5e- = 0.5N2 + 3H2O	N7	-140816.478	-20.2528	-0.1301	0.9999	-589.4578	-0.0848	-0.0005
2NO2- + 8H+ + 6e- = N2 + 4H2O	N8	-206401.155	-20.1139	-0.2264	0.9998	-863.9952	-0.0842	-0.0009
NO3- + 9H+ + 8e- = NH3 + 3H2O	N9	-149007.022	-35.1673	-0.1199	0.9999	-623.7434	-0.1472	-0.0005
Oxygen								
O2 + 4H+ + 4e- = 2H2O	O1	-113792.702	17.5605	-0.0416	0.9999	-476.3363	0.0735	-0.0002
Sulfur								
S + H+ + 2e- = HS-	S1	3107.4736	-10.5365	0.03688	0.9999	13.0079	-0.0441	0.0002
S + 2H+ +2e- = H2S	S2	-127020.088	-2.6852	-0.1192	0.9998	-531.7061	-0.0112	-0.0005
SO4-2 + 9H+ + 8e- = HS- + 4H2O	S3	-44105.4889	-71.3428	-0.1525	0.9999	-184.6256	-0.2986	-0.0006
SO4-2 + 10H+ + 8e- = H2S + 4H2O	S4	-53361.3532	-80.989	-0.2362	0.9999	-223.3706	-0.3390	-0.0010
HSO4- + 7H+ + 6e- = S + 4H2O	S5	-45083.4335	-38.7462	-0.1117	0.9999	-188.7193	-0.1622	-0.0005
SO4-2 + 8H+ + 6e- = S + 4H2O	S6	-47183.5454	-60.636	-0.1924	0.9999	-197.5103	-0.2538	-0.0008
SO2 + 4e- + 4H+ = S + 2H2O	S7	-41304.2847	-3.7158	0.0072	0.9991	-172.8997	-0.0156	0.0000
SO32- + 7H+ + 6e- = HS- + 3H2O	S8	-49176.8092	-66.8302	-0.1392	0.9999	-205.8541	-0.2798	-0.0006
2SO4-2 + 10H+ + 8e- = S2O3-2 + 5H2O	S9	-50416.0002	-79.053	-0.2149	0.9999	-211.0414	-0.3309	-0.0009
Hydrogen								
H+ + e- = 0.5H2	H1	387.1731	-15.3815	-4.99E-03	0.9999	1.6207	-0.0644	0.0000
Iron								
Fe2O3 + 6H+ + 6e- = 2Fe + 3H2O	F1	9142.5147	-41.3104	-0.0465	0.9999	38.2706	-0.1729	-0.0002
Fe2+ + 2e- = Fe	F2	22648.6398	-30.7865	-0.0188	0.9999	94.8072	-0.1289	-0.0001
Fe3+ + e- = Fe2+	F3	-16752.7104	-39.2684	-0.0344	0.9999	-70.1268	-0.1644	-0.0001
Fe3O4 + 8H+ + 8e- = 3Fe + 4H2O	F4	17107.4431	-50.4332	-0.0608	0.9999	71.6118	-0.2111	-0.0003
FeOOH + 3H+ + e- = Fe2+ + 2H2O	F5	-14875.6231	-86.2999	-0.0302	0.9999	-62.2694	-0.3613	-0.0001
Manganese								
MnO2 + 4H+ + 2e- = Mn2+ + 2H2O	M1	-58994.1105	64.9218	-0.2417	0.9168	-246.9493	0.2718	-0.0010
Mn3O4 + 8H+ + 2e- = 3Mn2+ + 4H2O	M2	-29541.3246	-7.0738	4.8045	0.9807	-123.6600	-0.0296	0.0201

DTN: MO9909SPAMING1.003

6.4.4.1.4 Model Specific Inputs

These include the following single-value items that are required to implement the conceptual model: temperature cutoff, humidity cutoff, tunnel diameter, tunnel length, porosity, and the energy cutoff.

6.4.4.2 Model Output

Output from MING is designed to define only the bulk system redox chemistry of the near-field system given the variable temperature and pH of the system, it does not reflect the actual chemical speciation or reactions that might occur at a more localized scale. The chemical output is designed to capture molar quantities of the production of byproducts (such as CO_2, H_2S, and H^+ ions) over one linear meter of repository drift. Output is also designed to enable the evaluation of the quantities of microbes produced, the limits to microbial growth from both nutrients and energy, and the stipulation of which nutrient is limiting growth in the repository.

MING V1.0 produces several output tables. The descriptions of these files are found in Section 1.4 of the MING V1.0 users manual (CRWMS M&O 1998d; pp. 36-40). The most used of these files are the "Time Output", "Reactions for Plot" and "Limiting Nutrients Tables". The time output table records a) the output year, b) the number of microbes that could be produced in the output year based on the available nutrient mass balance calculation, c) the total amount of free energy available in that year to create microbes, d) the number of microbes that could be produced in that year based on the available energy, and e) the actual number of microbes that are actually produced based on the lower value of items b and d above. For example, each test case reported in Table 81 (Section 6.7.2.2.1 below) is typical of any given year's output.

The reactions for plot table records the reactions that were used in each energy calculation, the ΔG that the particular reaction contributes to the total energy available, the pH of the incoming water, and the temperature at that timestep. Note: although the reactions are balanced, the code does not divide through the reaction to determine the smallest possible stoichiometric coefficients for each of the chemical species before generating the table.

Often, the terms "energy limited" or "nutrient limited" will be used to describe the conditions that limit microbial growth. Energy limited indicates that although there are sufficient nutrients available for growth, the redox conditions within the calculation constrain the amount of microbial growth that can happen. On the other hand, when something is termed nutrient limited, it means that there are not enough nutrients available to produce further microbial growth.

The limiting nutrients output table contains the starting and ending year in which a given nutrient (i.e. carbon, phosphorous, sulfur or nitrogen) is (or could limit if the results indicate that it is energy limiting) limiting microbial growth. In addition, the table may report whether the calculations are being limited by the RH dropping below or the temperature surpassing the thresholds for microbial activity of either RH = 90 or temperature = 120°C. These results may be reported either as a tabular result or in the written text depending on the complexity of the calculation. For most results presented below, the results are not reported in tabular form but can be verified by looking at the output table of interest.

Table 19 Atomic Masses for Each Element (Sargent-Welch 1979).

Element	Atomic Mass	Element	Atomic Mass	Element	Atomic Mass	Element	Atomic Mass	Element	Atomic Mass
Ar	40	Co	59	In	115	Pa	231	Sr	88
Ac	227	Cr	52	Ir	192	Pb	207	Ta	181
Ag	108	Cs	133	K	39	Pd	106	Tb	159
Al	27	Cu	64	Kr	84	Pm	145	Tc	98
Am	243	Dy	163	La	139	Po	209	Te	128
As	75	Es	252	Li	7	Pr	141	Th	232
At	210	Er	167	Lu	175	Pt	195	Ti	48
Au	197	Eu	152	Mg	24	Pu	244	Tl	204
B	11	F	19	Mn	55	Ra	226	Tm	169
Ba	137	Fe	56	Mo	96	Rb	85	U	238
Be	9	Fm	257	Md	258	Re	186	V	51
Bi	209	Fr	223	N	14	Rh	103	W	184
Bk	247	Ga	70	Na	23	Rn	222	Xe	131
Br	80	Gd	157	Nb	93	Ru	101	Y	89
C	12	Ge	73	Nd	144	S	32	Yb	173
Ca	40	H	1	Ne	20	Sb	122	Zn	65
Cd	112	He	4	Ni	59	Sc	45	Zr	91
Ce	140	Hf	178	Np	237	Se	79		
Cf	251	Hg	201	O	16	Si	28		
Cl	35	Ho	165	Os	190	Sm	150		
Cm	247	I	127	P	31	Sn	119		

6.5 MODEL INPUTS

The model inputs below were selected to account for both the no backfill design and the option to run sensitivity studies with a backfill option. In the cases below both backfill and no backfill results are shown so that the conservative bounding cases could be selected for input into other modeling activities. The cases below indicate that the greatest microbial mass is produced by using the backfill option and definitely bound the no backfill results.

6.5.1 Environmental Inputs

6.5.1.1 Percolation Flux into the Drift

MING requires as input the flux of water entering the drift. Figure 8 represents the percolation flux at the crown of the drift for both major waste package types for the backfill design. The backfill design results in higher percolation flux at the drift wall. This is because no backfill cases result in higher drift wall temperatures and lower RHs as shown *in Thermal Hydrology*

EBS Design Sensitivity Analyses (CRWMS M&O 2000q, Section 5.6). Therefore the bounding percolation flux that will allow microbial growth to be possible at an earlier timeframe is associated with the cooler temperatures from the backfill design. Therefore, the percolation flux shown on Figure 8 above generated for the backfill case can also be used to bound the no backfill case.

For the backfill sensitivity cases, ideally we would use the seepage into the drift combined with the integrated liquid flux into the drift due to the wicking due to backfill. This latter piece would be taken from the TH process model calculations that were abstracted in CRWMS M&O (2000c). Two problems inhibit the use of this approach. First, the actual seepage flux is not calculated until the percolation fluxes for all 600 locations are provided within the TSPA. Second, the integrated liquid flux into the drift from wicking is not actually output from the TH process model (CRWMS M&O 2000o).

In order to develop a reasonably bounding estimate for the backfill design option to replace the actual modeled values, the following bounding arguments apply.

(i) The integrated liquid flux into the drift from wicking is ubiquitous for all packages and much larger than the spatially uncommon seepage flux and we can therefore ignore the flux calculated directly with the Seepage model (CRWMS M&O 2000a).

(ii) The integrated liquid flux into the drift from wicking can be approximated by using some multiplier on the percolation fluxes that are provided in the TH abstraction model calculations (see Figure 8 below).

(iii) Given that the backfill interfaces essentially with the two drift side walls, and most of the percolation flux at the crown would either seep into the drift or be diverted along one of the two sides of the drift, the most percolation flux that could be brought into the drift through wicking would be three "sides" of the drift each seeing at most the percolation flux. This ignores the wicking at the base of the drift, but this can be shown to be small compared to the sides just using the model outputs of the TH process model work (CRWMS M&O 2000o).

Therefore, the results shown on Figure 8 below will be used directly for the no backfill cases and will be multiplied by three to produce the percolation flux curves that are used in the MING V1.0 inputs for the backfill sensitivity cases.

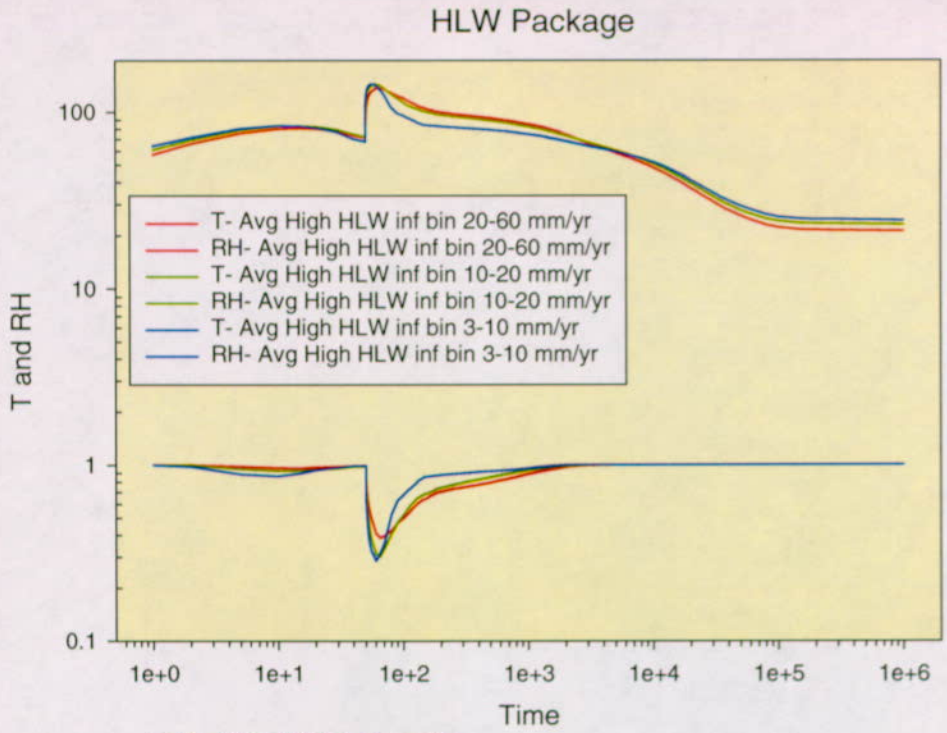

Figure 6. Average High Infiltration Temperature and RH Curves for HLW Packages from the TH Abstraction.

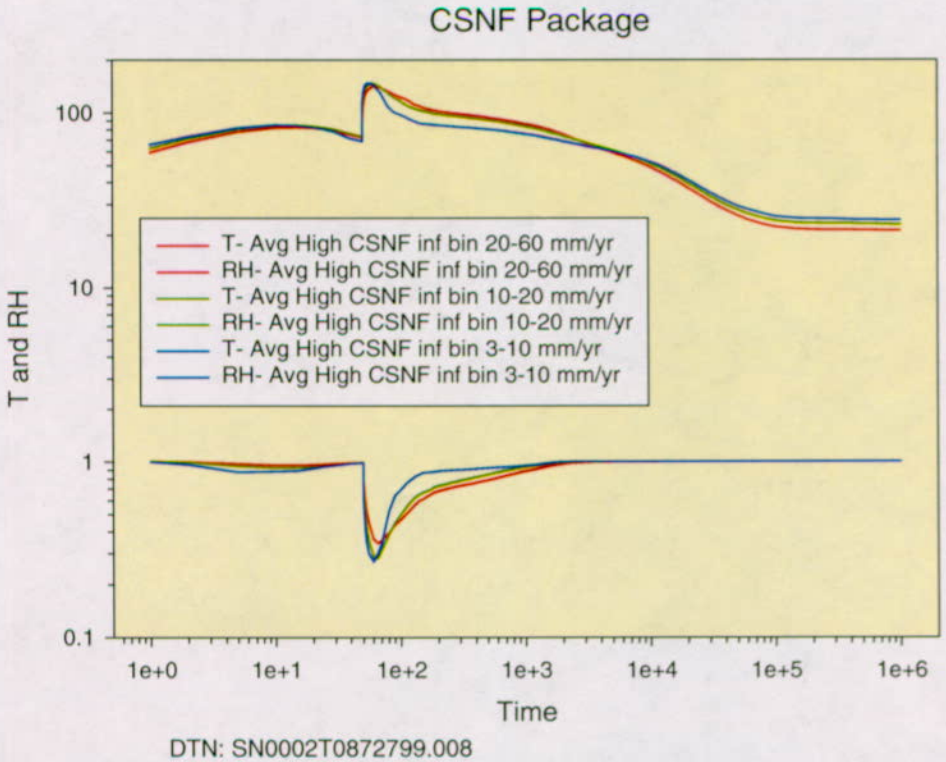

Figure 7. Average High Infiltration Temperature and RH Curves for CSNF Packages from the TH Abstraction.

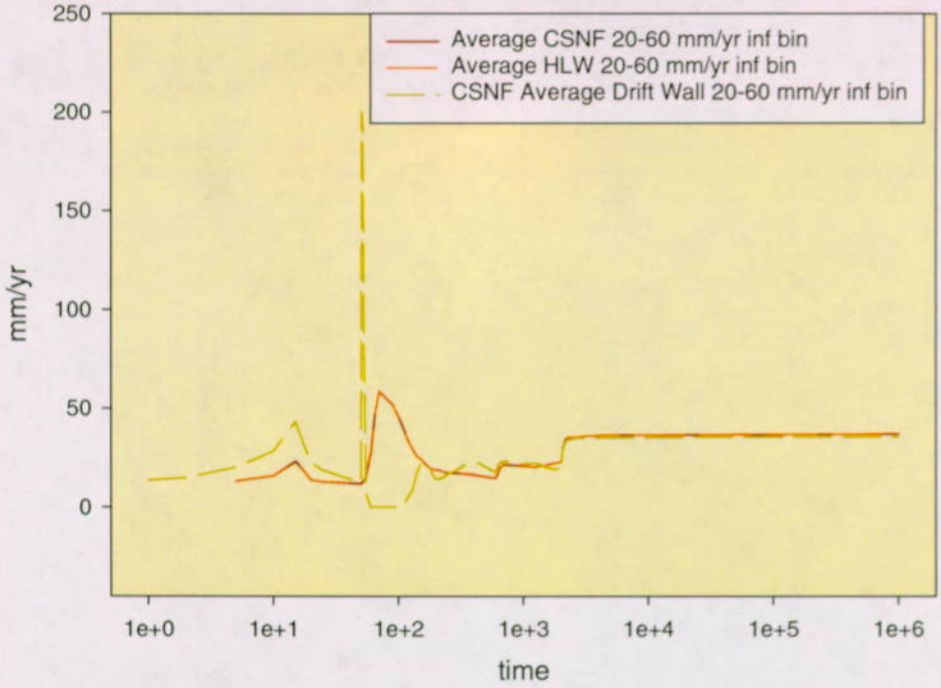

DTN: SN0001T0872799.006

Figure 8. Average Percolation Flux Under High Infiltration
(at 5 Meters from Drift Crown and at the Drift Wall)

6.5.1.2 Thermohydrology

MING requires input for combined temperature, and RH values for the drift wall (or another relevant location in the drift) that correspond to the selected infiltration rate and/or seepage into the drift through time. In order to be conservative and bounding, the T and RH curves provided in DTN: SN0002T0872799.008 were compared and the values that will allow for more microbial growth during the thermal phase were selected for use in MING V1.0. Based on that criterion, the cases that would be most conservative would be the values that would provide shortest duration of temperatures above the threshold of 120°C and the shortest duration of low RH for both CSNF and HLW cases. These values are associated with the infiltration bin (inf bin) data having average infiltration rates between 3-10 mm/yr for both the HLW and the CSNF packages (see High CSNF and HLW inf bin 3-10 mm/yr curves shown on Figures 6 and 7 above).

In the cases of the backfill and no backfill design options, the values for High CSNF and HLW inf bin 3-10 mm/yr curves shown on Figures 6 and 7 above would be the most conservative to use. This is because no backfill cases result in higher drift wall temperatures and lower RHs as shown *in Thermal Hydrology EBS Design Sensitivity Analyses* (CRWMS M&O 2000q, Section 5.6). Higher temperatures and lower RHs would thus be prevalent over longer periods in the drift. The cooler temperatures from the backfill design will allow microbial growth to be possible at an earlier timeframe. Therefore, the T and RHs from the DTN above generated for the backfill case will also be used in the no backfill case.

6.5.1.3 Incoming Water Compositions

Because MING requires water compositions entering the drift having units of kmol/m^3, the following values were abstracted and produced for PA calculations (see Table 20). These values represent the current abstraction of the thermal hydrological chemical (THC) inputs from the LBNL THC models as documented in CRWMS M&O (2000i).

Because the values on Table 20 do not include some of the key nutrients (DOC, Mn^{2+}, NO_3^-, and PO_4^{-3}) that are utilized for microbial growth and these values are present in the groundwater at Yucca Mountain (Harrar et al. 1990 and CRWMS M&O 1997b), Table 20 below was modified to include the values shown on Table 21 below. These values are derived from Assumption 5.11 and the following DTN: GS980908312322.008.

Assumption 2 is the basis for the value used for DOC (1 ppm). The conversion from 1 ppm to the proper units has been done previously in other documentation (see CRWMS M&O 1998a, Table 4-58). The converted value is found on Table 21 below.

Manganese abundance (5.697 µg/l) was determined from DTN: GS980908312322.008 by taking the average of all values excluding data from well WT-17. Two values were reported below detection limits. A maximum value of 3.99 was used for these two data points. These values were then converted to the correct units [(mg/l)/formula wt = mol/l = kmol/m^3] and are shown on Table 21.

Phosphate abundance (0.016975 mg/l) was derived from DTN: GS980908312322.008 by averaging the values from well WT-3, as the values from well WT-17 were excluded. One data point used was below detection and a maximum value of .0099 was used to represent this. These values were then converted to the correct units and are shown on Table 21.

The value for nitrate (0.790875 mg/l) was derived from DTN: GS980908312322.008 by taking the average of all values from the nitrogen oxides abundance excluding the data from well WT-17. Values below detection limits were assigned a maximum value of 0.049. These values were then converted to the correct units and are shown on Table 21.

Table 20. Water compositions taken from PA Initial THC Abstraction

Parameter Time	Preclosure Period 1 0 - 50 years	Boiling Period 2 50 - 1000 years	Transitional Cool-Down Period 3 1000 - 2000 years	Extended Cool-Down Period 4 2000 - 100,000 years
Time	0 - 50 years	50 - 1000 years	1000 – 2000 years	2000 - 100,000 years
Temperature, °C	80	96	90	50
log CO2, vfrac	-2.8	-6.5	-3.0	-2.0
pH	8.2	8.1	7.8	7.3
Ca^{2+}, molal	1.7E-03	6.4E-04	1.0E-03	1.8E-03
Na^{+}, molal	3.0E-03	1.4E-03	2.6E-03	2.6E-03
$SiO_2°$, molal	1.5E-03	1.5E-03	2.1E-03	1.2E-03
Cl^{-}, molal	3.7E-03	1.8E-03	3.2E-03	3.3E-03
HCO_3^{-}, molal	1.3E-03	1.9E-04	3.0E-04	2.1E-03
SO_4^{2-}, molal	1.3E-03	6.6E-04	1.2E-03	1.2E-03
Mg^{2+}, molal	4.0E-06	3.2E-07	1.6E-06	7.8E-06
K^{+}, molal	5.5E-05	8.5E-05	3.1E-04	1.0E-04
AlO_2^{-}, molal	1.0E-10	2.7E-07	6.8E-08	2.0E-09
$HFeO_2^{-}$, molal	1.1E-10	7.9E-10	4.1E-10	2.4E-11
F^{-}, molal	5.0E-05	2.5E-05	4.5E-05	4.5E-05

MO9912SPAPAI29.002

Table 21. Aqueous Concentrations (kmol/m^3) not included on Table 20 but required for microbial growth.

PO_4^{3-}	NO_3^{-}	DOC	Mn^{2+}
1.79E-07	1.28E-05	3.30E-05	1.04E-07

The THC values from Table 20 above were converted to kmol/m (molal = mol solute/kg water ≈ mol solute/(L of solution [for dilute solutions]) = mol/10^{-3} m^3 = kmol/m^3) and are shown on Table 22 below. Additionally, in order for MING to consider the iron and carbonate reactions from the composition of the water Fe^{2+} is assigned the concentration of $HFeO_2^{-}$ and HCO_3^{1-} is assigned to be the concentration of ΣCO_3^{2-}.

Table 22. Incoming water compositions for the Microbial Communities Model calculations.

Parameter Time	Preclosure Period 1	Boiling Period 2	Transitional Cool-Down Period 3	Extended Cool-Down Period 4
Time	0 - 50 years	50 - 1000 years	1000 – 2000 years	2000 - 100,000 years
pH	8.2	8.1	7.8	7.3
PO_4^{-3} kmol/m^3	1.79E-07	1.79E-07	1.79E-07	1.79E-07
NO_3^- kmol/m^3	1.28E-05	1.28E-05	1.28E-05	1.28E-05
DOC kmol/m^3	3.30E-05	3.30E-05	3.30E-05	3.30E-05
Mn^{2+} kmol/m^3	1.04E-07	1.04E-07	1.04E-07	1.04E-07
CO_3^{2-} kmol/m^3	1.3E-03	1.9E-04	3.0E-04	2.1E-03
SO_4^{-2} kmol/m^3	1.3E-03	6.6E-04	1.2E-03	1.2E-03
Fe^{2+} kmol/m^3	1.1E-10	7.9E-10	4.1E-10	2.4E-11

6.5.1.4 In-Drift Gas

MING requires input for time varying cumulative influx of O_2, N_2 and CO_2 (CH_4 if available) based on and corresponds with the repository temperature history derived from the thermohydrological calculations presented above. The values being generated by other modeling efforts for TSPA-SR and have not been finalized prior to the due date of this model. Therefore, the values presented on Table 7 derived in Assumption 5.10 above will be used.

6.5.1.5 Waste Package Design and Waste Form Materials

These inputs are documented in Attachments III and IV below. Values include both the masses of materials proposed materials as well as the composition of those materials. These materials represent a synthesis of preliminary design inputs transmitted via AP-3.14Q transmittals as well as use of other qualified and unqualified input to generate the appropriate inputs. The input tables are reported in Attachment III, Sections III-4.1, III-4.2, and Attachment IV, Section IV-5.

6.5.2 Model Specific Inputs

6.5.2.1 "Default Inputs"

Table 23 includes the user-elicited inputs that are required to make the modeling runs. These values are generally set as default parameters, but can be modified to run a specific sensitivity calculation. Table 23 not only reports the "default value" but also reports the source for the value selected. These values unless otherwise specified are used for all calculations within this report.

In the MING code, there is an option to turn on or off the availability of gas as both a nutrient and as an energy source. This is done by selecting or deselecting the appropriate button(s) on the main form of MING where the inputs are entered. Due to the availability of gas in the repository

(see Section 6.5.1.4 above) and the discussion on gas utilization by microbes as nutrients in Section 6.3.1.10 above, these buttons will be placed in the on position as the default input.

Table 23. Standard Default Input Parameters Used in MING Calculations.

Default MING Input Parameters	Value	Source
Temperature Cut off	120° C	See Section 6.3.1.3
Humidity Cut off	0.90	See Section 6.3.3.2.2
Tunnel Diameter	5.5 m	CRWMS M&O (2000s)
Tunnel length	1 m	Standard length of interest
MING V1.0 Near-Field Porosity	0	CRWMS M&O (1998h, p. 53)
Gas Buttons (N_2, CO_2, O_2)	On	See Section 6.3.1.10
Energy Cut Off	15 kJ/mol e^-	McKinley et al. (1997)

6.5.2.2 Reactant Compositions

Each repository or WP material modeled using MING has a given elemental composition, but that elemental composition has to be related to a given redox state and associated with the selected redox equations that represent the microbial metabolic pathways. Attachment V reports the derivation of the reactant composition values. These are reported on Table V-2 (Attachment V). These values represent the associated species for all of the materials that are documented in Section 6.5.2

6.5.2.3 Material Lifetime

Another input that may be varied in the calculations below is the material lifetimes used to calculate the availability of materials in both the nutrient and energy calculations. Material lifetime inputs for the calculations below are given in Table 32. The reference case values (median lifetimes) are thought to be a reasonable lifetime of the given material based on the calculations below.

In order to calculate a material lifetime, material thicknesses need to be specified that correspond to the general masses of materials in the drift. Material thickness is determined by taking the largest minimal dimension of all the items of the given material. Information for these inputs were taken from the AP-3.14Q input transmittals (CRWMS M&O 1999e, 1999g, and 1999h) and from an accepted data source (AISC 1989).

Table 24. Selected Material Thickness of Repository Materials

Material	Item	Thickness (mm)	Source
Alloy 22	Waste package outer barrier	20	CRWMS M&O (2000g)
316NG	Waste package inner barrier	50	CRWMS M&O (2000g)
316L	Pallet tube	9.525	CRWMS M&O (2000g)
Ti Grade 7	Drip Shield plate	15	CRWMS M&O (2000e)
Neutronit A978	Basket plate	7	CRWMS M&O (2000g)
Aluminum 6061	Basket plate	5	CRWMS M&O (2000g)
A516 Carbon Steel	Basket guide	10	CRWMS M&O (2000g)
ASTM F432-95	Rock Bolts	28.5	CRWMS M&O (1999g)
Unspecified	Welded wire fabric	4.95	CRWMS M&O (1999e)
ASTM A572 Steel	Invert	23.8	CRWMS M&O (1999e) AISC (1989)
ASTM A759-85 Steel	Gantry Rail	74.6	CRWMS M&O (1999e) AISC (1989)
Unspecified	Rail Fittings (Anchor Clips)	19.05	CRWMS M&O (1999e)

Values for general corrosion of Ti grade 7 and Alloy 22 were taken from Figures 9 and 10. In this case, the minimum, median and maximum values correspond to the 5th, 50th and 95th percentiles. These are shown on Table 25. Material lifetimes are then determined by dividing the material thickness as shown on Table 24 by the rates shown in Tables 25. The results are found on Table 32.

Table 25. Minimum, Median and Maximum General Corrosion Rates for Alloy 22 and Ti Grade 7.

Percentile	Alloy 22 (mm/yr)	Ti Grade 7 (mm/yr)
5th	3.8e-6	5.3e-6
50th	2.9e-5	2.5e-5
95th	1.1e-4	2.6e-4

DTN: MO0003SPASUP02.003

Stainless Steel corrosion rates are presented in Table 26. The median was determined using the following equation taken from Journel (1989, Equation 20). This equation is used to determine the median of a log normal distribution.

$$Y_p Y_{p\text{-}1} = M^2 \qquad \text{(Eq. 7)}$$

where:

Y_p = Lower bound
$Y_{p\text{-}1}$ = Upper bound
M = Median

Table 26. General Aqueous Corrosion Rates for 316L Stainless Steel.

Material	Lower Bound (mm/yr)	Upper Bound (mm/yr)	Median (mm/yr)
316L	8.79×10^{-5}	4.55×10^{-2}	2.0×10^{-3}

DTN: MO0004SPASMA05.004

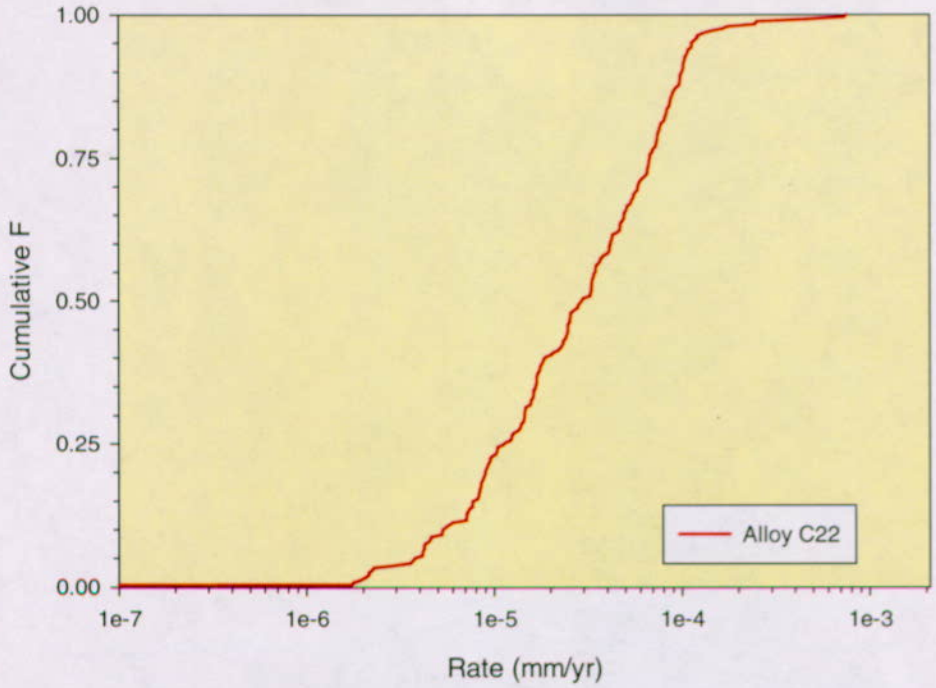

DTN: MO0003SPASUP02.003

Figure 9. Cumulative CDF for General Corrosion of Alloy 22.

Material lifetimes for 316L and 316NG are then determined by dividing the material thickness as shown on Table 24 by the rates from Table 26. The results are found on Table 29. These same results were then applied to 304L stainless steel (see Assumption 5.3) using the thickness of the canister wall as reported on Table 27.

Material lifetimes for DHLW glass are derived by taking the values from Table 27, determining the inner diameter [$2r$ = 6.1 m - 2(0.0095 m) = 0.591 m], then calculating the surface area of the glass waste (area=$2\pi rh$) in a 1 meter length of pour canister. This value is obtained by multiplying the surface area by the number of pour canisters (5) per waste package to get the total surface area (9.28 m^2). The total surface area is then modified by a factor of 30 to account for the fracturing of glass during cooling (see Assumption 5.7). This results in a total surface area of 278.50 m^2. The surface area is multiplied by the dissolution rate shown on Table 28 to obtain the number of grams per day. This value is then multiplied by 0.365 to convert g/day to kilograms per year as shown on Table 28. The mass of glass per meter of waste package found on Table IV-6 is divided by the rate to determine the material lifetime. These values are shown on Table 32.

Table 27. 304L Stainless Steel Pour Canister Properties from Savannah River HLW. (DOE 1992, Table 3.1.1)

Parameter	Value
Outside Diameter of HLW pour canister	0.61 m
Canister wall thickness	0.95 cm

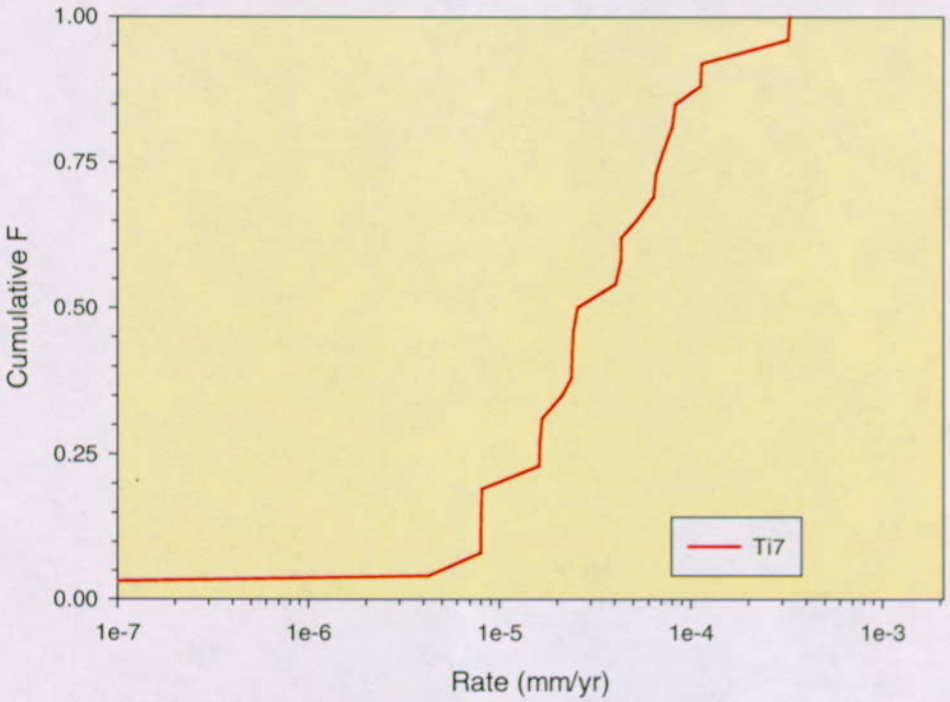

DTN: MO0003SPASUP02.003

Figure 10. Cumulative CDF for General Corrosion of Titanium Grade 7.

Table 28. Aqueous Dissolution Rates for HLW Glass.

Rate (g/m^2day)	Rate (kg/year)
1.00E-04	1.02E-02
3.00E-02	3.05E+00
3.00E-03	3.05E-01

DTN: SN9911T0811199.003

For carbon steel corrosion rates, data supplied by the following DTN LL980704605924.035 was used where 6-month corrosion tests for aqueous general corrosion of A387, A516 and cast carbon steel values were averaged. The minimum and maximum rates represent one standard

deviation of the average of these 12 values. The rates are given on Table 29. These rates are applied to the following materials: ASTM A572 Steel, ASTM A759-85 Steel, ASTM F432-95 Steel, C Steel ASTM A516, WWF Steel, and Rail Fittings. These rates will be divided by the average thickness of the material as shown on Table 24 and the results will be provided on Table 32.

Table 29. Selected Aqueous General Corrosion Rates for Mild Carbon Steel.

Minimum Rate (-1STD) (μm/yr)	Maximum Rate (+1STD) (μm/yr)	Median Rate (AVG) (μm/yr)
23.5	95.34	59.42

LL980704605924.035

For Neutronit A978 there are no documented corrosion rates available. However, a corrosion rate has been determined and documented for two similar materials, Bohler A976 SD and Nutrosorb Plus. These materials are both borated stainless steels. (Van Konynenburg, 1998). The single value is for Bohler A976 SD was used (see Assumption 5.8). The minimum and maximum values shown below were derived by taking an ±1 order of magnitude on the single (median) value. These values are shown on Table 30. The material thickness from Table 24 are then divided by these rates and added to Table 32 below.

Table 30. Surrogate General Aqueous Corrosion Rates for Neutronit A978 Borated Steel.

Material	Median (mm/yr)	Lower Bound (mm/yr)	Upper Bound (mm/yr)
Neutronit A978 (Bohler A976 SD)	0.04	0.004	0.4

DTN: LL980504105924.034

For Aluminum 6061, accepted data values for 10 and 20 year atmospheric corrosion rates on various types of aluminum have been reported in ASM International (1987, p. 601, Table 11). The median rate was determined by taking the average for the reported 10-year rates. The high rate was determined by taking the aggressive values for alloy 6061 from ASM International (1987, Table 8). The low value was taken from the 20-year desert atmosphere rate (ASM International 1987, p. 601, Table 11). These values are shown on Table 31. The material thickness from Table 24 are then divided by these rates and added to Table 32 below.

Table 31. General Aqueous Corrosion Rates for Aluminum 6061.

Material	Median Rate (μm/yr)	Low Rate (μm/yr)	High Rate (μm/yr)
Aluminum 6061	0.35	0.076	422

For CSNF, calculations have shown that aqueous dissolution of spent fuel can occur in 500 years or less (CRWMS M&O 1998a, Figure 4-57). In order to account for some range due to the potential for humid air corrosion, five fold increases to the minimum and median lifetimes will also be included. These values are shown on Table 32.

For Superplasticizer, Type K Cement and Silica Fume an assumption was made (see Assumption 5.4) for the median lifetimes shown, as no other information is known at this time. Minimum and maximum lifetimes are assumed to be a factor of 5 less and greater, respectively, than the median lifetime.

For the commo cable, no rates are available so the lifetimes are assumed so as to span the probable lifetime of the material (see Assumption 5.9).

Table 32. Minimum, Median and Maximum Material Lifetimes (years) used in the MING Calculations.

Material Name	Minimum Lifetime	Median Lifetime	Maximum Lifetime
304L Stainless Steel	208	4750	108077
316L Stainless Steel	209	4763	108362
316NG Stainless Steel	1099	25000	568828
Alloy C-22	181818	689655	5263158
Aluminum 6061	11.8	14286	65789
ASTM A572 Steel	250	401	1013
ASTM A759-85 Steel	782	1255	3174
ASTM F432-95 Steel	299	480	1213
C Steel ASTM A516	105	168	426
Commo Cable	100	1000	10000
CSNF Waste	500	2500	12500
DHLW Waste	718	7180	214705
Neutronit A978	17.5	175	1750
Rail Fittings	200	321	811
Silica Fume	2500	10000	50000
Superplasticizer	2500	10000	50000
Ti Grade 7	57692	600000	2830189
Type K Cement	2500	10000	50000
WWF Steel	52	83	211

6.5.2.4 Breakdown Codes

Some materials used in the design evaluated below contain complex organic compounds that are known to be resistant to biodegradation (i.e., superplasticizer admixtures in the grout formulation) as well as composite materials which contain organics, that are made up of more than one substance (i.e., communications cable). These materials cannot be directly broken down into their basic elemental compositions and fed into the nutrient and energy stream. MING allows for a special reactant flag that allows for partial breakdown and/or multiple reactant compositions (see Section 6.4.3). The input used below (Table 33) is derived in Attachment II.

Table 33. Reactant Compositions, Breakdown Codes and Molecular Masses for the Release of Organic Materials.

Reactant Composition	Breakdown Code	Molecular Mass
Superplasticizer		
CH_2O	5	278
CH_3OH	4	
$HCOO^-$	2	
SO_3^{2-}	1	
Wire Conductor		
CH_2O	15	88
CH_3OH	11	
Commo Cable		
CH_2O	2	28

6.5.2.5 Material Layer Designators

Until the drip shield and waste package outer barrier materials are penetrated, internal WP materials are not expected to be affected by microbial activity. This is primarily due to the lack of water availability. In order to account for the absence of water in waste packages, the values for the layer flag (see Section 6.4.3) in MING need to be entered to allow the sequential degradation of the materials in question. Table 34 provides input values for the case where there is no corrosion of the waste package internals until drip shield and outer barrier materials are breached (no drip case) and for the case where the drip shield does not divert the water from the waste package surface (drip case). Other values may be selected on a case by case basis to look at various issues that may arise. Note: the lower the layer number the sooner the material degrades.

Table 34. Material Layer Designators Used in MING V1.0 for the Sequential Degradation of Waste Package and Repository Materials.

Material Name	Drip Case Layer	No Drip Case Layer	Material Name	Drip Case Layer	No Drip Case Layer
304L Stainless Steel	2	3	CSNF Waste	2	3
316L Stainless Steel	0	2	DHLW Waste	2	3
316NG Stainless Steel	2	3	Neutronit A978	2	3
Alloy C-22**	1	2	Rail Fittings*	0	0
Aluminum 6061	2	3	Silica Fume	0	0
ASTM A572 Steel	0	0	Superplasticizer	0	0
ASTM A759-85 Steel	0	0	Ti Grade 7	0	1
ASTM F432-95 Steel	0	0	Type K Cement	0	0
C Steel ASTM A516	2	3	WWF Steel	0	0
Commo Cable	0	0			

* Not used, rolled up in ASTM A572 steel values.
** Decrease the layer designator by 1 for specific mass included in drip shield design.

6.6 MODEL RESULTS

6.6.1 Scenario Set Up

Because of the multiple parameters that are available for producing calculations, the following parameters have been selected as those that will be altered to produce the various results and show the variability in microbial communities in the EBS. They are as follows: Waste package type (CSNF (21 PWR), and HLW; Tables III-1 and III-3 below), Material Lifetime (Minimum, Median and Maximum; Table 32), Material layer designators (Dripping and No Dripping; Table 34), repository ground support options (lithophysal and Non-lithophysal locations; Table II-26 or II-27) and backfill vs. no backfill (3 times the results on Figure 8 for backfill or Figure 8 for no backfill; see Section 6.5.1.1 above) This combination of parameter variability will allow for 24 different no backfill calculations, twelve each for CSNF and HLW package types. These variable parameters along with the conservative bounding of the major environmental parameters discussed above should give results that generally will bound the total numbers of microbes that could be produced per lineal meter of repository drift. For backfill sensitivity, only the 5 cases (2 each for PWR and HLW and one BWR case) that produced the largest biomass of the 24 no backfill cases were rerun using 3 times the results on Figure 8 as the infiltration flux.

MING V1.0 was run for the cases discussed above and the results are shown below. The following input item numbers (See Table 2 in Section 4.1 above) are used as input to all calculations. They are as follows: 3-12, 17-23, 28-31, and 33-37. In addition, for CSNF calculations reported in Section 6.6.2 below, the following input item numbers from Table 2 are included: 32, 34, and either 24 or 25. For HLW canister calculations reported in Section 6.6.3 below, the inputs from Table 4 are 27 and 36. For the lithophysal locations the following inputs are used: 17-22 and 28. For the nonlithophysal areas all of the inputs for the lithophysal locations are included plus the following: 14-16 and 38. Items 1, 13, 24 and 35 vary depending on the scenario that is specified.

Six additional cases (Cases 29-34) were run with no waste package, backfill, drip shield or pallet present in the repository. Only the ground support options were selected. Therefore, the variable inputs are found on Tables 34, II-26 and II-27. These cases are reported in Section 6.6.4 below.

Plots showing the results for each of the cases are shown in Attachment VI.

6.6.2 CSNF Results

14 separate calculations (Cases 1-14 below) were run using the 21PWR waste package type. Two additional calculations were run using the inputs used for case one with the substitution of a 44 BWR waste package (Table III-2 below) to quantify the difference between the two CSNF fuel types and waste packages. Each of the specific inputs along with all of the universal inputs (Section 6.6.1 above) was entered into MING V1.0 and run.

6.6.2.1 No Backfill Design

Case 1

This case contains the following variable input parameters: minimum material lifetime, a non-lithophysal repository segment, and initial dripping on the waste package.

Results shown on Figure VI-1 indicate that the maximum biomass produced for the entire calculation is 90.48 g_{dry}/m of drift in year 181,830. During the preclosure ventilation period (0 to 51 years) the biomass production was between 25.66 and 51.34 g_{dry}/m of drift during times when the T and RH were below the threshold for growth. Otherwise, no growth occurred until well into the post closure period (in year 324) due to elevated temperatures or low RH. Maximum biomass growth from the degradation of ground support of 4.11 g_{dry}/m occurred in year 780 due to the degradation of the steel in the gantry rails. The biomass decreases to 0.84 g_{dry}/m of drift when the final ground support component (cement grout) is degraded in year 2,500. Later, the waste package outer barrier, drip shield, and pallet produced a maximum of 0.19 g_{dry}/m at year 150,000 and the natural ambient system produced a biomass of 0.07 g_{dry}/m after the waste form was degraded in year 182,917. Biomass production during the waste form degradation period (181,818 to 182,318) was at its peak (90.48 g_{dry}/m) due to the rapid degradation of the waste package inner barrier and the basket materials. For the majority of the lifetime of the waste form, the biomass produced ranged between 71.99 and 11.42 g_{dry}/m.

During most of the time period covered by the calculation, the biomass growth in the repository environment is generally nutrient limited by the lack of phosphorous (Table 35). This is due to the lack of phosphorous in the groundwater fluxing into the repository. Prior to year 324, the biomass is generally limited because the RH was too low and the temperature too high to sustain microbial growth. The only times that the calculation is energy limited was during the preclosure ventilation period and during waste form degradation. During times when the repository is limited by carbon, it is because there is not enough available in the materials being degraded in the repository.

Table 35. Limiting Condition for Case 1.

Start Year	Stop Year	Limiting Condition
1	9	Energy Limited
10	24	Humidity Too Low
25	51	Energy Limited
52	323	Humidity Too Low
324	782	Carbon
783	181817	Phosphorus
181818	182916	Energy Limited
182917	1000000	Phosphorus

Case 2

This case contains the following variable input parameters: minimum material lifetime, in a non-lithophysal repository segment with no initial dripping on the waste package.

Results shown on Figure VI-2 indicate that the maximum biomass produced for the entire calculation is 90.48 g_{dry}/m of drift in year 363,636. During the preclosure ventilation period (0 to 51 years) the biomass production was between 24.29 and 49.61 g_{dry}/m of drift during times when the T and RH were below the threshold for growth. Otherwise, no growth occurred until well into the post closure period (in year 324) due to elevated temperatures or low RH. Maximum biomass growth from the degradation of ground support of 4.10 g_{dry}/m occurred in year 780 due to the degradation of the steel in the gantry rails. The biomass decreases to 0.72 g_{dry}/m of drift when the final ground support component (cement grout) is degraded in year 2,500. Later, the drip shield produced a maximum of 0.071 g_{dry}/m at year 150,000 and the natural ambient system produced a biomass of 0.070 g_{dry}/m after the waste form was degraded in year 364,735. After the drip shield fails the waste package and pallet produce a maximum biomass of 11.09 g_{dry}/m during degradation of the stainless steel in the waste package pallet (pedestal) and a biomass of 0.19 g_{dry}/m for the C-22 alloy materials. Biomass production during the waste form degradation period (363,636 to 364,735) was at its peak (90.48 g_{dry}/m) due to the rapid degradation of the waste package inner barrier and the basket materials. For the majority of the lifetime of the waste form, the biomass produced ranged between 71.99 and 11.42 g_{dry}/m.

During most of the time period covered by the calculation, the biomass growth in the repository environment is generally nutrient limited by the lack of phosphorous (Table 36). This is due to the lack of phosphorous in the groundwater fluxing into the repository. Prior to year 324, the biomass is generally limited because the RH was too low and the temperature too high to sustain microbial growth. The only time that the calculation is energy limited was during the preclosure ventilation period. During times when the repository is limited by carbon, it is because there is not enough available in the materials being degraded in the repository.

Table 36. Limiting Condition for Case 2.

Start Year	Stop Year	Limiting Condition
1	9	Energy Limited
10	24	Humidity Too Low
25	51	Energy Limited
52	323	Humidity Too Low
324	782	Carbon
783	181817	Phosphorus
181818	182026	Carbon
182027	363635	Phosphorus
363636	364734	Carbon
364735	1000000	Phosphorus

Case 3

This case contains the following variable input parameters: minimum material lifetime, in a lithophysal repository segment and with initial dripping on the waste.

Results shown on Figure VI-3 indicate that the maximum biomass produced for the entire calculation is 90.48 g_{dry}/m of drift in year 181,830. During the preclosure ventilation period (0 to 51 years) the biomass production was between 27.67 and 36.84 g_{dry}/m of drift during times when the T and RH were below the threshold for growth. Otherwise, no growth occurred until well into the post closure period (in year 324) due to elevated temperatures or low RH. Maximum biomass growth from the degradation of ground support of 3.98 g_{dry}/m occurred in year 780 due to the degradation of the steel in the gantry rails. Later, the waste package outer barrier, drip shield, and pallet produced a maximum of 0.19 g_{dry}/m at year 150,000 and the natural ambient system produced a biomass of 0.069 g_{dry}/m after the waste form was degraded in year 182,917. Biomass production during the waste form degradation period (181,818 to 182,318) was at its peak (90.48 g_{dry}/m) due to the rapid degradation of the waste package inner barrier and the basket materials. For the majority of the lifetime of the waste form, the biomass produced ranged between 71.99 and 11.42 g_{dry}/m.

During most of the time period covered by the calculation, the biomass growth in the repository environment is generally nutrient limited by the lack of phosphorous (Table 37). This is due to the lack of phosphorous in the groundwater fluxing into the repository. Prior to year 324, the biomass is generally limited because the RH was too low and the temperature too high to sustain microbial growth. The only times that the calculation is energy limited was during the preclosure ventilation period and during waste form degradation. During times when the repository is limited by carbon, it is because there is not enough available in the materials being degraded in the repository.

Table 37. Limiting Condition for Case 3.

Start Year	Stop Year	Limiting Condition
1	9	Energy Limited
10	24	Humidity Too Low
25	51	Energy Limited
52	323	Humidity Too Low
324	782	Carbon
783	181817	Phosphorus
181818	182916	Energy Limited
182917	1000000	Phosphorus

Case 4

This case contains the following variable input parameters: minimum material lifetime, in a lithophysal repository segment with no initial dripping on the waste package.

Results shown on Figure VI-4 indicate that the maximum biomass produced for the entire calculation is 90.48 g_{dry}/m of drift in year 363,636. During the preclosure ventilation period (0 to 51 years) the biomass production was between 25.65 and 33.26 g_{dry}/m of drift during times when the T and RH were below the threshold for growth. Otherwise, no growth occurred until well into the post closure period (in year 324) due to elevated temperatures or low RH. Maximum biomass growth from the degradation of ground support of 3.98 g_{dry}/m occurred in year 780 due to the degradation of the steel in the gantry rails. Later, the drip shield produced a maximum of 0.071 g_{dry}/m at year 150,000 and the natural ambient system produced a biomass of 0.070 g_{dry}/m after the waste form was degraded in year 364,735. After the drip shield fails the waste package and pallet produce a maximum biomass of 11.09 g_{dry}/m during degradation of the stainless steel in the waste package pallet (pedestal) and a biomass of 0.19 g_{dry}/m for the C-22 alloy materials. Biomass production during the waste form degradation period (363,636 to 364,735) was at its peak (90.48 g_{dry}/m) due to the rapid degradation of the waste package inner barrier and the basket materials. For the majority of the lifetime of the waste form, the biomass produced ranged between 71.99 and 11.42 g_{dry}/m.

During most of the time period covered by the calculation, the biomass growth in the repository environment is generally nutrient limited by the lack of phosphorous (Table 38). This is due to the lack of phosphorous in the groundwater fluxing into the repository. Prior to year 324, the biomass is generally limited because the RH was too low and the temperature too high to sustain microbial growth. The only time that the calculation is energy limited was during the preclosure ventilation period. During times when the repository is limited by carbon, it is because there is not enough available in the materials being degraded in the repository.

Table 38. Limiting Condition for Case 4.

Start Year	Stop Year	Limiting Condition
1	9	Energy Limited
10	24	Humidity Too Low
25	51	Energy Limited
52	323	Humidity Too Low
324	782	Carbon
783	181817	Phosphorus
181818	182026	Carbon
182027	363635	Phosphorus
363636	364734	Carbon
364735	1000000	Phosphorus

Case 5

This case contains the following variable input parameters: median material lifetimes, in a non-lithophysal repository segment with initial dripping on the waste package.

Results shown on Figure VI-5 indicate that the maximum biomass produced for the entire calculation is 49.84 g_{dry}/m of drift in year 689,655. During the preclosure ventilation period (0 to 51 years) the biomass production was between 11.42 and 31.43 g_{dry}/m of drift during times when the T and RH were below the threshold for growth. Otherwise, no growth occurred until well into the post closure period (in year 324) due to elevated temperatures or low RH. Maximum biomass growth from the degradation of ground support of 12.24 g_{dry}/m occurred in year 400 due to the degradation of the steel in the steel sets. The biomass decreases to 0.26 g_{dry}/m of drift when the final ground support component (cement grout) is degraded in year 10,000. Later, the waste package outer barrier, drip shield, and pallet produced a maximum of 0.10 g_{dry}/m at year 600,001 and the natural ambient system produced a biomass of 0.070 g_{dry}/m after the waste form was degraded in year 714,655. Biomass production during the waste form degradation period (689,655 to 714,655) was at its peak (49.84 g_{dry}/m) due to the rapid degradation of the waste package inner barrier and the basket materials. For the majority of the lifetime of the waste form, the biomass produced ranged between 10.70 and 2.60 g_{dry}/m.

During most of the time period covered by the calculation, the biomass growth in the repository environment is generally nutrient limited by the lack of phosphorous (Table 39). This is due to the lack of phosphorous in the groundwater fluxing into the repository. Prior to year 324, the biomass is generally limited because the RH was too low and the temperature too high to sustain microbial growth. The calculation was not energy limited at any time. During times when the repository is limited by carbon, it is because there is not enough available in the materials being degraded in the repository.

Table 39. Limiting Condition for Case 5.

Start Year	Stop Year	Limiting
1	9	Carbon
10	24	Humidity Too Low
25	51	Carbon
52	323	Humidity Too Low
324	1189	Carbon
1190	689654	Phosphorus
689655	689822	Carbon
689823	1000000	Phosphorus

Case 6

This case contains the following variable input parameters: median material lifetimes, in a non-lithophysal repository segment with no initial dripping on the waste package.

Results shown on Figure VI-6 indicate that the maximum biomass produced for the entire post closure period in the calculation is 12.21 g_{dry}/m of drift in year 400. During the preclosure ventilation period (0 to 51 years) the biomass production was between 11.34 and 31.40 g_{dry}/m of drift during times when the T and RH were below the threshold for growth. Otherwise, no growth occurred until well into the post closure period (in year 324) due to elevated temperatures or low RH. Maximum biomass growth from the degradation of ground support of 12.21 g_{dry}/m occurred in year 400 due to the degradation of the steel in the steel sets. The biomass decreases to 0.23 g_{dry}/m of drift when the final ground support component (cement grout) is degraded in year 10,000. Later, the drip shield produced a maximum of 0.070 g_{dry}/m at year 600,000. After the drip shield fails the waste package and pallet produce a maximum biomass of 1.10 g_{dry}/m during degradation of the stainless steel in the waste package pallet (pedestal) and a biomass of 0.10 g_{dry}/m for the C-22 alloy materials. No other results were produced due to the longevity of the materials involved.

During most of the time period covered by the calculation, the biomass growth in the repository environment is generally nutrient limited by the lack of phosphorous (Table 40). This is due to the lack of phosphorous in the groundwater fluxing into the repository. Prior to year 324, the biomass is generally limited because the RH was too low and the temperature too high to sustain microbial growth. The calculation was not energy limited at any time. During times when the repository is limited by carbon, it is because there is not enough available in the materials being degraded in the repository.

Table 40. Limiting Condition for Case 6.

Start Year	Stop Year	Limiting Condition
1	9	Carbon
10	24	Humidity Too Low
25	51	Carbon
52	323	Humidity Too Low
324	480	Carbon
481	1000	Phosphorus
1001	1009	Carbon
1010	1000000	Phosphorus

Case 7

This case contains the following variable input parameters: median material lifetimes, in a lithophysal repository segment and with initial dripping on the waste package.

Results shown on Figure VI-7 indicate that the maximum biomass produced for the entire calculation is 49.84 g_{dry}/m of drift in year 689,655. During the preclosure ventilation period (0 to 51 years) the biomass production was between 15.87 and 25.77 g_{dry}/m of drift during times when the T and RH were below the threshold for growth. Otherwise, no growth occurred until well into the post closure period (in year 324) due to elevated temperatures or low RH. Maximum biomass growth from the degradation of ground support of 14.96 g_{dry}/m occurred in year 400 due to the degradation of the steel in the steel sets. The biomass decreases to 3.83 g_{dry}/m of drift when the final ground support component (gantry rail) is degraded in year 1,255. Later, the waste package outer barrier, drip shield, and pallet produced a maximum of 1.1 g_{dry}/m at year 4700. This decreases to 0.10 g_{dry}/m until the C-22 alloy in the waste package is degraded. The natural ambient system produced a biomass of 0.069 g_{dry}/m after the waste form was degraded in year 714,655. Biomass production during the waste form degradation period (689,655 to 714,655) was at its peak (49.84 g_{dry}/m) due to the rapid degradation of the waste package inner barrier and the basket materials. For the majority of the lifetime of the waste form, the biomass produced ranged between 10.70 and 2.60 g_{dry}/m.

During most of the time period covered by the calculation, the biomass growth in the repository environment is generally nutrient limited by the lack of phosphorous (Table 41). This is due to the lack of phosphorous in the groundwater fluxing into the repository. Prior to year 324, the biomass is generally limited because the RH was too low and the temperature too high to sustain microbial growth. The calculation was not energy limited at any time. During times when the repository is limited by carbon, it is because there is not enough available in the materials being degraded in the repository.

Table 41. Limiting Condition for Case 7.

Start Year	Stop Year	Limiting
1	9	Carbon
10	24	Humidity Too Low
25	51	Carbon
52	323	Humidity Too Low
324	1169	Carbon
1170	689654	Phosphorus
689655	689822	Carbon
689823	1000000	Phosphorus

Case 8

This case contains the following variable input parameters: median material lifetimes, in a lithophysal repository segment with no initial dripping on the waste package.

Results shown on Figure VI-8 indicate that the maximum biomass produced for the entire post closure period in the calculation is 14.94 g_{dry}/m of drift in year 400. During the preclosure ventilation period (0 to 51 years) the biomass production was between 15.80 and 25.65 g_{dry}/m of rift during times when the T and RH were below the threshold for growth. Otherwise, no growth occurred until well into the post closure period (in year 324) due to elevated temperatures or low RH. Maximum biomass growth from the degradation of ground support of 14.94 g_{dry}/m occurred in year 400 due to the degradation of the steel in the steel sets. The biomass decreases to 2.79 g_{dry}/m of drift when the final ground support component (gantry rail) is degraded in year 1,255. Later, the drip shield produced a maximum of 0.070 g_{dry}/m at year 600,000. After the drip shield fails the waste package and pallet produce a maximum biomass of 1.10 g_{dry}/m during degradation of the stainless steel in the waste package pallet (pedestal) and a biomass of 0.10 g_{dry}/m for the C-22 alloy materials. No other results were produced due to the longevity of the materials involved.

During most of the time period covered by the calculation, the biomass growth in the repository environment is generally nutrient limited by the lack of phosphorous (Table 42). This is due to the lack of phosphorous in the groundwater fluxing into the repository. Prior to year 324, the biomass is generally limited because the RH was too low and the temperature too high to sustain microbial growth. The calculation was not energy limited at any time. During times when the repository is limited by carbon, it is because there is not enough available in the materials being degraded in the repository.

Table 42. Limiting Condition for Case 8.

Start Year	Stop Year	Limiting
1	9	Carbon
10	24	Humidity Too Low
25	51	Carbon
52	323	Humidity Too Low
324	401	Carbon
402	1000000	Phosphorus

Case 9

This case contains the following variable input parameters: maximum material lifetimes, in a non-lithophysal repository segment with initial dripping on the waste package.

Results shown on Figure VI-9 indicate that the maximum biomass produced for the entire post closure period is 5.39 g_{dry}/m of drift in year 1,010. During the preclosure ventilation period (0 to 51 years) the biomass production was between 11.63 and 14.70 g_{dry}/m of drift during times when the T and RH were below the threshold for growth. Otherwise, no growth occurred until well into the post closure period (in year 324) due to elevated temperatures or low RH. Maximum biomass growth from the degradation of ground support of 5.39 g_{dry}/m occurred in year 1,010 due to the degradation of the steel in the steel sets. The biomass decreases to 0.12 g_{dry}/m of drift when the final ground support component (cement grout) is degraded in year 100,000. Later, the waste package outer barrier, drip shield, and pallet produced a maximum of 0.074 g_{dry}/m at year 1,000,000. No other results were produced due to the longevity of the materials involved.

During most of the time period covered by the calculation, the biomass growth in the repository environment is generally nutrient limited by the lack of phosphorous (Table 43). This is due to the lack of phosphorous in the groundwater fluxing into the repository. Prior to year 324, the biomass is generally limited because the RH was too low and the temperature too high to sustain microbial growth. The calculation was not energy limited at any time. During times when the repository is limited by carbon, it is because there is not enough available in the materials being degraded in the repository.

Table 43. Limiting Condition for Case 9.

Start Year	Stop Year	Limiting
1	9	Carbon
10	24	Humidity Too Low
25	51	Carbon
52	323	Humidity Too Low
324	1039	Carbon
1040	1000000	Phosphorus

Case 10

This case contains the following variable input parameters: maximum material lifetimes, in a non-lithophysal repository segment with no initial dripping on the waste package.

Results shown on Figure VI-10 indicate that the maximum biomass produced for the entire post closure period in the calculation is 5.39 g_{dry}/m of drift in year 1,010. During the preclosure ventilation period (0 to 51 years) the biomass production was between 11.63 and 14.70 g_{dry}/m of drift during times when the T and RH were below the threshold for growth. Otherwise, no growth occurred until well into the post closure period (in year 324) due to elevated temperatures or low RH. Maximum biomass growth from the degradation of ground support of 5.39 g_{dry}/m occurred in year 1,010 due to the degradation of the steel in the steel sets. The biomass decreases to 0.10 g_{dry}/m of drift when the final ground support component (cement grout) is degraded in year 50,000. Later, the drip shield produced a maximum of 0.070 g_{dry}/m at year 1,000,000. No other results were produced due to the longevity of the materials involved.

During most of the time period covered by the calculation, the biomass growth in the repository environment is generally nutrient limited by the lack of phosphorous (Table 44). This is due to the lack of phosphorous in the groundwater fluxing into the repository. Prior to year 324, the biomass is generally limited because the RH was too low and the temperature too high to sustain microbial growth. The calculation was not energy limited at any time. During times when the repository is limited by carbon, it is because there is not enough available in the materials being degraded in the repository.

Table 44. Limiting Condition for Case 10.

Start Year	Stop Year	Limiting Condition
1	9	Carbon
10	24	Humidity Too Low
25	51	Carbon
52	323	Humidity Too Low
324	1029	Carbon
1030	1000000	Phosphorus

Case 11

This case contains the following variable input parameters: maximum material lifetimes, in a lithophysal repository segment and with initial dripping on the waste package.

Results shown on Figure VI-11 indicate that the maximum biomass produced for the entire post closure period is 6.47 g_{dry}/m of drift in year 1,010. During the preclosure ventilation period (0 to 51 years) the biomass production was between 12.71 and 15.78 g_{dry}/m of drift during times when the T and RH were below the threshold for growth. Otherwise, no growth occurred until well into the post closure period (in year 324) due to elevated temperatures or low RH. Maximum biomass growth from the degradation of ground support of 6.48 g_{dry}/m occurred in year 1,010 due to the degradation of the steel in the steel sets. The biomass decreases to 1.20 g_{dry}/m until

year 3,175 when the gantry rails finish degrading. The biomass again decreases to 0.12 g_{dry}/m of drift when the waste package support pallet (pedestal) is degrading, which lasts until year 100,000. Later, the waste package outer barrier, drip shield, and pallet produced a maximum of 0.074 g_{dry}/m at year 1,000,000. No other results were produced due to the longevity of the materials involved.

During most of the time period covered by the calculation, the biomass growth in the repository environment is generally nutrient limited by the lack of phosphorous (Table 45). This is due to the lack of phosphorous in the groundwater fluxing into the repository. Prior to year 324, the biomass is generally limited because the RH was too low and the temperature too high to sustain microbial growth. The calculation was not energy limited at any time. During times when the repository is limited by carbon, it is because there is not enough available in the materials being degraded in the repository.

Table 45. Limiting Condition for Case 11.

Start Year	Stop Year	Limiting
1	9	Carbon
10	24	Humidity Too Low
25	51	Carbon
52	323	Humidity Too Low
324	1013	Carbon
1014	1000000	Phosphorus

Case 12

This case contains the following variable input parameters: maximum material lifetimes, in a lithophysal repository segment with no initial dripping on the waste package.

Results shown on Figure VI-12 indicate that the maximum biomass produced for the entire post closure period in the calculation is 6.47 g_{dry}/m of drift in year 1,010. During the preclosure ventilation period (0 to 51 years) the biomass production was between 12.71 and 15.78 g_{dry}/m of drift during times when the T and RH were below the threshold for growth. Otherwise, no growth occurred until well into the post closure period (in year 324) due to elevated temperatures or low RH. Maximum biomass growth from the degradation of ground support of 6.47 g_{dry}/m occurred in year 1,010 due to the degradation of the steel in the steel sets. The biomass decreases to 1.16 g_{dry}/m until year 3,175 when the gantry rails finish degrading. Later, the drip shield produced a maximum of 0.069 g_{dry}/m at year 1,000,000. No other results were produced due to the longevity of the materials involved.

During most of the time period covered by the calculation, the biomass growth in the repository environment is generally nutrient limited by the lack of phosphorous (Table 46). This is due to the lack of phosphorous in the groundwater fluxing into the repository. Prior to year 324, the biomass is generally limited because the RH was too low and the temperature too high to sustain microbial growth. The calculation was not energy limited at any time. During times when the

repository is limited by carbon, it is because there is not enough available in the materials being degraded in the repository.

Table 46. Limiting Condition for Case 12.

Start Year	Stop Year	Limiting Condition
1	9	Carbon
10	24	Humidity Too Low
25	51	Carbon
52	323	Humidity Too Low
324	1013	Carbon
1014	1000000	Phosphorus

6.6.2.2 Backfill Sensitivity Cases

Case 13

This case contains the following variable input parameters: minimum material lifetime, in a non-lithophysal repository segment with initial dripping on the waste package with backfill present.

Results shown on Figure VI-13 indicate that the maximum biomass produced for the entire calculation is 111.43 g_{dry}/m of drift in year 181,818. During the preclosure ventilation period (0 to 51 years) the biomass production was between 27.27 and 46.90 g_{dry}/m of drift during times when the T and RH were below the threshold for growth. Otherwise, no growth occurred until well into the post closure period (in year 324) due to elevated temperatures or low RH. Maximum biomass growth from the degradation of ground support of 5.32 g_{dry}/m occurred in year 780 due to the degradation of the steel in the gantry rails. The biomass decreases to 0.98 g_{dry}/m of drift when the final ground support component (cement grout) is degraded in year 2,500. Later, the waste package outer barrier, drip shield, and pallet produced a maximum of 0.32 g_{dry}/m at year 150,000 and the natural ambient system produced a biomass of 0.21 g_{dry}/m after the waste form was degraded in year 182,917. Biomass production during the waste form degradation period (181,818 to 182,318) was at its peak (111.42 g_{dry}/m) due to the rapid degradation of the waste package inner barrier and the basket materials. For the majority of the lifetime of the waste form, the biomass produced ranged between 92.93 and 32.35 g_{dry}/m.

During most of the time period covered by the calculation, the biomass growth in the repository environment is generally nutrient limited by the lack of phosphorous (Table 47). This is due to the lack of phosphorous in the groundwater fluxing into the repository. Prior to year 324, the biomass is generally limited because the RH was too low and the temperature too high to sustain microbial growth. The only times that the calculation is energy limited was during the preclosure ventilation period and during waste form degradation. During times when the repository is limited by carbon, it is because there is not enough available in the materials being degraded in the repository.

Table 47. Limiting Condition for Case 13.

Start Year	Stop Year	Limiting Condition
1	9	Energy Limited
10	24	Humidity Too Low
25	51	Energy Limited
52	323	Humidity Too Low
324	325	Carbon
326	564	Phosphorus
565	614	Carbon
615	181817	Phosphorus
181818	182916	Energy Limited
182917	1000000	Phosphorus

Case 14

This case contains the following variable input parameters: median material lifetimes, in a lithophysal repository segment and with initial dripping on the waste package with backfill present.

Results shown on Figure VI-14 indicate that the maximum biomass produced for the entire calculation is 70.77 g_{dry}/m of drift in year 689,655. During the preclosure ventilation period (0 to 51 years) the biomass production was between 19.18 and 35.30 g_{dry}/m of drift during times when the T and RH were below the threshold for growth. Otherwise, no growth occurred until well into the post closure period (in year 324) due to elevated temperatures or low RH. Maximum biomass growth from the degradation of ground support of 16.60 g_{dry}/m occurred in year 400 due to the degradation of the steel in the steel sets. The biomass decreases to 3.92 g_{dry}/m of drift when the final ground support component (gantry rail) is degraded in year 1,255. Later, the waste package outer barrier, drip shield, and pallet produced a maximum of 1.24 g_{dry}/m at year 4700. This decreases to 0.24 g_{dry}/m until the C-22 alloy in the waste package is degraded. The natural ambient system produced a biomass of 0.21 g_{dry}/m after the waste form was degraded in year 714,655. Biomass production during the waste form degradation period (689,655 to 714,655) was at its peak (70.77 g_{dry}/m) due to the rapid degradation of the waste package inner barrier and the basket materials. For the majority of the lifetime of the waste form, the biomass produced ranged between 10.84 and 2.74 g_{dry}/m.

During most of the time period covered by the calculation, the biomass growth in the repository environment is generally nutrient limited by the lack of phosphorous (Table 48). This is due to the lack of phosphorous in the groundwater fluxing into the repository. Prior to year 324, the biomass is generally limited because the RH was too low and the temperature too high to sustain microbial growth. The calculation was energy limited for the pre closure period. During times when the repository is limited by carbon, it is because there is not enough available in the materials being degraded in the repository.

Table 48. Limiting Condition for Case 14.

Start Year	Stop Year	Limiting Condition
1	9	Energy Limited
10	24	Humidity Too Low
25	51	Energy Limited
52	323	Humidity Too Low
324	401	Carbon
402	689654	Phosphorus
689655	689822	Carbon
689823	1000000	Phosphorus

6.6.2.3 44BWR Sensitivity Cases

44BWR No Backfill Case

This case is identical to Case 1 with the substitution of the 44 BWR waste package (Table III-2).

Results shown on Figure VI-15 indicate that the maximum biomass produced for the entire calculation is 106.93 g_{dry}/m of drift in year 181,830. During the preclosure ventilation period (0 to 51 years) the biomass production was between 25.66 and 51.34 g_{dry}/m of drift during times when the T and RH were below the threshold for growth. Otherwise, no growth occurred until well into the post closure period (in year 324) due to elevated temperatures or low RH. Maximum biomass growth from the degradation of ground support of 4.11 g_{dry}/m occurred in year 780 due to the degradation of the steel in the gantry rails. The biomass decreases to 0.84 g_{dry}/m of drift when the final ground support component (cement grout) is degraded in year 2,500. Later, the waste package outer barrier, drip shield, and pallet produced a maximum of 0.19 g_{dry}/m at year 150,000 and the natural ambient system produced a biomass of 0.070 g_{dry}/m after the waste form was degraded in year 182,917. Biomass production during the waste form degradation period (181,818 to 182,318) was at its peak (106.92 g_{dry}/m) due to the rapid degradation of the waste package inner barrier and the basket materials. For the majority of the lifetime of the waste form, the biomass produced ranged between 50.04 and 11.44 g_{dry}/m.

During most of the time period covered by the calculation, the biomass growth in the repository environment is generally nutrient limited by the lack of phosphorous (Table 49). This is due to the lack of phosphorous in the groundwater fluxing into the repository. Prior to year 324, the biomass is generally limited because the RH was too low and the temperature too high to sustain microbial growth. The calculation is energy limited was during the preclosure ventilation period. During times when the repository is limited by carbon, it is because there is not enough available in the materials being degraded in the repository.

Table 49. Limiting Condition for 44BWR No Backfill Case.

Start Year	Stop Year	Limiting Condition
1	9	Energy Limited
10	24	Humidity Too Low
25	51	Energy Limited
52	323	Humidity Too Low
324	782	Carbon
783	181817	Phosphorus
181818	182916	Carbon
182917	1000000	Phosphorus

44BWR Backfill Case

This case is identical to Case 1 with the substitution of the 44 BWR waste package (Table III-2) and backfill sensitivity instead of the no backfill design.

Results shown on Figure VI-16 indicate that the maximum biomass produced for the entire calculation is 127.86 g_{dry}/m of drift in year 181,830. During the preclosure ventilation period (0 to 51 years) the biomass production was between 27.27 and 46.90 g_{dry}/m of drift during times when the T and RH were below the threshold for growth. Otherwise, no growth occurred until well into the post closure period (in year 324) due to elevated temperatures or low RH. Maximum biomass growth from the degradation of ground support of 5.32 g_{dry}/m occurred in year 780 due to the degradation of the steel in the gantry rails. The biomass decreases to 0.98 g_{dry}/m of drift when the final ground support component (cement grout) is degraded in year 2,500. Later, the waste package outer barrier, drip shield, and pallet produced a maximum of 0.33 g_{dry}/m at year 150,000 and the natural ambient system produced a biomass of 0.21 g_{dry}/m after the waste form was degraded in year 182,917. Biomass production during the waste form degradation period (181,818 to 182,318) was at its peak (127.86 g_{dry}/m) due to the rapid degradation of the waste package inner barrier and the basket materials. For the majority of the lifetime of the waste form, the biomass produced ranged between 108.59 and 32.38 g_{dry}/m.

During most of the time period covered by the calculation, the biomass growth in the repository environment is generally nutrient limited by the lack of phosphorous (Table 50). This is due to the lack of phosphorous in the groundwater fluxing into the repository. Prior to year 324, the biomass is generally limited because the RH was too low and the temperature too high to sustain microbial growth. The only times that the calculation is energy limited was during the preclosure ventilation period and during waste form degradation. During times when the repository is limited by carbon, it is because there is not enough available in the materials being degraded in the repository.

Table 50. Limiting Condition for 44BWR Backfill Case.

Start Year	Stop Year	Limiting Condition
1	9	Energy Limited
10	24	Humidity Too Low
25	51	Energy Limited
52	323	Humidity Too Low
324	325	Carbon
326	564	Phosphorus
565	614	Carbon
615	181817	Phosphorus
181818	182916	Carbon
182917	1000000	Phosphorus

6.6.3 HLW Results

14 separate calculations (Cases 15-28) were run using the HLW package type. Each of the specific inputs called out below along with all of the universal inputs (Section 6.6.1 above) was entered into MING V1.0 and run. Each case documents the conditions of the calculation done in MING V1.0.

6.6.3.1 No Backfill Cases

Case 15

This case contains the following variable input parameters: minimum material lifetime, in a non-lithophysal repository segment and with initial dripping on the waste package.

Results shown on Figure VI-17 indicate that the maximum biomass produced for the entire calculation is 70.44 g_{dry}/m of drift in year 181,818. During the preclosure ventilation period (0 to 51 years) the biomass production was between 26.21 and 51.34 g_{dry}/m of drift during times when the T and RH were below the threshold for growth. Otherwise, no growth occurred until well into the post closure period (in year 324) due to elevated temperatures or low RH. Maximum biomass growth from the degradation of ground support of 4.11 g_{dry}/m occurred in year 780 due to the degradation of the steel in the gantry rails. The biomass decreases to 0.91 g_{dry}/m of drift when the final ground support component (cement grout) is degraded in year 2,500. Later, the waste package outer barrier, drip shield, and pallet produced a maximum of 0.26 g_{dry}/m at year 150,000 and the natural ambient system produced a biomass of 0.070 g_{dry}/m after the waste form was degraded in year 182,917. Biomass production during the waste form degradation period (181,818 to 182,318) was at its peak (70.44 g_{dry}/m) due to the rapid degradation of the waste package inner barrier and the basket materials. For the majority of the lifetime of the waste form, the biomass produced ranged between 13.74 and 11.78 g_{dry}/m.

During most of the time period covered by the calculation, the biomass growth in the repository environment is generally nutrient limited by the lack of phosphorous (Table 51). This is due to the lack of phosphorous in the groundwater fluxing into the repository. Prior to year 324, the

biomass is generally limited because the RH was too low and the temperature too high to sustain microbial growth. The only time that the calculation is energy limited was during the preclosure ventilation period. During times when the repository is limited by carbon, it is because there is not enough available in the materials being degraded in the repository.

Table 51. Limiting Condition for Case 15.

Start Year	Stop Year	Limiting Condition
1	9	Carbon
10	24	Humidity Too Low
25	51	Carbon
52	333	Humidity Too Low
334	782	Carbon
783	181817	Phosphorus
181818	182916	Carbon
182917	1000000	Phosphorus

Case 16

This case contains the following variable input parameters: minimum material lifetime, in a lithophysal repository segment with no initial dripping on the waste package.

Results shown on Figure VI-18 indicate that the maximum biomass produced for the entire calculation is 70.44 g_{dry}/m of drift in year 363,636. During the preclosure ventilation period (0 to 51 years) the biomass production was between 24.27 and 49.61 g_{dry}/m of drift during times when the T and RH were below the threshold for growth. Otherwise, no growth occurred until well into the post closure period (in year 324) due to elevated temperatures or low RH. Maximum biomass growth from the degradation of ground support of 4.10 g_{dry}/m occurred in year 780 due to the degradation of the steel in the gantry rails. The biomass decreases to 0.72 g_{dry}/m of drift when the final ground support component (cement grout) is degraded in year 2,500. Later, the drip shield produced a maximum of 0.071 g_{dry}/m at year 150,000 and the natural ambient system produced a biomass of 0.070 g_{dry}/m after the waste form was degraded in year 364,735. After the drip shield fails the waste package and pallet produce a maximum biomass of 11.09 g_{dry}/m during degradation of the stainless steel in the waste package pallet (pedestal) and a biomass of 0.26 g_{dry}/m for the C-22 alloy materials. Biomass production during the waste form degradation period (363,636 to 364,735) was at its peak (70.44 g_{dry}/m) due to the rapid degradation of the waste package inner barrier and the basket materials. For the majority of the lifetime of the waste form, the biomass produced ranged between 13.74 and 11.78 g_{dry}/m.

During most of the time period covered by the calculation, the biomass growth in the repository environment is generally nutrient limited by the lack of phosphorous (Table 52). This is due to the lack of phosphorous in the groundwater fluxing into the repository. Prior to year 324, the biomass is generally limited because the RH was too low and the temperature too high to sustain microbial growth. The only time that the calculation is energy limited was during the preclosure ventilation period. During times when the repository is limited by carbon, it is because there is not enough available in the materials being degraded in the repository.

Table 52. Limiting Condition for Case 16.

Start Year	Stop Year	Limiting Condition
1	9	Energy Limited
10	24	Humidity Too Low
25	51	Energy Limited
52	333	Humidity Too Low
334	782	Carbon
783	181817	Phosphorus
181818	182026	Carbon
182027	363635	Phosphorus
363636	364734	Carbon
364735	1000000	Phosphorus

Case 17

This case contains the following variable input parameters: minimum material lifetime, in a lithophysal repository segment and with initial dripping on the waste.

Results shown on Figure VI-19 indicate that the maximum biomass produced for the entire calculation is 70.44 g_{dry}/m of drift in year 181,818. During the preclosure ventilation period (0 to 51 years) the biomass production was between 27.64 and 36.67 g_{dry}/m of drift during times when the T and RH were below the threshold for growth. Otherwise, no growth occurred until well into the post closure period (in year 324) due to elevated temperatures or low RH. Maximum biomass growth from the degradation of ground support of 3.98 g_{dry}/m occurred in year 780 due to the degradation of the steel in the gantry rails. Later, the waste package outer barrier, drip shield, and pallet produced a maximum of 0.26 g_{dry}/m at year 150,000 and the natural ambient system produced a biomass of 0.070 g_{dry}/m after the waste form was degraded in year 182,917. Biomass production during the waste form degradation period (181,818 to 182,318) was at its peak (70.44 g_{dry}/m) due to the rapid degradation of the waste package inner barrier and the basket materials. For the majority of the lifetime of the waste form, the biomass produced ranged between 13.74 and 11.78 g_{dry}/m.

During most of the time period covered by the calculation, the biomass growth in the repository environment is generally nutrient limited by the lack of phosphorous (Table 53). This is due to the lack of phosphorous in the groundwater fluxing into the repository. Prior to year 324, the biomass is generally limited because the RH was too low and the temperature too high to sustain microbial growth. The only time that the calculation is energy limited was during the preclosure ventilation period. During times when the repository is limited by carbon, it is because there is not enough available in the materials being degraded in the repository.

Table 53. Limiting Condition for Case 17.

Start Year	Stop Year	Limiting
1	9	Energy Limited
10	24	Humidity Too Low
25	51	Energy Limited
52	333	Humidity Too Low
334	782	Carbon
783	181817	Phosphorus
181818	182916	Carbon
182917	1000000	Phosphorus

Case 18

This case contains the following variable input parameters: minimum material lifetime, in a lithophysal repository segment with no initial dripping on the waste package.

Results shown on Figure VI-20 indicate that the maximum biomass produced for the entire calculation is 70.44 g_{dry}/m of drift in year 363,636. During the preclosure ventilation period (0 to 51 years) the biomass production was between 25.62 and 34.02 g_{dry}/m of drift during times when the T and RH were below the threshold for growth. Otherwise, no growth occurred until well into the post closure period (in year 324) due to elevated temperatures or low RH. Maximum biomass growth from the degradation of ground support of 3.98 g_{dry}/m occurred in year 780 due to the degradation of the steel in the gantry rails. Later, the drip shield produced a maximum of 0.071 g_{dry}/m at year 150,000 and the natural ambient system produced a biomass of 0.070 g_{dry}/m after the waste form was degraded in year 364,735. After the drip shield fails the waste package and pallet produce a maximum biomass of 11.09 g_{dry}/m during degradation of the stainless steel in the waste package pallet (pedestal) and a biomass of 0.26 g_{dry}/m for the C-22 alloy materials. Biomass production during the waste form degradation period (363,636 to 364,735) was at its peak (70.44 g_{dry}/m) due to the rapid degradation of the waste package inner barrier and the basket materials. For the majority of the lifetime of the waste form, the biomass produced ranged between 13.74 and 11.78 g_{dry}/m.

During most of the time period covered by the calculation, the biomass growth in the repository environment is generally nutrient limited by the lack of phosphorous (Table 54). This is due to the lack of phosphorous in the groundwater fluxing into the repository. Prior to year 324, the biomass is generally limited because the RH was too low and the temperature too high to sustain microbial growth. The only time that the calculation is energy limited was during the preclosure ventilation period. During times when the repository is limited by carbon, it is because there is not enough available in the materials being degraded in the repository.

Table 54. Limiting Condition for Case 18.

Start Year	Stop Year	Limiting Condition
1	9	Energy Limited
10	24	Humidity Too Low
25	51	Energy Limited
52	333	Humidity Too Low
334	782	Carbon
783	181817	Phosphorus
181818	182026	Carbon
182027	363635	Phosphorus
363636	364734	Carbon
364735	1000000	Phosphorus

Case 19

This case contains the following variable input parameters: median material lifetimes, in a non-lithophysal repository segment with initial dripping on the waste package.

Results shown on Figure VI-21 indicate that the maximum biomass produced for the entire calculation is 46.17 g_{dry}/m of drift in year 689,655. During the preclosure ventilation period (0 to 51 years) the biomass production was between 10.40 and 31.43 g_{dry}/m of drift during times when the T and RH were below the threshold for growth. Otherwise, no growth occurred until well into the post closure period (in year 324) due to elevated temperatures or low RH. Maximum biomass growth from the degradation of ground support of 12.24 g_{dry}/m occurred in year 400 due to the degradation of the steel in the steel sets. The biomass decreases to 0.28 g_{dry}/m of drift when the final ground support component (cement grout) is degraded in year 10,000. Later, the waste package outer barrier, drip shield, and pallet produced a maximum of 0.12 g_{dry}/m at year 600,001 and the natural ambient system produced a biomass of 0.070 g_{dry}/m after the waste form was degraded in year 714,655. Biomass production during the waste form degradation period (689,655 to 714,655) was at its peak (46.16 g_{dry}/m) due to the rapid degradation of the waste package inner barrier and the basket materials. For the majority of the lifetime of the waste form, the biomass produced ranged between 10.63 and 3.72 g_{dry}/m.

During most of the time period covered by the calculation, the biomass growth in the repository environment is generally nutrient limited by the lack of phosphorous (Table 55). This is due to the lack of phosphorous in the groundwater fluxing into the repository. Prior to year 324, the biomass is generally limited because the RH was too low and the temperature too high to sustain microbial growth. The calculation was energy limited during the preclosure period. During times when the repository is limited by carbon, it is because there is not enough available in the materials being degraded in the repository.

Table 55. Limiting Condition for Case 19.

Start Year	Stop Year	Limiting Condition
1	9	Energy Limited
10	24	Humidity Too Low
25	51	Energy Limited
52	333	Humidity Too Low
334	1189	Carbon
1190	689654	Phosphorus
689655	689822	Carbon
689823	1000000	Phosphorus

Case 20

This case contains the following variable input parameters: median material lifetimes, in a non-lithophysal repository segment with no initial dripping on the waste package.

Results shown on Figure VI-22 indicate that the maximum biomass produced for the entire post closure period in the calculation is 12.21 g_{dry}/m of drift in year 400. During the preclosure ventilation period (0 to 51 years) the biomass production was between 10.31 and 31.40 g_{dry}/m of drift during times when the T and RH were below the threshold for growth. Otherwise, no growth occurred until well into the post closure period (in year 324) due to elevated temperatures or low RH. Maximum biomass growth from the degradation of ground support of 12.21 g_{dry}/m occurred in year 400 due to the degradation of the steel in the steel sets. The biomass decreases to 0.23 g_{dry}/m of drift when the final ground support component (cement grout) is degraded in year 10,000. Later, the drip shield produced a maximum of 0.070 g_{dry}/m at year 600,000. After the drip shield fails the waste package and pallet produce a maximum biomass of 1.12 g_{dry}/m during degradation of the stainless steel in the waste package pallet (pedestal) and a biomass of 0.11 g_{dry}/m for the C-22 alloy materials. No other results were produced due to the longevity of the materials involved.

During most of the time period covered by the calculation, the biomass growth in the repository environment is generally nutrient limited by the lack of phosphorous (Table 56). This is due to the lack of phosphorous in the groundwater fluxing into the repository. Prior to year 324, the biomass is generally limited because the RH was too low and the temperature too high to sustain microbial growth. The calculation was energy limited during the preclosure period. During times when the repository is limited by carbon, it is because there is not enough available in the materials being degraded in the repository.

Table 56. Limiting Condition for Case 20.

Start Year	Stop Year	Limiting Condition
1	9	Energy Limited
10	24	Humidity Too Low
25	51	Energy Limited
52	333	Humidity Too Low
334	480	Carbon
481	1000	Phosphorus
1001	1009	Carbon
1010	1000000	Phosphorus

Case 21

This case contains the following variable input parameters: median material lifetimes, in a lithophysal repository segment and with initial dripping on the waste package.

Results shown on Figure VI-23 indicate that the maximum biomass produced for the entire calculation is 46.17 g_{dry}/m of drift in year 689,655. During the preclosure ventilation period (0 to 51 years) the biomass production was between 15.87 and 24.60 g_{dry}/m of drift during times when the T and RH were below the threshold for growth. Otherwise, no growth occurred until well into the post closure period (in year 324) due to elevated temperatures or low RH. Maximum biomass growth from the degradation of ground support of 14.96 g_{dry}/m occurred in year 400 due to the degradation of the steel in the steel sets. The biomass decreases to 3.85 g_{dry}/m of drift when the final ground support component (gantry rail) is degraded in year 1,255. Later, the waste package outer barrier, drip shield, and pallet produced a maximum of 1.12 g_{dry}/m at year 4700. This decreases to 0.12 g_{dry}/m until the C-22 alloy in the waste package is degraded. The natural ambient system produced a biomass of 0.070 g_{dry}/m after the waste form was degraded in year 714,655. Biomass production during the waste form degradation period (689,655 to 714,655) was at its peak (46.17 g_{dry}/m) due to the rapid degradation of the waste package inner barrier and the basket materials. For the majority of the lifetime of the waste form, the biomass produced ranged between 10.63 and 3.72 g_{dry}/m.

During most of the time period covered by the calculation, the biomass growth in the repository environment is generally nutrient limited by the lack of phosphorous (Table 57). This is due to the lack of phosphorous in the groundwater fluxing into the repository. Prior to year 324, the biomass is generally limited because the RH was too low and the temperature too high to sustain microbial growth. The calculation was energy limited during the preclosure period. During times when the repository is limited by carbon, it is because there is not enough available in the materials being degraded in the repository.

Table 57. Limiting Condition for Case 21.

Start Year	Stop Year	Limiting Condition
1	9	Energy Limited
10	24	Humidity Too Low
25	51	Energy Limited
52	333	Humidity Too Low
334	1169	Carbon
1170	689654	Phosphorus
689655	689822	Carbon
689823	1000000	Phosphorus

Case 22

This case contains the following variable input parameters: median material lifetimes, in a lithophysal repository segment with no initial dripping on the waste package.

Results shown on Figure VI-24 indicate that the maximum biomass produced for the entire post closure period in the calculation is 14.94 g_{dry}/m of drift in year 400. During the preclosure ventilation period (0 to 51 years) the biomass production was between 17.08 and 24.48 g_{dry}/m of rift during times when the T and RH were below the threshold for growth. Otherwise, no growth occurred until well into the post closure period (in year 324) due to elevated temperatures or low RH. Maximum biomass growth from the degradation of ground support of 14.94 g_{dry}/m occurred in year 400 due to the degradation of the steel in the steel sets. The biomass decreases to 2.79 g_{dry}/m of drift when the final ground support component (gantry rail) is degraded in year 1,255. Later, the drip shield produced a maximum of 0.070 g_{dry}/m at year 600,000. After the drip shield fails the waste package and pallet produce a maximum biomass of 1.12 g_{dry}/m during degradation of the stainless steel in the waste package pallet (pedestal) and a biomass of 0.12 g_{dry}/m for the C-22 alloy materials. No other results were produced due to the longevity of the materials involved.

During most of the time period covered by the calculation, the biomass growth in the repository environment is generally nutrient limited by the lack of phosphorous (Table 58). This is due to the lack of phosphorous in the groundwater fluxing into the repository. Prior to year 324, the biomass is generally limited because the RH was too low and the temperature too high to sustain microbial growth. The calculation was energy limited during the preclosure period. During times when the repository is limited by carbon, it is because there is not enough available in the materials being degraded in the repository.

Table 58. Limiting Condition for Case 22.

Start Year	Stop Year	Limiting Condition
1	9	Energy Limited
10	24	Humidity Too Low
25	51	Energy Limited
52	333	Humidity Too Low
334	401	Carbon
402	1000000	Phosphorus

Case 23

This case contains the following variable input parameters: maximum material lifetimes, in a non-lithophysal repository segment with initial dripping on the waste package.

Results shown on Figure VI-25 indicate that the maximum biomass produced for the entire post closure period is 5.39 g_{dry}/m of drift in year 1,010. During the preclosure ventilation period (0 to 51 years) the biomass production was between 11.63 and 14.70 g_{dry}/m of drift during times when the T and RH were below the threshold for growth. Otherwise, no growth occurred until well into the post closure period (in year 324) due to elevated temperatures or low RH. Maximum biomass growth from the degradation of ground support of 5.39 g_{dry}/m occurred in year 1,010 due to the degradation of the steel in the steel sets. The biomass decreases to 0.12 g_{dry}/m of drift when the final ground support component (cement grout) is degraded in year 100,000. Later, the waste package outer barrier, drip shield, and pallet produced a maximum of 0.076 g_{dry}/m at year 1,000,000. No other results were produced due to the longevity of the materials involved.

During most of the time period covered by the calculation, the biomass growth in the repository environment is generally nutrient limited by the lack of phosphorous (Table 59). This is due to the lack of phosphorous in the groundwater fluxing into the repository. Prior to year 324, the biomass is generally limited because the RH was too low and the temperature too high to sustain microbial growth. The calculation was not energy limited at any time. During times when the repository is limited by carbon, it is because there is not enough available in the materials being degraded in the repository.

Table 59. Limiting Condition for Case 23.

Start Year	Stop Year	Limiting Condition
1	9	Carbon
10	24	Humidity Too Low
25	51	Carbon
52	333	Humidity Too Low
334	1039	Carbon
1040	1000000	Phosphorus

Case 24

This case contains the following variable input parameters: maximum material lifetimes, in a non-lithophysal repository segment with no initial dripping on the waste package.

Results shown on Figure VI-26 indicate that the maximum biomass produced for the entire post closure period in the calculation is 5.39 g_{dry}/m of drift in year 1,010. During the preclosure ventilation period (0 to 51 years) the biomass production was between 11.63 and 14.70 g_{dry}/m of drift during times when the T and RH were below the threshold for growth. Otherwise, no growth occurred until well into the post closure period (in year 324) due to elevated temperatures or low RH. Maximum biomass growth from the degradation of ground support of 5.39 g_{dry}/m occurred in year 1,010 due to the degradation of the steel in the steel sets. The biomass decreases to 0.10 g_{dry}/m of drift when the final ground support component (cement grout) is degraded in year 50,000. Later, the drip shield produced a maximum of 0.070 g_{dry}/m at year 1,000,000. No other results were produced due to the longevity of the materials involved.

During most of the time period covered by the calculation, the biomass growth in the repository environment is generally nutrient limited by the lack of phosphorous (Table 60). This is due to the lack of phosphorous in the groundwater fluxing into the repository. Prior to year 324, the biomass is generally limited because the RH was too low and the temperature too high to sustain microbial growth. The calculation was not energy limited at any time. During times when the repository is limited by carbon, it is because there is not enough available in the materials being degraded in the repository.

Table 60. Limiting Condition for Case 24.

Start Year	Stop Year	Limiting Condition
1	9	Carbon
10	24	Humidity Too Low
25	51	Carbon
52	333	Humidity Too Low
334	1029	Carbon
1030	1000000	Phosphorus

Case 25

This case contains the following variable input parameters: maximum material lifetimes, in a lithophysal repository segment and with initial dripping on the waste package.

Results shown on Figure VI-27 indicate that the maximum biomass produced for the entire post closure period is 6.48 g_{dry}/m of drift in year 1,010. During the preclosure ventilation period (0 to 51 years) the biomass production was between 12.71 and 15.78 g_{dry}/m of drift during times when the T and RH were below the threshold for growth. Otherwise, no growth occurred until well into the post closure period (in year 324) due to elevated temperatures or low RH. Maximum

biomass growth from the degradation of ground support of 6.48 g_{dry}/m occurred in year 1,010 due to the degradation of the steel in the steel sets. The biomass decreases to 1.21 g_{dry}/m until year 3,175 when the gantry rails finish degrading. The biomass again decreases to 0.12 g_{dry}/m of drift when the waste package support pallet (pedestal) is degrading, which lasts until year 100,000. Later, the waste package outer barrier, drip shield, and pallet produced a maximum of 0.076 g_{dry}/m at year 1,000,000. No other results were produced due to the longevity of the materials involved.

During most of the time period covered by the calculation, the biomass growth in the repository environment is generally nutrient limited by the lack of phosphorous (Table 61). This is due to the lack of phosphorous in the groundwater fluxing into the repository. Prior to year 324, the biomass is generally limited because the RH was too low and the temperature too high to sustain microbial growth. The calculation was not energy limited at any time. During times when the repository is limited by carbon, it is because there is not enough available in the materials being degraded in the repository.

Table 61. Limiting Condition for Case 25.

Start Year	Stop Year	Limiting Condition
1	9	Carbon
10	24	Humidity Too Low
25	51	Carbon
52	333	Humidity Too Low
334	1013	Carbon
1014	1000000	Phosphorus

Case 26

This case contains the following variable input parameters: maximum material lifetimes, in a lithophysal repository segment with no initial dripping on the waste package.

Results shown on Figure VI-28 indicate that the maximum biomass produced for the entire post closure period in the calculation is 6.47 g_{dry}/m of drift in year 1,010. During the preclosure ventilation period (0 to 51 years) the biomass production was between 12.71 and 15.78 g_{dry}/m of drift during times when the T and RH were below the threshold for growth. Otherwise, no growth occurred until well into the post closure period (in year 324) due to elevated temperatures or low RH. Maximum biomass growth from the degradation of ground support of 6.47 g_{dry}/m occurred in year 1,010 due to the degradation of the steel in the steel sets. The biomass decreases to 1.16 g_{dry}/m until year 3,175 when the gantry rails finish degrading. Later, the drip shield produced a maximum of 0.070 g_{dry}/m at year 1,000,000. No other results were produced due to the longevity of the materials involved.

During most of the time period covered by the calculation, the biomass growth in the repository environment is generally nutrient limited by the lack of phosphorous (Table 62). This is due to

the lack of phosphorous in the groundwater fluxing into the repository. Prior to year 324, the biomass is generally limited because the RH was too low and the temperature too high to sustain microbial growth. The calculation was not energy limited at any time. During times when the repository is limited by carbon, it is because there is not enough available in the materials being degraded in the repository.

Table 62. Limiting Condition for Case 26.

Start Year	Stop Year	Limiting Condition
1	9	Carbon
10	24	Humidity Too Low
25	51	Carbon
52	333	Humidity Too Low
334	1013	Carbon
1014	1000000	Phosphorus

6.6.3.2 Backfill Sensitivity Cases

Case 27

This case is the same as Case 21 with the backfill option included

Results shown on Figure VI-29 indicate that the maximum biomass produced for the entire calculation is 67.11 g_{dry}/m of drift in year 689,655. During the preclosure ventilation period (0 to 51 years) the biomass production was between 24.56 and 35.15 g_{dry}/m of drift during times when the T and RH were below the threshold for growth. Otherwise, no growth occurred until well into the post closure period (in year 324) due to elevated temperatures or low RH. Maximum biomass growth from the degradation of ground support of 16.61 g_{dry}/m occurred in year 400 due to the degradation of the steel in the steel sets. The biomass decreases to 3.93 g_{dry}/m of drift when the final ground support component (gantry rail) is degraded in year 1,255. Later, the waste package outer barrier, drip shield, and pallet produced a maximum of 1.26 g_{dry}/m at year 4700. This decreases to 0.26 g_{dry}/m until the C-22 alloy in the waste package is degraded. The natural ambient system produced a biomass of 0.21 g_{dry}/m after the waste form was degraded in year 714,655. Biomass production during the waste form degradation period (689,655 to 714,655) was at its peak (67.11 g_{dry}/m) due to the rapid degradation of the waste package inner barrier and the basket materials. For the majority of the lifetime of the waste form, the biomass produced ranged between 10.77 and 3.86 g_{dry}/m.

During most of the time period covered by the calculation, the biomass growth in the repository environment is generally nutrient limited by the lack of phosphorous (Table 63). This is due to the lack of phosphorous in the groundwater fluxing into the repository. Prior to year 324, the biomass is generally limited because the RH was too low and the temperature too high to sustain microbial growth. The calculation was energy limited during the preclosure period. During times when the repository is limited by carbon, it is because there is not enough available in the materials being degraded in the repository.

Table 63. Limiting Condition for Case 27.

Start Year	Stop Year	Limiting Condition
1	9	Energy Limited
10	24	Humidity Too Low
25	51	Energy Limited
52	333	Humidity Too Low
334	401	Carbon
402	689654	Phosphorus
689655	689822	Carbon
689823	1000000	Phosphorus

Case 28

This case is identical to Case 17 with the backfill added.

Results shown on Figure VI-30 indicate that the maximum biomass produced for the entire calculation is 91.38 g_{dry}/m of drift in year 181,818. During the preclosure ventilation period (0 to 51 years) the biomass production was between 27.26 and 48.08 g_{dry}/m of drift during times when the T and RH were below the threshold for growth. Otherwise, no growth occurred until well into the post closure period (in year 324) due to elevated temperatures or low RH. Maximum biomass growth from the degradation of ground support of 5.39 g_{dry}/m occurred in year 780 due to the degradation of the steel in the gantry rails. Later, the waste package outer barrier, drip shield, and pallet produced a maximum of 0.40 g_{dry}/m at year 150,000 and the natural ambient system produced a biomass of 0.21 g_{dry}/m after the waste form was degraded in year 182,917. Biomass production during the waste form degradation period (181,818 to 182,318) was at its peak (91.38 g_{dry}/m) due to the rapid degradation of the waste package inner barrier and the basket materials. For the majority of the lifetime of the waste form, the biomass produced ranged between 34.68 and 32.72 g_{dry}/m.

During most of the time period covered by the calculation, the biomass growth in the repository environment is generally nutrient limited by the lack of phosphorous (Table 64). This is due to the lack of phosphorous in the groundwater fluxing into the repository. Prior to year 324, the biomass is generally limited because the RH was too low and the temperature too high to sustain microbial growth. The only time that the calculation is energy limited was during the preclosure ventilation period. During times when the repository is limited by carbon, it is because there is not enough available in the materials being degraded in the repository.

Table 64. Limiting Condition for Case 28.

Start Year	Stop Year	Limiting Condition
1	9	Energy Limited
10	24	Humidity Too Low
25	51	Energy Limited
52	333	Humidity Too Low
334	339	Carbon
340	534	Phosphorus
535	619	Carbon
620	181817	Phosphorus
181818	182916	Carbon
182917	1000000	Phosphorus

6.6.4 Ground Support Only (No Emplaced Waste Package) Results

6 separate calculations (Cases 29-34 below) were run without backfill, the waste package, drip shield, and pallet to quantify the impact due to ground support materials. Each of the specific inputs along with all of the universal inputs (Section 6.6.1 above) was entered into MING V1.0 and run.

Case 29

This case contains the following variable input parameters: minimum material lifetime, in a non-lithophysal repository segment.

Results shown on Figure VI-31 indicate that during the preclosure ventilation period (0 to 51 years) the biomass production was between 24.29 and 49.60 g_{dry}/m of drift during times when the T and RH were below the threshold for growth. Otherwise, no growth occurred until well into the post closure period (in year 324) due to elevated temperatures or low RH. Maximum biomass growth from the degradation of ground support of 4.08 g_{dry}/m occurred in year 780 due to the degradation of the steel in the gantry rails. The biomass decreases to 0.70 g_{dry}/m of drift when the final ground support component (cement grout) is degraded in year 2,500.

During most of the time period covered by the calculation, the biomass growth in the repository environment is generally nutrient limited by the lack of phosphorous (Table 65). This is due to the lack of phosphorous in the groundwater fluxing into the repository. Prior to year 324, the biomass is generally limited because the RH was too low and the temperature too high to sustain microbial growth. The only time that the calculation is energy limited was during the preclosure ventilation period. During times when the repository is limited by carbon, it is because there is not enough available in the materials being degraded in the repository.

Table 65. Limiting Condition for Case 29.

Start Year	Stop Year	Limiting Condition
1	9	Energy Limited
10	24	Humidity Too Low
25	51	Energy Limited
52	323	Humidity Too Low
324	782	Carbon
783	1000000	Phosphorus

Case 30

This case contains the following variable input parameters: minimum material lifetime, in a lithophysal repository segment.

Results shown on Figure VI-32 indicate during the preclosure ventilation period (0 to 51 years) the biomass production was between 25.64 and 33.25 g_{dry}/m of drift during times when the T and RH were below the threshold for growth. Otherwise, no growth occurred until well into the post closure period (in year 324) due to elevated temperatures or low RH. Maximum biomass growth from the degradation of ground support of 3.96 g_{dry}/m occurred in year 780 due to the degradation of the steel in the gantry rails. At the end of the calculation, the natural ambient system produced a biomass of 0.070 g_{dry}/m.

During most of the time period covered by the calculation, the biomass growth in the repository environment is generally nutrient limited by the lack of phosphorous (Table 66). This is due to the lack of phosphorous in the groundwater fluxing into the repository. Prior to year 324, the biomass is generally limited because the RH was too low and the temperature too high to sustain microbial growth. The only time that the calculation is energy limited was during the preclosure ventilation period. During times when the repository is limited by carbon, it is because there is not enough available in the materials being degraded in the repository.

Table 66. Limiting Condition for Case 30.

Start Year	Stop Year	Limiting Condition
1	9	Energy Limited
10	24	Humidity Too Low
25	51	Energy Limited
52	323	Humidity Too Low
324	782	Carbon
783	1000000	Phosphorus

Case 31

This case contains the following variable input parameters: median material lifetime, in a non-lithophysal repository segment.

Results shown on Figure VI-33 indicate that during the preclosure ventilation period (0 to 51 years) the biomass production was between 11.34 and 31.40 g_{dry}/m of drift during times when the T and RH were below the threshold for growth. Otherwise, no growth occurred until well into the post closure period (in year 324) due to elevated temperatures or low RH. Maximum biomass growth from the degradation of ground support of 12.21 g_{dry}/m occurred in year 400 due to the degradation of the steel in the steel sets. It decreases to 5.05 g_{dry}/m with the degradation of the rock bolts in year 480 and to 2.96 g_{dry}/m with the degradation of the gantry rails in 1,255. The biomass decreases to 0.23 g_{dry}/m of drift when the final ground support component (cement grout) is degraded in year 10,000. Later, at the end of the calculation the natural ambient system produces a biomass of 0.070 g_{dry}/m.

During most of the time period covered by the calculation, the biomass growth in the repository environment is generally nutrient limited by the lack of phosphorous (Table 67). This is due to the lack of phosphorous in the groundwater fluxing into the repository. Prior to year 324, the biomass is generally limited because the RH was too low and the temperature too high to sustain microbial growth. The calculation is energy limited during the preclosure ventilation period. During times when the repository is limited by carbon, it is because there is not enough available in the materials being degraded in the repository.

Table 67. Limiting Condition for Case 31.

Start Year	Stop Year	Limiting Condition
1	9	Energy Limited
10	24	Humidity Too Low
25	51	Energy Limited
52	323	Humidity Too Low
324	480	Carbon
481	1000	Phosphorus
1001	1009	Carbon
1010	1000000	Phosphorus

Case 32

This case contains the following variable input parameters: median material lifetime, in a lithophysal repository segment.

Results shown on Figure VI-34 indicate that during the preclosure ventilation period (0 to 51 years) the biomass production was between 15.80 and 25.65 g_{dry}/m of drift during times when the T and RH were below the threshold for growth. Otherwise, no growth occurred until well into the post closure period (in year 324) due to elevated temperatures or low RH. Maximum

biomass growth from the degradation of ground support of 14.94 g_{dry}/m occurred in year 400 due to the degradation of the steel in the steel sets. It decreases to 2.79 g_{dry}/m with the degradation of the gantry rails in 1,255. Later, at the end of the calculation the natural ambient system produces a biomass of 0.070 g_{dry}/m.

During most of the time period covered by the calculation, the biomass growth in the repository environment is generally nutrient limited by the lack of phosphorous (Table 68). This is due to the lack of phosphorous in the groundwater fluxing into the repository. Prior to year 324, the biomass is generally limited because the RH was too low and the temperature too high to sustain microbial growth. The calculation is energy limited during the preclosure ventilation period. During times when the repository is limited by carbon, it is because there is not enough available in the materials being degraded in the repository.

Table 68. Limiting Condition for Case 32.

Start Year	Stop Year	Limiting Condition
1	9	Energy Limited
10	24	Humidity Too Low
25	51	Energy Limited
52	323	Humidity Too Low
324	401	Carbon
402	1000000	Phosphorus

Case 33

This case contains the following variable input parameters: maximum material lifetime, in a non-lithophysal repository segment.

Results shown on Figure VI-35 indicate that during the preclosure ventilation period (0 to 51 years) the biomass production was between 11.63 and 14.70 g_{dry}/m of drift during times when the T and RH were below the threshold for growth. Otherwise, no growth occurred until well into the post closure period (in year 324) due to elevated temperatures or low RH. Maximum biomass growth from the degradation of ground support of 5.39 g_{dry}/m occurred in year 1,010 due to the degradation of the steel in the steel sets. It decreases to 2.64 g_{dry}/m with the degradation of the rock bolts in year 1,210 and to 1.19 g_{dry}/m with the degradation of the gantry rails in 3,150. The biomass decreases to 0.10 g_{dry}/m of drift when the final ground support component (cement grout) is degraded in year 50,000. Later, at the end of the calculation the natural ambient system produces a biomass of 0.070 g_{dry}/m.

During most of the time period covered by the calculation, the biomass growth in the repository environment is generally nutrient limited by the lack of phosphorous (Table 69). This is due to the lack of phosphorous in the groundwater fluxing into the repository. Prior to year 324, the biomass is generally limited because the RH was too low and the temperature too high to sustain microbial growth. The calculation is always nutrient limited. During times when the repository is

limited by carbon, it is because there is not enough available in the materials being degraded in the repository.

Table 69. Limiting Condition for Case 33.

Start Year	Stop Year	Limiting Condition
1	9	Carbon
10	24	Humidity Too Low
25	51	Carbon
52	323	Humidity Too Low
324	1029	Carbon
1030	1000000	Phosphorus

Case 34

This case contains the following variable input parameters: maximum material lifetime, in a lithophysal repository segment.

Results shown on Figure VI-36 indicate that during the preclosure ventilation period (0 to 51 years) the biomass production was between 12.71 and 15.78 g_{dry}/m of drift during times when the T and RH were below the threshold for growth. Otherwise, no growth occurred until well into the post closure period (in year 324) due to elevated temperatures or low RH. Maximum biomass growth from the degradation of ground support of 6.47 g_{dry}/m occurred in year 1,010 due to the degradation of the steel in the steel sets. It decreases to 1.16 g_{dry}/m with the degradation of the gantry rails in year 3,150. Later, at the end of the calculation the natural ambient system produces a biomass of 0.070 g_{dry}/m.

During most of the time period covered by the calculation, the biomass growth in the repository environment is generally nutrient limited by the lack of phosphorous (Table 70). This is due to the lack of phosphorous in the groundwater fluxing into the repository. Prior to year 324, the biomass is generally limited because the RH was too low and the temperature too high to sustain microbial growth. The calculation is always nutrient limited. During times when the repository is limited by carbon, it is because there is not enough available in the materials being degraded in the repository.

Table 70. Limiting Condition for Case 34.

Start Year	Stop Year	Limiting Condition
1	9	Carbon
10	24	Humidity Too Low
25	51	Carbon
52	323	Humidity Too Low
324	1013	Carbon
1014	1000000	Phosphorus

6.6.5 TSPA SR Abstraction

6.6.5.1 Calculation Comparisons

CSNF No Backfill

Figure 11 depicts a comparison between all the backfill calculations done for the CSNF waste form. These cases show the maximum biomass that could be present on the waste package and the waste form given the uncertainty in the repository due to various environmental conditions.

The material lifetime has a significant impact on peak growth for any microbial community that could be present on the waste package. With shorter material lifetimes the biofilm growth is limited because the material degrades before the environmental conditions will allow the growth of microbes. With longer lifetimes the nutrient availability is not as abundant. Longer lifetimes also delay the large growth due to degradation of the waste package internal components.

For dripping cases, there is increased growth due to additional material availability. The non-dripping cases tend to decrease the numbers of microbes that can interact with the waste package, but only delay the large peaks after the waste package is breached.

Finally, the biomass produced from the degradation of the ground support in the non-lithophysal areas as opposed to the lithophysal areas is higher due to increased nutrient and energy availability.

CSNF Backfill Sensitivity Figure 12 depicts the comparison between the backfill sensitivity calculations. The only significant difference between the backfill and no backfill calculations was the increase in percolation flux into the drift. This three-fold difference caused a notable increase in microbial abundance. Clearly the backfill cases will yield more microbes.

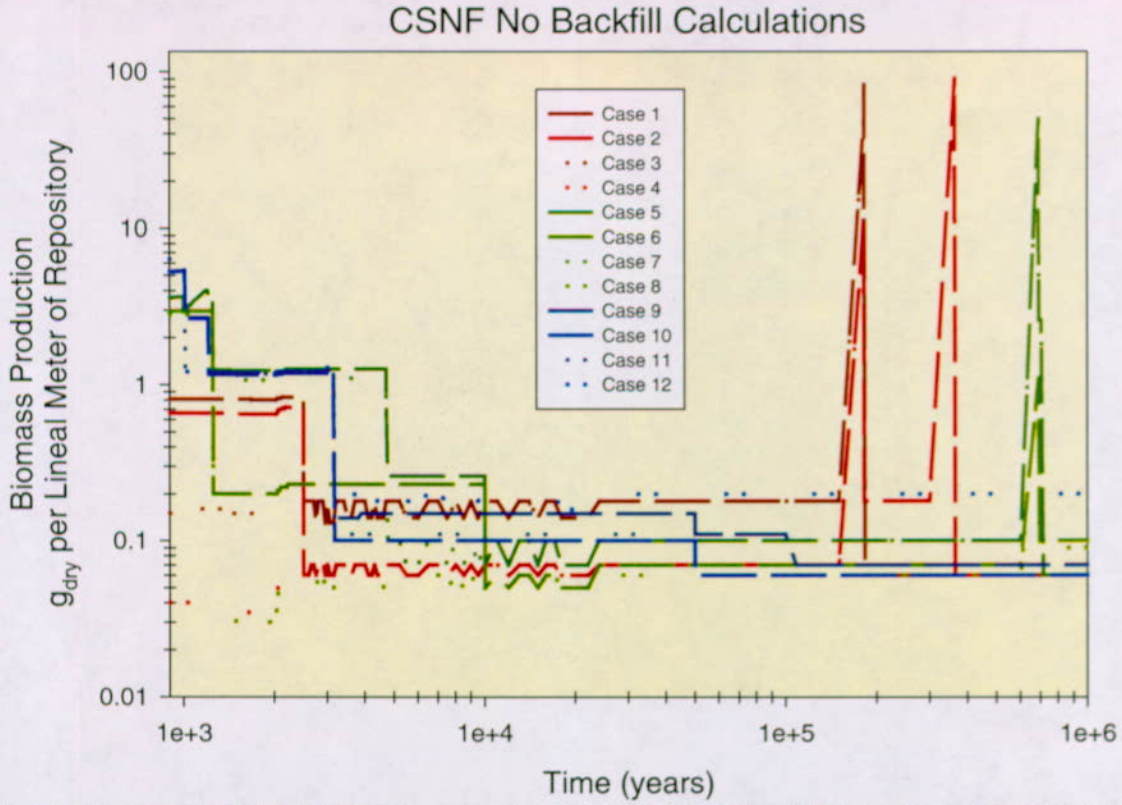

Figure 11. Results of CSNF Calculations for the No Backfill Design Option where the Dashed Lines Represent the Non-lithophysal Portions of the Repository Drift and Dotted Lines Represent the Lithophysal Portions of the Drift. The Dark Colors Represent the Dripping Cases and the Lighter Colors Represent the No Dripping Cases. The Red, Green, and Blue Colors Represent Minimum, Median, and Maximum Material Lifetimes, Respectively.

CSNF BWR PWR Comparison

Figure 13 shows a sensitivity comparison between a PWR waste package and a BWR waste package. The results seem to indicate that there is no real significant difference. However, there is a slight increase in biomass due to the waste package internals.

The material lifetime has a significant impact on peak growth for any microbial community that could be present on the waste package. With shorter material lifetimes the biofilm growth is limited because the material degrades before the environmental conditions will allow the growth of microbes. With longer lifetimes the nutrient availability is not as abundant. Longer lifetimes also delay the large growth due to degradation of the waste package internal components.

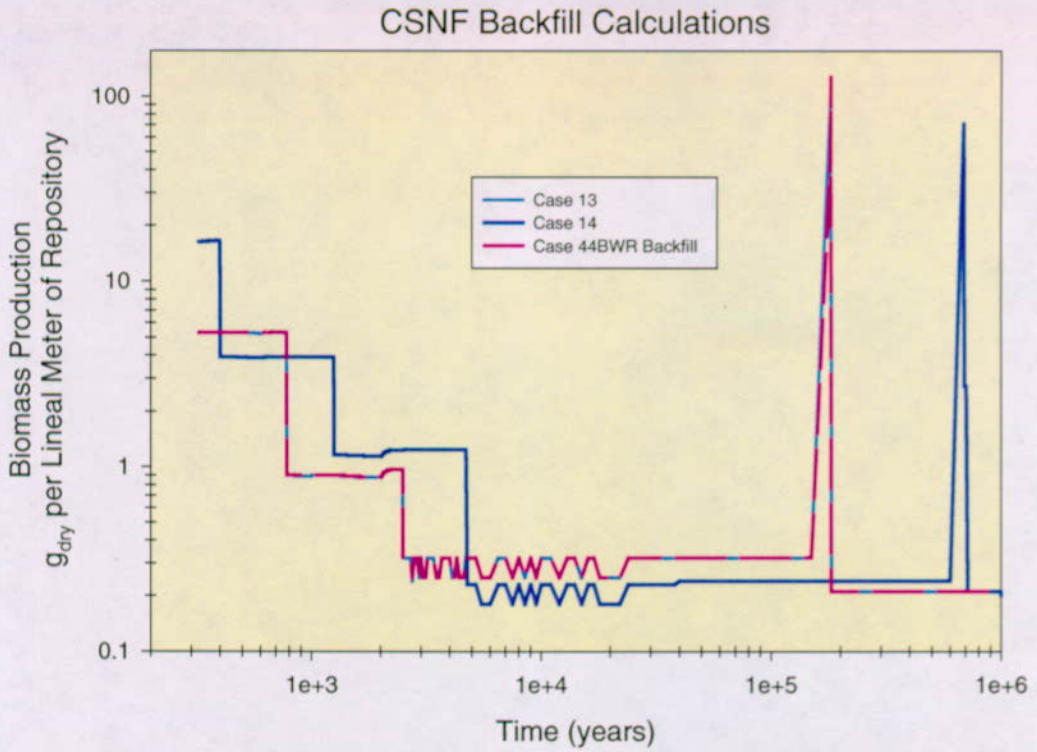

Figure 12. Results of CSNF Calculations for the Backfill Design Sensitivity

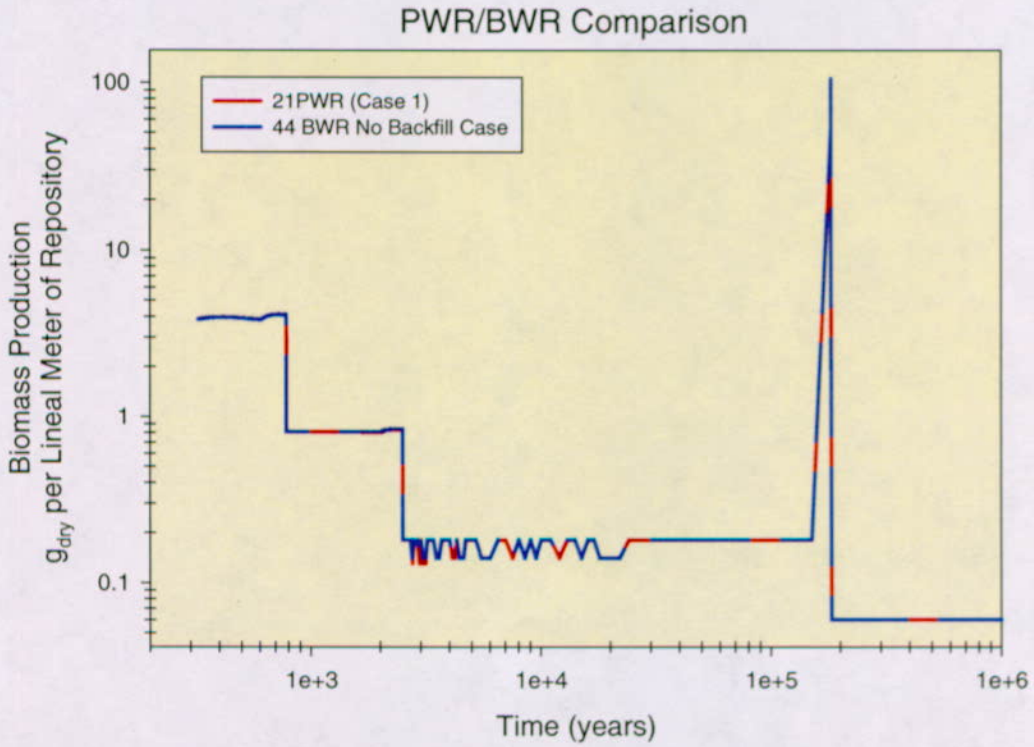

Figure 13. Results of Comparison Between 21PWR (Case 1) and 44 BWR Calculations.

HLW No Backfill Cases

Figure 14 depicts a comparison between all the no backfill calculations done for the HLW glass waste form. These cases show the maximum biomass that could be present on the waste package and the waste form given the uncertainty in the repository due to various environmental conditions.

For dripping cases, there is increased growth due to additional material availability. The non-dripping cases tend to decrease the numbers of microbes that can interact with the waste package, but only delay the large peaks after the waste package is breached.

Finally, the biomass produced from the degradation of the ground support in the non-lithophysal areas as opposed to the lithophysal areas are higher due to increased nutrient and energy availability.

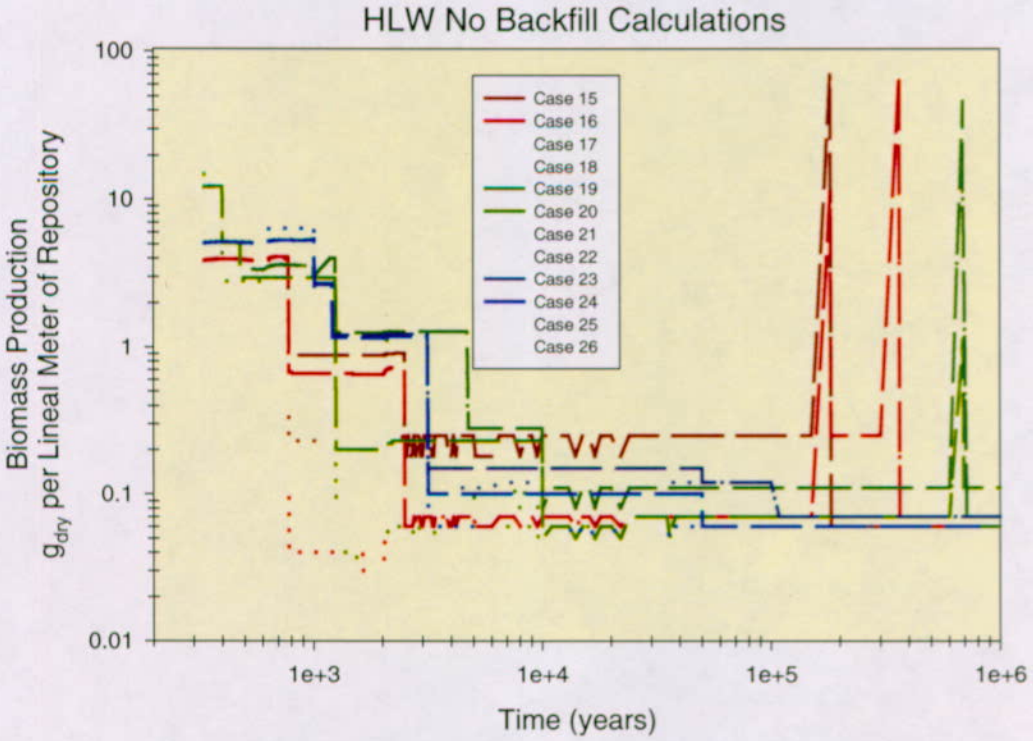

Figure 14. Results of HLW Calculations for the No Backfill Design Option where the Dashed Lines Represent the Non-lithophysal Portions of the Repository Drift and Dotted Lines Represent the Lithophysal Portions of the Drift. The Dark Colors Represent the Dripping Cases and the Lighter Colors Represent the No Dripping Cases. The Red, Green, and Blue Lines Represent Minimum, Median, and Maximum Material Lifetimes, Respectively.

HLW Backfill Sensitivity

Figure 15 depicts the comparison between all the backfill sensitivity calculations. The only significant difference between the backfill and no backfill calculations was the increase in percolation-flux into the drift. This three-fold difference caused a notable decrease in microbial abundance. Clearly, the backfill cases will yield more microbes.

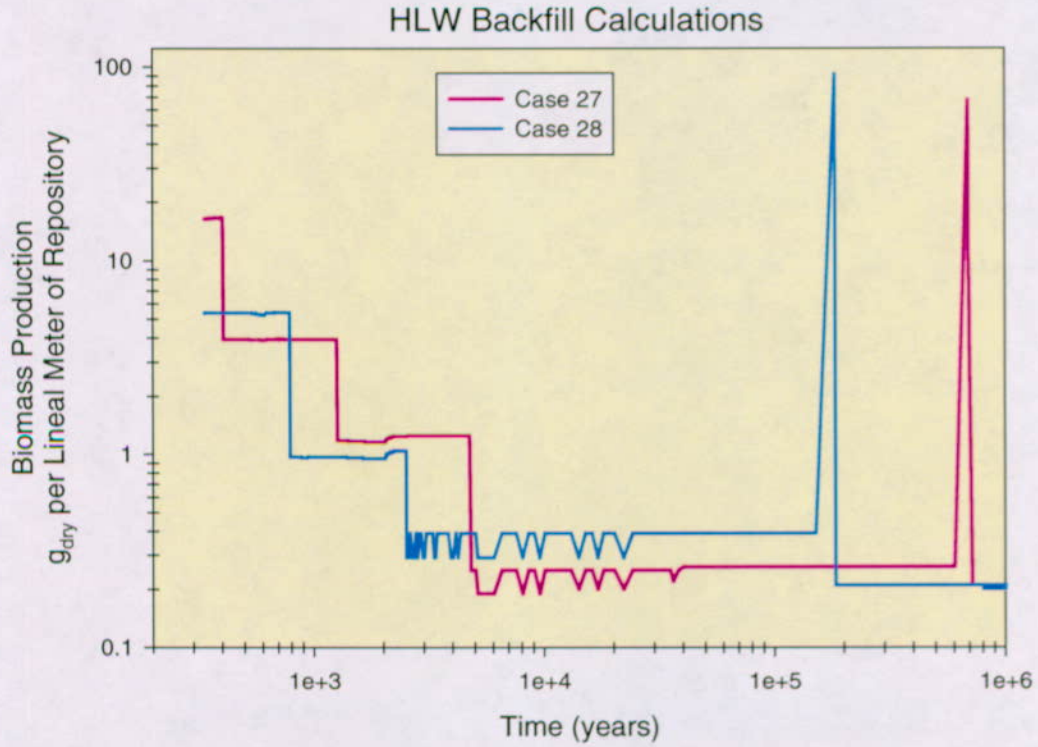

Figure 15. Results of HLW Calculations for the Backfill Design Sensitivity.

Ground Support Only

Figure 16 shows a comparison of results that only include calculations where the ground support was considered (the waste package and pallet was excluded). This figure shows that the material lifetime is the most significant factor with the type of ground support materials (non-lithophysal areas as opposed to the lithophysal areas) the second largest factor behind the biomass produced as a result of the ground support.

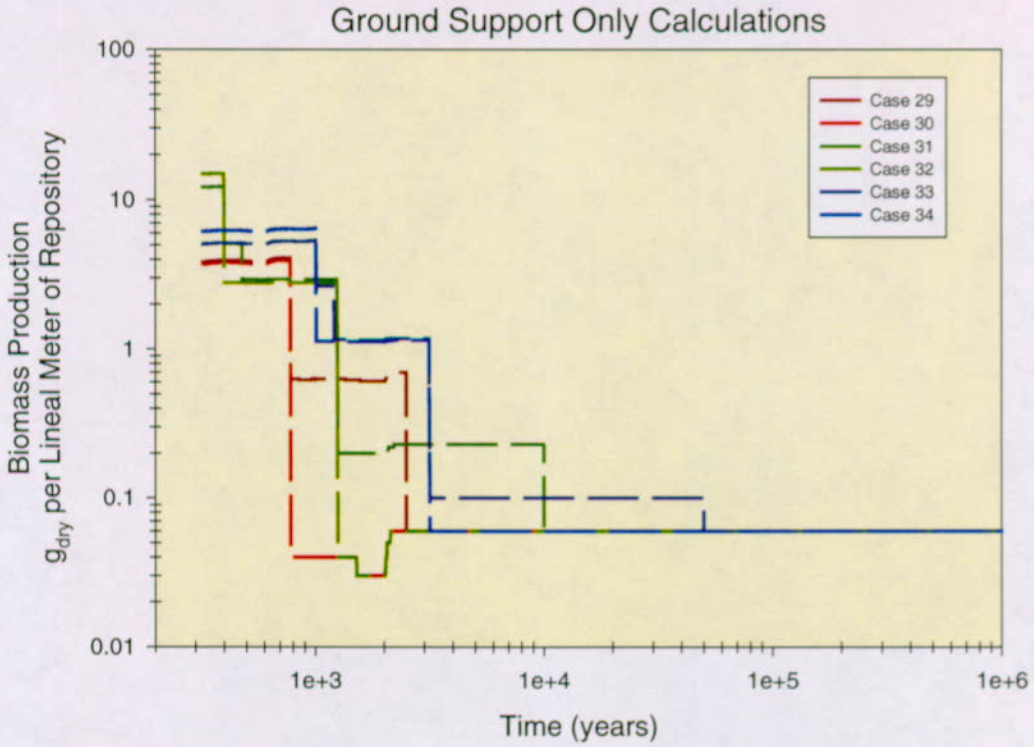

Figure 16. Results of Ground Support Only Calculations.

Other Issues

When one compares the differences between the HLW results and the CSNF results, the glass waste does produce about half the peak growth due to the nature of the glass waste.

In addition to the differences in results, the model does show that for all calculations the limiting nutrients are chiefly phosphorous and at times carbon. Additionally, the amount of percolation flux into the drift does impact the results as we see three fold increases in biomass produced in the post EBS materials degradation environment due to the backfill versus no backfill.

6.6.5.2 Potential Colloids

As discussed in Section 6.3.1.13, microbes can be thought of as colloids because they show some of the same behaviors that abiotic colloidal particles do. Table 71 reports an abstraction of results where only the most bounding (in terms of numbers of microbes produced) cases are shown. In order to estimate the potential numbers of microbial "organic" colloids that could be available from these cases for transport out of the repository drift, the numbers of microbes have to be determined. This is done by taking the maximum biomass produced from the cases shown on

Table 71 and applying the same method as outlined in Section 6.6.3.3 below where Equation 8 is used on a per meter of drift basis (see note below on Table 71). The MING results selected are shown on Table 71 below.

After the numbers of microbes are determined, the numbers of particles per ml of flux is then determined. This is done by dividing the # of microbes from Table 71 by the product of the long-term percolation flux (Table 72) and the cross sectional area of 1 meter of drift wall (5.5m drift diameter x 1 meter length of drift x π = 17.28 m^2). The results are shown on Table 73.

Table 71. Bounding Cases and The Numbers of Microbes Produced Per Meter of Drift.

Description	CSNF			HLW		
	Case #	MING Results (g_{dry}/m)	# of Microbes	Case #	MING Results (g_{dry}/m)	# of Microbes
Bounding Values for WP Surface and Ground Support Components	7	14.96	9.97E+13	21	14.96	9.97E+13
Bounding Values for PWR/HLW Waste Forms	1 to 4	90.48	6.03E+14	15 to 18	70.44	4.70E+14
Bounding Values for BWR Waste Form	44BWR No Backfill	106.93	7.13E+14	N/A	N/A	N/A
Bounding Values for the Waste Form in the Backfill Cases	44BWR With Backfill	127.86	8.52E+14	28	91.38	6.09E+14
Ambient Value for No Backfill Cases*	All	0.070	4.67E+11	All	0.070	4.67E+11
Ambient Value for Backfill Cases*	All	0.21	1.40E+12	All	0.21	1.40E+12

*Results are identical for HLW and CSNF

Note The mass of an average microbe is determined by taking the information for average water content (99% by wt.) and microbial volume (1.5E-13 cm^3) from DTN: MO9909SPAMICRO.001 (Table 17) and calculating the mass of a microbe (1.5E-13 g) using assumption 2 in Attachment I.

Table 72. Long-term Percolation Flux for No Backfill and Backfill Cases.

Long-term Percolation Flux	Backfill Cases	No Backfill Cases
For all cases as abstracted from Figure 7 (time = 1,000,000)	107 mm/yr	35.5 mm/yr

Table 73. Potential In-Drift and Waste Form Microbial Colloids.

Description	CSNF (Microbes per ml of flux)	HLW (Microbes per ml of flux)
Bounding Values for WP Surface and Ground support components	1.63E+11	1.63E+11
Bounding Values for WP internals and waste form components	(PWR) 9.83E+11 (BWR) 1.16E+12	7.66E+11
Ambient Value (No Backfill)	7.61E+08	7.61E+08

6.6.5.3 Bounding Biofilm Size

Because biofilms are known to form (Section 6.3.1.14) and can cause MIC and production of extracellular organic polymers, bounding the extent that a biofilm might form on a waste package or the fuel assembly is prudent. The size of the biofilm that could be present on the waste package can be determined by bounding the dimensionality of the potential biofilm. Thus, the most conservative biofilm that could be applied to the waste package or fuel assembly surface would be a biofilm that was a single microbe thick. This would allow for the largest affected area on the waste package or fuel assembly. This is based on the understanding that biofilms tend to form microcolonies or films (Little et al. 1997) and would be present on the waste package or fuel assembly in localized areas.

Calculations for the both the waste package surface and fuel assembly surface using this bounding argument is presented below with results shown on Table 74. First calculations of the surface area of one meter of spent fuel and the waste package surface need to be determined. The most conservative surface areas are on non-corroded waste packages and waste forms. Surface area will only increase over time due to corrosion or other destructive processes. Then the surface area covered by the available microbes has to be determined. Once these values have been determined then the ratio of waste package area to microbial surface area will give the total surface area of the waste package or spent fuel that can be covered by the bounding biofilm.

The most conservative surface area of one meter of waste package having a outer shell diameter of 1.564 meters (CRWMS M&O 2000g) was determined using the formula for surface area of a right curricular cylinder ($2\pi rh$). The most conservative surface area of one meter of spent fuel in the PWR waste package with 21 assemblies per package and 264 rods per assembly with each fuel rod having a diameter of 0.95 cm (CRWMS M&O 2000m) was determined in the same manner. The results are shown on Table 74.

For the surface area of microbes, Table 71 gives the bounding numbers of microbes that could be present on the waste package or the waste form. These values are then converted to a single microorganism layer biofilm using the following arguments. First, the volume of an average microbe is converted to m^3 (1.5 E-13 ml [from Table 17] x 1.0E-6 m^3/ml = 1.5E-19 m^3). This value is then used to determine the surface area that can be occupied by a microbe. Microbes are often thought of as rod or spherical shaped, therefore the volume can be used to determine the

diameter of a sphere or the radius of a right circular cylinder using the mathematical formulas for calculating the volume of a sphere ($\pi d^3/6$) or a cylinder ($h\pi r^2$). For this calculation, a spherical shape was used and results in a diameter of 6.59E-07 m. This diameter (6.59E-07 m) was used to determine the individual surface area that one microbe can occupy or the area of a circle (πr^2) resulting in a surface area of 3.41E-13 m^2. This area is then multiplied by the number of microbes available to both the waste package surface (9.97E+13) and the BWR spent fuel (7.13E+14) found on Table 71 to give the calculated surface area covered by microbes. The results are shown on Table 74. To determine the percent of material surface area covered by a one microbe thick biofilm the surface area available from the microbes is divided by the surface area of the material to determine the biofilm coverage or the percent of the material surface area covered by the microbes. This percent is shown in the last column in Table 74.

Table 74. Determination of Biofilm Coverage on One Meter of Waste Package and Spent Fuel Assembly Surface.

Material	Calculated Surface Area--Microbes (m^2)	Calculated Surface Area--Material (m^2)	Percent of Material Surface Area Covered
Waste Package Surface	34.0	4.91	692.56%
Spent Fuel (PWR)	205.81	165.46	124.39%

6.6.5.4 Generation of CO_2 Gas and Consumption of O_2 Gas Via Microbial Respiration

In order to understand the impacts of CO_2 gas generation on the in-drift geochemical environment, a bounding estimate is discussed below and is based on assumption 5.12 above. The calculation is based on the methodology discussed in Morel and Hering (1993, Chapter 4 Section 7.1) where protoplasm term for a chemical reaction is equated to the major elements in an algal biomass and the respiratory process is defined by the following reactions:

$$\text{Protoplasm} = C_{106}H_{263}O_{110}N_{16}P_1$$

$$\text{Protoplasm} + 138O_2 \Rightarrow 106CO_2 + 16NO_3^- + H_2PO_4^- + 122H_2O + 17H^+$$

Therefore, if we equate our microbe stoichiometric formula [$C_{160}(H_{280}O_{80})N_{30}P_2S$; Table 17] to the protoplasm term, we can then determine the an estimate of the number of moles of CO_2 that could be generated by a given number of moles of microbes. Thus, a maximum of 160 moles of CO_2 could be produced for every mole of microbes that would respire.

Using this term we can then derive a bound on the generation of CO_2 through time for any of the MING outputs. This is determined by taking the molecular dry wt of a microbe (3,998.1 g mol^{-1}, see Section 6.4.2) and determining how many moles of microbe this would represent (i.e. for the maximum biomass from a PWR waste package shown on Table 71; 106.93g / 3998.1 g mol^{-1} = 0.027 mol) and multiplying this by the number of moles of CO_2 (i.e. 160*0.027=4.28 mol produced from 106.93g of biomass) that could be produced. In order to determine the moles of gas per unit volume we divide this result by the volume of a lineal meter of drift or 23.76 m^3 (i.e.

4.28/23.76=0.181 mol/m^3). Figure 17 below was generated in this manner by taking the mass of microbes from each of the case outputs found in Attachment VI, and calculating the moles of CO_2 per cubic meter of drift. Bounding values for the bounding cases are shown on Table 75 below.

Table 75. Bounding Cases and the Moles of CO_2 Produced per Meter of Drift.

Description	CSNF			HLW		
	Case #	MING Results (g_{dry}/m)	Moles CO_2/m	Case #	MING Results (g_{dry}/m)	Moles CO_2/m
Bounding Values for WP Surface and Ground Support Components	7	14.96	0.599	21	14.96	0.599
Bounding Values for PWR Waste Form	1 to 4	90.48	3.62	15 to 18	70.44	2.82
Bounding Values for BWR Waste Form	44BWR No Backfill	106.93	4.28	N/A	N/A	N/A
Bounding Values for the Waste Form in the Backfill Cases	44BWR With Backfill	127.86	5.12	28	91.38	3.66
Ambient Values*	All No Backfill Cases	0.069	0.0027	All Backfill cases	0.21	0.0084

*Results are identical for HLW and CSNF

To understand the significance of this quantity of gas we can compare it to the average yearly flux of CO_2 calculated from Table 8 where we take the 1 million year cumulative flux value and derive an average yearly flux in moles (19.951 x 10^3 g per m^2 per m of drift / 1,000,000 years / 44g CO_2 per mol = 4.5 x 10^{-3} moles/m^3 of drift) and compare it to results from the maximum values from Table 71 calculated above (4.28 moles per meter of drift / 23.7 m^3 per meter of drift = 0.181 moles per m^3). This implies that CO_2 gas generated from microbial respiration could provide up to two orders of magnitude more CO_2 than the average yearly flux calculated from Table 8 during the time when the waste form and waste package internals are being degraded. One caveat needs to be made in that the impact of this generation of gas is dependent on the total flux of gas in the environment. If diffusion of CO_2 into the drift were slow, this would be a significant impact. If diffusive transport is high or advective transport via fractures dominates the flow, the larger volume of gases being transported into the drift would dominate the geochemical environment.

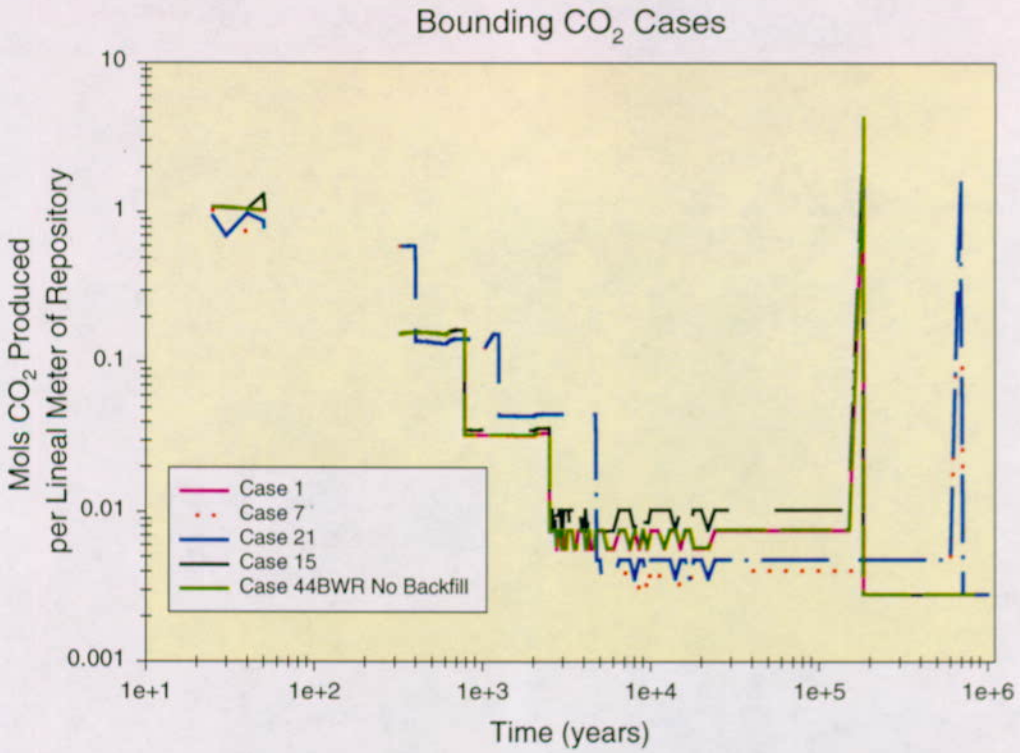

Figure 17. Bounding Cases for CO_2 Gas Generation via Microbial Respiration.

In turn the production of CO_2 gas will consume O_2 gas. If we write out a balanced equation for O_2 consumption based on the microbe stoichiometric formula [$C_{160}(H_{280}O_{80})N_{30}P_2S$; Table 17] and the reactions above we get:

$$C_{160}(H_{280}O_{80})N_{30}P_2S + 209O_2 \Rightarrow 160CO_2 + 80H_2O + 30NO_3^- + 2H_2PO_4^- + H_2S + 114H^+$$

Thus, 209 moles of O_2 would be consumed for each mol of microbes producing CO_2. We can determine the number of moles utilized based on the dry molecular weight of a microbe (3,998.1 g mol^{-1}, see Section 6.4.2) and determining how many moles of microbe this would represent (i.e. for the maximum biomass for PWR waste packages shown on Table 71; 106.92g / 3998.1 g mol^{-1} = 0.027 mol). Multiplying this by the number of moles of O_2 results in 209*0.027=5.59 mol O_2 consumed per 106.92g of biomass or (5.59 mol/m of drift)/(23.7 m^3/m of drift) = 0.236 mol/m^3).

Compare this value to the average yearly flux of O_2 calculated from Table 8 where we take the 1 million year cumulative flux value and derive an average yearly flux of (4.623 x 10^9 g per m^2 per m of drift / 1,000,000 years / 32g O_2 per mol = 144.46 mol/m^3 of drift). These results indicate that there could be sufficient O_2 to produce the calculated quantity of CO_2 gas. Additionally we can determine on a bulk chemistry basis that as long as the O_2 flux remained at levels such as those shown on Table 8, the microbes would not consume the available O_2 during microbial respiration and the drift would remain oxidizing. A mass balance calculation in the *In-Drift Gas Flux and Composition* AMR (CRWMS M&O 2000l) produced a mass balance calculation that indicated that O_2 utilization from the corrosion of steels and alloys in the drifts after 4000 years

was only 14% of the total flux. Therefore, even with the utilization by the microbes there would still remain sufficient O_2 to keep the repository in an oxidizing environment.

6.6.6 Potential Impacts to Bulk Geochemistry

During the first 10,000 years a maximum of eight grams of microbes produced from the materials in a 23.76 m^3 volume (one linear meter of repository) does not seem to be significant, especially when compared to the masses of materials that are to be used in ground support and WPs. In order to put the bulk impact into perspective, during the first 10,000 years for any given year, a maximum of 14.96 grams of microbial mass might be generated from 7154.5 kg (calculated from Tables II-17, III-1, III-5 and III-6 for a 21 PWR waste package in a non lithophysal host rock) of material. This is equivalent to approximately 2.1 parts per million (14.9 ppm for waste form effects). Based on the dry molecular weight of a microbe (3.998.1 g mol^{-1}, see Section 6.4.2) and the number of moles that this represents over the entire volume of the drift segment (i.e. 14.96 or 106.93g / 3998.1 g mol^{-1} / 23.76 m^3), for the waste package effects this would be equivalent to 1.57 x 10^{-4} mol/ m^3 and for waste form effects 1.13 x 10^{-3} mol/m^3. Based on this small mass or abundance of microbes being generated, effects on the bulk chemistry in the drift are expected to be negligible, with the exception of the CO_2 gas generation by this level of microbial activity. Nevertheless, there exists the potential to induce localized impacts to the in-drift geochemistry. Microbes are known to produce inorganic acids, methane, organic byproducts, and other chemical species that could change the longevity of materials and the transport of radionuclides from the drift.

Certainly, 14.96 (or 106.93 for the waste form) grams of microbes would have an impact on corrosion if they were located on a 1-meter segment of WP (or spent fuel) as multiple biofilms, which could then greatly enhance the pitting corrosion of a WP. As currently calculated in Section 6.6.5.3 above 14.96 (or 106.93) grams represent a single biofilm that could cover over 692 percent (or 147 percent for the waste form) of the waste package surface. Fifteen grams of microbes do represent a rather large number of potential organic colloids where the particle flux of 1.63 × 10^{11} microbes/ml (1.16 × 10^{12} for the waste form) could then be released from the repository each year (see Section 6.6.5.4 above).

Not only is the potential number of colloids a significant concern, but microbes tend to stabilize natural colloids by facilitating colloidal agglomeration (see Section 6.3.5.6) and act as chelating agents via production of siderophores (see Section 6.3.5.2). Microbes can also act as surface reactants for dissolved metals (see Section 6.3.5.1). These three qualities can be significant in determining microbial impacts on the transport of radionuclides. With the quantity of gas that could be produced (up to 0.181 moles/m^3 of drift), there could be significant impacts on waste form dissolution and complexation due to the interaction CO_2 has on aqueous carbonate speciation and pH.

6.7 MODEL VALIDATION TEST CASES

The analyses presented below represent model validation tests designed to insure that the conceptual model, software and inputs can be used to assess the microbial growth that may occur

within a potential repository at Yucca Mountain. This will allow evaluation of whether or not microbes should be an issue within the overall bulk geochemistry affecting the water composition within the drift, or if the microbial aspects of the system should be treated further only as they affect localized chemical conditions.

Presented below are three different test sets. The first represents our duplication of the results in the Swiss repository program (see Section 6.7.1). The second set of tests represent a depiction of ambient conditions found in the ESF and at Rainier Mesa (a natural analog) are shown in Section 6.7.2 and the third test set represents the duplication of independent lab experiments conducted at LLNL (Horn et al. 1998a and 1998b; Davis et al. 1998) and are shown in Section 6.7.3.

Our presentation of the Swiss case (Section 6.7.1) demonstrates that MING V1.0 code functions adequately when compared to previous modeling activities using the same type of conceptual model and software code. The ambient tests (Section 6.7.2) demonstrate that the selection of redox equations (Table 18) and how we handle the elemental breakdown of materials (Table V-2) are adequate to produce results that are reasonable when compared to the actual measured system at Yucca Mountain. Finally, duplication of the LLNL lab experiments (Section 6.7.3) will give us a feeling of how much uncertainty can be associated with the modeled results.

In addition to the test cases presented below, the microbial effects model (CRWMS M&O 2000k) which was developed independently of and much later than the concepts in this model (see Section 3.2) shows that the concepts documented above are representative of the microbial processes that are important to be modeled herein. The thresholds discussed in CRWMS M&O (2000k) were the same thresholds that were developed in the conceptual model above, namely no microbial growth in the repository environment above 120°C and no growth below RH of 90. When these two conditions are met CRWMS M&O (2000k) reports that the microbial communities could attack and utilize all EBS materials for energy and nutrients and that the limiting factors are generally the availability of water and nutrients such as phosphate.

6.7.1 Swiss Low-Level Test Case

To build confidence that MING was incorporating the portions of the Swiss LLW/ILW model correctly (Grogan and McKinley 1990, Capon and Grogan 1991), we ran MING using the Swiss model input parameters. Both Grogan and McKinley (1990), and Capon and Grogan (1991) can be used as the source of parameter inputs. For detailed information on how the Swiss model parameter inputs were incorporated into a MING calculation, refer to CRWMS M&O (1998h).

Before results of the benchmark calculation are presented below, two model differences should be spelled out that cause our results to differ very slightly from those reported in Grogan and McKinley (1990) and Capon and Grogan (1991). First, MING does not divide the Swiss calculation into an oxic and an anoxic phase. Therefore, the initial oxygen conditions are not reported in our results. The Swiss model limited this period to the time required to consume the oxygen, which was introduced into a normally anoxic environment due to construction. If we were to incorporate the early oxic phase, the results would be limited to the first year of the calculations, and would not show up in a significant way on our results plots. Second, MING

does not incorporate radiolytic products that are generated within the WP. Early on during MING model development, a decision was made not to incorporate this type of effect as there is little evidence that it would be of concern in a Yucca Mountain repository. This was based on the assessment that radiolysis outside WP should be negligible for the given design thickness (Van Konynenburg 1996; see Section 6.3.1.4 above).

The results indicate that the portions of the nutrient and energy models used in the Swiss model and which are used in MING are operating the same. Figure 18 shows a result comparison for both the energy and nutrient calculations reported by Capon and Grogan (1991) with those calculated with MING. From Figure 18, it can be seen that the results are virtually identical. However, examination of a table of results (Table 76) indicates that there is a slight difference in the energy calculations during the 271- to 3,030-year period. The difference is attributed to not incorporating into MING the radiolytic products produced in the Swiss repository. This indicates that not incorporating those radiolytic effects for the Swiss case resulted in only very minor changes to the results.

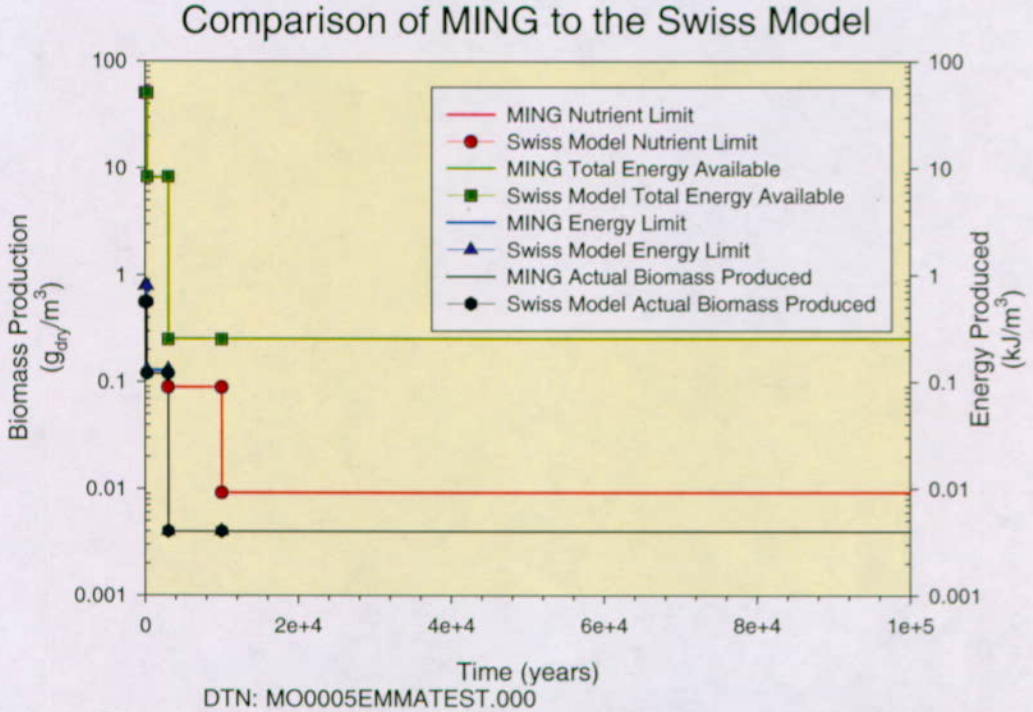

DTN: MO0005EMMATEST.000

Figure 18. Comparison of Swiss Model Results (Capon and Grogan 1991) with MING Calculations of the Swiss Model.

Table 76. Comparison of the Swiss Model Results Using EMMA (Capon and Grogan 1991) with that of the Same Swiss Model Parameters Used in MING.

Time Period (a)	Maximum Energy (kJ/a)		Maximum Biomass (g/a)	
	EMMA	MING	EMMA	MING
0-270	50.6	50.6	0.79	0.791
271-3,030	8.3	8.14	0.13	0.127
3,031-10,000	2.5E-01	2.54E-01	4.0E-03	3.97E-03
10,001+	2.5E-01	2.54E-01	4.0E-03	3.97E-03

DTN: MO0005EMMATEST.000

6.7.2 Ambient ESF and Natural Analog Test Cases

To compare the modeled results of the ambient system in MING with the measurements presented in Section 6.3.2, the ambient populations have to be converted to the equivalent unit of measurement that is reported by MING. Table I-9 reports the grams (dry wt) of microbes in a one-meter length segment of TSw2 tuff having a repository drift radius of 2.55 m. Documentation of this calculation is found in Attachment I. Therefore, based on the ESF measurements, the mass of microbes in one linear meter of repository drift ranges between 0.12 to 1.34 grams (dry). If we were to do an equivalent calculation for low and high values for the Rainier Mesa natural analog site (see assumption 5.6), the value would be as low as 0.36 to 1.81 grams (dry) per linear meter of repository drift.

6.7.2.1 General Ambient Test Case Inputs

Eighteen ambient calculations were done using MING to build confidence in the model and to bound the overall way that MING handles nutrient and energy calculations. The general intent of these calculations is to show that MING gives a reasonable answer. Then we can assume that it would provide estimates that are at least in the order-of-magnitude range for the potential microbial abundance in the near field. These sorts of estimates form the starting point for evaluating which pieces of the system microbial-driven chemistry could have some capacity to influence in-drift geochemistry. Three separate test case sets were developed, each dependant on the nutrient and energy sources that were likely to be encountered: biotite, altered tuff and unaltered tuff.

In all 18 ambient case calculations the following input parameters were utilized: the average composition of J-13 water (Table 77); an average cumulative influx of O_2, N_2 and CO_2 (Table 79) ; a repository temperature of 25°C; and a RH of 0.99 (see assumption 5.2). The average J-13 water chemistry values were taken from Harrar et al. (1990). These values are found on Table 33. Also included with the J-13 water composition was the addition of 1 ppm dissolved organic carbon ([DOC]; converted to the appropriate units and represented as CH_2O in our simplified redox model; see Table V-2) which seems to be the approximate value for DOC in the groundwater at Yucca Mountain (CRWMS M&O 1997b).

Each of the three test case sets differed by altering two inputs that were thought to be the biggest factors to natural microbial variability. They are the water infiltration rate and the material lifetime of the rock.

Due to cyclic climatic change, the water infiltration rate at the surface of Yucca Mountain is thought to fluctuate. Therefore, two cases were used to look at the variability that infiltration has on the ambient system. The values selected were identical to the values used in TSPA-VA calculations (CRWMS M&O 1998a) as shown on Table 78.

In addition to the infiltration rate, the material lifetime for the alteration of the repository host rock seems to be the most uncertain parameter. Because this rate can provide different quantities of nutrients and energy, this parameter was varied.

Each of the three test cases below were run using the matrix of infiltration rates and material lifetimes as shown on Table 78.

Table 77. J-13 Water Compositions Used in MING Calculations.

Groundwater Constituent	Concentration (kmol/m^3)
HCO_3^-	2.12E-03
O_2	1.75E-04
NO_3^-	1.42E-04
SO_4^{2-}	1.92E-04
Mn^{2+}	8.00E-07
Fe^{2+}	5.80E-07
PO_4^{3-}	3.80E-06
*DOC	3.30E-05
pH	7.4

* Data derived from Assumption 5.11.

DTN: MO9909SPA00J13.006

Table 78. Infiltration Rates and Material Lifetimes used in TSPA-VA Ambient Test Cases (see Assumption 5.5).

Test Case	Material Lifetime (years)	Infiltration Rate (mm/yr)
1	10,000,000	7.8
2	1,000,000	7.8
3	100,000	7.8
4	10,000,000	42.06
5	1,000,000	42.06
6	100,000	42.06

DTN: MO9807MWDEQ3/6.005

Cumulative gas flux into the drift values used in the TSPA-VA ambient test cases (CRWMS M&O 1998a) were also used and are shown on Table 79 below.

Table 79. Cumulative Gas Flux Values (kg/m^2) used in the Ambient Test Case Calculations.

Year	CO_2	O_2	N_2	CH_4
1	2.00E-5	4.64E-3	1.85E-2	0
50	1.00E-3	2.32E-1	9.25E-1	0
200	4.00E-3	9.28E-1	3.70E-0	0
3,000	6.00E-2	1.39E+1	5.55E+1	0
5,000	1.00E-1	2.32E+1	9.25E+1	0
27,560	5.55E-1	1.27E+2	5.10E+2	0
28,000	5.60E-1	1.30E+2	5.17E+2	0
50,000	1.00E-0	2.32E+2	9.25E+2	0
100,001	2.00E-0	4.64E+2	1.85E+3	0
1,000,000	2.00E+1	4.64E+3	1.85E+4	0

DTN: MO9911SPACGF04.000

6.7.2.2 Ambient Case Calculations

These analyses are presented in terms of the resultant growth of microbial mass. The mass of microbes that could be produced based on the limiting nutrient or the energy limitations of the system are given in the figures and tables shown below.

6.7.2.2.1 Biotite as Energy Source Test Cases

The first test case set uses the long-term release rate of Fe^{2+} from biotite dissolution (see assumption 5.5). The determination of the maximum mass of biotite that could be potentially found within a 1-meter repository drift volume (460 kg/m) and the available quantity (wt. percent) of Fe that could be released from that amount of biotite (32.7 percent) are documented in Attachment I and are used in these calculations.

In order to utilize biotite as well as the altered and unaltered tuff in the model the biotite parameters from Table 80 need to be entered into MING. These parameters (see Table 80) are based on the same premise used to develop the layer designators and reactant compositions found on Table 34 and Table V-2 respectively, as discussed in Sections 6.5.2.5 and Attachment V.

Table 80. Reactant Compositions and Layer Designator for Biotite (Table I-7, Attachment I), Altered, and Unaltered Tuff (Table 15).

Material Name	Reactant Compositions	Layer Designator
Altered tuff	Fe, Mn^{2+}	0
Unaltered tuff	Fe, Mn^{2+}	0
Biotite	Fe^{2+}	0

Test Specific Conditions

Case 1: This calculation was run in MING using a material lifetime on the biotite (Table I-7) of 10,000,000 years and an infiltration rate of 7.8 mm/yr from Table 78, the gas compositions found on Table 79, and J-13 water (Table 77).

Case 2: This calculation was run in MING using a material lifetime on the biotite (Table I-7) of 1,000,000 years and an infiltration rate of 7.8 mm/ Table 78, the gas compositions found on Table 79, and J-13 water (Table 77).

Case 3: This calculation was run in MING using a material lifetime on the biotite (Table I-7) of 100,000 years and an infiltration rate of 7.8 mm/yr from Table 78, the gas compositions found on Table 79, and J-13 water (Table 77).

Case 4: This calculation was run in MING using a material lifetime on the biotite (Table I-7) of 10,000,000 years and an infiltration rate of 42.06 mm/yr from Table 78, the gas compositions found on Table 79, and J-13 water (Table 77).

Case 5: This calculation was run in MING using a material lifetime on the biotite (Table I-7) of 1,000,000 years and an infiltration rate of 42.06 mm/yr from Table 78, the gas compositions found on Table 79, and J-13 water (Table 77).

Case 6: This calculation was run in MING using a material lifetime on the biotite (Table I-7) of 100,000 years and an infiltration rate of 42.06 mm/yr from Table 78, the gas compositions found on Table 79, and J-13 water (Table 77).

Test Results

Table 81 shows that the system is energy limited. There are sufficient nutrients to produce more microbes. However, the system is limited by phosphorous.

Table 81. Results from MING for Biotite Test Cases 1 to 6.

Test Case	Mass of microbes from available nutrients (g dry)	Energy available in system (kJ mol^{-1})	Mass of microbes from available energy (g dry)	Calculated Mass of microbes (g dry)
1	0.3018745	0.1036498	0.001619529	0.001619529
2	0.3018745	0.8705462	0.01360228	0.01360228
3	0.3018745	8.53951	0.1334298	0.1334298
4	1.6278	0.1846402	0.002885003	0.002885003
5	1.6278	0.9515365	0.01486776	0.01486776
6	1.6278	8.6205	0.1346953	0.1346953

6.7.2.2.2 Altered Tuff Test Cases

Test Specific Conditions

Case 1: This calculation was run in MING using a altered tuff material lifetime (Table 15) of 10,000,000 years and an infiltration rate of 7.8 mm/yr from Table 78, the gas compositions found on Table 79, and J-13 water (Table 77).

Case 2: This calculation was run in MING using an altered tuff material lifetime (Table 15) of 1,000,000 years and an infiltration rate of 7.8 mm/yr from Table 78, the gas compositions found on Table 79, and J-13 water (Table 77).

Case 3: This calculation was run in MING using an altered tuff material lifetime (Table 15) of 100,000 years and an infiltration rate of 7.8 mm/yr from Table 78, the gas compositions found on Table 79, and J-13 water (Table 77).

Case 4: This calculation was run in MING using an altered tuff material lifetime (Table 15) of 10,000,000 years and an infiltration rate of 42.06 mm/yr from Table 78, the gas compositions found on Table 79, and J-13 water (Table 77).

Case 5: This calculation was run in MING using an altered tuff material lifetime (Table 15) of 1,000,000 years and an infiltration rate of 42.06 mm/yr from Table 78, the gas compositions found on Table 79, and J-13 water (Table 77).

Case 6: This calculation was run in MING using an altered tuff material lifetime (Table 15) of 100,000 years and an infiltration rate of 42.06 mm/yr from Table 78, the gas compositions found on Table 79, and J-13 water (Table 77).

Test Results

Table 82 shows that the system is energy limited. There are sufficient nutrients to produce more microbes. However, the system is limited by phosphorous.

Table 82. Results from MING for Altered Tuff Test Cases 1 to 6.

Test Case	Mass of microbes from available nutrients (g dry)	Energy available in system ($kJ\ mol^{-1}$)	Mass of microbes from available energy (g dry)	Calculated Mass of microbes (g dry)
1	0.3569763	0.7591901	0.01186235	0.01186235
2	0.8528919	7.44353	0.1163052	0.1163052
3	2.28205	101.9634	1.593177	1.593177
4	1.682902	0.8316002	0.01299375	0.01299375
5	2.178818	7.51594	0.1174366	0.1174366
6	7.137974	74.35934	1.161865	1.161865

6.7.2.2.3 Unaltered Tuff Test Cases

Test Specific Conditions

Case 1: This calculation was run in MING using an unaltered tuff material lifetime (Table 15) of 10,000,000 years and an infiltration rate of 7.8 mm/yr from Table 78, the gas compositions found on Table 79, and J-13 water (Table 77).

Case 2: This calculation was run in MING using an unaltered tuff material lifetime (Table 15) of 1,000,000 years and an infiltration rate of 7.8 mm/yr from Table 78, the gas compositions found on Table 79, and J-13 water (Table 77).

Case 3: This calculation was run in MING using an unaltered tuff material lifetime (Table 15) of 100,000 years and an infiltration rate of 7.8 mm/yr from Table 78, the gas compositions found on Table 79, and J-13 water (Table 77).

Case 4: This calculation was run in MING using an unaltered tuff material lifetime (Table 15) of 10,000,000 years and an infiltration rate of 42.06 mm/yr from Table 78, the gas compositions found on Table 79, and J-13 water (Table 77).

Case 5: This calculation was run in MING using an unaltered tuff material lifetime (Table 15) of 1,000,000 years and an infiltration rate of 42.06 mm/yr from Table 78, the gas compositions found on Table 79, and J-13 water (Table 77).

Case 6: This calculation was run in MING using an unaltered tuff material lifetime (Table 15) of 100,000 years and an infiltration rate of 42.06 mm/yr from Table 78, the gas compositions found on Table 79, and J-13 water (Table 77).

Test Results

Table 83 shows that the system is energy limited. There are sufficient nutrients to produce more microbes. However, the system is limited by phosphorous.

Table 83. Results from MING for Unaltered Tuff Test Cases 1 to 6.

Test Case	Mass of microbes from available nutrients (g dry)	Energy available in system (kJ mol^{-1})	Mass of microbes from available energy (g dry)	Calculated Mass of microbes (g dry)
1	0.3294254	0.5592371	0.008738079	0.008738079
2	0.5773832	5.444	0.0850625	0.0850625
3	2.28205	74.50928	1.164207	1.164207
4	1.655351	0.6316471	0.009869485	0.009869485
5	1.903309	5.51641	0.0861939	0.0861939
6	4.382887	54.36403	0.849438	0.849438

6.7.2.3 Ambient Case Results

Figure 19 compares the results provided in the three test cases above with the actual measurements taken at Rainer Mesa and in the ESF. They show that all of the measurements are within an order of magnitude and seem reasonable in comparison to the inputs.

Two factors may affect the variability of the results. First there could be some sort of nutrient contamination (not accounted for before sampling) or enhanced growth that allowed the measured ESF and Rainer Mesa tunnel values to be elevated because the sampling took place well after the tunnels were constructed (Kieft et al. 1993, Haldeman and Amy 1993). Second, our model is simplified, and therefore, we may not have included a measurable quantity of an energy-providing nutrient, especially in the Rainier Mesa tests, because TSw2 tuff and J-13 water serve as approximations to the composition of *in situ* materials (see assumption 5.6).

Even with the above factors in mind, the ambient case results seem to indicate that we are modeling the ambient system adequately. The results also indicate the dependence of groundwater composition and flux on microbial growth, especially since the ESF experiments indicate that water is the limiting nutrient in the ambient system (Kieft et al. 1997).

To some extent, the modeling results also indicate that the composition and material lifetime of the altered and unaltered tuff can also play a role in the abundance of microbes. Phosphorous is less abundant in the unaltered tuff and its availability is generally limited to the concentrations found in the tuff. This point is also discussed in the Lawrence Livermore National Laboratory (LLNL) experiments modeled in Section 6.7.3 below. Therefore, the ambient case allows us to have increased confidence that MING can produce reasonable modeling results for the repository system.

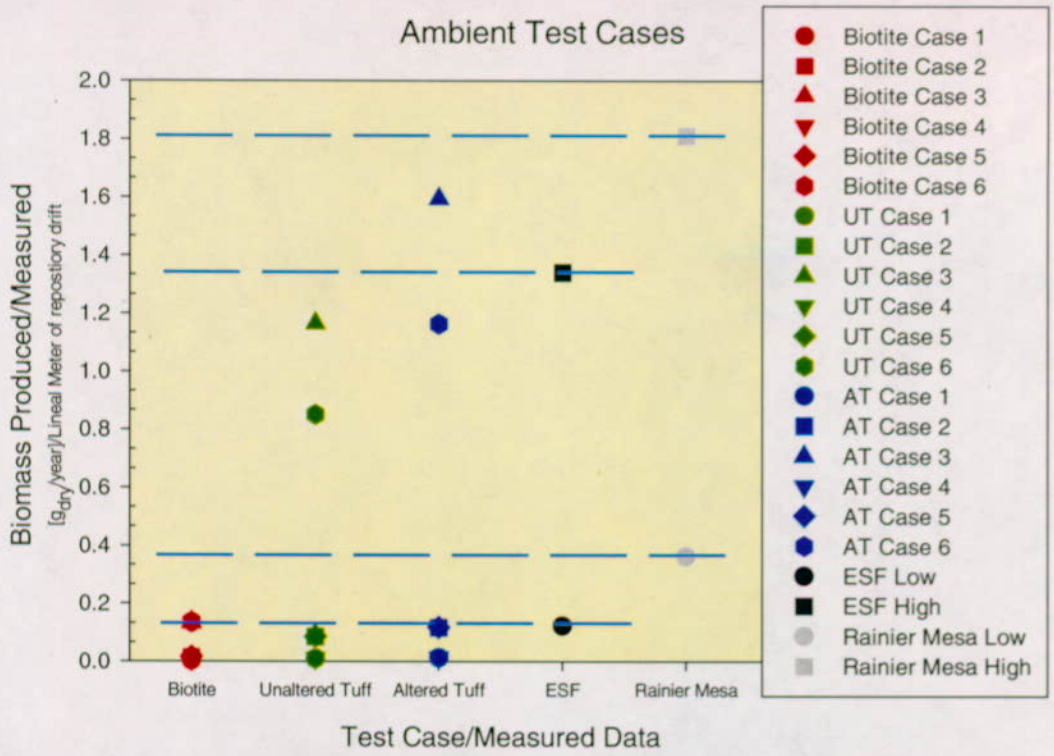

Figure 19. Comparison of Modeled Results to Ambient Measurements. ESF and Rainier Mesa Low and High Values are Taken from Table I-9.

6.7.3 LLNL *In Situ* Limiting Nutrient Experiment Test Cases

Experiments conducted at LLNL to determine limiting nutrients to microbial growth in the YMP environment and to give bounds on MIC on waste packages are utilized in this model to assist in model validation. These experiments were conducted independent of model development and are intended to be a "blind test" on the results of the simulated tests calculated from MING V1.0. A description of these results are reported in Horn et al. (1998a and 1998b) and Davis et al. (1998). Positive test results using this "blind testing" method should determine to what "level of certainty" this model is valid.

6.7.3.1 Experimental Description

The experiments reported in Horn et al. (1998a and 1998b) and Davis et al. (1998) utilize several different growth media to grow microbes (see Table 84). Each of these media was selected to determine the limiting nutrients in the host rock at YM. Each media shown on Table 85 below was specifically selected to enable the determination of limiting nutrients in the repository environment. The reader is referred to Horn et al. (1998a and 1998b) and Davis et al. (1998) for more detailed descriptions of the experiments.

Table 84. Details of LLNL Batch Experiments used as Inputs to MING V1.0 (Horn et al. 1998a).

Input Item	Value
Flask Volume	125 ml
pH of Growth Media	7.2
Mass of Crushed Tuff	5 g
Temperature	30°C
Volume of Growth Media	20 ml

DTN: LL000206105924.126

Each of these media was placed in a flask in addition to a known quantity of Topopah Spring tuff (see Table 15) and was cultured for approximately seven days to determine the optimum growth rates. Growth rates were determined by taking samples of the media and periodically subjecting them to live plating.

Two different types of tests were conducted. First, a set of microcosm experiments where the crushed tuff was exposed to a continuous feed of growth media and second, a set of batch experiments where the crushed tuff was exposed to a single aliquot of growth media. The experiments that best fit the setup of MING V1.0 to model are the batch experiments as they use easily duplicated conditions. Table 84 reports the specifics of the batch experiments that are required by MING to duplicate the batch tests. The results of the growth tests for both the batch and microcosm tests are shown below in Figures 20 and 21 respectively.

Table 85. Growth Media Compositions (mmol) from the LLNL Lab Experiments.

Component	YM complete	Dilute Complete	J13-NO3	J13-SO4	Phosphate deficient	Carbon deficient
NH_4^+	3.75E-03	3.80E-04	0.00E+00	0.00E+00	1.90E-02	3.75E-03
NO_3^-	1.50E-02	1.50E-03	1.00E-04	1.96E-02	1.00E-03	1.50E-02
SO_4^{2-}	9.74E-03	9.70E-04	9.98E-03	1.70E-04	5.79E-02	9.74E-03
PO_4^{3-}	5.71E-02	5.71E-03	6.40E-02	6.40E-02	0.00E+00	5.71E-02
HCO_3^-	1.89E-02	1.89E-03	1.90E-02	1.90E-02	1.90E-02	1.89E-02
Glucose	5.55E-03	5.60E-04	5.55E-03	5.55E-03	5.55E-03	0.00E+00

DTN: LL980608505924.035

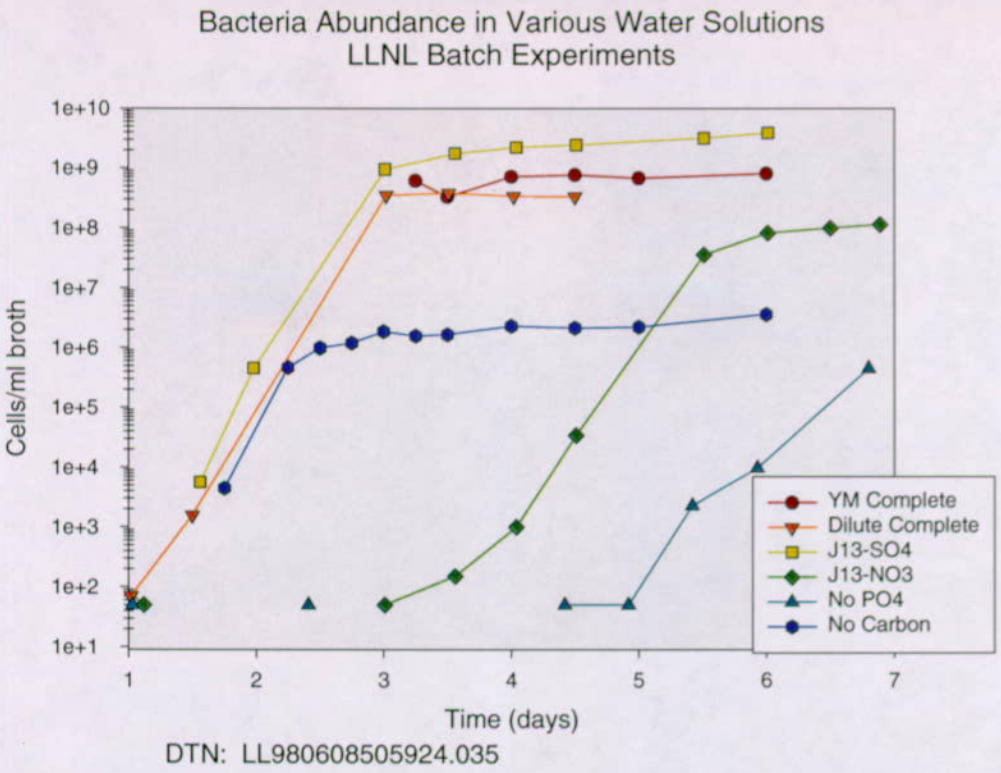

Figure 20. Results of LLNL *In Situ* Limiting Nutrient Batch Test Growth Experiments.

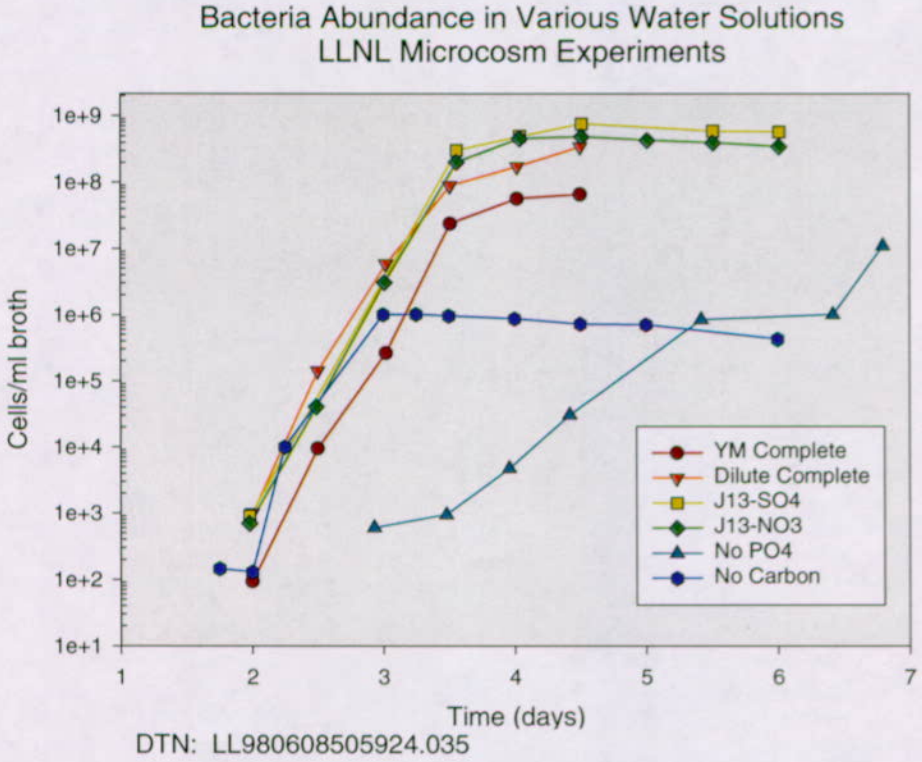

Figure 21. Results of LLNL *In Situ* Limiting Nutrient Microcosm Test Growth Experiments.

6.7.3.2 Input Development

6.7.3.2.1 General MING Inputs

The following general inputs were used in the test calculations: Tables 18, 19 and 23 with the exception of the values that are substituted on Table 23 as discussed in Section 6.7.3.2.2. Two other parameters that have no consequence on these calculations but have to be entered are the RH value (0.999, equivalent to saturated conditions, see Assumption 5.2 above) and the layer designator parameters for the altered and unaltered tuff (Table 80 above).

6.7.3.2.2 Test Specific Inputs

Lab Values

In addition to the inputs specifically discussed in the sections below the following tables were used as inputs: Table 15 (composition of altered and unaltered tuff), Table 85 (compositions of the various growth media), and Table 84 (various required inputs used to simulate the lab experiments). The same method as discussed in Attachment V was used to generate the "reactant compositions" for the altered and unaltered tuff. They are shown on Table 80.

Any parameters that were altered for sensitivity cases are presented as part of the discussion in Sections 6.7.3.4.2 and 6.7.3.4.3.

Scaling of Time

MING V1.0 uses a year as its standard time unit; however, to scale the MING calculation all time units need to be scaled to days. This is a simple fix as the only real time dependant variable that gets entered as an input is the material lifetimes from which are calculated the material degradation rates. These yearly rates can be simply modified by multiplying the material lifetime by 365 to get the rate in days. Therefore, if the parameter "material lifetime" of altered tuff (AT) were determined to be 10 years, the value 3650 would be entered into the appropriate input table in MING. Additionally, the groundwater "infiltration rate" is usually entered in mm/year; however, with the batch experiment there is only a one-time addition of media to the flask so the time dependence does not interfere with the calculation.

Scaling of Volume

MING V1.0 requires that you input a "tunnel length" and a "tunnel diameter" as default input parameters to all model calculations. In order to account appropriately for gas flow, the scaling of the 125 ml flasks used in the LLNL microcosm experiments (Horn et al. 1998a, 1998b, and Davis et al. 1998) needs to be calculated.

Attachment I documents the development of necessary volume input parameters for model validation test case inputs that are used to replace the default input parameters (tunnel diameter and tunnel length) shown in Table 23. In order to simulate the lab experiments appropriate volume had to be defined. Sections I-2.3, I-4.3, and I-5.3 document the derivation of appropriate

volume conditions within the flasks. The results of the derivation that are direct inputs into MING are found on Table I-10.

6.7.3.2.3 Gas Input

MING V1.0 requires gas flux into the drift in units of kg/m^2 year. However, to scale the lab experiments properly, the values entered in MING need to be scaled on the order of days and not years. When scaling MING, as long as all time units are input as the same unit there are no conversion problems.

Attachment I documents the development of necessary gas input parameters for model validation test case inputs. In order to simulate the lab experiments appropriate gas conditions had to be defined. Sections I-2.3, I-4.3 and I-5.3 document the derivation of appropriate gas conditions within a 125 ml flask. The results of this derivation used as direct inputs into MING are found on Table I-11.

6.7.3.3 Test Results

Results calculated in MING using the inputs above are reported in grams (dry weight) of microbes per unit volume. In order to compare the MING results to the growth experiments, the values calculated in MING need to be converted to the number of cells per ml of growth media. This is done using the following two formulas.

$$\mu/\alpha=\phi \qquad \text{(Eq. 8)}$$

$$\phi/\lambda=\beta \qquad \text{(Eq. 9)}$$

where:

μ = MING result (g) $_{dry}$ per flask
α = Mass of average microbe (g) $_{dry}$ (see value from Table I-2)
ϕ = # of microbes in flask
λ = Volume of growth media in flask (ml) (See value from Table 84)
β = # of microbes per ml growth media

Equations 8 and 9 are used to create the results tables presented in the sections below. These tables are used in creating the figures shown below. The calculated results presented on these tables are plotted against both the batch and microcosm results shown in Figures 20 and 21 above.

6.7.3.3.1 YM Complete Test

Test Specific Conditions

This calculation was run in MING using a material lifetime on the altered tuff (Table 15) of 10 years (3650 days), the gas compositions found on Table I-11, and the YM-Complete (YMC) growth media composition from Table 85.

Test Results

Table 86 shows that the system is energy limited. There are sufficient nutrients to produce more microbes. Applying equations 8 and 9 to the calculated mass reported on Table 86 gives the values shown on Table 87. This calculated concentration (1.89E+09 cells/ml) is plotted against the batch and microcosm results and shown on Figure 22.

Table 86. Results from MING for YMC Test.

Mass of microbes from available nutrients (g dry)	Energy available in system ($kJ\ mol^{-1}$)	Mass of microbes from available energy (g dry)	Calculated Mass of microbes (g dry)
0.006077383	0.3621332	0.005658332	0.005658332

Table 87. Calculated Abundance of Microbes per ml of YMC Growth Media using Equations 8 and 9.

Calculated Mass (g dry) (μ)	Mass of Average microbe (α)	# of Microbes in Flask (ϕ)	ml of growth media in flask (λ)	# of Microbes per ml of broth (β)
5.66E-03	1.50E-13	3.77E+10	20	1.89E+09

6.7.3.3.2 Dilute Complete Test

Test Specific Conditions

This calculation was run in MING using a material lifetime on the altered tuff (Table 15) of 10 years (3650 days), the gas compositions found on Table I-11, and the Dilute Complete (DC) growth media composition from Table 85.

Test Results

Table 88 shows that the system is energy limited. There are sufficient nutrients to produce more microbes. Applying equations 8 and 9 to the calculated mass reported on Table 88 gives the values shown on Table 89. This calculated concentration (1.92E+08 cells/ml) is plotted against the batch and microcosm results and shown on Figure 23.

Table 88. Results from MING for DC Test.

Mass of microbes from available nutrients (g dry)	Energy available in system (kJ mol^{-1})	Mass of microbes from available energy (g dry)	Calculated Mass of microbes (g dry)
0.0007697311	0.03683817	0.0005755964	0.0005755964

Table 89. Calculated Abundance of Microbes per ml of DC Growth Media using Equations 8 and 9.

Calculated Mass (g dry) (μ)	Mass of Average microbe (α)	# of Microbes in Flask (ϕ)	ml of growth media in flask (λ)	# of Microbes per ml of broth (β)
5.76E-04	1.50E-13	3.84E+09	20	1.92E+08

6.7.3.3.3 J-13-NO_3 Test

Test Specific Conditions

This calculation was run in MING using a material lifetime on the altered tuff (Table 15) of 10 years (3650 days), the gas compositions found on Table I-11, and the J-13-NO_3 growth media composition from Table 85.

Test Results

Table 90 shows that the system is energy limited. There are sufficient nutrients to produce more microbes. Applying equations 8 and 9 to the calculated mass reported on Table 90 gives the values shown on Table 91. This calculated concentration (1.85E+09 cells/ml) is plotted against the batch and microcosm results and shown on Figure 24.

Table 90. Results from MING for J-13-NO_3 Test.

Mass of microbes from available nutrients (g dry)	Energy available in system (kJ mol^{-1})	Mass of microbes from available energy (g dry)	Calculated Mass of microbes (g dry)
0.007665622	0.3549707	0.005546418	0.005546418

Table 91. Calculated Abundance of Microbes per ml of J-13-NO_3 Growth Media using Equations 8 and 9.

Calculated Mass (g dry) (μ)	Mass of Average microbe (α)	# of Microbes in Flask (ϕ)	ml of growth media in flask (λ)	# of Microbes per ml of broth (β)
5.55E-03	1.50E-13	3.69E+10	20	1.85E+09

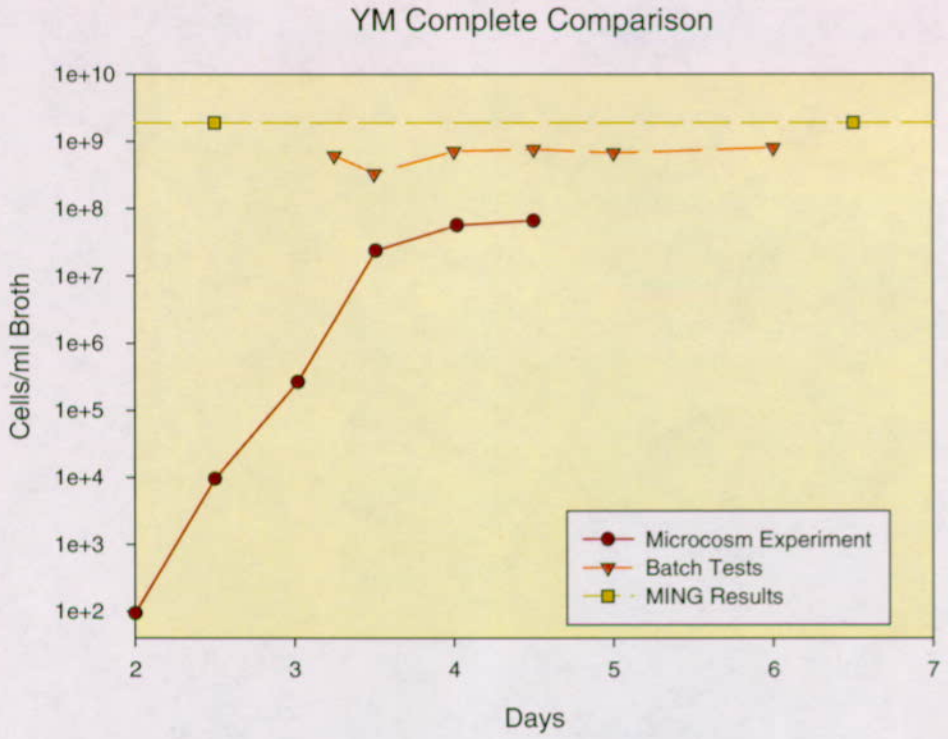

Figure 22. Comparison of Growth Rate Experiments in YMC Growth Media with Calculated Values in MING V1.0.

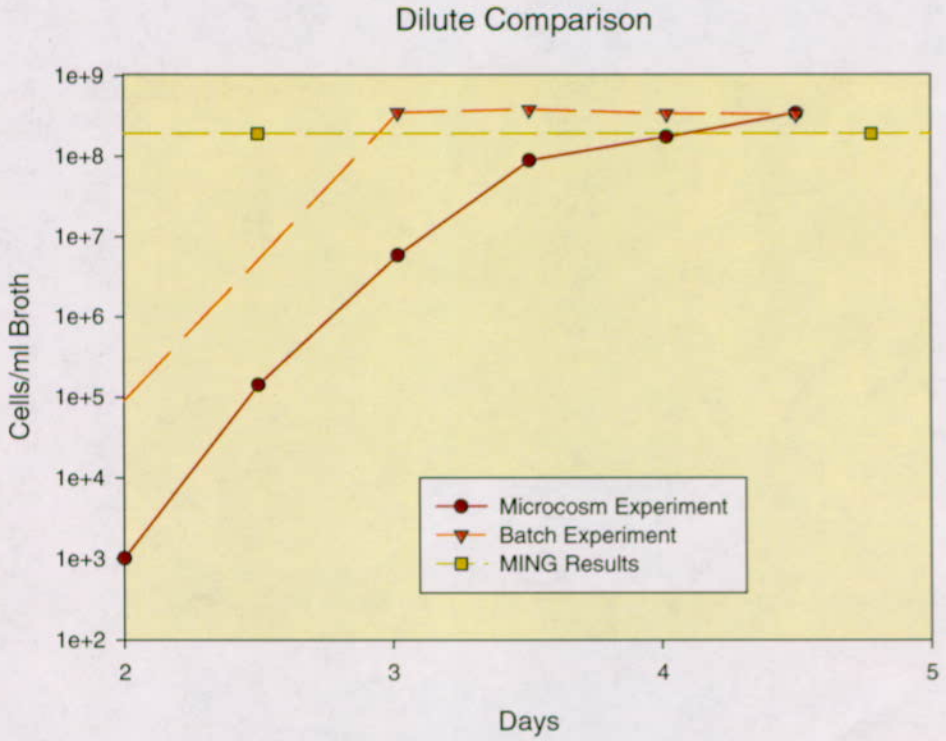

Figure 23. Comparison of Growth Rate Experiments in DC Growth Media with Calculated Values in MING V1.0.

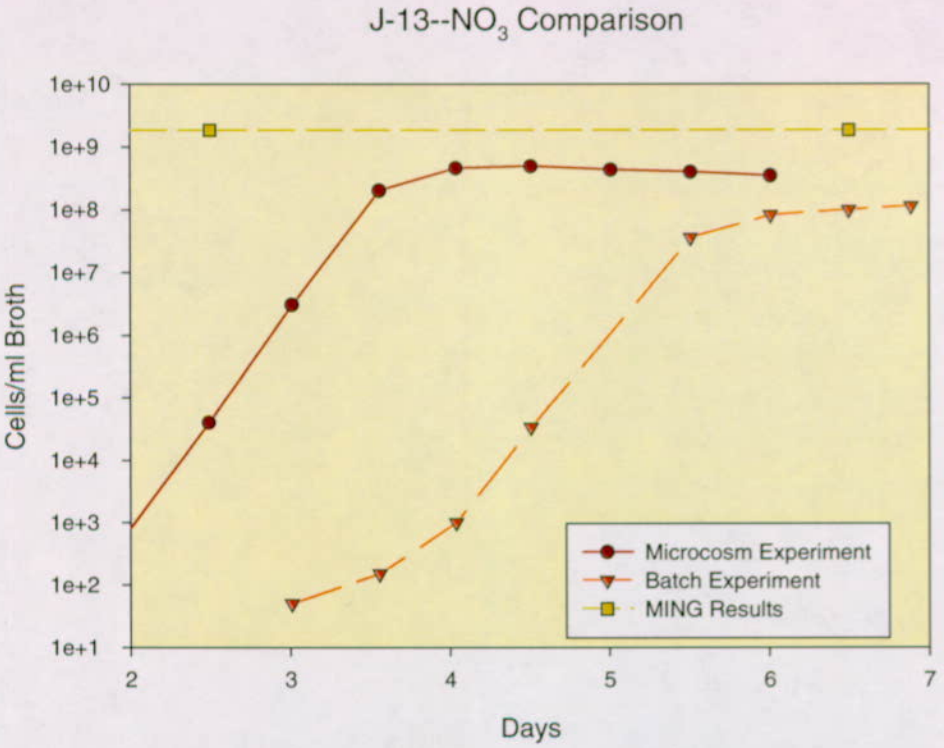

Figure 24. Comparison of Growth Rate Experiments in J-13-NO_3 Growth Media with Calculated Values in MING V1.0.

6.7.3.3.4 J-13-SO_4 Test

Test Specific Conditions

This calculation was run in MING using a material lifetime on the altered tuff (Table 15) of 10 years (3650 days), the gas compositions found on Table I-11, and the J-13-SO_4 growth media composition from Table 85.

Test Results

Table 92 shows that the system is energy limited. There are sufficient nutrients to produce more microbes. Applying equations 8 and 9 to the calculated mass reported on Table 92 gives the values shown on Table 93. This calculated concentration (1.85E+09 cells/ml) is plotted against the batch and microcosm results and shown on Figure 25.

Table 92. Results from MING for J-13-SO_4 Test.

Mass of microbes from available nutrients (g dry)	Energy available in system (kJ mol^{-1})	Mass of microbes from available energy (g dry)	Calculated Mass of microbes (g dry)
0.007665622	0.3549707	0.005546418	0.005546418

Table 93. Calculated Abundance of Microbes per ml of J-13-SO_4 Growth Media using Equations 8 and 9.

Calculated Mass (g dry) (μ)	Mass of Average microbe (α)	# of Microbes in Flask (ϕ)	ml of growth media in flask (λ)	# of Microbes per ml of broth (β)
5.55E-03	1.50E-13	3.70E+10	20	1.85E+09

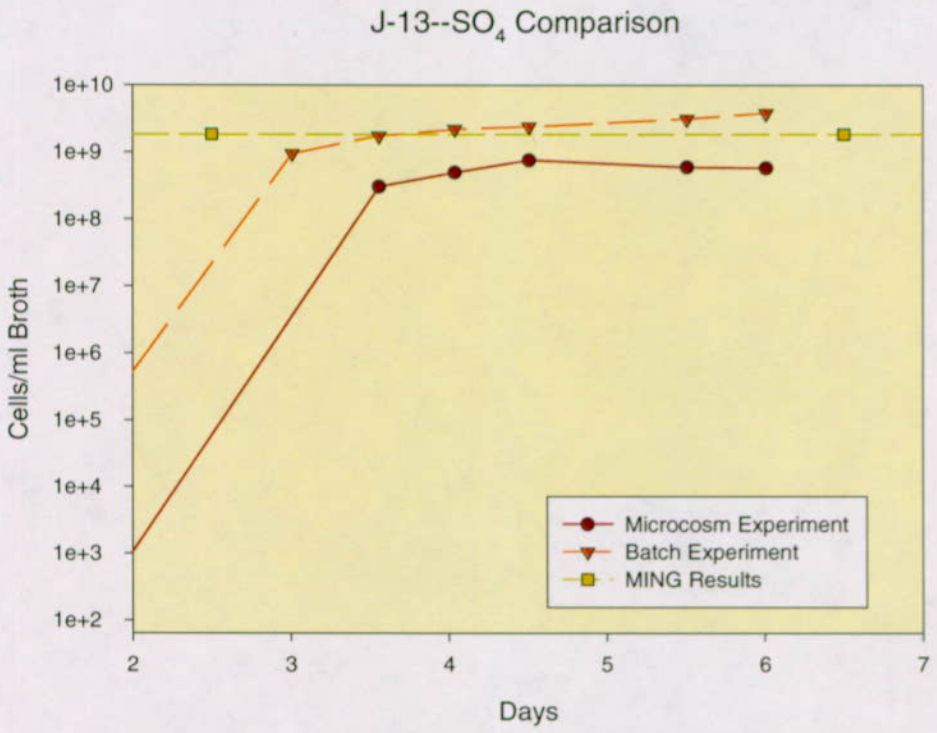

Figure 25. Comparison of Growth Rate Experiments in J-13-SO_4 Growth Media with Calculated Values in MING V1.0.

6.7.3.3.5 Phosphate Deficient Test

Test Specific Conditions

This calculation was run in MING using a material lifetime on the altered tuff (Table 15) of 10 years (3650 days), the gas compositions found on Table I-11, and the Phosphate Deficient (PD) growth media composition from Table 85.

Test Results

Table 94 shows that the system is nutrient limited. There is sufficient energy to produce more microbes. Applying equations 8 and 9 to the calculated mass reported on Table 94 gives the values shown on Table 95. This calculated concentration (1.47E+05 cells/ml) is plotted against the batch and microcosm results and shown on Figure 26.

Table 94. Results from MING for PD Test.

Mass of microbes from available nutrients (g dry)	Energy available in system (kJ mol^{-1})	Mass of microbes from available energy (g dry)	Calculated Mass of microbes (g dry)
4.412285E-07	0.4114369	0.006428701	4.412285E-07

Table 95. Calculated Abundance of Microbes per ml of PD Growth Media using Equations 8 and 9.

Calculated Mass (g dry) (μ)	Mass of Average microbe (α)	# of Microbes in Flask (ϕ)	ml of growth media in flask (λ)	# of Microbes per ml of broth (β)
4.41E-07	1.50E-13	2.94E+06	20	1.47E+05

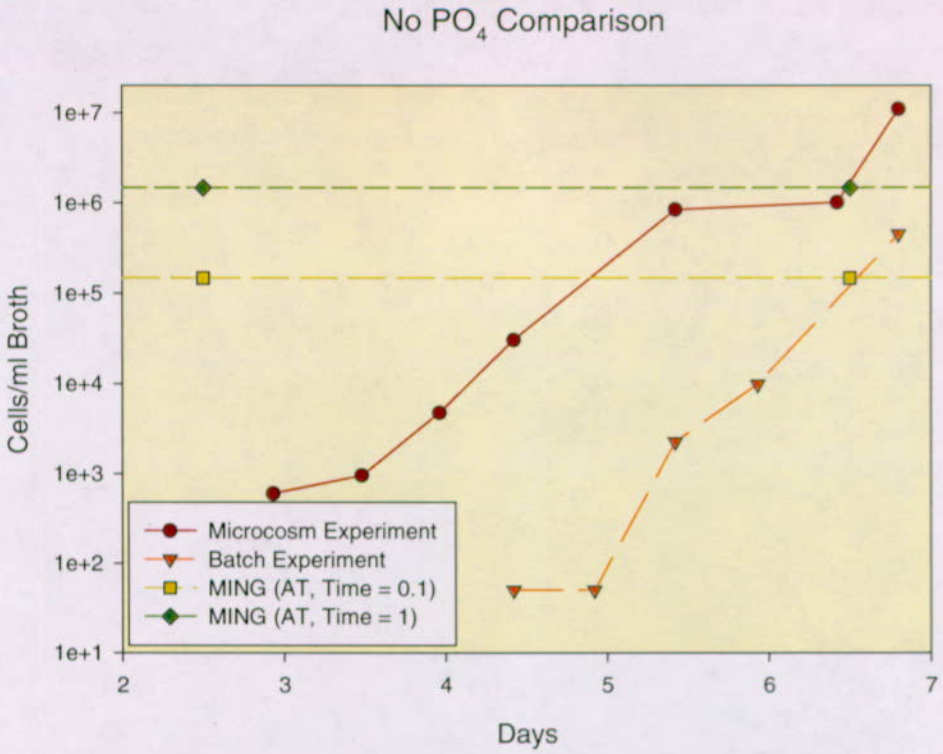

Figure 26. Comparison of Growth Rate Experiments in PD Growth Media with Calculated Values in MING V1.0. A Sensitivity Calculation (see Section 6.7.3.4.2 below) using a Modified Material Lifetime for Altered Tuff of One Year (365 Days) is also Shown.

6.7.3.3.6 Carbon Deficient Test

Test Specific Conditions

This calculation was run in MING using a material lifetime on the altered tuff (Table 15) of 10 years (3650 days), the gas compositions found on Table I-11, and the Carbon Deficient (CD) growth media composition from Table 85.

Test Results

Table 96 shows that the system is energy limited. There are sufficient nutrients to produce more microbes. Applying equations 8 and 9 to the calculated mass reported on Table 96 gives the values shown on Table 97. This calculated concentration (1.88E+09 cells/ml) is plotted against the batch and microcosm results and shown on Figure 27.

Table 96. Results from MING for CD Test.

Mass of microbes from available nutrients (g dry)	Energy available in system (kJ mol^{-1})	Mass of microbes from available energy (g dry)	Calculated Mass of microbes (g dry)
0.00590302	0.3614834	0.005648179	0.005648179

Table 97. Calculated Abundance of Microbes per ml of CD Growth Media using Equations 8 and 9.

Calculated Mass (g dry) (μ)	Mass of Average microbe (α)	# of Microbes in Flask (ϕ)	ml of growth media in flask (λ)	# of Microbes per ml of broth (β)
5.65E-03	1.50E-13	3.77E+10	20	1.88E+09

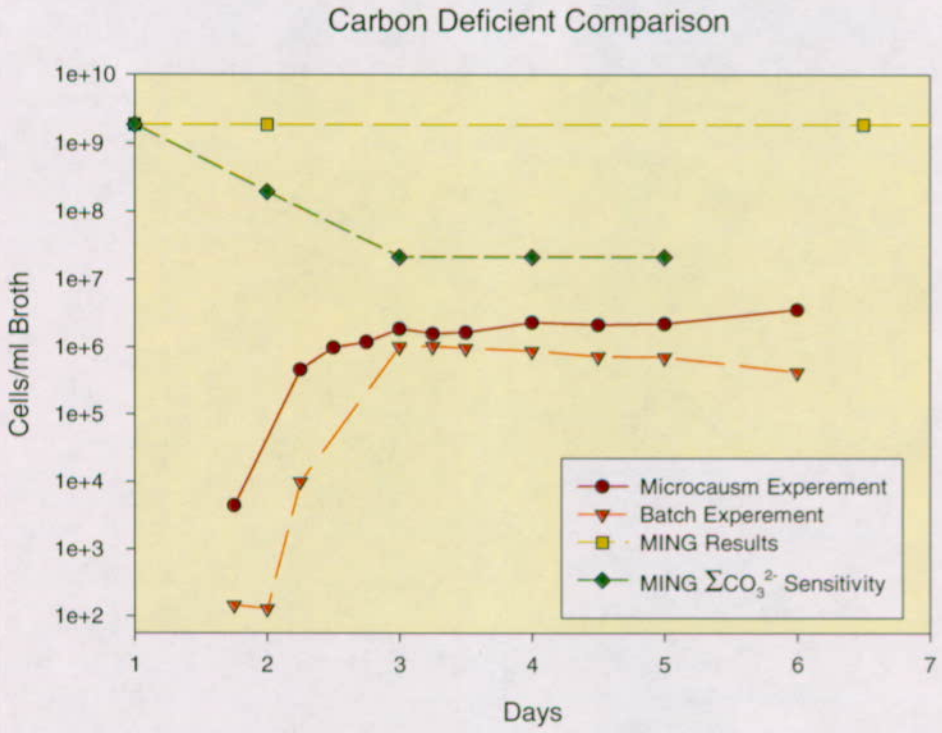

Figure 27. Comparison of Growth Rate Experiments in CD Growth Media with Calculated Values in MING V1.0. A Sensitivity Calculation using Modified Aqueous Carbonate Compositions from Table 85 Spanning Two Orders of Magnitude Decrease is also Shown.

6.7.3.4 Sensitivities to Inputs

6.7.3.4.1 Gas Sensitivity Tests

Test Specific Conditions

These sensitivity calculations were run in MING using a material lifetime on the altered tuff (Table 15) of 10 years (3650 days), the gas compositions found on Table I-11, and the CD growth media composition from Table 85. Each sensitivity calculation was done using a different gas composition. In MING, this is done by turning on or off the various gas switches in the code then proceeding with the calculation. Figure 28 below shows the various gas switches that were selected for each run.

Test Results

Seven separate calculations were done in addition to the calculation presented in Section 6.7.3.3.6. Applying equations 8 and 9 to the calculated masses reported on Table 98 gives the values shown on Figure 28.

6.7.3.4.2 Material Lifetime Sensitivity Tests

Test Specific Conditions

These sensitivity calculations were run in MING using a variable material lifetime on altered (AT) and unaltered tuff (UT) (Table 15) ranging from 1 year to 10,000 years, the gas compositions found on Table I-11, and the YMC and PD growth media composition from Table 85. Each sensitivity calculation was done using a different material lifetime, growth media composition or rock type. Figures 29 and 30 below show the various parametric selections used in each calculation. YMC media and PD media were selected to observe the affects of a nutrient vs. energy limited system. A nutrient-limited system should show an incremental increase in microbial abundance but an energy-limited system should show no effects of the additional nutrients available to the system.

Test Results

Twelve separate calculations were done in addition to the calculations presented in Section 6.7.3.3.1 and 6.7.3.3.5 Applying equations 8 and 9 to the calculated masses reported on Table 99 gives the values shown on Figures 29 and 30.

The results are essentially identical for all cases run. In all of these calculations, the results indicate that the mass of microbes produced is limited by the available energy. However, there is a slight increase when the redox energy from the O_2 is available. The difference in the calculations with and without the oxygen gas (0.00002 grams) indicates that the calculations are insensitive to the nutrients and energy that the gas inputs provide.

Table 98. Results of Gas Sensitivity Calculations.

Gas Switches on in Sensitivity Test	Calculated Mass of microbes (g dry)
N_2 and O_2	5.65E-03
CO_2 and O_2	5.65E-03
N_2 and CO_2	5.63E-03
N_2	5.63E-03
O_2	5.65E-03
CO_2	5.63E-03
All	5.65E-03
None	5.63E-03

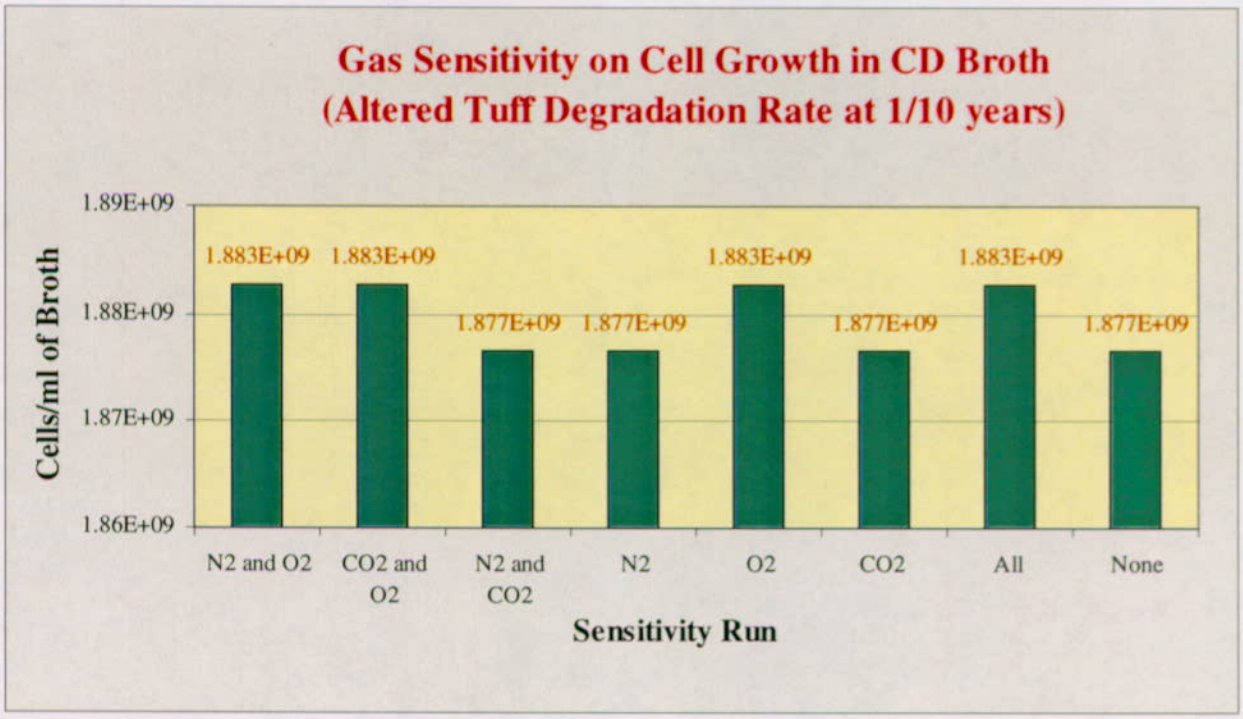

Figure 28. Comparison of Gas Sensitivity on Cell Growth using Modeled Results from the CD Growth Media.

Table 99. Results of Material Lifetime Sensitivity Calculations.

Parameters Selected	Calculated Mass of microbes (g dry)
YMC, AT, ML=1	5.66E-03
YMC, AT, ML=10	5.66E-03
YMC, AT, ML=1,000	5.66E-03
YMC, AT, ML=10,000	5.66E-03
YMC, UT, ML=10	5.66E-03
YMC, UT, ML=1,000	5.66E-03
YMC, UT, ML=10,000	5.66E-03
PD, UT, ML=10	2.21E-07
PD, UT, ML=1,000	2.21E-09
PD, UT, ML=10,000	2.21E-10
PD, AT, ML=1	4.41E-06
PD, AT, ML=10	4.41E-07
PD, AT, ML=1,000	4.41E-09
PD, AT, ML=10,000	4.41E-10

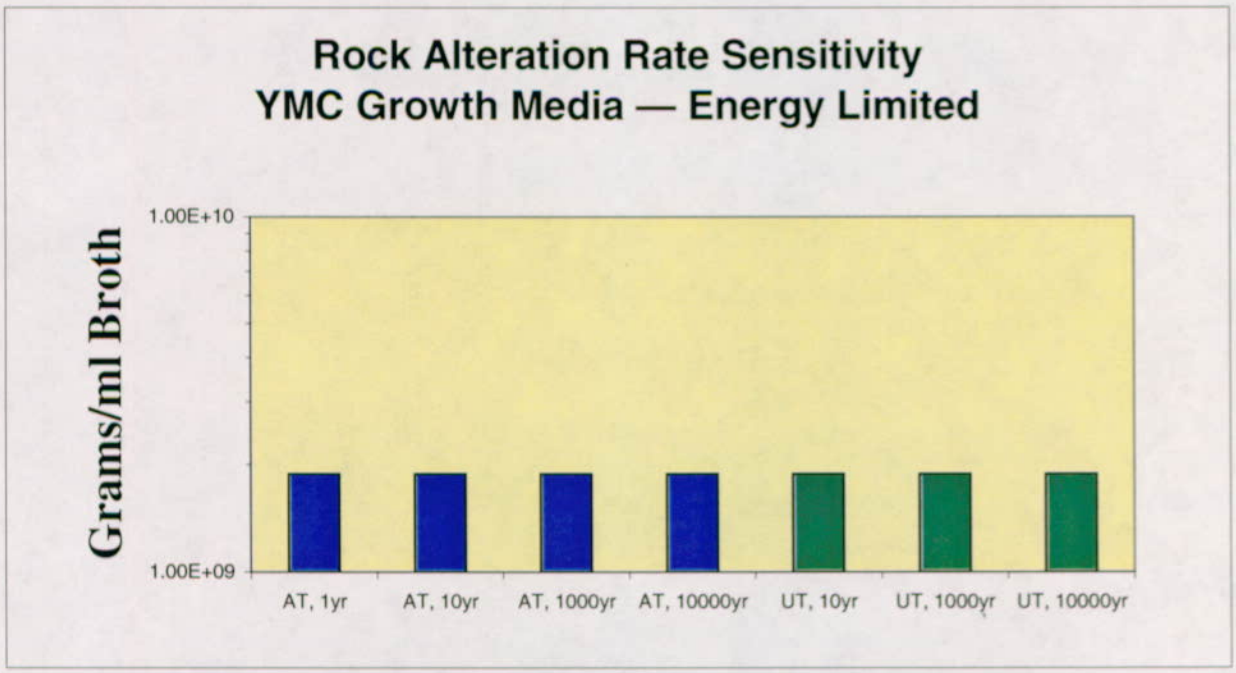

Figure 29. Results of Material Lifetime Sensitivity Calculations for Altered and Unaltered Tuff (Table 14) in an Energy Limited System using the YMC Growth Media.

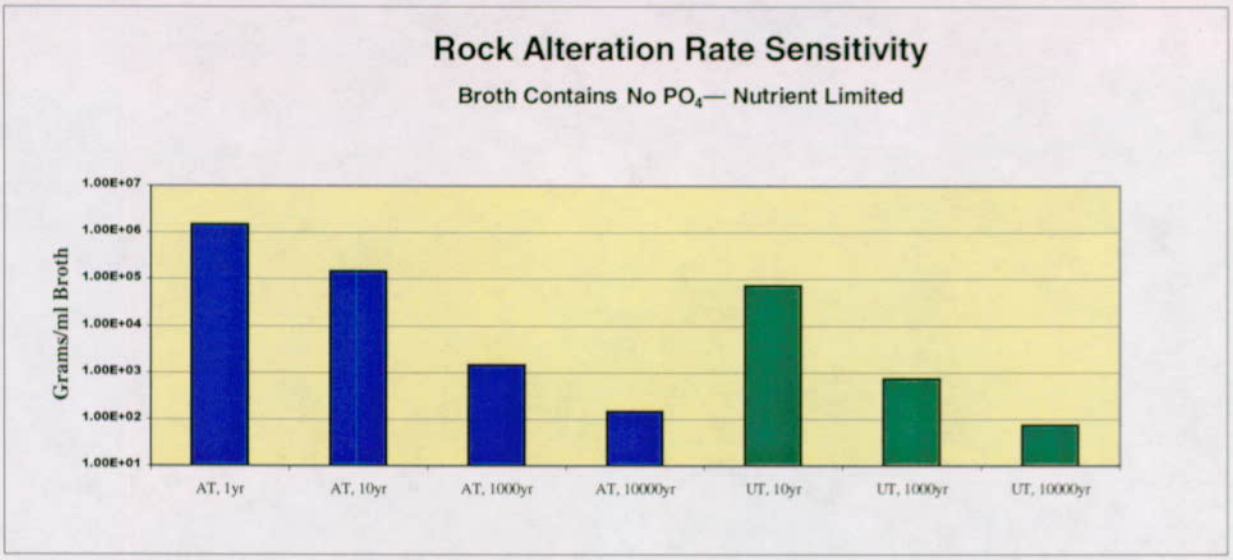

Figure 30. Results of Material Lifetime Sensitivity Calculations for Altered and Unaltered Tuff (Table 14) in a Nutrient Limited System using the PD Growth Media.

6.7.3.4.3 Groundwater Concentration and pH Sensitivity

Test Specific Conditions

This calculation was run in MING using a material lifetime on the altered tuff (Table 15) of 10 years (3650 days) and the gas compositions found on Table I-11. These sensitivity calculations were run in MING using the Yucca Mountain Complete (YMC) media and modifying the concentration by ± 10%. In addition, pH was altered by one pH unit so that the range was between 6.2 and 8.2. Figure 31 below shows the various parametric selections used in each calculation.

The carbon deficient media was also modified by altering the ΣCO_3 values in order to explain the discrepancies in the results (Figure 27). This was done by taking the values for CO_3 on Table 85 and decreasing them by two orders of magnitude during the five time step (day) modeling run. At day 2, the first order of magnitude drop was entered and at day three, the second order of magnitude drop was entered in the input.

Test Results

Nine separate calculations were done in addition to the calculations presented in Section 6.7.3.3.6. Applying equations 8 and 9 to the calculated masses reported on Tables 100 and 101 give the values shown on Figures 31 and 27, respectively.

In all of these calculations, the results indicate that the mass of microbes produced is limited by the available energy. If these runs were nutrient limited, the effects of the pH variation would not

appear, although the amount of energy available to the system would vary. The results from Figure 31 show that there is an energy minimum produced at pH of 7.2. This is possible due to the hydrogen ion dependence in most of the half reactions shown on Table 18. Because of this dependence, some of the full reactions that produce the energy above the 15kJ limit at a given pH may not produce the same energy at a different pH. This difference may force the reaction below the 15kJ limit, which will cause the reaction to be discarded by MING.

In these cases, an unmeasured variation in pH for the experimental broth formulas (Tables 84 and 85) of ± 1 pH unit will not force the validation calculations to fall outside the one order of magnitude level. Whether a greater variation on pH would cause larger impacts to an energy-limited system is unknown at this time.

6.7.3.5 LLNL Test Case Comparison

For tests shown on Figures 22, 23, 24, and 25, the results show that MING V1.0 adequately replicates the lab tests to within one order of magnitude. For the PD test, the results of MING V1.0 are extremely sensitive to the material lifetime of the tuff (see Figures 26 and 30). The tests reflect the nutrient limiting conditions set up in the lab. By altering the material lifetime of the tuff the MING results of the lab tests can be favorably compared to the actual tests and be found within an order of magnitude. No impact is noted to energy limiting situations as shown on Figure 29.

For the CD test case there are some problematic results. The MING results show a three order of magnitude discrepancy with the values measured in the lab. However, when sensitivity calculations are done on the ΣCO_3 to account for a decrease in ΣCO_3 due to the potential precipitation of calcite or an unknown imposed CO_2 fugacity on the CD growth media, the values approach those measured in the lab experiments (Figure 27).

There does not seem to be sensitivity to gas conditions. There is a slight increase in population when O_2 is accounted for in the redox calculations. Otherwise, there is no impact on results due to sensitivities on gas utilization.

Groundwater and pH sensitivities do not show a large dependence on the minor fluctuations to concentration or a variance of ± 1 unit in pH (Figure 31). These differences are insignificant when compared to the general order of magnitude of the results shown on Figures 22, 23, 24, and 25.

Table 100. Results of YMC Growth Media Concentration and pH Sensitivity Calculations.

Parameters Selected	Calculated Mass of microbes (g dry)	# of Microbes per ml of broth (β)
pH 6.2, -10%	6.60E-03	2.20E+09
pH 6.2, +10%	8.07E-03	2.69E+09
pH 6.2, YMC	5.86E-03	1.95E+09
pH 7.2, -10%	5.17E-03	1.72E+09
pH 7.2, +10%	6.33E-03	2.11E+09
pH 8.2, -10%	5.92E-03	1.97E+09
pH 8.2, +10%	7.20E-03	2.40E+09
pH 8.2, YMC	5.70E-03	1.90E+09

Table 101. Results of a Sensitivity Study on the Effects to CD Growth Media by Altering ΣCO_3 by Two Orders of Magnitude.

Time step	Calculated Mass of microbes (g dry)	# of Microbes per ml of broth (β)
1	0.00564818	1.88E+09
2	0.00059503	1.98E+08
3	6.4232E-05	2.14E+07

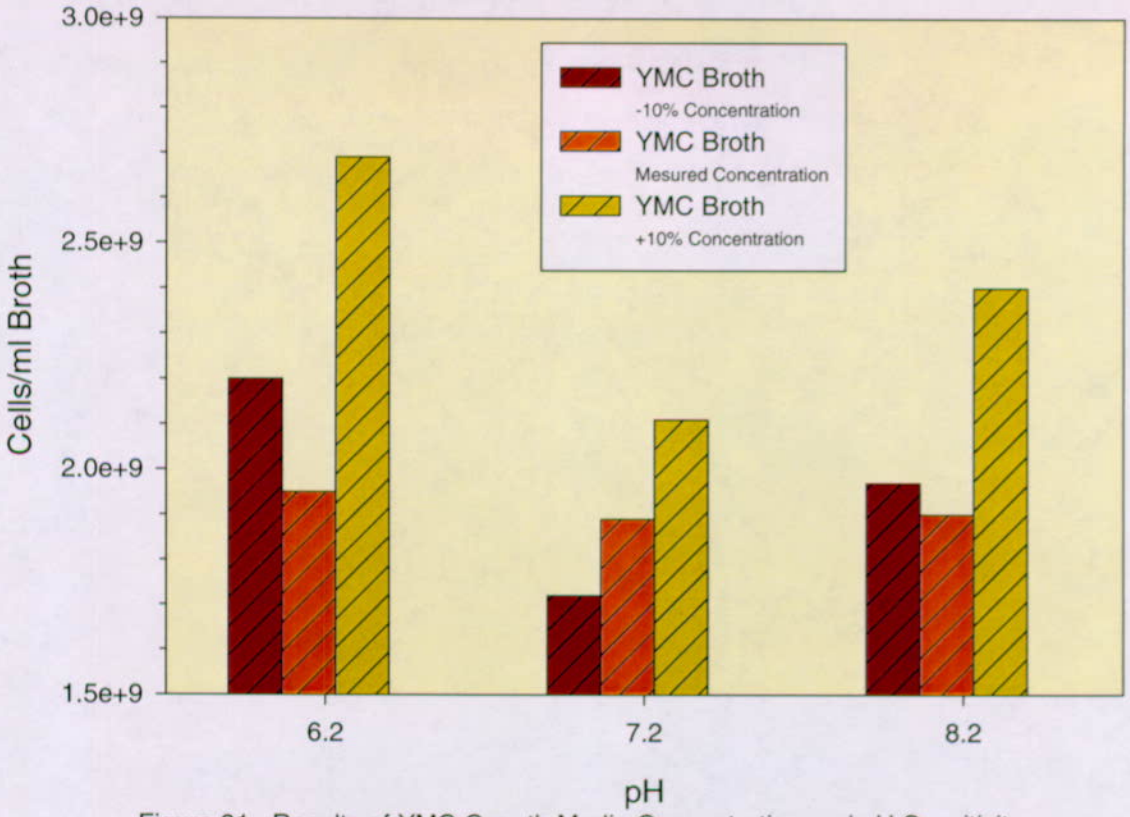

Figure 31. Results of YMC Growth Media Concentration and pH Sensitivity.

7. CONCLUSIONS

7.1 CONCEPTUAL MODEL SUMMARY

The reader is referred to Section 6.3.6 for the summary of the conceptual model.

7.2 MODEL SUMMARY

As discussed in Section 6.2 there are general parts to the model. These parts are the conceptual model, the software code MING V1.0, and the required parameter inputs. These items are summarized below.

1. The results of the conceptual model were incorporated within the MING V1.0 software during software development or are incorporated directly as parameter inputs.
2. MING V1.0 software was developed using approved QA procedures and has passed its software validation.
3. The required model parameters have been developed within the body of this report.

In general, the model uses the constraints on the supply rates of the nutrients to build an idealized microbial composition, comprised of carbon, nitrogen, sulfur, and potassium in addition to the

water components. The rates of supply of these constituents are input as constant release rates for each introduced material in the system by specifying the mass and composition of the material and its degradation lifetime. The other major constraint evaluated is the energy available for microbes to grow based on the pH corrected, standard state free energy released from oxidation/reduction reactions. Other constraints on microbial growth are temperature and RH thresholds in the model that limit the start of microbial activity until the boiling period is over. Although microbes could be sterilized out of the drifts during the highest temperature period, because they are present in the water-rock system they will return as water drips back into potential drifts.

It is important to note that the conceptual model discusses potential repository impacts due to microbial transport and localized colonization (biofilm formation and MIC, see Section 6.6.5.3). However, the model as presented herein does not yet address the specific effects of the localized impacts of biofilm development, colloid formation, and the production of inorganic acids, methane, organic byproducts, carbon dioxide, and other chemical species that could change the longevity of materials. The transport of radionuclides from the near field was not investigated.

This model is designed to be able to bound the microbial communities that could be present within a given length of repository drift. The bounding calculations for microbial growth for the given model cases are found on Table 71. They seem to indicate that for the waste package surface the bounding biomass is 14.96 grams dry per meter of waste package whether it is either a CSNF or HLW package. For the waste form the biomass is between 70.44 to 106.92 grams dry per meter of waste package depending on whether it is either CSNF or HLW waste form. These values would be higher if backfill were used.

Bounding values for CO_2 gas generation is shown on Figure 17 and on Table 75 and is discussed in Section 6.6.5.4.

Bounding values for colloid generation is found on Table 73 and is discussed in Section 6.6.5.2.

Additionally, results of the model calculations above show that:

- The estimates of microbe masses growing in the potential repository system suggest that effects to the bulk in-drift geochemistry should be small with the exception of CO_2 gas generation.
- Microbial influenced corrosion (MIC) and other localized microbial attack of materials cannot be precluded as the calculated masses of microbes can be shown to create conservative biofilms that can cover both the waste package and the waste form.
- Consideration of microbes as colloids might be pursued in future work.
- In-drift gas compositions used in other geochemical modeling work should include the production of CO_2 gas from microbial sources.
- There is some potential for additional ligands generated locally due to chelation and other microbial processes; however, the radionuclides would have to directly compete with many other available multivalent metals.

7.3 MODEL VALIDATION SUMMARY

Three general tests were conducted in Section 6.7 above. The first test duplicated the model that was constructed for the Swiss low level repository (see Figure 18). This test indicates that our model handles the types of calculations that are required on a repository level where natural barrier components are combined with the engineered barrier components to calculate microbial growth.

The second test (see Figure 19) demonstrates that the model is able to replicate the ambient system, not only within the ESF but also with other natural analog measurements in arid volcanic tuff. These values are reasonable when compared to the inputs and fall within an order of magnitude of the measured results.

The second test also confirms the results reported by Kieft et al. (1997) where water availability seemed to be a limiting factor to microbial growth. Calculated results shown on Figure 19 also show a dependence on the availability of redox energy to the system. This is demonstrated by a noticeable increase in energy produced when the material lifetimes are decreased. When these two factors are combined, we are able to match the variability in the natural system.

Finally, the results of the third test (Figures 22 - 31) show that the numbers of organisms reported by MING are within an order of magnitude of measured values. The replication of these tests shows that the model as a whole does a good job at estimating the microbial growth in the system.

From the results, we reach the same conclusions that were reported with the lab experiments (Horn et al. 1998a and 1998b; Davis et al. 1998). Namely, the results indicate that the availability of water (growth media) was the primary factor contributing to microbial growth. In addition, we were able to determine that the primary limiting nutrient in the repository system is phosphorous. This same conclusion was reached by Davis et al. (1998). We also show that in energy limited systems there are limited impacts due to gas availability, slight variations in pH and water chemistry, and material lifetimes. However, in nutrient limited systems, there are larger impacts to cell growth due to large variations in water chemistry and material lifetimes.

Finally, the conceptual model developed herein is corroborated by the Microbial Effects Model documented in CRWMS M&O (2000k) Results of all three tests and conceptual model corroboration indicate that a) the model will function as intended, and b) the model predictions are accurate to within one order of magnitude of measured values.

7.4 TO BE VERIFIED (TBV) IMPACT

It is important to note that with the exception of the parameter and data inputs to this model, all other aspects of model qualification have been met. As seen on the input tables (Tables 1-5) there are several unqualified or preliminary inputs. The uncertainty of many of these inputs could have a large impact on the results of the model. Other inputs may have a rather insignificant impact. Yet again, some input may not have a large impact but their status, as TBV/TBD without any sensitivity analysis, will effect the qualification status of any results.

Because there are multiple TBV/TBD's in this revision of the model documentation and it is difficult to determine which of the TBV/TBD's are the most important, no evaluation of each individual TBV/TBD is included. Three areas of focus that will go a long way toward resolving many of the TBV/TBD's are a) the documentation of a qualified repository design, b) the qualification of the natural system models and data that feed these models, and c) the qualification of the thermochemical data used in the energy calculations.

7.5 EVALUATION OF NRC IRSR CRITERIA

From Section 4.2.1.1 (Data and Model Justification Acceptance Criteria), Criteria 1, 2, 3, 4, 5, and 6 are addressed in this model. However, in accordance with Criterion 3 much of the data used in this model needs further work both to its abundance and to acquisition. Criterion 7 is outside the scope of this model because it involves activities that are part of the performance confirmation program.

- With respect to this model, Criterion 1 is addressed in Section 4.
- With respect to this model, Criterion 2 is addressed in Section 6.3.
- With respect to this model, Criterion 3 is addressed in Section 4. However, in accordance with Criterion 3 some of the data used in this model needs further work on qualification.
- Criterion 4 is addressed explicitly by this model. This model as documented in Section 6 above provides nutrient and energy inventory calculations and does document the potential for microbial activity that could impact the waste package chemical environment. It is important to note that the Microbial Effects Model documented in the *Engineered Barrier System: Physical and Chemical Environment Model* document (CRWMS M&O 2000k) does not address this specific criterion and was not designed to do so.
- Criterion 5 is addressed by the project based on the findings of this model. Based on the calculations and the fulfillment of criterion 4 above the project now has adequate documentation to allow for MIC (see Section 6.6 above) using the constraints of temperature, humidity and dripping (see Section 6.3 above). It is important to note that the Microbial Effects Model documented in the *Engineered Barrier System: Physical and Chemical Environment Model* document (CRWMS M&O 2000k) does not in and of itself completely address this specific criterion and was not designed to do so.
- For Criterion 6 sensitivity and uncertainty analyses were conducted in the model validation section. The results of the model validation section seem to indicate that the uncertanties were within an order of magnitude, which is sufficient for TSPA analysis (see Section 6.7).

From Section 4.2.1.2 (Data Uncertainty and Verification Acceptance Criteria), Criteria 1, 2, 3, and 4 are addressed in this model. Criterion 5 is outside the scope of this model because it involves activities that are part of the performace confirmation program.

- With respect to this model, Criteria 1 through 4 are addressed as a result of this document. Inputs are discussed in Section 4, assumptions in Section 5, and how they were used is discussed in Section 6.

From Section 4.2.1.3 (Model Uncertainty Acceptance Criteria), Criterion 1 was addressed in this model. Criteria 2 and 3 are outside the scope of this model as alternative conceptual models that are designed to address Criterion 4 in Section 4.2.1.1 have not been developed. Discussion of the types of models that could be developed is briefly discussed in Section 6.4.1. This section (6.4.1) also discusses the reasons why a kinetic approach is not used.

- With respect to this model, Criterion 1 does consider to the extent possible the interaction of all of the 5 issues listed above.

From Section 4.2.1.4 (Model Verification Acceptance Criteria), Criteria 1, 2, and 3, are addressed in this model.

- With respect to this model, Criterion 1 has been met by the detailed documentation of this model and the use of a qualified software code.

- With respect to this model, Criterion 2 has been met by the detailed documentation of this model and the use of a qualified software code.

- With respect to this model, Criterion 3 has been met by the detailed documentation of this model.

7.6 FEATURE, EVENT OR PROCESS (FEP) EVALUATION

Table 6 above documents the FEPs that this model could potentially address. Each of these numbered FEPs will be discussed below.

1. The reduction and oxidation potential in the waste and EBS can be effected by the presence of microbial communities. However, this model only addresses the conceptual processes. It does list many of the redox half reactions that are used by microbes in their metabolic processes. These are discussed in Sections 6.3.1.1 and 6.3.1.2 above. In addition, it discusses the effects of biofilm development in the alteration of local redox environments (see Section 6.3.1.14).

2. The production of organics in the waste and EBS would be directly effected by the presence of microbial communities. This is a general result of the effects of biofilm growth (see Section 6.3.1.14). Other sources and information (e.g. production of siderophores) are documented in Section 6.3.5. Results are reported in Section 6.6.

3. The results of this model can be used to generate the abundance of microbes in the drift through time. These microbes can be used as a source of potential colloids in other modeling work. These conceptual concepts are discussed in Section 6.3.5. Results are discussed in Section 6.6

4. This model was developed to answer this FEP. Results are discussed in Section 6.6.

5. This model was developed to answer this FEP. Results are discussed in Section 6.6..

6. The sorption potential in the waste and EBS can be effected by the presence of microbial communities. However, this model only addresses the conceptual processes. It does discuss the sorption onto microbes. These are discussed in Section 6.3.5.

7.7 RECOMMENDATIONS FOR FUTURE REVISION OR CHANGE

The biggest need for this model is to qualify the input data and parameters. Data qualification directly impacts the results and status of this model. Section 7.4 above discusses the major areas of concern.

One technical issue may be added in a future revision of the model. Redox half reactions for uranium, along with their temperature dependant parameters, should be incorporated. This is due to two reasons. First, some species of microbes derive their metabolic energy from half reactions involving uranium (see Section 6.3.1.1). Second, there will be a large abundance of uranium in the waste. In general, however this will only impact results during the expected lifetimes of the CSNF and HLW.

A slight modification to the software would be helpful in resolving some of the scaling issues as is discussed in Attachment I. With modification, the documentation for drift (or borehole, flask, etc.) scaling would be more efficient.

Finally, more sensitivity to uncertain parameters should be conducted and evaluated.

7.8 MODEL OUTPUT DATA

Section 8.4 lists the DTNs that have been submitted to the TDMS as a result of this model.

8. INPUTS AND REFERENCES

8.1 DOCUMENTS CITED

Abdelouas, A.; Yongming, L.; Lutze, W.; and Nuttall, H. E. 1998. "Reduction of U(VI) to U(IV) by Indigenous Bacteria in Contaminated Ground Water." *Journal of Contaminant Hydrology, 35,* 217-233. Amsterdam, The Netherlands: Elsevier Science. TIC: 244766.

AISC (American Institute of Steel Construction) 1989. *Manual of Steel Construction, Allowable Stress Design.* 9th Edition. Chicago, Illinois: American Institute of Steel Construction. TIC: 205770.

Amy, P.S. 1997. "Microbial Dormancy and Survival in the Subsurface." Chapter 11 of *The Microbiology of the Terrestrial Deep Subsurface.* Amy, P.S. and Haldeman, D.L., eds. Boca Raton, Florida: CRC Lewis Publishers. TIC: 232570.

Amy, P.S. and Haldeman, D.L. 1997. *The Microbiology of the Terrestrial Deep Subsurface.* Boca Raton, Florida: CRC Lewis Publishers. TIC: 232570.

Arthur, R.C. and Murphy, W.M. 1989. "An Analysis of Gas-Water-Rock Interactions During Boiling in Partially Saturated Tuff." *Science Geology Bulletin, 42,* (4), 313-327. Strasbourg, France: Sciences Geologiques Bulletin Publisher Strasbourg, Universite Louis Pasteur de Strasbourg. TIC: 235013.

ASM International 1987. *Corrosion.* Volume 13 of *Metals Handbook.* 9th Edition. Metals Park, Ohio: ASM International. TIC: 209807.

Bachofen, R. 1991. "Gas Metabolism of Microorganisms." *Experientia, 47,* 508-513. Basel, Switzerland: Birkhäuser Verlag. TIC: 236441.

Banfield, J.F. and Nealson, K.H., eds. 1997. *Geomicrobiology: Interactions Between Microbes and Minerals.* Reviews in Mineralogy Volume 35. Washington, D.C.: Mineralogical Society of America. TIC: 236757.

Bennet, P.C.; Siegel, D.E.; Baedecker, M.J.; and Hult, M.F. 1993. "Crude Oil in a Shallow Sand and Gravel Aquifer-I. Hydrogeology and Inorganic Geochemistry." *Applied Geochemistry, 8,* 529-549. Oxford, Great Britain: Pergamon Press. TIC: 236423.

Bhattacharyya, K.K. 2000. "Request for Approval of Analysis and Modeling Report Input as 'Accepted Data' - Composition of Silica Fume." Letter from K.K. Bhattacharyya (CRWMS M&O) to S.P. Mellington (DOE/YMSCO), February 15, 2000, LV.SSFD.KKB.02/00-001, with attachments. ACC: MOL.20000504.0594.

Capon, P. and Grogan, H. 1991. *EMMA, A User Guide and Description of the Program.* IM2661-2. Wettingen, Switzerland: Nationale Genossenschaft fur die Lagerung radioaktiver Abfalle. TIC: 240697.

Chapelle, F.H. 1993. *Ground-Water Microbiology and Geochemistry.* New York, New York: John Wiley & Sons. TIC: 248402.

Chen, Y.; Engel, D.W.; McGrail, B.P.; and Lessor, K.S. 1995. *AREST-CT V1.0 Software Verification.* PNL-10692. Richland, Washington: Pacific Northwest Laboratory. ACC: MOL.19960415.0236.

Choppin, G.R. 1992. "The Role of Natural Organics in Radionuclide Migration in Natural Aquifer Systems." *Radiochimica Acta, 58/59,* 113-120. New York, New York: Academic Press. TIC: 222387.

Codell, R.B. and Murphy, W.M. 1992. "Geochemical Model for 14C Transport in Unsaturated Rock." *High Level Radioactive Waste Management, Proceedings of the Third International Conference, Las Vegas, Nevada, April 12-16, 1992. 2,* 1959-1965. La Grange Park, Illinois: American Nuclear Society. TIC: 204231.

CRWMS M&O 1995. *Total System Performance Assessment - 1995: An Evaluation of the Potential Yucca Mountain Repository.* B00000000-01717-2200-00136 REV 01. Las Vegas, Nevada: CRWMS M&O. ACC: MOL.19960724.0188.

CRWMS M&O 1997a. *Near-Field Geochemical Environment Abstraction/Testing Workshop Results.* B00000000-01717-2200-00188. Las Vegas, Nevada: CRWMS M&O. ACC: MOL.19980612.0027.

CRWMS M&O 1997b. *Performance Implications to the Potential Yucca Mountain Repository by the Addition of Organics to the Site Surface: The Relations Between Soil Organic Carbon, CO_2 from Soil Respiration and Their Interactions with Groundwater.* BA0000000-01717-2200-00008. Las Vegas, Nevada: CRWMS M&O. ACC: MOL.19970604.0498.

CRWMS M&O 1997c. *Materials for Emplacement Drift Ground Support.* BCAA00000-01717-0200-00003 REV 00. Las Vegas, Nevada: CRWMS M&O. ACC: MOL.19971029.0493

CRWMS M&O 1998a. "Near-Field Geochemical Environment." Chapter 4 of *Total System Performance Assessment-Viability Assessment (TSPA-VA) Analyses Technical Basis Document.* B00000000-01717-4301-00004 REV 01. Las Vegas, Nevada: CRWMS M&O. ACC: MOL.19981008.0004.

CRWMS M&O 1998b. "Thermal Hydrology." Chapter 3 of *Total System Performance Assessment-Viability Assessment (TSPA-VA) Analyses Technical Basis Document.* B00000000-01717-4301-00003 REV 01. Las Vegas, Nevada: CRWMS M&O. ACC: MOL.19981008.0003.

CRWMS M&O 1998c. "Waste Package Degradation Modeling and Abstraction." Chapter 5 of *Total System Performance Assessment-Viability Assessment (TSPA-VA) Analyses Technical Basis Document.* B00000000-01717-4301-00005 REV 01. Las Vegas, Nevada: CRWMS M&O. ACC: MOL.19981008.0005.

CRWMS M&O 1998d. *Computer Software Documentation and Users Manual, MING Microbial Impacts to the Near-Field Environment Geochemistry Version 1.0 CSCI 30018 V1.0.* CSCI: 30018 V1.0. DI: 30018-2003, Rev. 0. Las Vegas, Nevada: CRWMS M&O. ACC: MOL.19980803.0618.

CRWMS M&O 1998e. *MING Parameter Input: Reactant Compositions, Breakdown Codes and Molecular Masses for Release of Organic Materials.* B00000000-01717-0200-00171 REV 00. Las Vegas, Nevada: CRWMS M&O. ACC: MOL.19980904.0553.

CRWMS M&O 1998f. *MING Parameter Input: Temperature Dependant Delta G Relationships for Selected Redox Half Reactions of C, N, S, Fe, Mn, H, and O.* B00000000-01717-0200-00170 REV 00. Las Vegas, Nevada: CRWMS M&O. ACC: MOL.19980904.0551.

CRWMS M&O 1998g. *MING Parameter Input: Waste Package Design Compositional Information.* B00000000-01717-0200-00168 REV 00. Las Vegas, Nevada: CRWMS M&O. ACC: MOL.19980904.0547.

CRWMS M&O 1998h. *Software Qualification Report MING Microbial Impacts to the Near-Field Environment Geochemistry Version 1.0.* CSCI: 30018 V1.0 . DI: 30018-2003, Rev. 00. Las Vegas, Nevada: CRWMS M&O. ACC: MOL.19981029.0153.

CRWMS M&O 1998i. *Software Code: MING V1.0* . V1.0. 30018 V1.0.

CRWMS M&O 1999a. *Conduct of Performance Assessment.* Activity Evaluation, September 30, 1999. Las Vegas, Nevada: CRWMS M&O. ACC: MOL.19991028.0092.

CRWMS M&O 1999b. *Evaluation of Alternative Materials for Emplacement Drift Ground Control.* BCAA00000-01717-0200-00013 REV 00. Las Vegas, Nevada: CRWMS M&O. ACC: MOL.19990720.0198.

CRWMS M&O 1999c. *License Application Design Selection Report.* B00000000-01717-4600-00123 REV 01 ICN 01. Las Vegas, Nevada: CRWMS M&O. ACC: MOL.19990908.0319.

CRWMS M&O 1999d. Not Used.

CRWMS M&O 1999e. *Nominal Thickness of Steel Repository Materials.* Input Transmittal PA-SSR-99403.T. Las Vegas, Nevada: CRWMS M&O. ACC: MOL.19991209.0054.

CRWMS M&O 1999f. *Provide Sub-Models for the Physical and Chemical Environmental Abstraction Model for TSPA-LA.* TDP-WIS-MD-000006 REV 00. Las Vegas, Nevada: CRWMS M&O. ACC: MOL.19990902.0450.

CRWMS M&O 1999g. *Request for Repository Subsurface Design Information to Support TSPA-SR.* Input Transmittal PA-SSR-99218.Ta. Las Vegas, Nevada: CRWMS M&O. ACC: MOL.19990901.0312.

CRWMS M&O 1999h. *Waste Package Design Input for Geochemical Analysis.* Input Transmittal PA-WP-99294.Ta. Las Vegas, Nevada: CRWMS M&O. ACC: MOL.19991015.0303.

CRWMS M&O 1999i. *Waste Package Materials Properties.* BBA000000-01717-0210-00017 REV 00. Las Vegas, Nevada: CRWMS M&O. ACC: MOL.19990407.0172.

CRWMS M&O 2000a. *Abstraction of Drift Seepage.* ANL-NBS-MD-000005 REV 00. Las Vegas, Nevada: CRWMS M&O. ACC: MOL.20000322.0671.

CRWMS M&O 2000b. *Abstraction of Drift-Scale Coupled Processes.* ANL-NBS-HS-000029 REV 00. Las Vegas, Nevada: CRWMS M&O. ACC: MOL.20000525.0371.

CRWMS M&O 2000c. *Abstraction of NFE Drift Thermodynamic Environment and Percolation Flux.* ANL-EBS-HS-000003 REV 00. Las Vegas, Nevada: CRWMS M&O. ACC: MOL.20000504.0296.

CRWMS M&O 2000d. *Design Analysis for the Defense High-Level Waste Disposal Container.* ANL-DDC-ME-000001 REV 00. Las Vegas, Nevada: CRWMS M&O. ACC: MOL.20000627.0254.

CRWMS M&O 2000e. *Design Analysis for the Ex-Container Components.* ANL-XCS-ME-000001 REV 00. Las Vegas, Nevada: CRWMS M&O. ACC: MOL.20000525.0374.

CRWMS M&O 2000f. *Design Analysis for the Naval SNF Waste Package.* ANL-VDC-ME-000001 REV 00. Las Vegas, Nevada: CRWMS M&O . ACC: MOL.20000615.0029.

CRWMS M&O 2000g. *Design Analysis for UCF Waste Packages.* ANL-UDC-MD-000001 REV 00. Las Vegas, Nevada: CRWMS M&O. ACC: MOL.20000526.0336.

CRWMS M&O 2000h. *The Development of Information Catalogued in REV00 of the YMP FEP Database.* TDR-WIS-MD-000003 REV 00. Las Vegas, Nevada: CRWMS M&O. ACC: MOL.20000705.0098.

CRWMS M&O 2000i. *Drift-Scale Coupled Processes (DST and THC Seepage) Models.* MDL-NBS-HS-000001 REV 00. Las Vegas, Nevada: CRWMS M&O. ACC: MOL.19990721.0523.

CRWMS M&O 2000j. *Engineered Barrier System Degradation, Flow, and Transport Process Model Report.* TDR-EBS-MD-000006 REV 00. Las Vegas, Nevada: CRWMS M&O. ACC: MOL.20000324.0558.

CRWMS M&O 2000k. *Engineered Barrier System: Physical and Chemical Environment Model.* ANL-EBS-MD-000033 REV 00. Las Vegas, Nevada: CRWMS M&O. ACC: MOL.20000706.0206.

CRWMS M&O 2000l. *In-Drift Gas Flux and Composition.* ANL-EBS-MD-000040 REV 00. Las Vegas, Nevada: CRWMS M&O. ACC: MOL.20000523.0154.

CRWMS M&O 2000m. *Initial Cladding Condition.* ANL-EBS-MD-000048 REV 00. Las Vegas, Nevada: CRWMS M&O. ACC: MOL.20000523.0150.

CRWMS M&O 2000n. *Inventory Abstraction.* ANL-WIS-MD-000006 REV 00. Las Vegas, Nevada: CRWMS M&O. ACC: MOL.20000414.0643.

CRWMS M&O 2000o. *Multiscale Thermohydrologic Model.* ANL-EBS-MD-000049 REV 00. Las Vegas, Nevada: CRWMS M&O. ACC: MOL.20000609.0267.

CRWMS M&O 2000p. Not Used.

CRWMS M&O 2000q. *Draft of Calculation Thermal Hydrology EBS Design Sensitivity Analysis (CAL-EBS-HS-000003).* Input Transmittal 00361.T. Las Vegas, Nevada: CRWMS M&O. ACC: MOL.20000918.0525.

CRWMS M&O 2000r. *Yucca Mountain Site Description.* TDR-CRW-GS-000001 REV 01. Las Vegas, Nevada: CRWMS M&O. ACC: MOL.20000717.0292.

CRWMS M&O 2000s. *Monitored Geologic Repository Project Description Document.* TDR-MGR-SE-000004 REV 01 ICN 02. Las Vegas, Nevada: CRWMS M&O. ACC: MOL.20001005.0281

Daughney, C.J.; Fein, J.B.; and Yee, N. 1998. "A Comparison of the Thermodynamics of Metal Adsorption onto Two Common Bacteria." *Chemical Geology, 144,* 161-176. Amsterdam, The Netherlands: Elsevier Science. TIC: 244490.

Davis, M.A.; Martin, S.; Miranda, A.; and Horn, J.M. 1998. *Sustaining Native Microbial Growth with Endogenous Nutrients at Yucca Mountain.* URCL-JC-129185. Livermore, California: Lawrence Livermore National Laboratory. ACC: MOL.19980521.0038.

Diercks, M.; Sand, W.; and Bock, E. 1991. "Microbial Corrosion of Concrete." *Experientia, 47,* 514-516. Basal, Switzerland: Birkhäuser Verlag. TIC: 244488.

DOE (U.S. Department of Energy) 1992. *Characteristics of Potential Repository Wastes.* DOE/RW-0184-R1. Four volumes. Washington, D.C.: U.S. Department of Energy, Office of Civilian Radioactive Waste Management. ACC: HQO.19920827.0001; HQO.19920827.0002; HQO.19920827.0003; HQO.19920827.0004.

Dyer, J.R. 1999. "Revised Interim Guidance Pending Issuance of New U.S. Nuclear Regulatory Commission (NRC) Regulations (Revision 01, July 22, 1999), for Yucca Mountain, Nevada." Letter from J.R. Dyer (DOE/YMSCO) to D.R. Wilkins (CRWMS M&O), September 3, 1999, OL&RC:SB-1714, with enclosure, "Interim Guidance Pending Issuance of New NRC Regulations for Yucca Mountain (Revision 01)." ACC: MOL.19990910.0079.

Fein, J.B.; Daughney, C.J.; Yee, N.; and Davis, T.A. 1997. "A Chemical Equilibrium Model for Metal Adsorption onto Bacterial Surfaces." *Geochimica et Cosmochimica Acta, 61,* (16), 3319-3328. New York, New York: Pergamon Press. TIC: 238695.

Flint, L.E. 1998. *Characterization of Hydrogeologic Units Using Matrix Properties, Yucca Mountain, Nevada.* Water-Resources Investigations Report 97-4243. Denver, Colorado: U.S. Geological Survey. ACC: MOL.19980429.0512.

Francis, A.J.; Dodge, C.J.; Lu, F.; Halada, G.P.; and Clayton, C.R. 1994. "XPS and XANES studies of Uranium Reduction by Clostridium sp." *Environmental Science Technology, 28,* 636-639. Easton, Pennsylvania: American Chemical Society. TIC: 244487.

Geesey, G. 1993. *A Review of the Potential for Microbially Influenced Corrosion of High-Level Nuclear Waste Containers.* Cragnolino, G.A., ed. CNWRA 93-014. San Antonio, Texas: Center for Nuclear Waste Regulatory Analyses. TIC: 215011.

Glassley, W. 1997. *Chemical Composition of Water Before Contact with Repository Materials.* Milestone SPLA1M4. Livermore, California: Lawrence Livermore National Laboratory. ACC: MOL.19971210.0031.

Glassley, W.E. 1994. *Report on Near-Field Geochemistry: Water Composition Changes Due to Evaporation.* Milestone M0L26. Draft. Livermore, California: Lawrence Livermore National Laboratory. ACC: MOL.19950406.0153.

Grogan, H.A. and McKinley, I.G. 1990. *An Approach to Microbiological Modeling: Application to the Near Field of a Swiss Low/Intermediate-Level Waste Repository.* Technical Report 89-06. Baden, Switzerland: Nationale Genossenschaft fur die Lagerung radioaktiver Abfalle. TIC: 239189.

Haldeman, D.L. and Amy, P.S. 1993. "Bacterial Heterogeneity in Deep Subsurface Tunnels at Rainier Mesa, Nevada Test Site." *Microbial Ecology, 25,* (2), 185-194. New York, New York: Springer-Verlag. TIC: 238373.

Hardin, E.L. 1998. *Near-Field/Altered-Zone Models Report.* UCRL-ID-129179. Livermore, California: Lawrence Livermore National Laboratory. ACC: MOL.19980630.0560.

Harrar, J.E.; Carley, J.F.; Isherwood, W.F.; and Raber, E. 1990. *Report of the Committee to Review the Use of J-13 Well Water in Nevada Nuclear Waste Storage Investigations.* UCID-21867. Livermore, California: Lawrence Livermore National Laboratory. ACC: NNA.19910131.0274.

Hersman, L. 1995. *Microbial Effects on Colloidal Agglomeration.* LA-12972-MS. Los Alamos, New Mexico: Los Alamos National Laboratory. ACC: MOL.19971210.0253.

Hersman, L.E. 1997. "Subsurface Microbiology: Effects on the Transport of Radioactive Wastes in the Vadose Zone." Chapter 16 of *The Microbiology of the Terrestrial Deep Subsurface.* Amy, P.S. and Haldeman, D.L., eds. Boca Raton, Florida: CRC Lewis Publishers. TIC: 232570.

Hersman, L.E.; Palmer, P.D.; and Hobart, D.E. 1993. "The Role of Siderophores in the Transport of Radionuclides." *Scientific Basis for Nuclear Waste Management XVI, Symposium held November 30-December 4, 1992, Boston, Massachusetts.* Interrante, C.G. and Pabalan, R.T., eds. *294,* 765-770. Pittsburgh, Pennsylvania: Materials Research Society. TIC: 208880.

Horn, J.M. and Meike, A. 1995. "Microbial Activity at Yucca Mountain." Part I: *Microbial Metabolism, Adaptation and the Repository Environment.* UCRL-ID-122256. Livermore, California: Lawrence Livermore National Laboratory. TIC: 222145.

Horn, J.M.; Davis, M.; Martin, S.; Lian, T.; and Jones, D. 1998a. *Assessing Microbiologically Induced Corrosion of Waste Package Materials in the Yucca Mountain Repository.* URCL-JC-130567. Livermore, California: Lawrence Livermore National Laboratory. TIC: 244465.

Horn, J.M.; Rivera, A.; Lian, T.; and Jones, D. 1998b. "MIC Evaluation and Testing for the Yucca Mountain Repository." *Proceedings of Corrosion 98, March 22-27, San Diego, California.* Pages 152/2 to 152/14. Houston, Texas: NACE International. TIC: 237146.

Journel, A.G. 1989. "Fundamentals of Geostatistics in Five Lessons." *Short Course in Geology, Presented at the 28th International Geological Congress, Washington, D.C.* Volume 8 . Washington, D.C.: American Geophysical Union. TIC: 240472.

Kieft, T.L. and Phelps, T.J 1997. "Life in the Slow Lane: Activities of Microorganisms in the Subsurface." Chapter 9 of *The Microbiology of the Terrestrial Deep Subsurface.* Amy, P.S. and Haldeman, D.L., eds. New York, New York: Lewis Publishers. TIC: 236530.

Kieft, T.L.; Amy, P.S.; Brockman, F.J.; Fredrickson, J.K.; Bjornstad, B.N.; and Rosacker, L.L. 1993. "Microbial Abundance and Activities in Relation to Water Potential in the Vadose Zones of Arid and Semiarid Sites." *Microbial Ecology, 26,* 59-78. New York, New York: Springer-Verlag. TIC: 236436.

Kieft, T.L.; Kovacik, W.P., Jr.; Ringelberg, D.B.; White, D.C.; Haldeman, D.L.; Amy, P.S.; and Hersman, L.E. 1997. "Factors Limiting Microbial Growth and Activity at a Proposed High-Level Nuclear Repository, Yucca Mountain, Nevada." *Applied and Environmental Microbiology, 63,* (8), 3128-3133. Washington, D.C.: American Society for Microbiology. TIC: 236444.

Klein, C. and Hurlbut, C.S., Jr. 1985. *Manual of Mineralogy.* 20th Edition. New York, New York: John Wiley & Sons. TIC: 242818.

Kugler, A. 1997. Sheet and Plate for Nuclear Engineering, Bohler Neutronit A976. Houston, Texas: Bohler Bleche GmbH. TIC: 246410.

Lichtner, P.C. and Seth, M. 1996. "Multiphase-Multicomponent Nonisothermal Reactive Transport in Partially Saturated Porous Media." *Proceedings of the 1996 International Conference on Deep Geological Disposal of Radioactive Waste, September 16-19, 1996, Winnipeg, Manitoba, Canada.* Toronto, Ontario, Canada: Canadian Nuclear Society. TIC: 233923.

Little, B.J.; Wagner, P.A.; and Lewandowski, Z. 1997. *Spatial Relationships Between Bacteria and Mineral Surfaces.* Geomicrobiology: Interactions Between Microbes and Minerals. Banfield, J.F. and Nealson, K.H., eds. Reviews in Mineralogy Volume 35, 123-159. Washington, D.C.: Mineralogical Society of America. TIC: 236425.

Lovley, D.R. and Phillips, E.J.P. 1992. "Reduction of Uranium by Desulfovibrio Desulfuricans." *Applied and Environmental Microbiology, 58,* (3), 850-856. Washington, D.C.: American Society for Microbiology. TIC: 245045.

Lovley, D.R.; Phillips, E.J.P.; Gorby, Y. A.; and Land, E.R. 1991. "Microbial Reduction of Uranium." *Nature, 350,* (6317), 414-416. London, United Kingdom: Macmillan Publishers. TIC: 245130.

Lovley, D.R.; Widman, P.K.; Woodward, J.C.; and Phillips, E.J.P. 1993. "Reduction of Uranium by Cytochrome c^3 of Desulfovibrio Vulgaris." *Applied and Environmental Microbiology, 59,* (11), 3572-3576. Washington, D.C.: American Society for Microbiology. TIC: 244486.

MacKinnon, R.J. 2000. "EBS Performance Process Control Evaluation for Supplement V." Interoffice correspondence from R.J. MacKinnon (CRWMS M&O) to Records Processing Center (RPC), November 2, 2000, LV.PA.RJM.11/00-090, with attachment. ACC: MOL.20001103.0011.

McKinley, I.G. and Grogan, H.A. 1991. "Consideration of Microbiology in Modelling the Near Field of a L/ILW Repository." *Experientia, 47,* 573-577. Basel, Switzerland: Birkhäuser Verlag. TIC: 236438.

McKinley, I.G.; Hagenlocher, I.; Alexander, W.R.; and Schwyn, B. 1997. "Microbiology in Nuclear Waste Disposal: Interfaces and Reaction Fronts." *FEMS Microbiology Reviews, 20,* (3-4), 545-556. Amsterdam, The Netherlands: Elsevier Science B.V. TIC: 235823.

Meike, A. and Wittwer, C. 1993. "Formation of Colloids from Introduced Materials in the Post-Emplacement Environment: A Report on the State of Understanding." *Proceedings of the Topical Meeting on Site Characterization and Model Validation, Focus '93, September 26-29, 1993, Las Vegas, Nevada.* Pages 95-102. La Grange Park, Illinois: American Nuclear Society. TIC: 102245.

Mills, A.L. 1997. "Movement of Bacteria in the Subsurface." Chapter 13 of *The Microbiology of the Terrestrial Deep Subsurface* . Amy, P.S. and Haldeman, D.L., eds. New York, New York: CRC Lewis Publishers. TIC: 232570.

Minai, Y.; Choppin, G.R.; and Sisson, D.H. 1992. "Humic Material in Well Water from the Nevada Test Site." *Radiochimica Acta, 56,* 195-199. München, Germany: R. Oldenbourg Verlag. TIC: 238763.

Morel, F.M.M. and Hering, J.G. 1993. *Principles and Applications of Aquatic Chemistry.* New York, New York: John Wiley & Sons. TIC: 248465.

Morita, R.Y. 1990. "The Starvation-Survival State of Microorganisms in Nature and Its Relationship to the Bioavailable Energy." *Experientia, 46,* 813-817. Basel, Switzerland: Birkhäuser Verlag. TIC: 236763.

Morrison, R.T. and Boyd, R.N. 1992. *Organic Chemistry.* 6th Edition. Englewood Cliffs, New Jersey: Prentice Hall. TIC: 245883.

Murphy, W.M. 1991. "Performance Assessment Perspectives with Reference to the Proposed Repository at Yucca Mountain, Nevada." *Proceedings from the Technical Workshop on Near-Field Performance Assessment for High-Level Waste held in Madrid, October 15-17, 1990,.* P. Sellen, M. Apted, and J. Gago, eds. Pages 11-22. Stockholm, Sweden: Swedish Nuclear Fuel and Waste Management Company. TIC: 237757.

Murphy, W.M. 1993. "Geochemical Models for Gas-Water-Rock Interactions in a Proposed Nuclear Waste Repository at Yucca Mountain." *Proceedings of the Topical Meeting on Site Characterization and Model Validation, Focus '93, September 26-29, 1993, Las Vegas, Nevada.* Pages 115-121. La Grange Park, Illinois: American Nuclear Society. TIC: 102245.

Murphy, W.M. and Pabalan, R.T. 1994. *Geochemical Investigations Related to the Yucca Mountain Environment and Potential Nuclear Waste Repository.* NUREG/CR-6288. San Antonio, Texas: Southwest Research Institute. TIC: 227032.

Nealson, K.H. and Stahl, D.H. 1997. *Microorganisms and Biogeochemical Cycles: What Can We Learn from Layered Microbial Communities?.* Geomicrobiology: Interactions Between Microbes and Minerals. J.F. Banfield and K.H. Nealson, eds. Reviews in Mineralogy, Volume 35, 5-34. Washington, D.C.: Mineralogical Society of America. TIC: 236424.

Pedersen, K. 1999. "Subterranean Microorganisms and Radioactive Waste Disposal in Sweden." *Engineering Geology, 52,* 163-176. New York, New York: Elsevier Science. TIC: 244755.

Pedersen, K. and Karlsson, F. 1995. *Investigations of Subterranean Microorganisms: Their Importance for Performance Assessment of Radioactive Waste Disposal.* SKB 95-10. Stockholm, Sweden: Swedish Nuclear Fuel and Waste Management Company. TIC: 221443.

Perfettini, J.V.; Revertegat, E.; and Langomazino, N. 1991. "Evaluation of Cement Degradation Induced by the Metabolic Products of Two Fungal Strains." *Experientia, 47,* 527-532. Basel, Switzerland: Birkhäuser Verlag. TIC: 239327.

Peters, C.A.; Yang, I.C.; Higgins, J.D.; and Burger, P.A. 1992. "A Preliminary Study of the Chemistry of Pore Water Extracted from Tuff by One-Dimensional Compression." *Proceedings of the 7th International Symposium on Water-Rock Interaction, Park City, Utah, July 13-18, 1992.* Kharaka, Y.K. and Maest, A.S., eds. *1,* 741-745. Rotterdam, The Netherlands: A.A. Balkema. TIC: 208527.

Pitonzo, B. 1996. *Characterization of Microbes Implicated in Microbially-Influenced Corrosion from the Proposed Yucca Mountain Repository.* Ph.D. dissertation. Las Vegas, Nevada: University of Nevada, Las Vegas. TIC: 236608.

Ringelberg, D.B.; Amy, P.S.; Clarkson, W.W.; Haldeman, D.L.; Khalil, M.K.; Kieft, T.L.; Krumholtz, L.R.; Stair, J.O.; Suflita, J.M.; White, D.C.; and Hersman, L.E.H. 1997. *Microbial Community Composition in a Volcanic Tuff, Yucca Mountain, Nevada.* Rough draft. Vicksburg, Mississippi: U.S. Army Corps of Engineers Waterways Experiment Station. TIC: 234025.

Rogers, J.R.; Bennett, P.C.; and Choi, W.J. 1998. "Feldspars as a Source of Nutrients for Microorganisms." *American Mineralogist, 83,* 1532-1540. Washington, D.C.: Mineralogical Society of America. TIC: 244489.

Sargent-Welch Scientific Company 1979. *Periodic Table of the Elements.* Catalog Number S-18806. Skokie, Illinois: Sargent-Welch Scientific Company. TIC: 245069.

Stone, A.T. 1997. "Reactions of Extracellular Organic Ligands with Dissolved Metal Ions and Mineral Surfaces." Chapter 9 of *Geomicrobiology: Interactions Between Microbes and Minerals.* Banfield, J.F. and Nealson, K.H., eds. Reviews in Mineralogy 35. Washington, D.C.: Mineralogical Society of America. TIC: 236757.

Stroes-Gascoyne, S. 1989. *The Potential for Microbial Life in a Canadian High-Level Nuclear Fuel Waste Disposal Vault: A Nutrient and Energy Source Analysis.* AECL-9574. Pinawa, Manitoba, Canada: Atomic Energy of Canada Limited. TIC: 236580.

Van Konynenburg, R.A. 1996. "Radiation Effects." Chapter 5 of *Near-Field and Altered-Zone Environment Report.* Wilder, D.G., ed. UCRL-LR-124998. Volume II. Livermore, California: Lawrence Livermore National Laboratory. ACC: MOL.19961212.0122.

Van Konynenburg, R.A.; Curtis, P.G.; and Summers, T.S.E. 1998. *Scoping Corrosion Tests on Candidate Waste Package Basket Materials for the Yucca Mountain Project.* UCRL-ID-130386. Livermore, California: Lawrence Livermore National Laboratory. ACC: MOL.19980727.0385.

Vaniman, D.T.; Bish, D.L.; Chipera, S.J.; Carlos, B.A.; and Guthrie, G.D., Jr. 1996. *Chemistry and Mineralogy of the Transport Environment at Yucca Mountain.* Volume I of *Summary and Synthesis Report on Mineralogy and Petrology Studies for the Yucca Mountain Site Characterization Project.* Milestone 3665. Los Alamos, New Mexico: Los Alamos National Laboratory. ACC: MOL.19961230.0037.

Weast, R.C., ed. 1979. *CRC Handbook of Chemistry and Physics.* 60th Edition, 1979 - 1980. Boca Raton, Florida: CRC Press. TIC: 245312.

West, J.M.; Christofi, N.; and McKinley, I.G. 1985. "An Overview of Recent Microbiological Research Relevant to the Geological Disposal of Nuclear Waste." *Radioactive Waste Management and the Nuclear Fuel Cycle, 6,* (1), 79-95. New York, New York: Harwood Academic Publishers. TIC: 244498.

West, J.M.; McKinley, I.G.; and Vialta, A. 1989. "The Influence of Microbial Activity on the Movement of Uranium at OSAMU UTSUMI Mine, Poços de Caldas, Brazil." *Scientific Basis for Nuclear Waste Management XII, Symposium held October 10-13, 1988, Berlin, Germany.* Lutze, W. and Ewing, R.C., eds. *127,* 771-777. Pittsburgh, Pennsylvania: Materials Research Society. TIC: 203660.

Wilder, D.G., ed. 1996. *Near-Field and Altered-Zone Environment Report.* UCRL-LR-124998. Volume II. Livermore, California: Lawrence Livermore National Laboratory. ACC: MOL.19961212.0121; MOL.19961212.0122.

Wolery, T.J. 1992. *EQ3/6, A Software Package for Geochemical Modeling of Aqueous Systems. Package Overview and Installation Guide (Version 7.0).* UCRL-MA-110662 PT I. Livermore, California: Lawrence Livermore National Laboratory. TIC: 205087.

Yang, I.C. 1992. "Flow and Transport through Unsaturated Rock – Data from Two Test Holes, Yucca Mountain, Nevada." *High Level Radioactive Waste Management, Proceedings of the Third International Conference, Las Vegas, Nevada, April 12-16, 1992. 1,* 732-737. La Grange Park, Illinois: American Nuclear Society. TIC: 204231.

Yang, I.C.; Davis, G.S.; and Sayre, T.M. 1990. "Comparison of Pore-Water Extraction by Triaxial Compression and High-Speed Centrifugation Methods." *Proceedings of Conference on Minimizing Risk to the Hydrological Environment, American Institute of Hydrology.* Pages 250-259. Dubuque, Iowa: American Institute of Hydrology. TIC: 224435.

Yang, I.C.; Turner, A.K.; Sayre, T.M.; and Montazer, P. 1988. *Triaxial-Compression Extraction of Pore Water from Unsaturated Tuff, Yucca Mountain, Nevada.* Water-Resources Investigations Report 88-4189. Denver, Colorado: U.S. Geological Survey. ACC: NNA.19890309.0161.

8.2 CODES, STANDARDS, REGULATIONS, AND PROCEDURES

64 FR 8640. Disposal of High-Level Radioactive Wastes in a Proposed Geologic Repository at Yucca Mountain, Nevada. Readily available.

AP-SV.1Q, Rev. 0, ICN 2. *Control of the Electronic Management of Information.* Washington, D.C.: U.S. Department of Energy, Office of Civilian Radioactive Waste Management. ACC: MOL.20000831.0065.

ASME (American Society of Mechanical Engineers) 1995. "Specification for Low-Carbon Nickel-Molybdenum, and Low Carbon Nickel-Chromium-Molybdenum-Tungsten Alloy Plate, Shee, and Strip." SB-575. *Section II: Materials, Part B - Nonferrous Material Specifications.* 1995 ASME Boiler and Pressure Vessel Code. New York, New York: American Society of Mechanical Engineers. TIC: 245287.

ASTM A 185-97. 1997. *Standard Specification for Steel Welded Wire Fabric, Plain, for Concrete Reinforcement.* Philadelphia, Pennsylvania: American Society for Testing and Materials. TIC: 246271.

ASTM A 240/A 240M-97a. 1997. *Standard Specification for Heat-Resisting Chromium and Chromium-Nickel Stainless Steel Plate, Sheet, and Strip for Pressure Vessels.* West Conshohocken, Pennsylvania: American Society for Testing and Materials. TIC: 239431.

ASTM A 276-91a. 1991. *Standard Specification for Stainless and Heat-Resisting Steel Bars and Shapes.* Philadelphia, Pennsylvania: American Society for Testing and Materials. TIC: 240022.

ASTM A 516/A 516M - 90. 1991. *Standard Specification for Pressure Vessel Plates, Carbon Steel, for Moderate- and Lower-Temperature Service.* Philadelphia, Pennsylvania: American Society for Testing and Materials. TIC: 240032.

ASTM A 572/A 572M-99a. 1999. *Standard Specification for High-Strength Low-Alloy Columbium-Vanadium Structural Steel.* West Conshohocken, Pennsylvania: American Society for Testing and Materials. TIC: 246273.

ASTM A 759-85 (Reapproved 1992). *Standard Specification for Carbon Steel Crane Rails.* West Conshohocken, Pennsylvania: American Society for Testing and Materials. TIC: 246309.

ASTM B 209M-92a. 1992. *Standard Specification for Aluminum and Aluminum-Alloy Sheet and Plate [Metric]1.* Philadelphia, Pennsylvania: American Society for Testing and Materials. TIC: 240034.

ASTM C 1174-97. 1998. *Standard Practice for Prediction of the Long-Term Behavior of Materials, Including Waste Forms, Used in Engineered Barrier Systems (EBS) for Geological Disposal of High-Level Radioactive Waste.* West Conshohocken, Pennsylvania: American Society for Testing and Materials. TIC: 246015.

ASTM C 845-96. 1996. *Standard Specification for Expansive Hydraulic Cement.* West Conshohocken, Pennsylvania: American Society for Testing and Materials. TIC: 246401.

ASTM F 432-95. 1995. *Standard Specification for Roof and Rock Bolts and Accessories.* Philadelphia, Pennsylvania: American Society for Testing and Materials. TIC: 241007.

DOE (U.S. Department of Energy) 2000. *Quality Assurance Requirements and Description.* DOE/RW-0333P, Rev. 10. Washington, D.C.: U.S. Department of Energy, Office of Civilian Radioactive Waste Management. ACC: MOL.20000427.0422.

NLP-2-0, REV. 5 ICN 1, *Determination of Importance Evaluations*, Las Vegas, Nevada: CRWMS M&O. MOL.20000713.0360.

NRC (U.S. Nuclear Regulatory Commission) 1998. *Issue Resolution Status Report Key Technical Issue: Evolution of the Near-Field Environment.* Rev. 1. Washington, D.C.: U.S. Nuclear Regulatory Commission. ACC: MOL.19981106.0144.

NRC (U.S. Nuclear Regulatory Commission) 1999. *Issue Resolution Status Report Key Technical Issue: Evolution of the Near-Field Environment.* Rev. 2. Washington, D.C.: U.S. Nuclear Regulatory Commission. ACC: MOL.19990810.0640.

QAP-2-0, Rev. 5. *Conduct of Activities.* Las Vegas, Nevada: CRWMS M&O. ACC: MOL.19980826.0209.

QAP-2-3, Rev 10, *Classification of Permanent Items*, Las Vegas, Nevada: CRWMS M&O. MOL.19990316.0006.

8.3 SOURCE DATA, LISTED BY DATA TRACKING NUMBER

GS931208314211.047. Graphical Lithologic Log of Borehole Ue-25 UZ#16. Submittal date: 11/22/1993.

GS960908312231.004. Characterization of Hydrogeologic Units Using Matrix Properties at Yucca Mountain, Nevada. Submittal date: 09/12/1996.

GS980908312322.008. Field, Chemical, and Isotopic Data from Precipitation Sample Collected Behind Service Station in Area 25 and Ground Water Samples Collected at Boreholes UE-25 C #2, UE-25 C #3, USW UZ-14, UE-25 WT #3, UE-25 WT #17, and USW WT-24, 10/06/97 to 07/01/98. Submittal date: 09/15/1998.

LA000000000086.002. Mineralogic Variation in Drill Core UE-25 UZ#16 Yucca Mountain, Nevada. Submittal date: 03/28/1995.

LALH831342AQ96.002. Summary and Synthesis of Biological Sorption and Transport. Submittal date: 08/28/1996.

LL000206105924.126. Assessing Microbiologically Induced Corrosion of Waste Material in the Yucca Mountain Repository. Submittal date: 2/16/2000.

LL980504105924.034. Scoping Corrosion Tests on Candidate Waste Package Basket Materials for the YMP. Submittal date: 05/14/1998.

LL980608505924.035. Sustaining Microbial Growth with Endogenous Nutrients at Yucca Mountain. Submittal date: 06/26/1998.

LL980704605924.035. Engineering Material Characterization Report, Volume 3. Submittal date: 07/17/1998.

LL981209705924.059. Biochemical Contributions to Corrosion of Carbon Steel and Alloy 22 in a Continual Flow System. Submittal date: 12/15/1998.

MO0003SPASUP02.003. Supporting Media for Calculation of General Corrosion Rate of Drip Shield and Waste Package Outer Barrier to Support WAPDEG Analysis. Submittal date: 03/02/2000.

MO0004SPASMA05.004. Supporting Media for Abstraction of Models for Stainless Steel Structural Material Degradation. Submittal date: 04/05/2000.

MO0005EMMATEST.000. Results of EMMA Test Case Using MING V1.0 and MING Calculated Microbial Abundance, Redox Energy and Energy-Limited Biomass. Submittal date: 05/24/2000.

MO9807MWDEQ3/6.005. Chapter 4 TSPA-VA Technical Basis Document Near-Field Geochemical Environment. EQ3/6: Microbe Model. Submittal date: 08/06/1998.

MO9909SPA00J13.006. J-13 Water Compositions Used in MING Calculations. Submittal date: 09/28/1999.

MO9909SPABMASS.000. Biomass in Rock Samples Taken from Rainier Mesa Tunnels. Submittal date: 09/01/1999.

MO9909SPAMICRO.001. Average Microbial Volume, Water Content, and Microbial Composition. Submittal date: 09/01/1999.

MO9909SPAMING1.003. Temperature Dependant Delta G Relationships for Selected Redox Half Reactions Used in MING V1.0. Submittal date: 09/14/1999.

MO9911SPACGF04.000. Cumulative Gas Flux Values (KG/M^2) Used in the TSPA-VA Ambient Case MING Calculations. Submittal date: 11/22/1999.

MO9912DTMKCCOF.000. Chemical Compositions of Silica Fume. Submittal date: 12/07/1999.

MO9912SEPMKTDC.000. Chemical Compositions of TYPE E-1 (K) Cement. Submittal date: 12/07/1999.

MO9912SPAPAI29.002. PA Initial Abstraction of THC Model Chemical Boundary Conditions. Submittal date: 01/11/2000.

SN0001T0872799.006. In-Drift Thermodynamic Environment and Percolation Flux. Submittal date: 01/27/2000.

SN0002T0872799.008. Infiltration Bin Averaged Drift Wall Temperature and Relative Humidity. Submittal date: 02/01/2000.

SN9911T0811199.003. Calculations of Physical and Chemical Properties of Fast Flux Test Facility (FFTF) Waste Package. Submittal date: 11/15/99.

8.4 OUTPUT DATA, LISTED BY DATA TRACKING NUMBER

MO0010MWDMIN38.031. MING V1.0 Calculations for the In-Drift Microbial Communities Model. Submittal date: 10/11/00.

MO0010MWDMIN38.032. In-Drift Microbial Community Model Results for TSPA-SR. Submittal date: 10/11/00.

9. ATTACHMENTS

Attachment	Title
I	Model Validation Test Case Input Parameters
II	Repository Subsurface Design Input Parameters
III	Waste Package Design Input Parameters
IV	Waste Form Composition Determinations
V	Reactant Composition Determinations
VI	Plotted Results for Sections 6.6.2, 6.6.3, and 6.6.4

ATTACHMENT I: MODEL VALIDATION TEST CASE INPUT PARAMETERS

I-1. PURPOSE

The purpose of this attachment is to create the appropriate parameter input for MING 1.0 (CSCI 30018 V1.0, CRWMS M&O 1998d) that will allow the testing of the MING code with both scientific measurements of microbial populations at the site and natural analogs to the site. This is being done for the QA model validation of the in-drift microbial communities model as directed in CRWMS M&O (1999e).

I-2. METHOD

This section has three parts: 1) the determination of the iron bearing minerals in the host rock, 2) to determine the numbers of microbes in one lineal meter of repository drift, 3) the generation of gas inputs for the LLNL lab experiments and for ambient conditions within the repository host rock.

I-2.1 PART 1: DRIFT MINERALS

The following steps were used to calculate the quantity of iron bearing minerals in the host rock.

1. Calculate the volume of rock in one lineal meter of repository drift.
2. Calculate the mass of ambient materials in one lineal meter of repository drift.
3. Determine the mass of iron bearing minerals found in one lineal meter of repository drift.
4. Determine the wt % composition of iron in the iron bearing minerals in one lineal meter of repository drift.

I-2.2 PART 2: MICROBIAL COUNTS

The following steps were used to calculate the number of microbes in the host rock.

1. Convert mass (kg) of rock in 1 lineal meter of repository drift to grams.
2. Multiply number of cells per gram of crushed tuff (from input) times the number of grams of tuff per lineal meter of repository drift.
3. Multiply the cells per lineal meter of repository by the microbial bulk density to obtain the mass of cells per lineal meter of repository.

I-2.3 PART 3: GAS INPUTS

I-2.3.1 Flask to Drift Scaling

The following steps were used to calculate the appropriate MING V1.0 input parameters:

1. Assume a radius of the open end of a flask.
2. Determine the surface area of the flask opening.
3. Determine MING V1.0 input parameter "drift diameter" by calculating the radius of the flask having a given surface area and a volume of 125 ml.
4. Determine MING V1.0 input parameter "tunnel length" by calculating the length of a flask having a given radius and a volume of 125 ml.

I-2.3.2 Lab Gas

MING V1.0 requires gas flux into the drift in units of kg/m^2 year. The following steps are used to calculate the flux of atmospheric gas into a 125 ml flasks.

1. Determine the mass of atmospheric gases in air.
2. Determine the total gas available to enter the flask (kg/m^2)
3. Determine the daily flux into the flask (kg/m^2 day)
4. Determine the total cumulative flux (over 7 days) into the flask (kg/m^2).

I-3. ASSUMPTIONS

1. Because no specific mineral was designated, the composition of mica group mineral reported in DTN LA000000000086.002 is biotite [Used in Section I-5.1].

The rationale for this assumption is that this mineral was chosen to maximize the amount of iron in the system. Other mica group minerals reported in Klein and Hurlbut (1985, p. 430-433), a standard reference for mineralogy, have less potential iron in their elemental structures. In addition, biotite is considered the most abundant mafic silicate phenocryst in the tuffs at Yucca Mountain (Vaniman et al. 1989, Section 4.1.3.5).

2. Bulk density of a microbe is equal to the bulk density of water (1 g/cm^3) [Used in Section I-5.1].

The rationale for this assumption is because 99% of a microbe's mass is water as reported in DTN MO9909SPAMICRO.001. The remaining mass is not expected to change this value significantly.

3. The minerals sampled within borehole UZ-16 are representative of repository conditions and will serve as an appropriate surrogate for site wide properties. [Used in Section I-5.1].

The rationale for this assumption is based on Vaniman et al. (1989). A review of this synthesis report indicates that although there are differences in mineralogy from borehole to borehole, they do not significantly vary. The same sorts of minerals are found in each borehole within the given lithology.

4. The radius of the open end of a flask is 2.5 cm. [Used in Section I-5.1].

The rationale for this assumption is that although the radius was not reported in Horn et al. (1998a and 1998b) or Davis et al. (1998), a reasonable guess can be made based on the fact that a 125 ml flask is not a large flask and the changing the radius will not affect the results in any significant way because gas abundance in the flask is primarily dependant on the volume of the flask.

5. The only gas available over seven days time is in the flask [Used in Section I-4.3.2].

The rationale for this assumption is that this value bounds the maximum length of experimental days for the experiments conducted at LLNL that were used in the model validation runs (see Figures 11 and 12, Section 6.6.3.1). Although there could be gas entering the flask from the culture samples taken to do microbial counts, gas consumption or generation within the flask over this time should not significantly affect the calculations. This validity of this assumption was demonstrated in Section 6.6.3.4.1 where including gas as a nutrient or energy source did not significantly impact the results.

I-4. INPUTS

I-4.1 PART 1: DRIFT MINERALS

I-4.1.1 Inputs

Chemical formulas for biotite [$K(Mg,Fe)_3(AlSi_3O_{10})(OH)_2$] and hematite ($Fe_2O_3$) were taken from Klein and Hurlbut (1985). Fe^{2+} and Fe^{3+} can both substitute for the Mg in the crystal structure (Klein and Hurlbut 1985). In order to maximize the amount of Fe available in the biotite, Mg is ignored in the formula and the following is used: $KFe_3(AlSi_3O_{10})(OH)_2$.

The Topopah Spring tuff middle nonlithophysal (TMN) and lower lithophysal (TLL) are the rock units where the repository is currently located. DTN GS931208314211.047 shows the depth of the TMN unit to range from 549.0 ft. to 690 ft. and the TLL to go from 690 ft to at least 1054.6 ft. ESF is an abbreviation for the exploratory studies facility.

Table I-1. Input Values, their DTN #'s, and their Qualification Status for Part 1 Calculations.

Iron Mineral Types	Reported maximum mineral % in repository horizon tuff (borehole UZ 16)	Mineral GFW	Fe GFW	Wt. Fraction Fe	Bulk Density in repository horizon tuff (TMN, Flint 1998)
LA000000000086.002	LA000000000086.002 GS931208314211.047 (See Assumption # 3)	(Sargent-Welch 1979)	(Sargent-Welch 1979)	Fe GFW /Mineral GFW	GS960908312231.004 (See Assumption # 3)
Qualified Data	Qualified Data	Accepted Data	Accepted Data	Qualified	Qualified Data
Biotite (Mica; see Assumption # 1 above)	1%	511.885	167.54	0.3273	2.25 g/cm^3
Hematite	1%	159.692	111.694	0.6994	

I-4.1.2 Formulas Used

The following formulas were used to produce the results in Section I-5.1.

1. $\pi r^2 h$ — used to calculate the volume of tuff in 1 lineal meter of repository drift.
2. **Bulk Density * Volume** — used to determine the mass of tuff per lineal meter of drift.
3. **Mass per lineal meter * mineral % in host rock** — used to determine the mass of material available in the repository drift.
4. **Elemental GFW / Mineral GFW** — used to determine the weight % of each element.

I-4.2 PART 2: MICROBIAL COUNTS

I-4.2.1 Inputs

Table I-2. Input Values, their DTN #'s, and their Qualification Status for Part 2 Calculations.

Microbial Modeling Parameters	Microbial Volume and Mass (calculated)	Microbes/Biomass in Crushed Tuff (Cells/g)			
Water Content 99% by weight MO9909SPAMICRO.001	Microbial Volume 1.5E-13 cm^3, MO9909SPAMICRO.001	LALH831342AQ96.002		MO9909SPABMASS.000	
Accepted Data	Accepted Data	Qualified Data		Accepted Data	
Microbial Composition $C_{160}(H_{260}O_{80})N_{30}P_2S$ MO9909SPAMICRO.001	Microbial Mass Average Microbe volume * Bulk Density of H_2O (see Assumption # 2)	ESF Low Count	ESF High Count	Rainier Mesa Low Count	Rainier Mesa High Count
Accepted Data	1.5E-13 g	1.78E+04	1.95E+05	5.25E+04	2.63E+05

I-4.2.2 Formulas Used

The following formulas were used to produce the results in Section I-5.2.

1. **Mass of tuff in one meter of repository drift * # of cells per gram of crushed tuff** — used to get the # of cells per lineal meter of repository.

2. **# of cells per lineal meter of repository * average microbial mass** — used to get the mass of cells per lineal meter of repository.

I-4.3 PART 3: GAS INPUTS

I-4.3.1 Flask to Drift Scaling

Table 39 above reports the specifics of the batch experiments that are required by MING to duplicate the batch tests. MING V1.0 requires that you input a "tunnel length" and a "drift diameter" as inputs to all model calculations. In order to appropriately account for gas flow, the scaling of the 125 ml flasks used in the LLNL microcosm experiments (Table 39) needs to be calculated.

Because in MING the gas flow into the drift is across the cylindrical walls as opposed to axially along the drift, gas flow in an upright flask has to be scaled appropriately. To scale the gas flow, the surface area of the opening on the flask has to be equal to the surface area of the cylinder formed by the drift wall and the dimensions of the tunnel length and drift diameter have to match the given surface area. The scaling is set up so that the flask walls are generally impermeable to gas flow and the only allowable surface area for gas flow is at the flask opening. Therefore, using assumption 4 in Section I-3 above and the formula for area of a circle (πr^2), the area of the flask opening is 19.63 cm^2. The convex surface area of the "tunnel length" as entered into MING V1.0 has to be equal to the surface area of the flask opening (19.63 cm^2). The formula for the area of the convex surface for a right circular cylinder ($2\pi rh$) is used along with the volume of a right circular cylinder ($\pi r^2 h$) to determine the "tunnel length" and "drift diameter" of the MING V1.0 input.

$$19.63\ cm^2 = 2\pi rh \qquad \text{(Eq. I-1)}$$

$$125\ cm^3 = \pi r^2 h \qquad \text{(Eq. I-2)}$$

Solving Equation I-1 for h and substituting the results for h in Equation I-2 to solve for r gives:

$$r = 12.73\ cm$$

Substituting the value of r or a drift diameter of $2r$=25.46 cm or about 0.25m into Equation I-3 and solving for h gives the tunnel length:

$$h = 0.2454\ cm = 0.002454\ m$$

I-4.3.2 Lab Gas

MING V1.0 requires gas flux into the drift in units of kg/m^2 year. However, as long as all time units input into MING are the same there are no conversion problems. The actual air that would be generally present in the 125 ml flask over the 7 day time frame of the LLNL experiments is assumed to be the volume of air in the flask (see assumption 6). The following steps are used to calculate the flux of atmospheric gas into a 125 ml flask.

Step 1 is to determine the grams of each gas (O_2, N_2, and CO_2) in a liter of air. This is calculated using Equation I-4 below.

(Volume fraction of gas in air)(Gram Formula Weight)/(22.4 $L_{(gas)}$/1 $mol_{(gas)}$) (Eq. I-4)

Inputs for this calculation are provided in Table I-3. Argon gas is not included, as it is not a constituent for microbial growth. Table I-4 shows results of step 1.

Table I-3. Composition of Air. Accepted Handbook Data Taken from Weast (1979, page F-211) and Sargent-Welch (1979)

Component	% by Volume	GFW, g/mol
N_2	78.084	28
O_2	20.946	32
CO_2	0.033	44

Table I-4. Results of step 1

Gas Component	Mass in Air g/l
N_2	9.76E-01
O_2	2.99E-01
CO_2	6.48E-04

Step 2: This mass of gas that resides in the flask is assumed to flux into the fluid in the flask over the a surface area corresponding to the diameter of the flask (see assumption 4 above) or 1.96 x 10^{-3} m^2. The flask is filled with ~25 ml of fluid and crushed tuff, thus leaving ~0.1 L of gas in the flask. Thus, Table I-5 is calculated using the following formula

[(mass of gas) (volume of gas in flask)]/(Surface Area) (Eq. I-5)

Table I-5. Total Gas Available to Enter a 125 cm^3 Flask.

Component	Total Gas (kg/m^2)
N_2	4.971E-02
O_2	1.524E-02
CO_2	3.301E-05

Step 3: MING V1.0 requires the gas be entered as a cumulative flux over time. Therefore, we convert the total gas entering the flask to a daily flux. This is done by taking the total flux of gas into the flask and dividing by 7 days (approximate duration of the LLNL experiments), as shown on Table I-6

Table I-6. Gas Flux into a 125 cm^3 Flask (kg/m^2 day).

Component	Daily Flux (kg/m^2 day)
N_2	7.101E-03
O_2	2.177E-03
CO_2	4.716E-06

I-5. RESULTS

I-5.1. PART 1: DRIFT MINERALS

The volume of tuff in one lineal meter of repository drift is calculated using the equation for a right circular cylinder ($\pi r^2 h$) and using a drift radius of 2.75 m ($r=D/2$ where D is 5.5 m, see Table 19). Thus, the volume is 23.76 m^3. The mass of one lineal meter of tuff in an area equaling the repository drift is determined, by multiplying the bulk density of Topopah Spring tuff (Table I-1 above) by the volume and converting grams to kilograms. The results give a mass of 53,460 kg.

The mass of biotite and hematite in the drift is determined by multiplying 53,460 by 1% (percent of biotite and hematite in the tuff). Thus, the mass of each mineral per meter of drift is ~535 kg.

Table I-7. Wt Fraction of Elements Comprising the Mineral Biotite and its Mass in Tuff of an Area Equal to one Lineal Meter of Repository Drift.

Biotite	535 kg/m
Fe	0.327
Al	0.053
Si	0.164
O	0.375
H	0.004
K	0.076

Note: K, Al, Si, O and H are not needed in the MING calculations and are only presented for consistency.

Table I-8. Wt Fraction of Elements Comprising the Mineral Hematite and its Mass in Tuff of an Area Equal to One Lineal Meter of Repository Drift.

Hematite	535 kg/m
Fe	0.7
O	0.3

I-5.2 PART 2: MICROBIAL COUNTS

Table I-9. Determination of the Abundance of Microbes in an Area Equaling a One Lineal Meter of Repository Drift.

Microbial Abundance	ESF Low Value	ESF High Value	Rainier Mesa Low Value	Rainier Mesa High Value
# of cells per g of crushed tuff (Table I-2)	1.78E+04	1.95E+05	5.25E+04	2.63E+05
# of cells per linear m of repository	8.18E+11	8.96E+12	2.41E+12	1.21E+13
Average microbial mass (g) (Table I-2)	1.50E-13	1.50E-13	1.50E-13	1.50E-13
Mass (g) of cells per lineal meter of repository	1.23E-01	1.34E+00	3.62E-01	1.81E+00

I-5.3 PART 3: GAS INPUTS

I-5.3.1 Flask to Drift Scaling

The results of the calculations in section I-4.3 are necessary inputs for MING V1.0 in conducting model validation tests using the LLNL microcosm tests experimental data (Horn et al. 1998a, Davis et al. 1998). The results shown on Table I-10 can be considered qualified.

Table I-10. 125 ml Flask Dimensions used in Model Validation Tests Using LLNL Lab Experimental Data.

MING V1.0 Parameter	Value
"Drift Diameter"	0.25 m
"Tunnel Length"	0.0025 m

I-5.3.2 Lab Gas

Table I-6 gives the daily gas flux (kg/m^2). This is the starting value for the gas tables that need to be entered into MING V1.0. To construct the input table for a 7 day modeling run we multiply the daily value by the number of days as shown on Table I-11. These values are considered qualified values.

Table I-11. Cumulative Gas Flux (kg/m^2) in Closed 125 ml Flask under Atmospheric Conditions for 7 days.

Day	N_2	O_2	CO_2
1	7.101E-03	2.177E-03	4.716E-06
2	1.420E-02	4.354E-03	9.432E-06
3	2.130E-02	6.531E-03	1.415E-05
4	2.841E-02	8.708E-03	1.886E-05
5	3.551E-02	1.089E-02	2.358E-05
6	4.261E-02	1.306E-02	2.830E-05
7	4.971E-02	1.524E-02	3.301E-05

ATTACHMENT II: REPOSITORY SUBSURFACE DESIGN INPUT PARAMETERS

II -1. PURPOSE

This attachment reduces the information reported to PA from EBSO (CRWMS M&O 1999g) to useable parameters required as input to MING V1.0 (CSCI 30018 V1.0) for calculation of the effects of potential in-drift microbial communities as part of the microbial communities model as outlined in CRWMS M&O (1999e).

II -2. METHOD

Data that have been delivered to PA may be complete and necessary for other PA calculations but for use in MING may be overly detailed or in a format that cannot be directly used. This calculation extracts the necessary information from the AP-3.14Q Input Transmittals and places it into a format that can be used. This calculation also reduces the extemporaneous data from the sources and tabulates the results.

MING requires all chemical compositions of the repository design materials to be reported in two ways.

1- The material compositions (wt %) are required as a minimum for the following elements: C, N, P, S, Mn, and Fe.
2- The mass of each material in the design should be in terms of kilograms per lineal meter of either waste package or repository.

All input information is converted into this format depending on how the Repository Subsurface Design information was reported to Performance Assessment Operations via input transmittal (CRWMS M&O 1999g).

II -3. ASSUMPTIONS

1. Even though information was reported about the specific composition of all Swellex rock bolt sets components, all compositional data reported are based on the composition of the bolts only [used in Section II-5.1].

2. Due to lack of information about the specific composition of the steel and copper in the rail fittings, a composition of 75% A572 steel and 25% Cu was assumed [used in Section II-4.7].

3. Due to the lack of information on the composition of the steel fittings that are part of the conductor bar, the fittings were assumed to be A572 steel [used in Section II-4.7].

4. Due to lack of information about the composition of ceramic insulators, this material is not included in the information to be evaluated for the rail fittings [used in Section II-4.6].

5. Due to the lack of information, neoprene is assumed the composition of the insulation on the wire conductors [used in Section II-4.6].

The general rationale and/or basis for all of the assumptions above are encompassed in one or the other of the following two reasons. First, the composition of materials assumed will be a good approximation for the replaced materials as the masses and compositions are not going to be dramatically different from those assumed. For example, comparing the compositions of the various steel alloys reported in Section II-5.1 below, the steels are similar in composition. Second, the masses of these materials are generally small in comparison to the masses of some of the major alloys that are used in the system. For example, the mass of the commo cable is two orders of magnitude less than that of the steel invert (See Table II-26 below).

6. Superplasticizer has a composition of 60% H_2O and 40% Calcium Naphthalene Sulfonate (CNS) [used in Section II-4.4].

The rationale for this composition is that, as reported in CRWMS M&O (1997c Section 7.4.5) the most commonly used superplasticizers are naphthalene superplasticizers available as calcium or sodium salts and have a solids content between 38.5 and 42.5% (CRWMS M&O 1997c, Attachment II).

7. Because the composition of silica fume can vary in composition (CRWMS M&O 1997c Table 7.2 and DTN MO9912DTMKCCOF.000) and is used to lower the pH of concrete emplaced in the repository environment by the presence of elevated SiO_2, the values selected for use are found on Table II-3 [used in Section II-4.4].

The rationale for this assumption is that the values reported in CRWMS M&O (1997c) and in DTN MO9912DTMKCCOF.000 show Table II-3 to have the highest SiO_2 content. This composition is more likely to be used by design than the values with lower SiO_2 content based on the desire to lower the pH of the cement because of the uncertainty in using cement in the repository (CRWMS M&O 1997c, Section 7.4.3), even though the higher iron and sulfur contents for silica fume are found on Table 7.2. and would provide more nutrients and energy for microbial catalysis. Additionally, the values on Table II-3 have been reported as representative of the silica fume produced in North America (Bhattacharyya 2000, Attachment II, page 1).

8. The following allow for the creation of the appropriate breakdown codes and reactant compositions. Carbon functional groups are assumed to break down to form CH_2O unless the chemical structure warrants the formation of CH_3OH or COOH. The breakdown of nitrogen will form NO_3^-. The compounds that contain sulfur but no oxygen will break down to form H_2S otherwise they are assumed to form SO_3^-. [used in section II-5.3]

The rationale for these assumptions are that they simplify the model and seem reasonable based on the chemistry of the materials.

II-4. INPUTS

II-4.1 QA STATUS OF INPUTS

The source of most information found herein is CRWMS M&O (1999g) and is based on preliminary design information. Of the information provided in CRWMS M&O (1999g) and used in this calculation, the sources from ASTM standards (see Section 4.3.2) are considered to be accepted data. Perhaps data found in CRWMS M&O (1997c) which is used for the composition of silica fume may potentially be qualified or can eventually be classified as accepted data. However, it and all other data used from this reference (CRWMS M&O 1999g) are considered to be unqualified.

Two other sources of information used in this calculation are the periodic table of elements (Sargent–Welch Scientific Company 1979) and the chemical formulas for various organic materials found in a widely used organic chemistry text book (Morrison and Boyd 1992).

II-4.2 TYPE K CEMENT COMPOSITION

Type K cement is part grout formulation used to anchor rock bolts in the repository drift ground support (CRWMS M&O 1999g) and its characteristics are found in the following DTN: MO9912SEPMKTDC.000. Compositions of Type K cement are given in oxide weight percentage. These have to be converted to elemental weight percentage in order to be fed into MING as input. The oxide composition is shown in Table II-1 below.

Step 1: Calculate formula weights for each oxide. This is done by multiplying each elements formula weight (Sargent-Welch 1979) by the number of atoms of that element and summing all of the values (e.g., for SiO_2 do the following 1[Si]*28+2[O]*16 = 60).

Step 2: Determine the fraction of the oxide weight % for each element then sum the resulting elemental weight percents. This is done by taking the elemental weight % and multiplying by the number of atoms of each element then dividing by the oxide formula weight and then multiplying by the oxide weight % (e.g. for P in P_2O_5: 31*2/142*0.1=0.044). This gives the fraction of the element in the oxide in terms of the oxide weight %. These values are then summed for each element to give the elemental weight %. Results are found on Table II-20 below.

Table II-1. Oxide Composition of Type K Expansive Cement Manufactured to ASTM C 845-96.

Oxide Component	Wt %
SiO_2	19.4
Al_2O_3	5.2
Fe_2O_3	2.8
CaO	61.9
MgO	1.4
SO_3	6.9
Na_2O	0.1
K_2O	0.59
SrO	0.05
ZnO	0.02
TiO_2	0.28
P_2O_5	0.1
MnO_3	0.04
LOI	1.1
Total	99.88

DTN: MO9912SEPMKTDC.000

Table II-2. Formula Weights for Elements and Minerals in Type K Cement.

Element	Formula Wt	Oxide	Formula Wt
Ca	40	SiO_2	60
Si	28	Al_2O_3	102
O	16	Fe_2O_3	160
Al	27	CaO	56
Fe	56	MgO	40
S	32	SO_3	80
K	39	Na_2O	62
Na	23	K_2O	94
Mg	24	SrO	104
Sr	88	ZnO	81
Zn	65	TiO_2	80
Ti	48	P_2O_5	142
Mn	55	MnO_3	103
P	31		

II-4.3 SILICA FUME COMPOSITION

Silica fume is part of the cement admixtures used in the grout formulation to anchor rock bolts in the repository drift ground support (CRWMS M&O 1999g). The source of the oxide composition of silica fume (Table II-3) is discussed in assumption 7 above. These values need to be converted to elemental weight percentages so that they can be used directly in MING V1.0. This is done following the same steps used to calculate the elemental formula weight percents in the Type K cement (see Section II-4.2). Data for the formula weights were taken from Sargent-Welch (1979). Results are found on Table II-21 below.

Table II-3. Oxide Composition of Silica Fume.

Oxide	Wt %
SiO_2	95.0
Al_2O_3	0.7
Fe_2O_3	0.3
CaO	0.3
MgO	0.2
Na_2O	0.3
K_2O	0.3
SO_3	0.8
C	1.3

Table II-4. Formula Weights for Elements and Oxides Found in this Section.

Element	Formula Wt	Oxide	Formula Wt
Ca	40	SiO_2	60
Si	28	Al_2O_3	102
O	16	Fe_2O_3	160
Al	27	CaO	56
Fe	56	MgO	40
S	32	Na_2O	62
K	39	K_2O	94
Na	23	SO_3	80
Mg	24		

II-4.4 SUPERPLASTICIZER COMPOSITION

Superplasticizer is part of the cement admixtures used in the grout formulation to anchor rock bolts in the repository drift ground support (CRWMS M&O 1999g). This section represents the necessary calculations to determine the appropriate elemental wt % to enter into MING V1.0 for

the superplasticizer composition. Information for the rock bolt grout chemistry is found in assumption 6 above and formula weight data was taken from Sargent-Welch Scientific Company (1979). The chemical structure for calcium naphthalene sulfonate (CNS) is found on Figure II-1 and is reported in CRWMS M&O (1998e, Table 1).

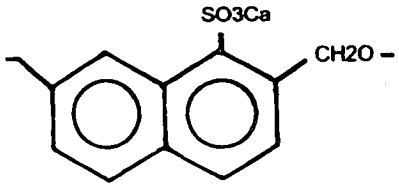

Figure II-1. Chemical Structure of CNS (CRWMS M&O 1998e).

Step 1: Determine appropriate proportions of mass in one m^3 of cement (i.e. 15 * 0.6 = 9).

Table II-5. Step 1 Results.

Superplasticizer (15 kg) (CRWMS M&O 1999g)	% Composition	mass (kg)
H2O	60	9
Calcium Naphthalene Sulfonate (CNS)	40	6

Step 2: Determine the appropriate elemental mass of H_2O by first determining the fraction of hydrogen and oxygen in the formula (Formula Wt / Total Formula Wt), then calculate the elemental mass by taking the mass (kg) from above and multiplying by the fraction (mass kg * fraction).

Table II-6. Step 2 Results.

	H*2	O	H_2O Total
Formula Wt	2.0158	15.9994	18.0152
Fraction	0.1119	0.8881	1.000
Elemental Mass (kg)	1.007	7.993	9.000

Step 3: Determine the appropriate elemental mass of CNS by multiplying the fraction composition reported in CRWMS M&O (1999g, Item 1, p. III-3) by the masses determined in Step 1.

Table II-7. Step 3 Results.

CNS	C	H	S	O	Ca	Cl	Total
Wt. Fr. (CRWMS M&O 1999g)	0.403	0.033	0.107	0.322	0.134	0.001	1.0
Mass (mass kg * Wt. Fr.)	2.418	0.198	0.642	1.932	0.804	0.006	6.0

Step 4: Develop input for MING V1.0 by adding the mass for each element (from steps 2 and 3 above) then using the formula [Mass (kg)/ Total Mass (kg)] to calculate the weight fraction (Wt fr.).

Table II-8. Step 4 Results.

Element	Mass (kg) [sums of Mass]	Wt fr.
C	2.418	0.1612
H	1.205	0.0803
S	0.642	0.0428
O	9.925	0.6617
Cl	0.006	0.0004
Ca	0.804	0.0536
Totals	15.000	1.0000

These weight fraction values are reported as weight % values in Table II-22 below.

II-4.5 QUANTITY OF TYPE K CEMENT, SILICA FUME, AND SUPERPLASTICIZER

CRWMS M&O (1999g) reports 91 kg per meter of repository of cement grout will be used in portions of the repository drift ground support. CRWMS M&O (1999b, Attachment II) reports the maximum case masses of grout per meter of drift would be 280 kg per meter of repository. Because PA calculations are designed to be bounding and conservative, both values will be reported in this calculation. Table II-9 below shows the composition of the grout in terms of mass per volume.

Step 1: In order to distribute the appropriate mass of grout between the three materials calculate the proportion of the mass of each of the three materials (Type K Cement, Silica Fume, and Superplasticizer) The percentage of each material in terms of total mass needs to be determined.

Table II-9. Composition of Rock Bolt Grout as Reported in CRWMS M&O (1999g)

Component	Mass per volume (kg/m^3)
Type K cement	1420
Water	525
Silica Fume	75
Superplasticizer	15

This is done by finding the total mass of material per unit volume (2035 kg) and dividing this value into the masses of each material and multiplying by 100 as shown on Table II-10.

Table II-10. Grout Components as a Percentage of Total Mass.

Component	% of total mass
Type K cement	69.8
Water	25.8
Silica Fume	3.7
Superplasticizer	0.7

Step 2: The percentages found on Table II-10 are then multiplied by 280 kg/meter and 91 kg/meter to determine the mass of each material per linear meter of drift.

Table II-11. Masses of Grout Components per Meter of Drift.

Component	For 280 kg (kg/m)	For 91 kg (kg/m)
Type K cement	195.44	63.50
Water	72.24	23.48
Silica Fume	10.36	3.35
Superplasticizer	1.96	0.67
Total	280.00	91.00

II-4.6 WIRE AND CABLE COMPOSITION

Wire conductor and commo cables are part of the repository drift ground support design reported in CRWMS M&O (1999g). This attachment represents the calculations to determine the appropriate elemental Wt % of both materials for the wire conductor to enter into MING. Data were taken from CRWMS M&O (1999g, Attachment III). Composition of the functional groups for polyethylene polymer, neoprene polymer and cellulose were taken from Morrison and Boyd (1992). The assumption (see assumption 5 Section II-3) was made to use neoprene as the jacket/insulating material because CRWMS M&O (1999g, Attachment III) did not specify the exact composition of the EPR used in the wire conductor. Formula weights for each element were taken from Sargent-Welch Scientific Company (1979).

Step 1: Determine the appropriate Wt fraction of polyethylene found in the commo cable by taking the composition reported in Morrison and Boyd (1992, CH_2CH_2, Page 350) and formula weights (FW) found in Sargent-Welch Scientific Company (1979), and dividing the elemental FW by the total FW. The values are then normalized to 50% based on design input that the cable is 50% (by weight) polyethylene (CRWMS M&O 1999g, Attachment III).

Table II-12. Results of Step 1.

CH_2CH_2	2*C	4*H	Total
FW (from periodic table)	24.022	4.0316	28.0536
Wt fraction (FW/ total FW)	0.8563	0.1437	1.00000
Normalized Wt fraction (50%)	0.4282	0.0718	0.50000

Step 2: Determine the appropriate Wt fraction of neoprene found in the wire conductor by taking the composition reported in Morrison and Boyd (1992, C_4H_5Cl, Page 420), formula weights (FW) found in from Sargent-Welch Scientific Company (1979), and dividing the elemental FW by the total FW. The values are then normalized to 5% based on design input that the wire conductor insulation is 5% (by weight) (CRWMS M&O 1999g, Attachment III).

Table II-13. Results of Step 2.

C_4H_5Cl	4*C	5*H	Cl	Total
FW (from periodic table)	48.04400	5.03950	35.45300	88.53650
Wt fraction (FW/ total FW)	0.54265	0.05692	0.40043	1.00000
Normalized Wt fraction (5%)	0.02713	0.00285	0.02002	0.05000

Step 3: Determine the appropriate Wt fraction of cellulose found in the wire conductor by taking the composition reported in Morrison and Boyd (1992, $C_6H_{10}O_5$, Page 1200), formula weights (FW) found in from Sargent-Welch Scientific Company (1979), and dividing the elemental FW by the total FW. The values are then normalized to 1% based on design input that the wire conductor separator is 1% (by weight) (CRWMS M&O 1999g, Attachment III).

Table II-14. Results of Step 3.

Cellulose	6*C	10*H	O*5	Total
FW (from periodic table)	72.06600	10.07900	79.99700	162.14200
Wt fraction (FW/ total FW)	0.44446	0.06216	0.49338	1.00000
Normalized Wt fraction (1%)	0.00444	0.00062	0.00493	0.01000

Table II-25 below was developed from the values in step 1 above and the commo cable composition assumptions from CRWMS M&O (1999g, Attachment III).

- 50% Cu
- 50% Polyethylene

Table II-24 below was developed from the values in steps 2 and 3 above and the wire conductor composition assumptions from CRWMS M&O (1999g, Attachment III).

- 94% Cu.
- 5% Neoprene.
- 1% Cellulose.

II-4.7 RAIL FITTINGS COMPOSITION

This section calculates the appropriate composition for rail fittings given an unknown steel composition from CRWMS M&O (1999g, Attachment III) and a 75% to 25% steel copper mix. Because the steel composition is unspecified, we have chosen to use an A572 composition (See assumptions 2 and 3 in Section II-3 above).

Step 1: Convert steel values found in Table II-16 below to values at 75% using the following formula (Formula = Wt % (from Table II-16 below) * 0.75).

Table II-15. Results of Step 1.

Element	Wt %
C	0.1725
P	0.03
S	0.0375
Si	0.3
Mn	1.2375
V	0.1125
Fe	73.11

Step 2: Create Table II-23 below by taking the values above and adding 25% Cu.

II-5. RESULTS

The results of each calculation are presented in the individual attachment. The tables presented here are the necessary input tables that need to be entered into MING software code. The results in the tables are either the value generated from the above calculations and/or a simple recompilation of the data provided in CRWMS M&O (1999g).

II-5.1 MATERIAL COMPOSITIONS

The values found on Tables II-16 to II-18 are considered accepted data having been taken from the ASTM standards listed in Section 4.3.2. Note that assumptions 2 and 3 apply to the use of Table II-16.

Table II-16. Composition of ASTM A572 Steel Used in Conductor Bar Fittings, Steel Set Ground Support, Inverts, and Loading Dock.

Element	Wt %
C	0.23
P	0.04
S	0.05
Si	0.4
Mn	1.65
V	0.15
Fe	97.48

Table II-17. Composition of ASTM-F432-95 Steel used in Rock Bolts. Note: Bolt Component Values used for All Components of the Set.

Element	Wt %
C	0.79
P	0.058
S	0.13
Fe	99.022

Table II-18. Composition of A759-85 Steel used in Gantry Rails

Element	Wt %
C	0.82
Mn	1
P	0.04
Si	0.05
S	0.5
Fe	97.59

Values found on Table II-19 were taken directly from CRWMS M&O (1999g).

Table II-19. Composition of Steel used in WWF

Element	Wt %
C	1.0
P	0.1
S	0.1
Fe	98.8

The values found on Table II-20 below show the elemental composition of Type K Cement. These data are considered accepted data.

Table II-20. Composition of Type K Cement as Calculated in Section II-4.2.

Element	Wt %
Ca	44.21
Si	9.05
O	36.34
Al	2.75
Fe	1.96
S	2.76
K	0.49
Na	0.07
Mg	0.84
Sr	0.04
Zn	0.02
Ti	0.17
Mn	0.02
P	0.04

The values found on Table II-21 below show the composition of silica fume.

Table II-21. Elemental Composition of Silica Fume as Calculated in Section II-4.3

Element	Wt %
Ca	0.214
Si	44.333
O	51.860
Al	0.371
Fe	0.21
S	0.32
K	0.249
Na	0.223
Mg	0.12
C	1.30

Table II-22. Composition of Superplasticizer as Calculated in Section II-4.4

Element	Wt %
C	16.12
H	8.03
S	4.28
O	66.17
Cl	0.04
Ca	5.36

The results found on Table II-23 below are based on assumption 2 reported in Section II-3 above.

Table II-23. Composition of Rail Fittings as Calculated in Section II-4.7.

Element	Wt %
C	0.1725
P	0.03
S	0.0375
Si	0.30
Mn	1.2375
V	0.1125
Fe	73.11
Cu	25.00

The results found on Table II-24 below are based on assumption 5 reported in Section II-3 above.

Table II-24. Composition of Wire Conductor as Calculated in Section II-4.6.

Element	Wt %
Cu	94.000
C	3.158
H	0.347
Cl	2.002
O	0.493

The results found on Table II-25 below are based on assumption 6 reported in Section II-3 above.

Table II-25. Composition of Commo Cable as Calculated in Section II-4.6.

Element	WT %
Cu	50.000
C	42.82
H	7.18

II-5.2 MATERIAL QUANTITIES

The masses reported below are taken and summarized from in CRWMS M&O (1999g). Note that assumptions 1, 3, and 4 apply to the use of the following tables where appropriate.

Table II-26. Quantities of Materials in a One Lineal Meter Segment of Repository Drift for Lithophysal Areas (~70% of Emplacement Drift Length)

Item	Elemental Composition	Quantity kg/m
Steel Set Ground Support	Table II-16	369*
WWF Steel	Table II-19	70
Gantry Rail	Table II-18	133.9
Rail fittings	Table II-23	10.05*
Steel Invert	Table II-16	587*
Conductor Bar Fittings	Table II-16	0.2*
Commo cable	Table II-25	0.79

*Total amount of ASTM A572 for input into MING is 966.25 kg/m

Table II-27. Quantities of Materials in a One Lineal Meter Segment of Repository Drift Nonlithophysal Areas (~30% of Emplacement Drift Length)

Item	Elemental Composition	Quantity kg/m
Rock Bolts/Plates	Table II-17	48
WWF Steel	Table II-19	70
Rail fittings	Table II-23	10.05*
Steel Invert	Table II-16	587*
Gantry Rail	Table II-18	133.9
Type K Cement	Table II-20	63.5
Silica Fume	Table II-21	3.35
Superplasticizer	Table II-22	0.67
Conductor Bar Fittings	Table II-16	0.2*
Commo cable	Table II-25	0.79

*Total amount of ASTM A572 for input into MING is 597.25 kg/m

II-5.3 BREAKDOWN CODES

As discussed in Section 6.5.3.5, breakdown codes are required to evaluate organic compounds that can break down into several different reactant compositions (see Attachment V). The breakdown code is analogous to the fraction of the total mass of material that the designated reactant composition would form when broken down into the smaller functional groups. Table 33

shows the required elements for input into MING. They are the reactant composition, the breakdown code and the molecular mass. These items are determined below using assumption 8 above.

II-5.3.1 Superplasticizer

As discussed in Chapelle (1993, Section 12.6) the degradation of aromatic hydrocarbons can be accomplished aerobically under Fe(III)-reducing conditions. Because naphthalene degradation is analogous to benzene degradation the reactant compositions required can be derived by looking at the breakdown of the benzene structure during microbial degradation. The breakdown creates in succession the formation of a catechol which is broken down into various CHO, HCOO and CH_3COOH functional groups. Therefore, the following breakdown codes (in parentheses) and reactant composition can be derived from the functional groups formed from naphthalene based on the appropriate half reactions found on Table 18. They are CH_3OH (4), $HCOO^-$ (2) and CH_2O (5). From the Figure II-1 above the chemical formula for the CNS is $C_{10}H_8O_3S \bullet CH_2O \bullet Ca$. Thus, the molecular mass of CNS using Table 19 above is 278.

II-5.3.2 Wire Conductor

For the mixture of the neoprene and cellulose that comprise the wire conductor, there is 5 times as much neoprene as cellulose so the resulting breakdown codes will reflect this abundance. The chemical formula for neoprene is shown on Table II-13. Thus, the molecular mass of neoprene using Table 19 above is 88. Based on the structure of neoprene (Morrison and Boyd 1992, page 420) the breakdown into applicable breakdown codes (in parentheses) and reactant composition would be CH_3OH (2), and CH_2O (2). For the cellulose (see Morrison and Boyd 1992, page 1200) the breakdown into applicable breakdown codes (in parentheses) and reactant composition would be CH_3OH (1), and CH_2O (5). Therefore, multiplying the neoprene results by 5 and adding to the cellulose gives us the following for a composite: CH_3OH (11), and CH_2O (15).

II-5.3.3 Commo Cable

For the commo cable the material is polyethylene. The chemical formula is found on Table II-12 above. The molecular mass for the base functional group is 28 using Table 19 above. Based on the structure of polyethylene (Morrison and Boyd 1992, page 356) the breakdown into applicable breakdown code (in parentheses) and reactant composition would be CH_3OH (2).

ATTACHMENT III: WASTE PACKAGE DESIGN INPUT PARAMETERS

III-1. PURPOSE

This attachment reduces the information reported to PA from WPO (CRWMS M&O 2000d, 2000e, 2000f, 2000g and 1999h) to useable parameters required as input to MING V1.0 (CSCI 30018 V1.0) for calculation of the effects of potential in-drift microbial communities as part of the microbial communities model as outlined in CRWMS M&O (1999e).

III-2. METHOD

Data that have been delivered to PA may be complete and necessary for other PA calculations but for use in MING may be overly detailed or in a format that cannot be directly used. This calculation extracts the necessary information from CRWMS M&O (2000d, 2000e, 2000f, and 2000g) and places it into a format that can be used. This calculation also reduces the extemporaneous data from the sources and tabulates the results.

MING requires all chemical compositions of the repository design materials to be reported in two ways.

1- The material compositions (wt%) are required as a minimum for the following elements: C, N, P, S, Mn, and Fe.
2- The mass of each material in the design should be in terms of kilograms per lineal meter of either waste package or repository.

All input info is converted into this format depending on how the Waste Package Design information found in CRWMS M&O (2000d, 2000e, 2000f, and 2000g) and was reported to Performance Assessment Operations via input transmittal (CRWMS M&O 1999h).

III-3. ASSUMPTIONS

III-1 The composition of Ti Grade 24 is assumed to be the same as Ti Grade 7.

The rationale for this assumption is that the materials are similar and the compositions should not differ significantly [used in section III-4.2 below].

III-2 The composition of Neutronit A978 steel is assumed to be the composition shown on Table III-13 below.

The rationale for this assumption is that the amount of Boron, Chromium, and Molybdenum can be varied in Neutronit A978 steel according to customer specifications (Kugler 1997). Partial material specifications for repository components have been proposed (CRWMS M&O 1999i) but have not been finalized yet (CRWMS M&O, 1999h). For the purposes of this model, the elemental composition of B and Fe of 1.6% and 66.66% respectively are used. Small variations

in the elemental composition should not significantly effect the results of this model [used in Section III-4.2 below]

III-4. INPUTS AND RESULTS

III-4.1 MATERIAL QUANTITIES

The source of the information found herein was taken from DOE (1992) and is based on preliminary design information. Therefore, the values reported are considered to be unqualified.

CRWMS M&O (CRWMS M&O 2000d, 2000e, 2000f, and 2000g) report 4 major waste package types: 21-PWR, 44-BWR, 5-DHLW and Naval SNF. The tables below report the waste package materials and the masses for each type. In addition, average lengths of the waste packages are reported and are included in the tables below.

Table III-1. Masses and Materials for a 21-PWR Waste Package with Length of 5.165 Meters Taken from CRWMS M&O (2000g, Attachment I).

Material	Mass (kg)	Mass per meter of Waste Package (kg/m)
Alloy C-22	6663	1290
316NG	11249	2178
A516	5724	1108
Neutronit A978	2064	400
Aluminum 6061	336	65

Table III-2. Masses and Materials for a 44-BWR Waste Package with Length of 5.165 Meters Taken from CRWMS M&O (2000g, Attachment II).

Material	Mass (kg)	Mass per meter of Waste Package (kg/m)
Alloy C-22	6812	1319
316NG	11531	2233
A516	7245	1403
Neutronit A978	2152	417
Aluminum 6061	336	65

Typical Hanford, Savannah River, and INEL DHLW pour canisters are reported to weigh 500kg each (DOE 1992, Table 3.1.1). Each DHLW waste package will contain 5 canisters; therefore, the mass of 304L stainless steel for each package would be 2500 kg.

Table III-3. Masses and Materials for a 5-DHLW Short Waste Package (Including Pour Canisters) with Length of 3.590 Meters

Taken from CRWMS M&O (2000d, Attachment III).

Material	Mass (kg)	Mass per meter of Waste Package (kg/m)
Alloy C-22	8260	2301
316NG	11296	3147
A516	3805	1060
304L	2500	651

No information has been provided on the Naval SNF waste package internal materials or fuel types; therefore, only the waste package outer and inner barrier materials are presented here.

Table III-4. Masses and Materials for a Naval SNF Waste Package with Length of 6.065 Meters Taken from CRWMS M&O (2000f, Attachment II).

Material	Mass (kg)	Mass per meter of Waste Package (kg/m)
Alloy C-22	10594	1747
316NG	17407	2870

In addition to the waste packages, two additional items are included in the waste package design, namely, the titanium drip shield and the waste package pallet. Each of these items has been reported in CRWMS M&O (2000g) and the materials and masses are reported below.

Table III-5. Masses and Materials for the Drip Shield Design using a Drip Shield Length of 6.105 Meters Taken from CRWMS M&O (2000e, Attachment II).

Material	Mass (kg)	Mass per meter of Waste Package (kg/m)
Alloy C-22	110	18
Titanium Grade 7	3264	534
Titanium Grade 24	829*	136*

*Include with Ti Grade 7 masses as input into MING (Total 670 kg/m, see Assumption III-1 above)

Table III-6. Masses and Materials for the Waste Package Pallet Design using a Pallet Length of 4.147 Meters Taken from CRWMS M&O (2000e, Attachment III).

Material	Mass (kg)	Mass per meter of Waste Package (kg/m)
Alloy C-22	1423	343
316L	684	165

III-4.2 MATERIAL COMPOSITIONS

Special instructions for compositions of 316NG stainless steel and Neutronit A978 are given in CRWMS M&O (1999h), where the composition of 316NG is the same as 316L with the exception of the carbon and nitrogen content as specified in American Society for Metals (1987) and the boron content is set at 1.6% in the composition of Neutronit A978. With the exception of data for Neutronit A978, the compositions listed in the tables below are based on the appropriate standard as listed in Section 4.3.2 above and can be considered accepted data. The composition of Neutronit A978 is based on Assumption III-2 above.

Table III-7. Composition of 304L Stainless Steel (ASTM A240/A 240M-97a).

Element	Percent
C	0.03
Mn	2.00
P	0.045
S	0.03
Si	0.75
Cr	20.00
Ni	12.00
N	0.10
Fe	65.045

Table III-8. Composition of 316L Stainless Steel (ASTM A276-91a).

Element	Percent
Mn	2.00
Si	1.00
P	0.045
S	0.03
Cr	18.00
N	0.10
Mo	3.00
Fe	61.795
Ni	14.00
C	0.03

Table III-9. Composition of 316NG Stainless Steel (ASTM A276-91a and ASM 1987).

Element	Percent
C	0.02
Mn	2.00
Si	1.00
P	0.045
S	0.03
Cr	18.00
N	0.10
Mo	3.00
Fe	61.805
Ni	14.00

Table III-10. Composition of Alloy C-22. (ASME Section II B SB-575).

Element	Percent
Mo	14.50
Cr	22.50
Fe	6.00
W	3.50
Co	2.50
C	0.015
Si	0.08
Mn	0.50
V	0.35
P	0.02
S	0.02
Ni	50.015

Table III-11. Composition of Aluminum 6061 (ASTM B 209M-92a).

Element	Percent
Si	0.80
Fe	0.70
Cu	0.40
Mn	0.15
Mg	1.20
Cr	0.35
Zn	0.25
Ti	0.15
Al	96.00

Table III-12. Composition of A516 Carbon Steel.
(ASTM A516/A516M-90).

Element	Percent
C	0.27
Mn	1.30
P	0.035
S	0.035
Si	0.45
Fe	97.91

Table III-13. Composition of Neutronit A978
(CRWMS M&O 1999h and Assumption III-2).

Element	Percent
C	0.04
Cr	18.50
Ni	13.00
Co	0.20
B	1.60
Fe	66.66

Table III-14. Composition of Titanium Grade 7
and Titanium Grade 24 (see Assumption III-1 above)
(ASME 1995).

Element	Percent
N	0.03
C	0.10
H	0.015
O	0.25
Fe	0.30
Pd	0.25
Ti	99.055

ATTACHMENT IV: WASTE FORM COMPOSITION DETERMINATIONS

IV-1. PURPOSE

This attachment reduces the data from the following DTN's: SN9911T0811199.003 and MO9912SPADWR90.007 to useable parameters required as input to MING V1.0 (CSCI 30018 V1.0) for calculation of the effects of potential in-drift microbial communities as part of the microbial communities model as outlined above. It also points to CRWMS M&O (1998g) for the source of the remainder of the information in this attachment.

IV -2. METHOD

Data that have been delivered to PA may be complete and necessary for other PA calculations but for use in MING may be overly detailed or in a format that cannot be directly used. The calculation extracts the necessary information from the DTN's or other documents and places it into a format that can be used. This calculation also reduces the extemporaneous data from the sources and tabulates the results.

MING requires all chemical compositions of the design materials to be reported in two ways.

1- The material compositions (weight percentage) are required as a minimum for the following elements: C, N, P, S, Mn, and Fe.
2- Composition should include U for potential sensitivity studies on U redox reactions.
3- The mass of each material in the design should be in terms of kilograms per lineal meter of waste package.

IV-3. ASSUMPTIONS

IV-1. The composition used in MING calculations of the CSNF is taken from CRWMS M&O (1998g) as shown on Tables IV-4 and IV-5.

The rationale for this assumption is that there is no current qualified source for composition of the spent fuel and assemblies and the determination of qualified explicit average compositions of CSNF is unrealistic given the different sources and burnup histories of the fuel. In addition, management expectations for radionuclide inventories are such that there is not an explicit composition for the spent fuel as discussed in *Inventory Abstraction* (CRWMS M&O 2000n). Therefore the work documented in CRWMS M&O (1998g) is representative of the composition of a particular fuel type with a burnup of 1000 years and should be sufficient to capture the effects of the waste form in the calculations.

IV-4. INPUTS

Table IV-1. Composition of HLW Glass.

Element	Wt%
O	44.51858
U	1.866878
Np	0.000947
Pu	0.014798
Ba	0.112037
Al	2.318745
S	0.128728
Ca	0.658172
P	0.01398
Cr	0.082104
Ni	0.730782
Pb	0.060619
Si	21.76507
Ti	0.593414
B	3.192673
Li	1.468034
F	0.031673
Cu	0.151784
Fe	7.349219
K	2.971929
Mg	0.820129
Mn	1.548915
Na	8.579966
Cl	0.115259
Total	99.09444

DTN: SN9911T0811199.003

Table IV-2. Mass of HLW Glass per Pour Canister from Savannah River.

Material	Mass
HLW	1682 kg per canister

DTN: MO9912SPADWR90.007

IV-5. RESULTS

DHLW values can be used directly from Table IV-1, however not all elements are important. Therefore, only the elements that are necessary for MING V1.0 calculations are included in Table IV-3 below.

Table IV-3. Abstracted DHLW Glass Composition for use in MING

Element	Wt%
U	1.87
S	0.13
P	0.014
Fe	7.35
Mn	1.55

DTN: SN9911T0811199.003

PWR values can be used directly from CRWMS M&O (1998g, Attachment I) based on the discussion in Assumption IV-1 above. The values are shown on Table IV-4 below.

Table IV-4 Abstracted CSNF PWR Composition for use in MING

Element	Wt%
P	0.01
Fe	1.85
Mn	0.05
C	0.01
N	0.01

BWR values can be used directly from CRWMS M&O (1998g, Attachment III) based on the discussion in Assumption IV-1 above. The values are shown on Table IV-5 below.

Table IV-5. Abstracted CSNF BWR Composition for use in MING

Element	Wt%
Fe	1.63
Mn	0.05
C	0.01
N	0.01

The mass of DHLW needs to be converted to a per meter of waste package basis. Therefore, the mass per canister based on Assumption 5.13 (Table IV-2) is multiplied by 5 (5 pour canisters per waste package) to obtain the appropriate mass of glass per waste package. This is equal to 8410 kg of glass. This is then divided by the length of a DHLW package (3.59 m, CRWMS M&O 2000d) resulting in a mass per meter of waste package as shown on Table IV-6. Masses and lengths and numbers of fuel assemblies for BWR and PWR wastes are taken from CRWMS M&O (2000g, Attachments I and II) and calculated in the same manner.

Table IV-6. Mass of Each Waste Form per Meter of Package.

Material	Mass (kg) per meter of waste package
PWR	3145
BWR	2798
DHLW	2342

ATTACHMENT V: REACTANT COMPOSITION DETERMINATIONS

V-1. PURPOSE

This attachment uses the data developed in attachments II, III and IV along with the inputs below to develop a useable parameter set for reactant compositions required as input to MING V1.0 (CSCI 30018 V1.0) for calculation of the energy limit to growth as part of the microbial communities model as outlined in CRWMS M&O (1999e).

V-2. METHOD

In order for MING V1.0 to conduct its energy calculations, each of the materials needs to be broken down into the associated chemical species termed "reactant compositions". In order to determine which chemical species can be selected and used within MING V1.0, Table V-1 is used to outline the available redox half reactions that can occur. Each material is then assigned the appropriate reactant compositions based on its chemical composition and general redox state. As an example, for steel set ground support which should be in its most reduced state, whose composition is found on Table II-16, a reactant composition would be assigned for each of the elements: Fe, S, C and Mn of Fe, S, CH_2O and Mn^{2+}, respectively. For the organic materials, which are comprised of several available functional groups (e.g. superplasticizer is comprised of Calcium Naphthalene Sulfonate, which has two functional groups that are attached to the naphthalene structure [SO_3Ca and CH_2O, see Figure 1, Attachment II]) the derivation of the organic reactant compositions have been previously assigned and is discussed in Attachment II.

Table V-2 shows the reactant compositions for all repository materials.

V-3. ASSUMPTIONS

1. The following allow for the creation of the appropriate breakdown codes and reactant compositions. Carbon functional groups are assumed to break down to form CH_2O unless the chemical structure warrants the formation of CH_3OH or COOH. The breakdown of nitrogen will form NO_3^-. The compounds that contain sulfur but no oxygen will break down to form H_2S otherwise they are assumed to form SO_3^-. [Used in section II-5.3]

The rationale for these assumptions is that they simplify the model and seem reasonable based on the chemistry of the materials.

V-4. INPUTS

Table V-1. Redox Half Reactions Associated with Microbial Catalysis.

Redox half reaction	Redox half reaction
Carbon	**Iron**
$CO_2 + H^+ + 2e^- = HCOO^-$	$Fe_2O_3 + 6H^+ + 6e^- = 2Fe + 3H_2O$
$CO_2 + 4H^+ + 4e^- = CH_2O + H_2O$	$Fe^{2+} + 2e^- = Fe$
$CO_2 + 6H^+ + 6e^- = CH_3OH + H_2O$	$Fe^{3+} + e^- = Fe^{2+}$
$HCOO^- + 3H^+ + 2e^- = CH_2O + H_2O$	$Fe_3O_4 + 8H^+ + 8e^- = 3Fe + 4H_2O$
$CO_2 + 8H^+ + 8e^- = CH_4 + 2H_2O$	$FeOOH + 3H^+ + e^- = Fe^{2+} + 2H_2O$
$CH_2O + 2H^+ + 2e^- = CH_3OH$	**Manganese**
$HCOO^- + 7H^+ + 6e^- = CH_4 + 2H_2O$	$MnO_2 + 4H^+ + 2e^- = Mn^{2+} + 2H_2O$
$CH_2O + 4H^+ + 4e^- = CH_4 + H_2O$	$Mn_3O_4 + 8H^+ + 2e^- = 3Mn^{2+} + 4H_2O$
$CH_3OH + 2H^+ + 2e^- = CH_4 + H_2O$	**Sulfur**
$CO_3^{2-} + 10H^+ + 8e^- = CH_4 + 3H_2O$	$S + H^+ + 2e^- = HS^-$
$CO_3^{2-} + 6H^+ + 4e^- = CH_2O + 2H_2O$	$S + 2H^+ + 2e^- = H_2S$
$CO_3^{2-} + 8H^+ + 6e^- = CH_3OH + 2H_2O$	$SO_4^{-2} + 9H^+ + 8e^- = HS^- + 4H_2O$
$CO_3^{2-} + 3H^+ + 2e^- = HCOO^- + H_2O$	$SO_4^{-2} + 10H^+ + 8e^- = H_2S + 4H_2O$
Nitrogen	$HSO_4^- + 7H^+ + 6e^- = S + 4H_2O$
$N_2 + 6H^+ + 6e^- = 2NH_3$	$SO_4^{-2} + 8H^+ + 6e^- = S + 4H_2O$
$N_2 + 8H^+ + 6e^- = 2NH_4^+$	$SO_2 + 4e^- + 4H^+ = S + 2H_2O$
$NO_2^- + 7H^+ + 6e^- = NH_3 + 2H_2O$	$SO_3^{2-} + 7H^+ + 6e^- = HS^- + 3H_2O$
$NO_3^- + 2H^+ + 2e^- = NO_2^- + H_2O$	$2SO_4^{-2} + 10H^+ + 8e^- = S_2O_3^{-2} + 5H_2O$
$NO_3^- + 10H^+ + 8e^- = NH_4^+ + 3H_2O$	**Hydrogen**
$NO_2^- + 8H^+ + 6e^- = NH_4^+ + 2H_2O$	$H^+ + e^- = 0.5H_2$
$NO_3^- + 6H^+ + 5e^- = 0.5N_2 + 3H_2O$	**Oxygen**
$2NO_2^- + 8H^+ + 6e^- = N_2 + 4H_2O$	$O_2 + 4H^+ + 4e^- = 2H_2O$
$NO_3^- + 9H^+ + 8e^- = NH_3 + 3H_2O$	

MO9909SPAMING1.003

All other inputs are taken from Attachments II, III, and IV.

V-5. RESULTS

Table V-2. Reactant Compositions Used in the Energy Calculations for Each Material in the Repository and Waste Package Designs.

Material Name	Reactant Compositions
Aluminum 6061	Fe, Mn^{2+}
ASTM A572 Steel	Fe, Mn^{2+}, S, CH_2O
ASTM A579-85 Steel	Fe, Mn^{2+}, S, CH_2O
ASTM F432-95 Steel	Fe, S, CH_2O
304L Stainless Steel	CH_2O, Fe, Mn^{2+}, S
316L Stainless Steel	CH_2O, Fe, Mn^{2+}, NO_3^-, S
316NG Stainless Steel	CH_2O, Fe, Mn^{2+}, NO_3^-, S
C Steel ASTM A516	CH_2O, Fe, Mn^{2+}, S
Neutronit A978	CH_2O, Fe,
Wire Conductor	CH_2O, CH_3OH
Alloy C-22	Fe, Mn^{2+}, S, CH_2O
Conductor Bar fittings	CH_2O, Fe
Type K Cement	Fe^{2+}, SO_4^{2-},
Gantry Rail	CH_2O, Fe, S, Mn^{2+}
Rail Fittings	CH_2O, Fe, S
Ti Grade 7	NO_3^-, CH_2O, Fe
Superplasticizer	$HCOO^-$, CH_3OH, CH_2O, SO_3^{2-}
Commo Cable	CH_3OH
WWF Steel	CH_2O, Fe, S
Silica Fume	Fe^{2+}, SO_4^{2-}, CH_2O
CSNF PWR	Fe, NO_3^-, CO_3^{2-}, S, Mn^{2+}
CSNF BWR	Fe, NO_3^-, CO_3^{2-}, S, Mn^{2+}
DHLW	Fe, SO_4^{2-}, Mn^{2+}

ATTACHMENT VI

PLOTTED RESULTS FOR SECTIONS 6.6.2, 6.6.3, AND 6.6.4

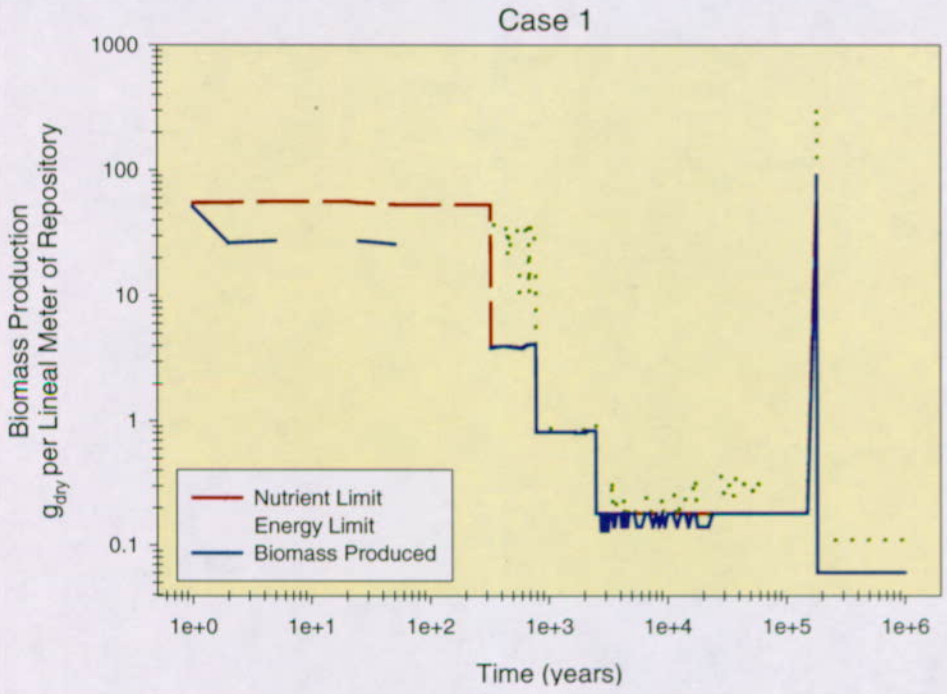

Figure VI-1. Case 1 Results.

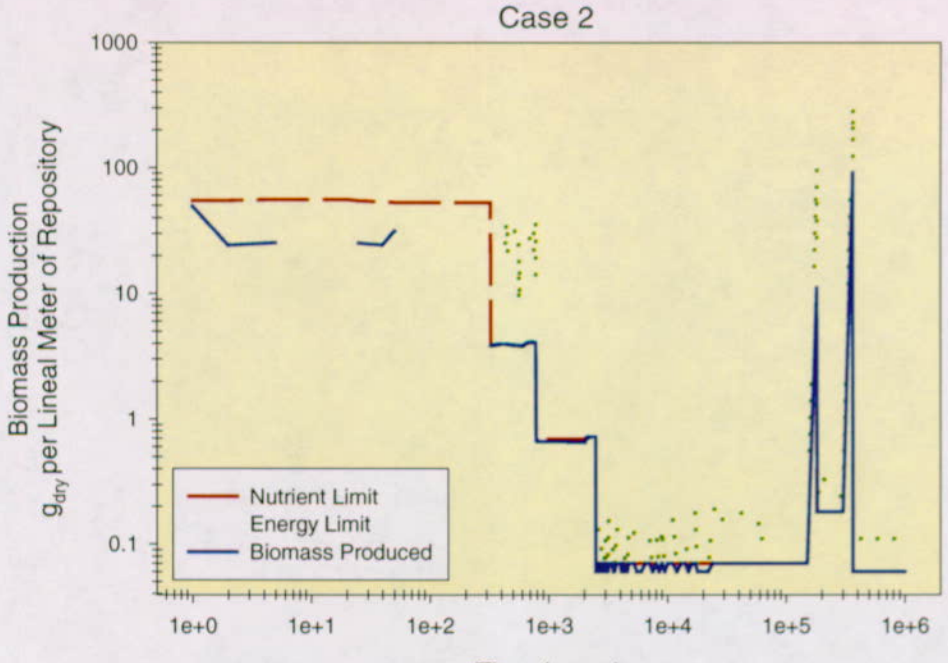

Figure VI-2. Case 2 Results.

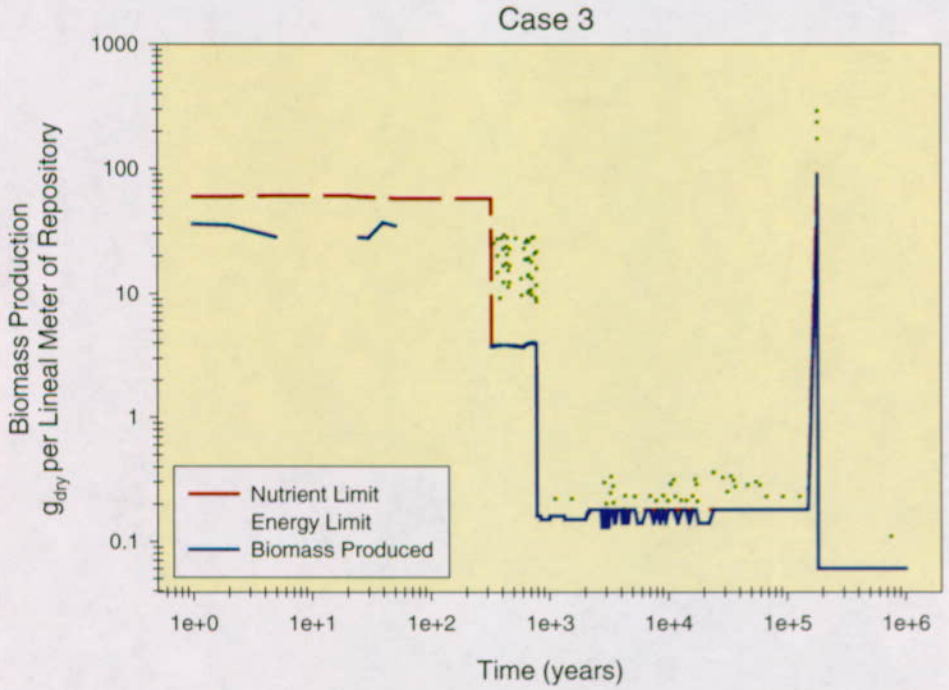

Figure VI-3. Case 3 Results.

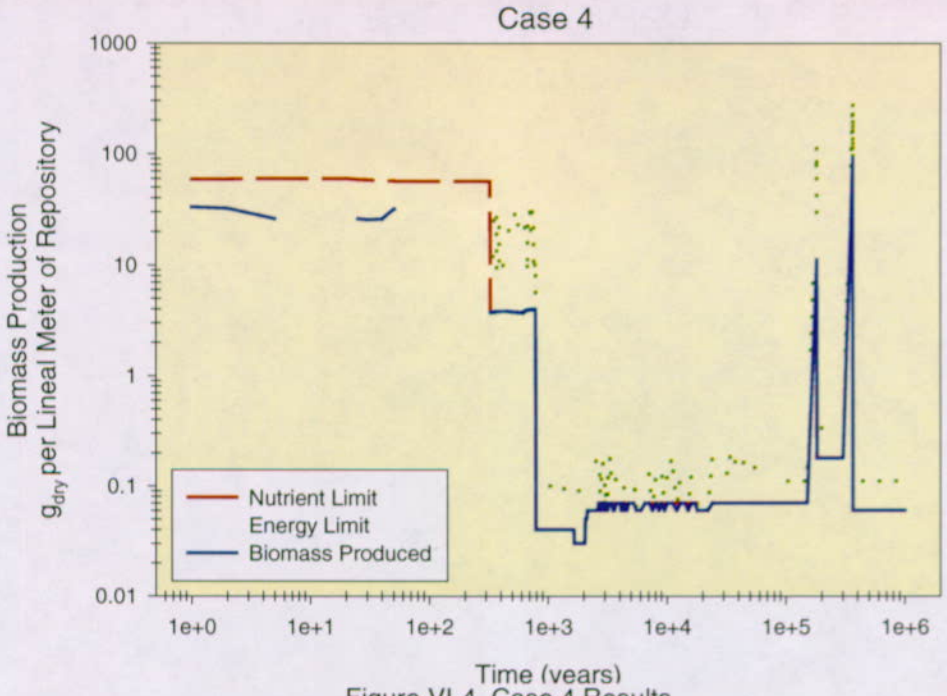

Figure VI-4. Case 4 Results.

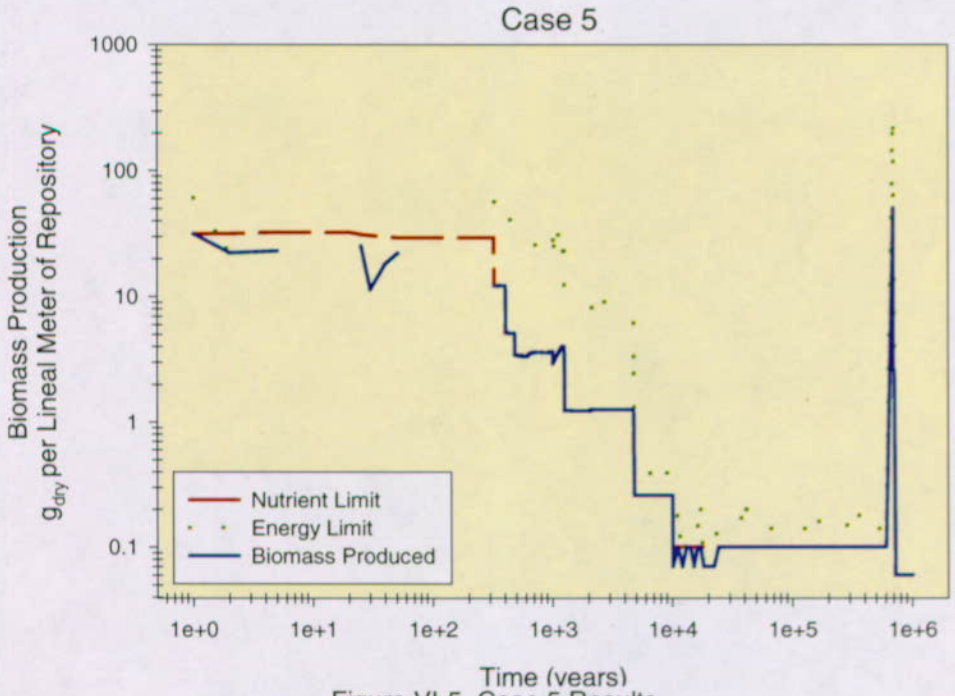

Figure VI-5. Case 5 Results.

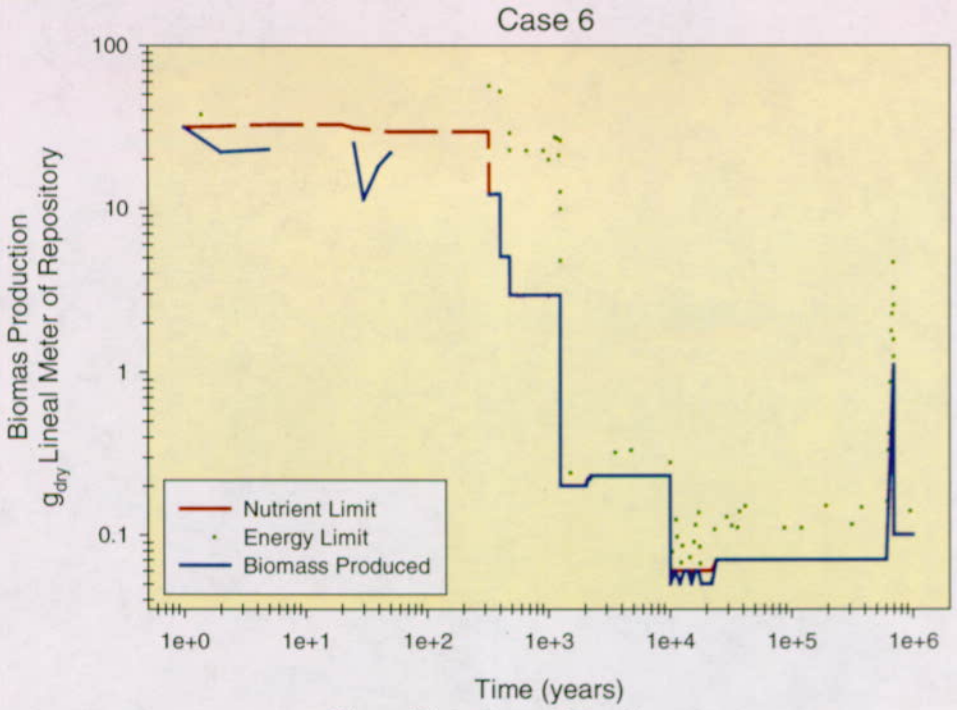

Figure VI-6. Case 6 Results.

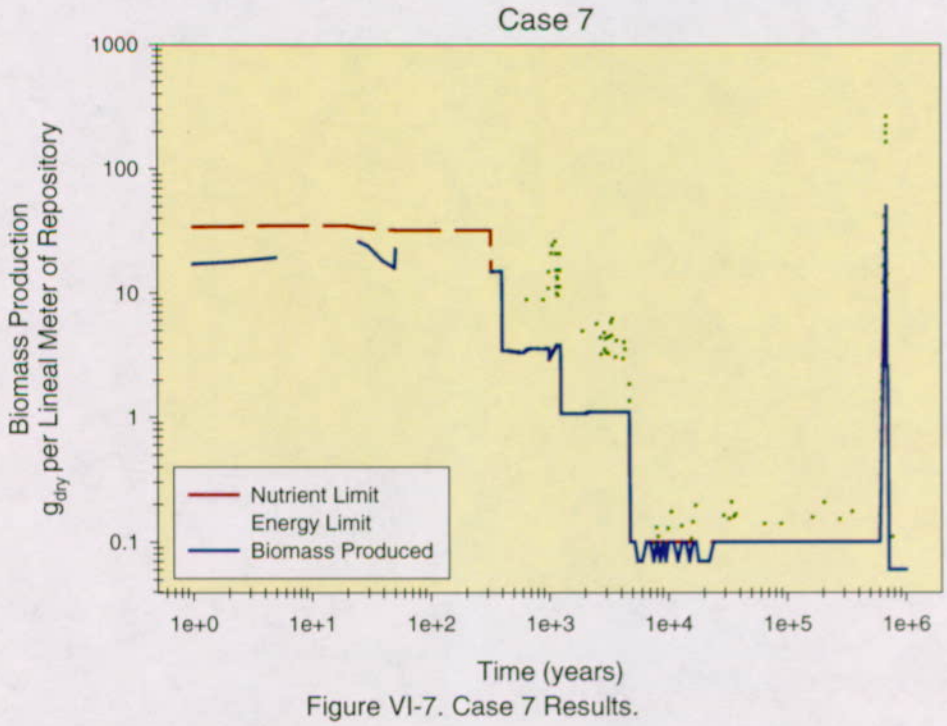

Figure VI-7. Case 7 Results.

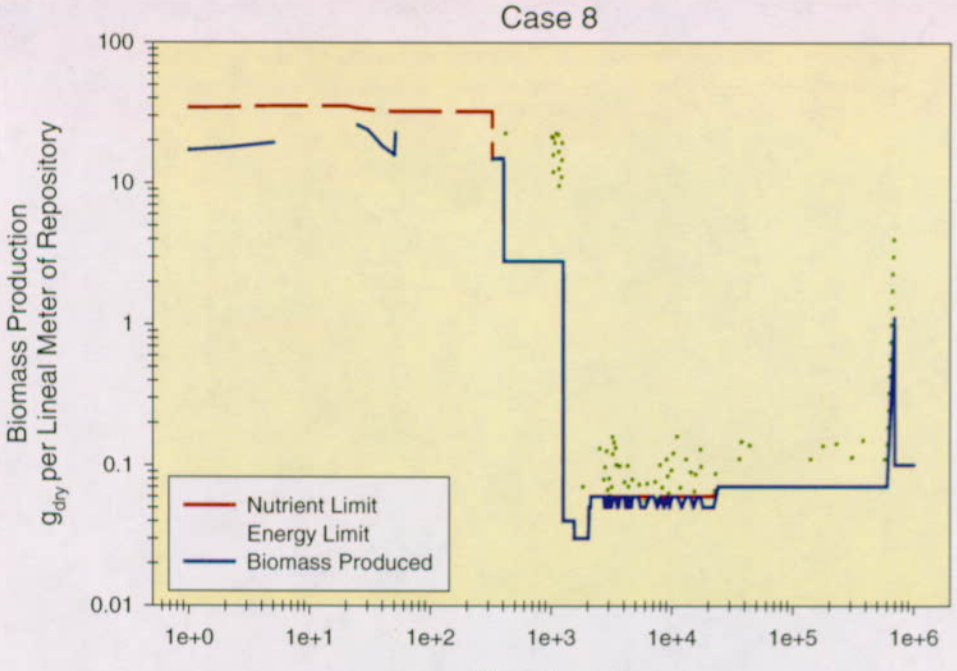

Figure VI-8. Case 8 Results.

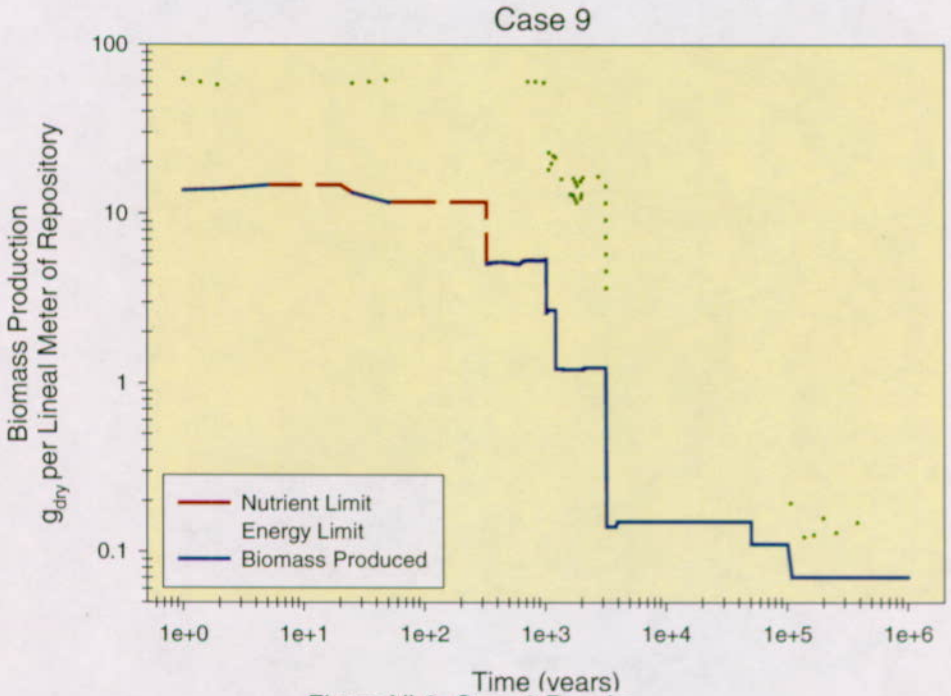

Figure VI-9. Case 9 Results.

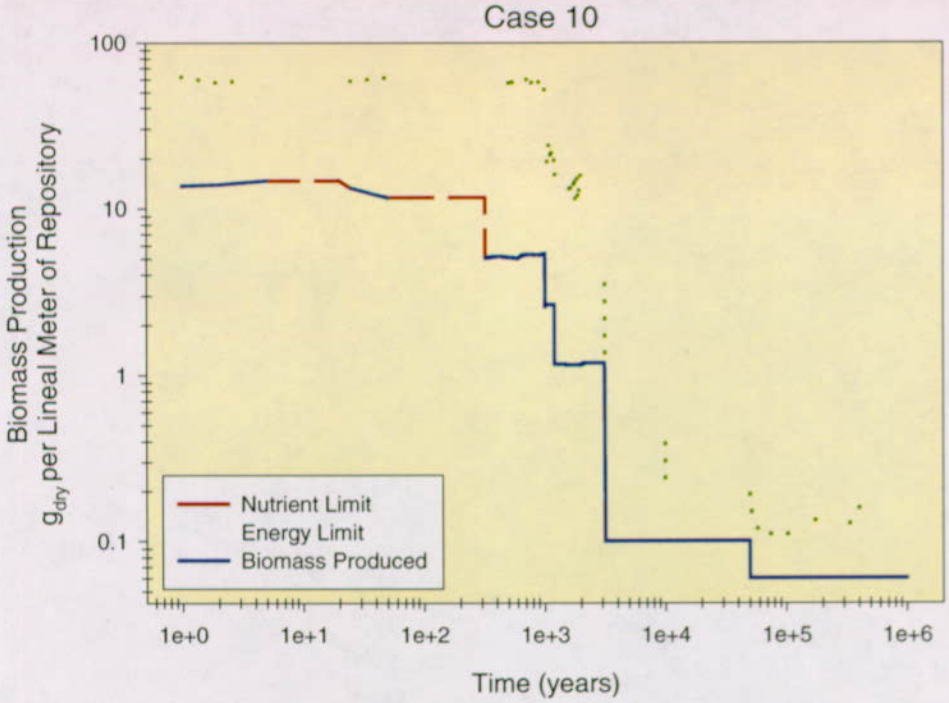

Figure VI-10. Case 10 Results.

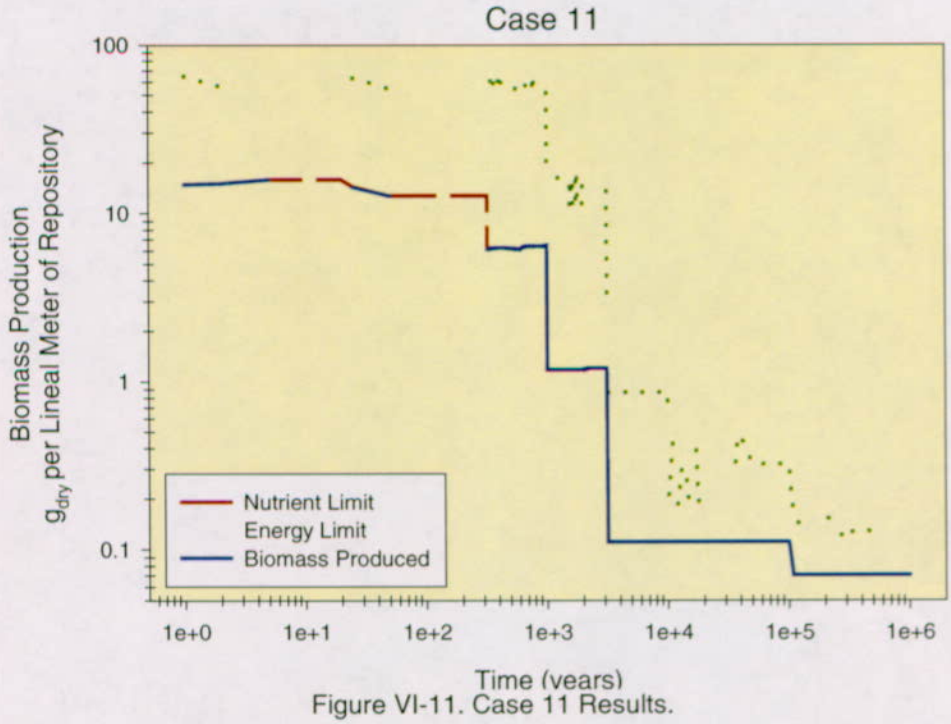

Figure VI-11. Case 11 Results.

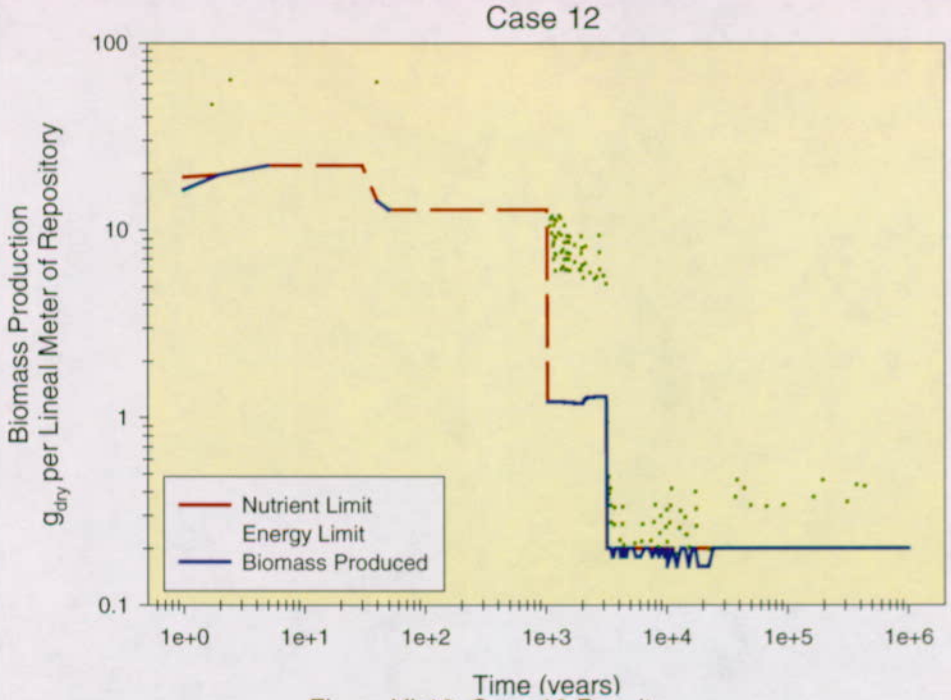

Figure VI-12. Case 12 Results.

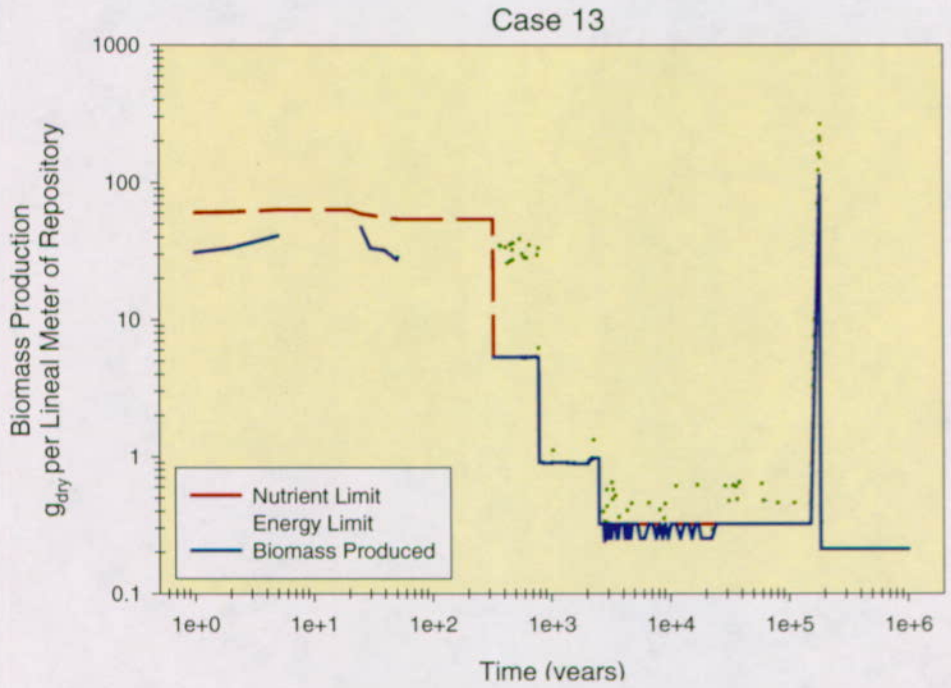

Figure VI-13. Case 13 Results.

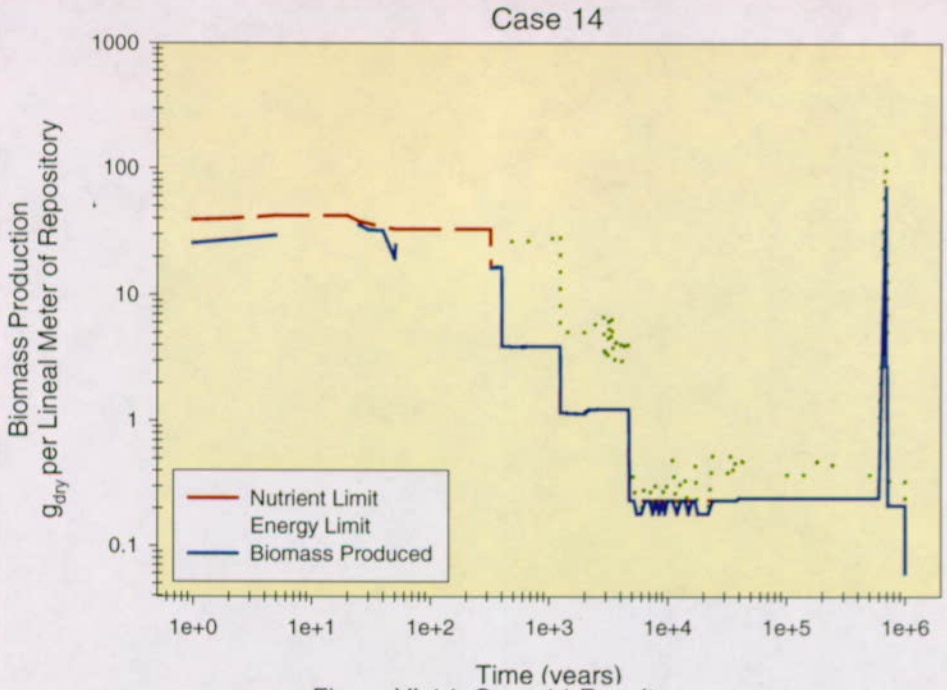

Figure VI-14. Case 14 Results.

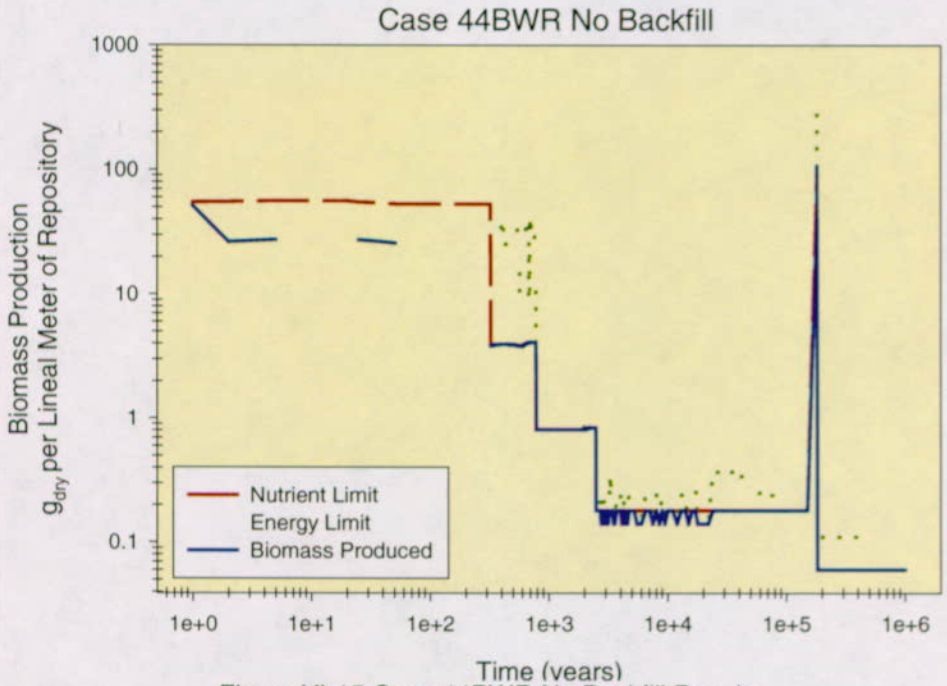

Figure VI-15 Case 44BWR No Backfill Results.

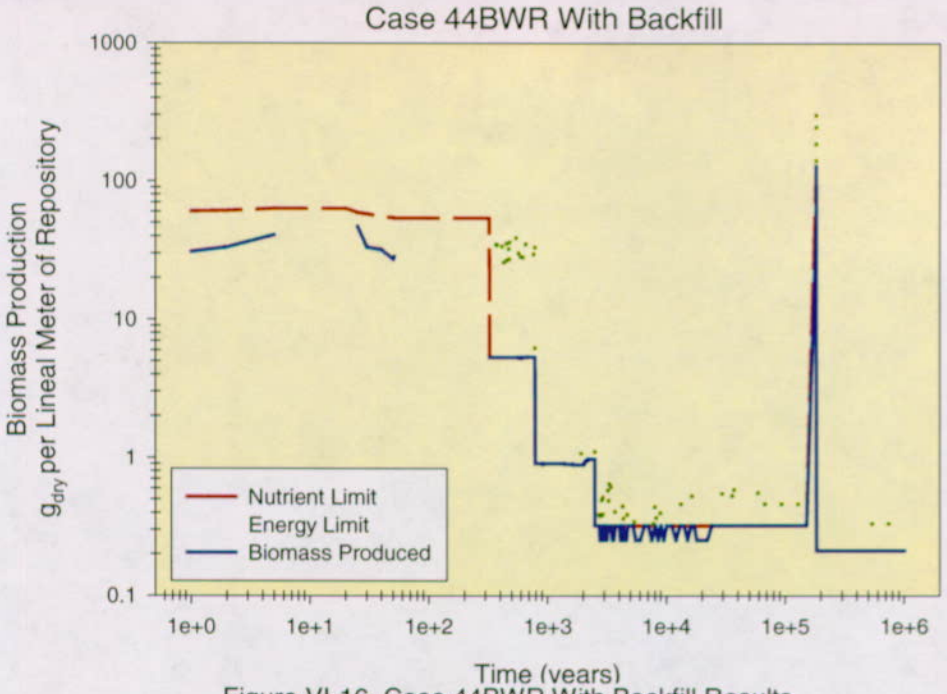

Figure VI-16. Case 44BWR With Backfill Results.

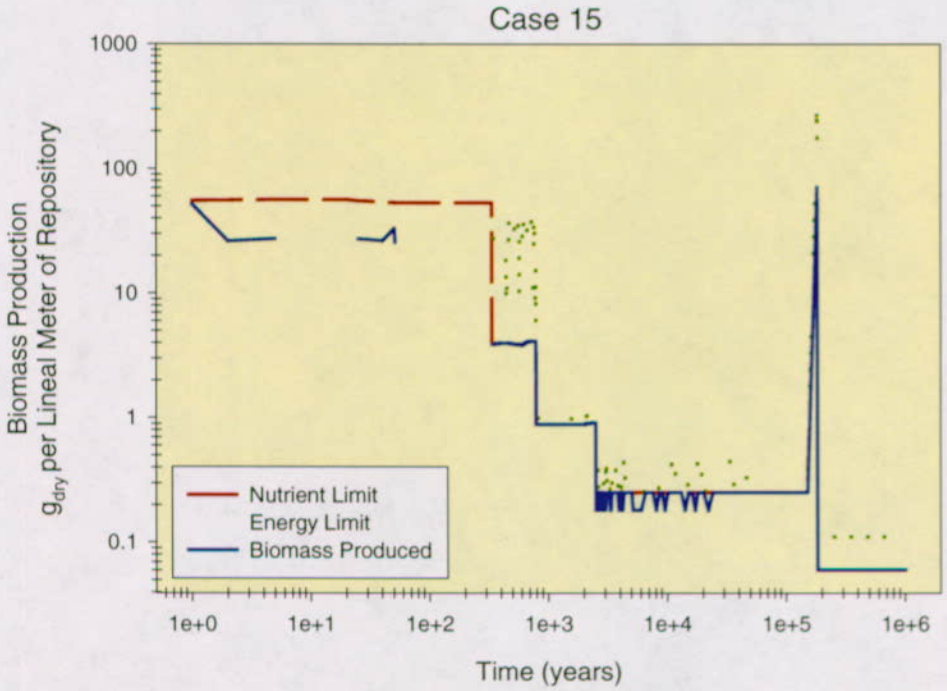

Figure VI-17. Case 15 Results.

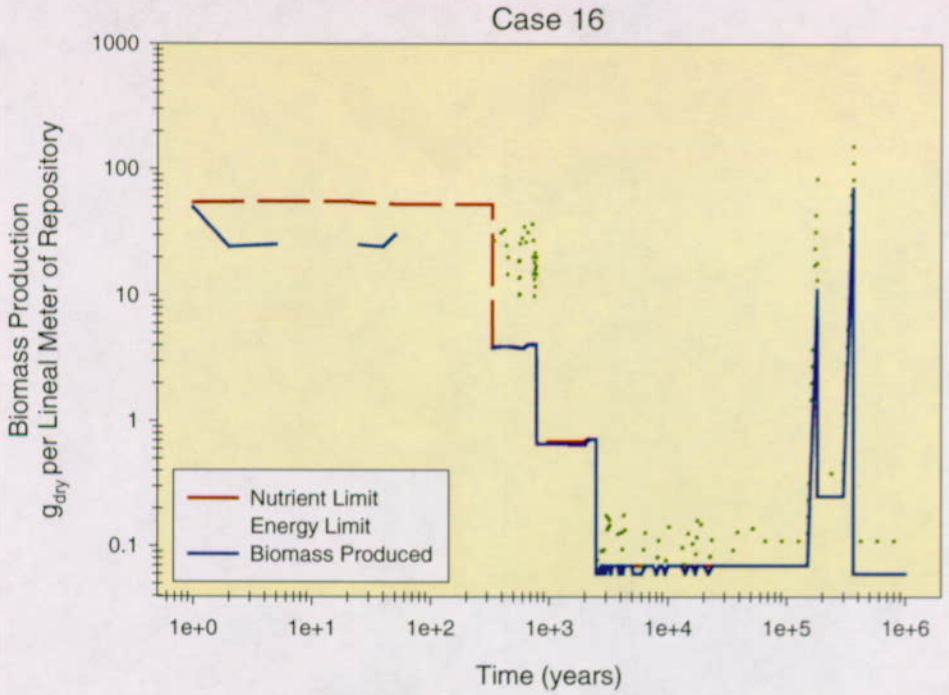

Figure VI-18. Case 16 Results.

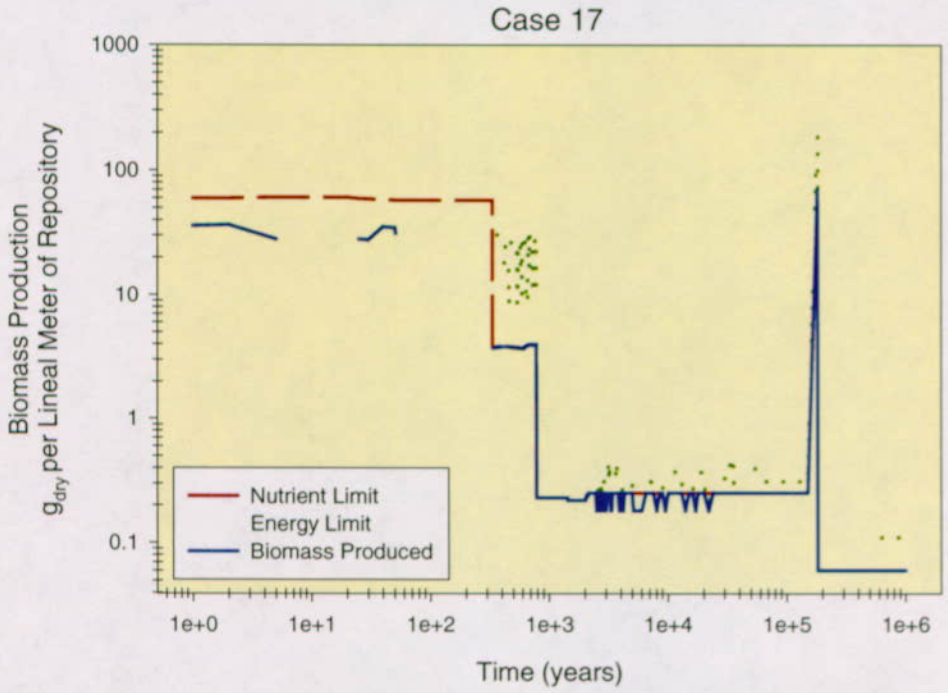

Figure VI-19. Case 17 Results.

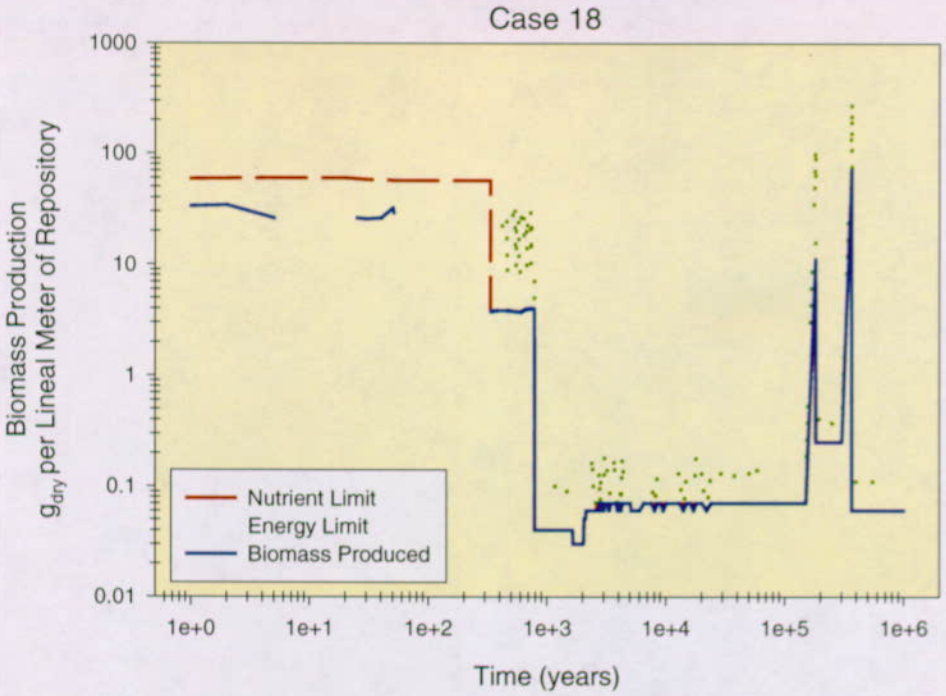

Figure VI-20. Case 18 Results.

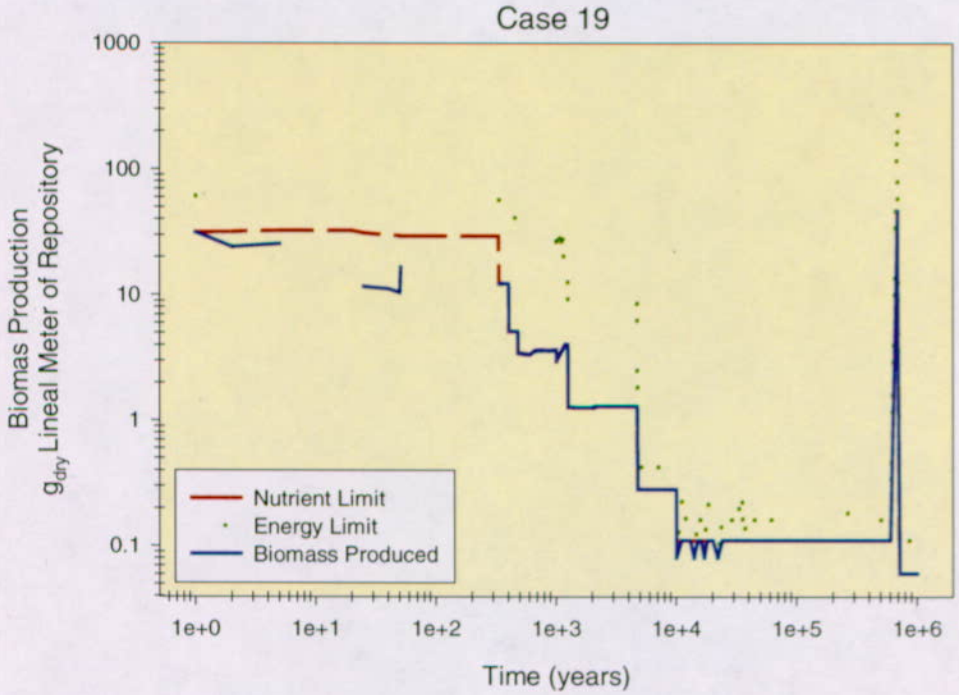

Figure VI-21. Case 19 Results.

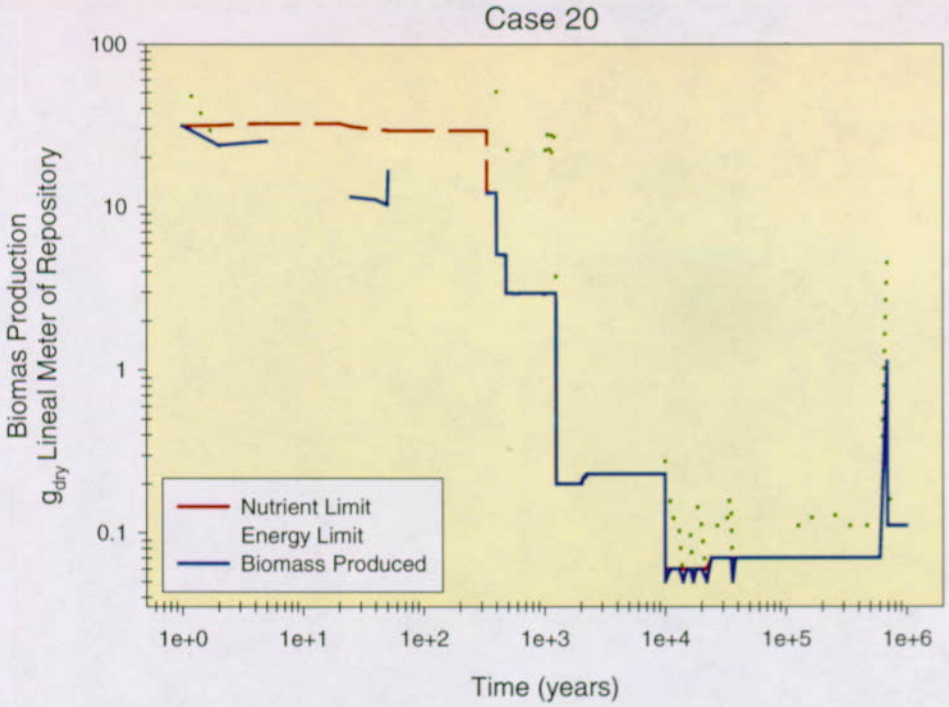

Figure VI-22. Case 20 Results.

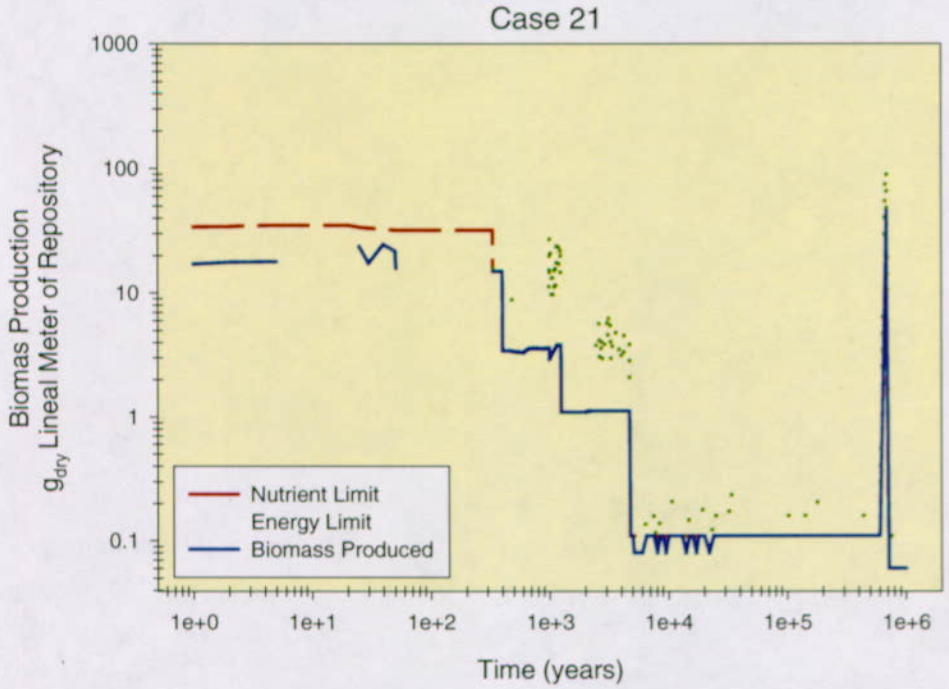

Figure VI-23. Case 21 Results.

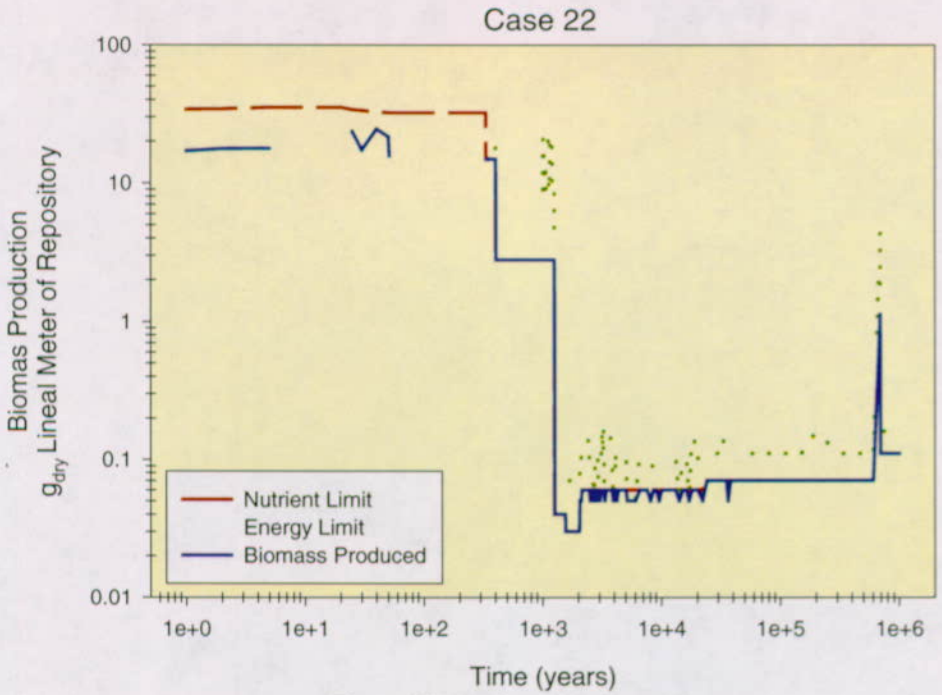

Figure VI-24. Case 22 Results.

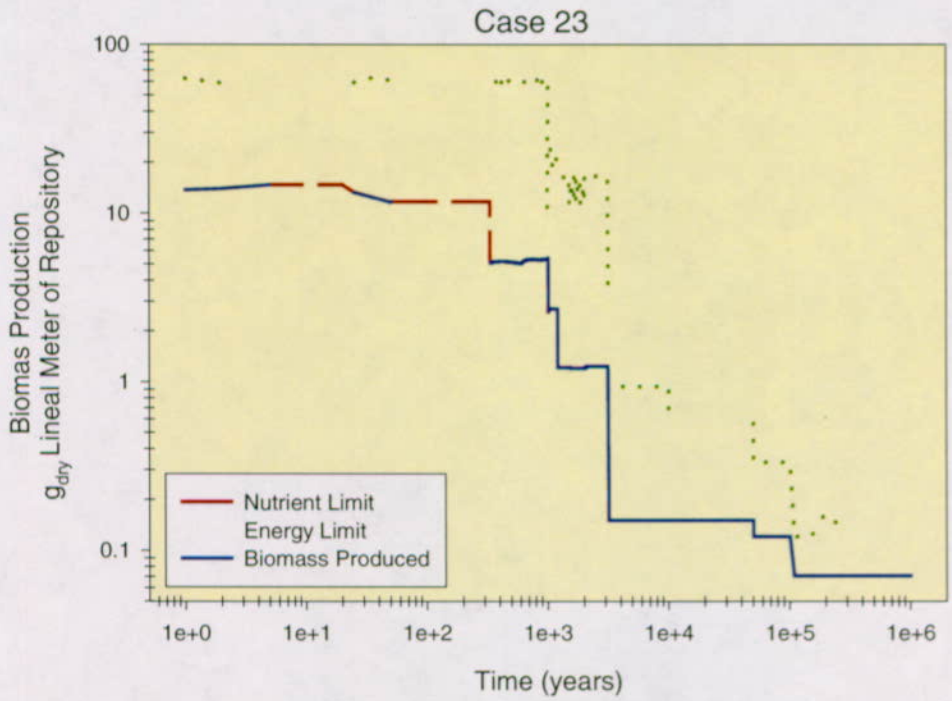

Figure VI-25. Case 23 Results.

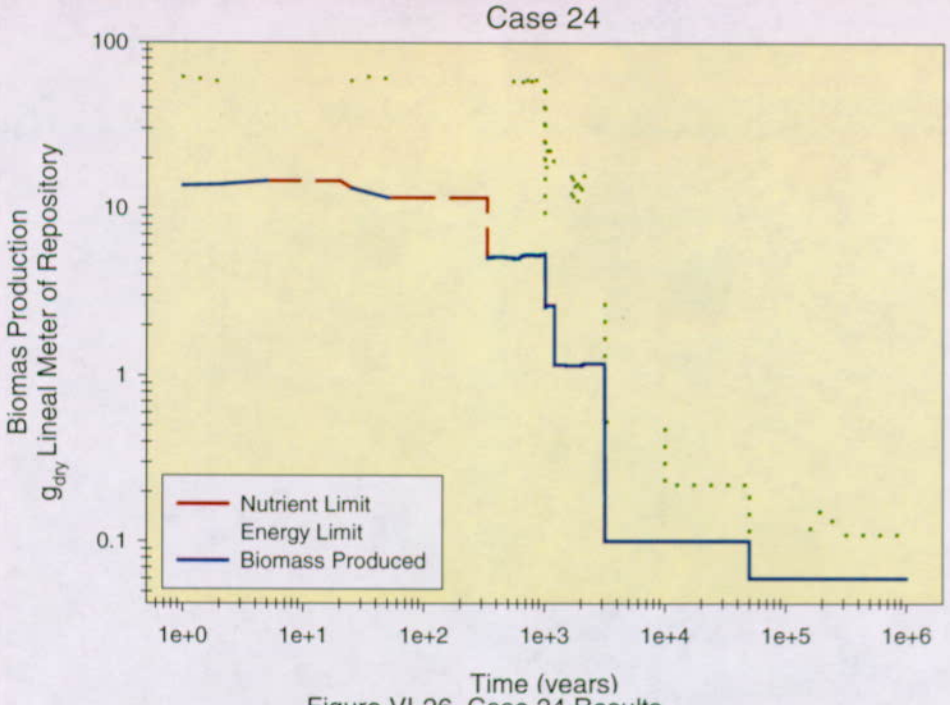

Figure VI-26. Case 24 Results.

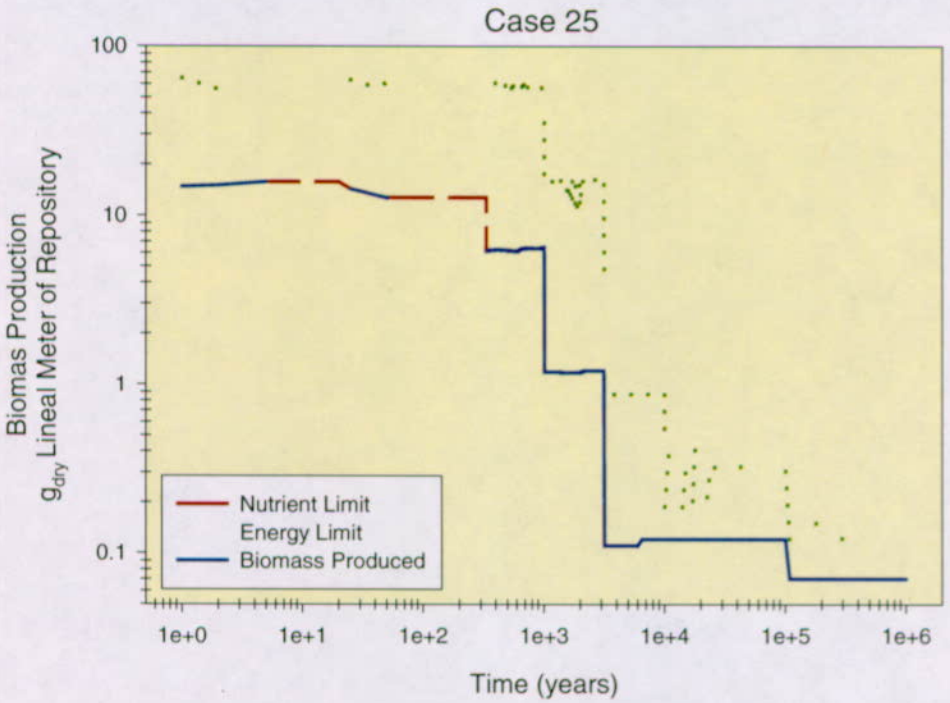

Figure VI-27. Case 25 Results.

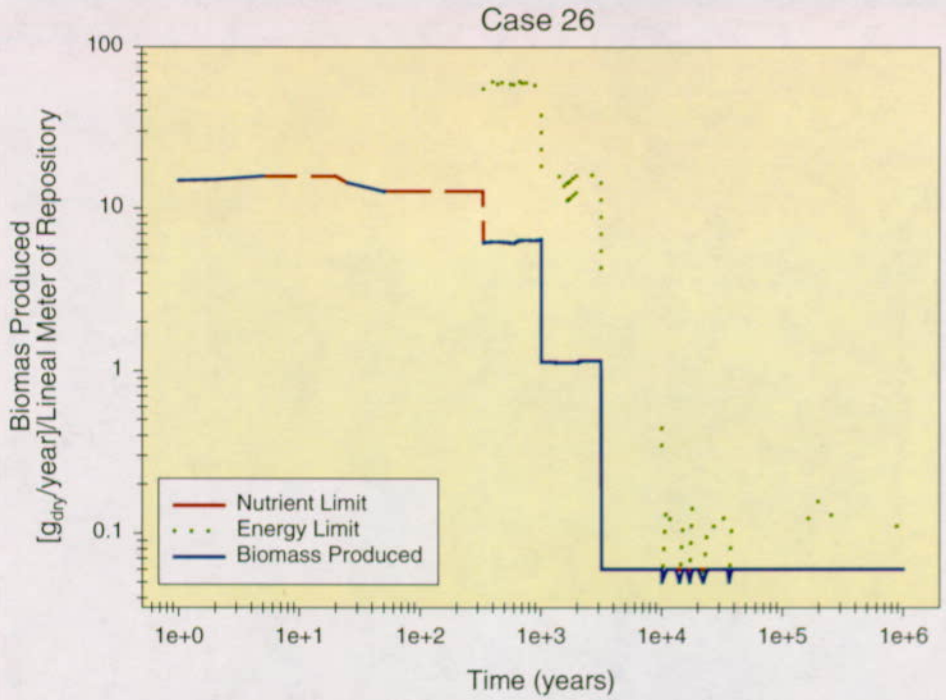

Figure VI-28. Case 26 Results.

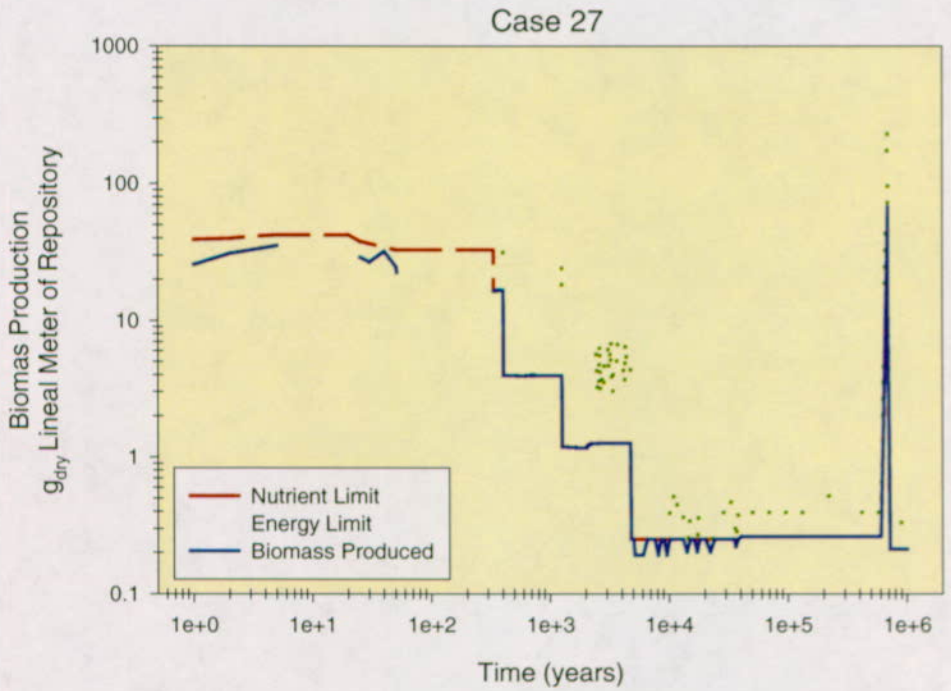

Figure VI-29. Case 27 Results.

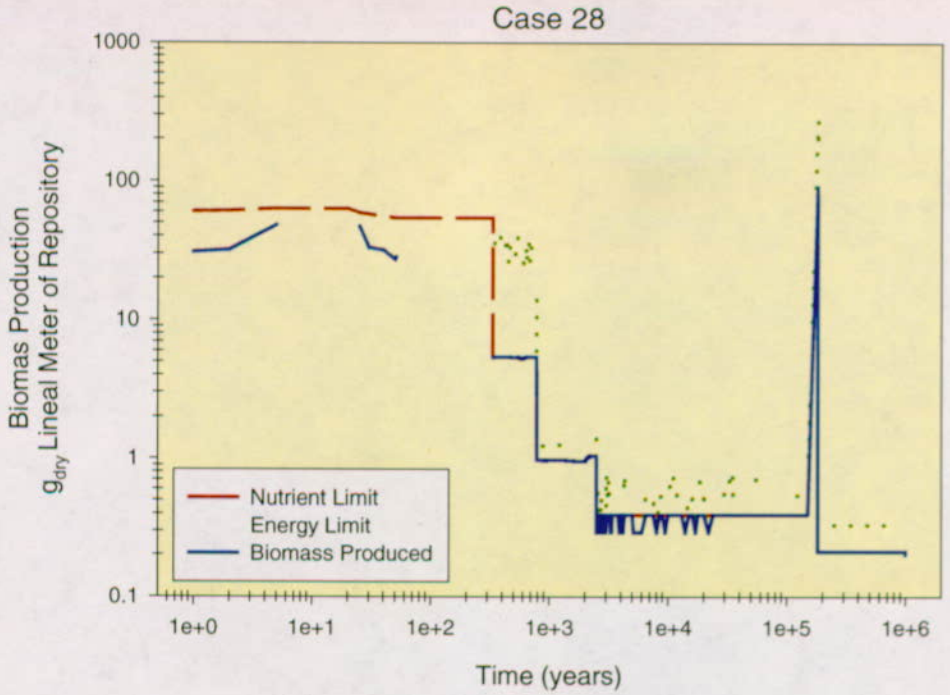

Figure VI-30. Case 28 Results.

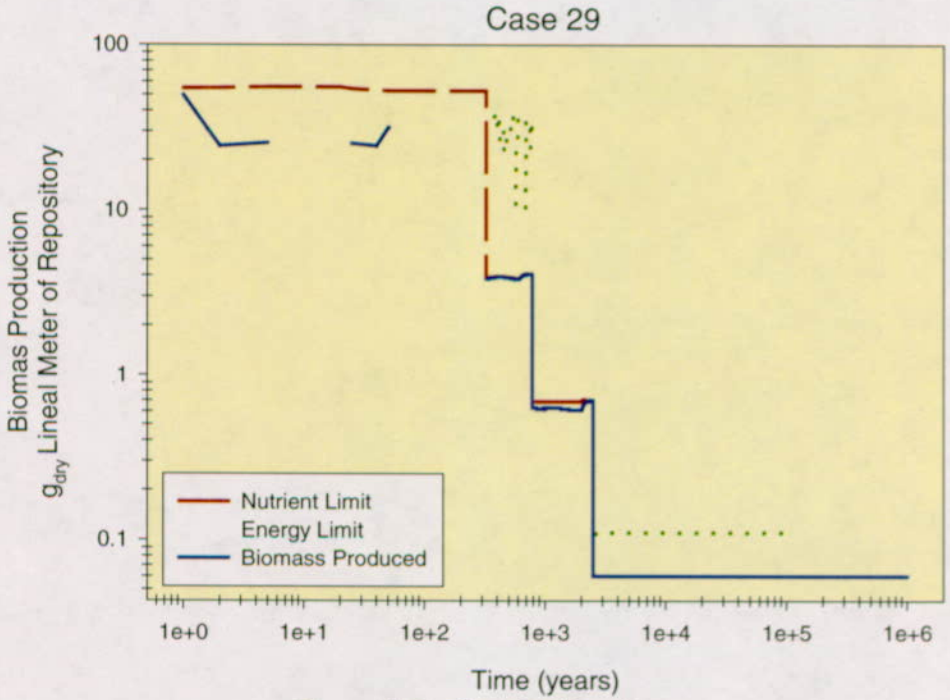

Figure VI-31. Case 29 Results.

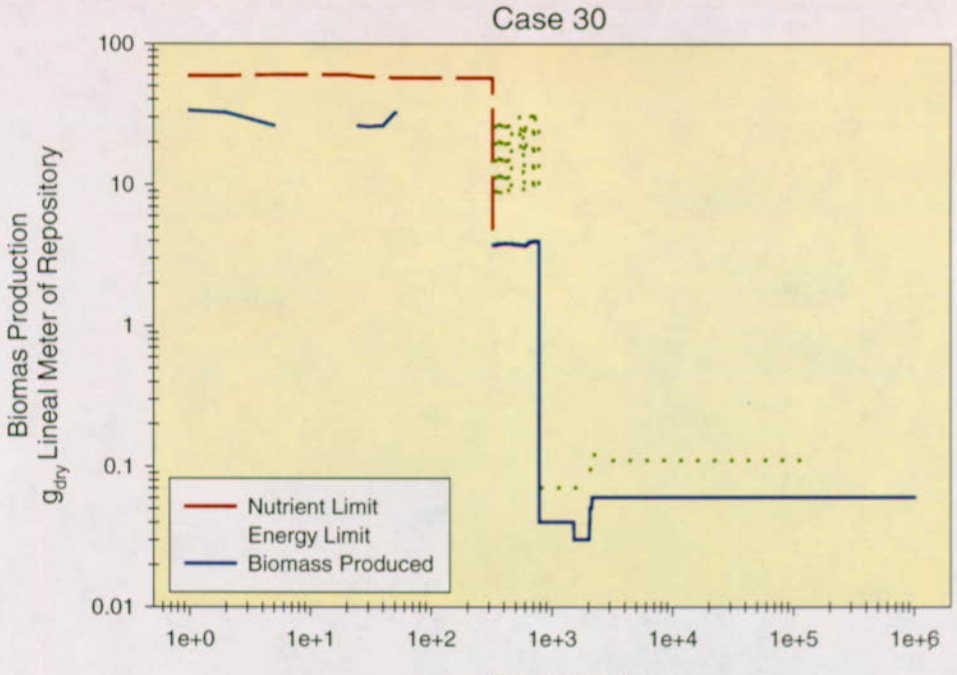

Figure VI-32. Case 30 Results.

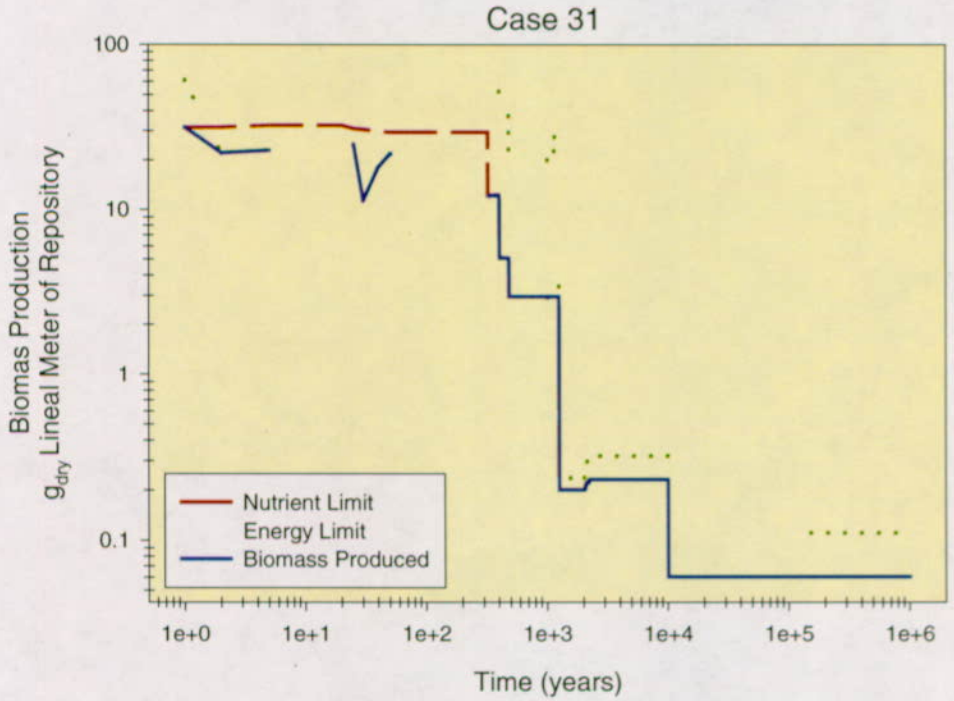

Figure VI-33. Case 31 Results.

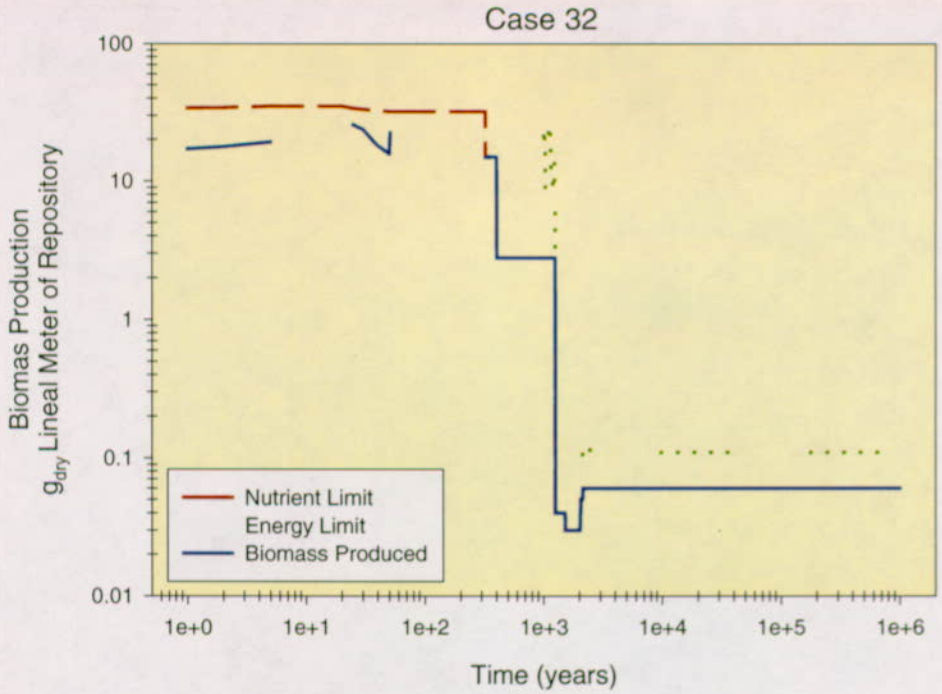

Figure VI-34. Case 32 Results.

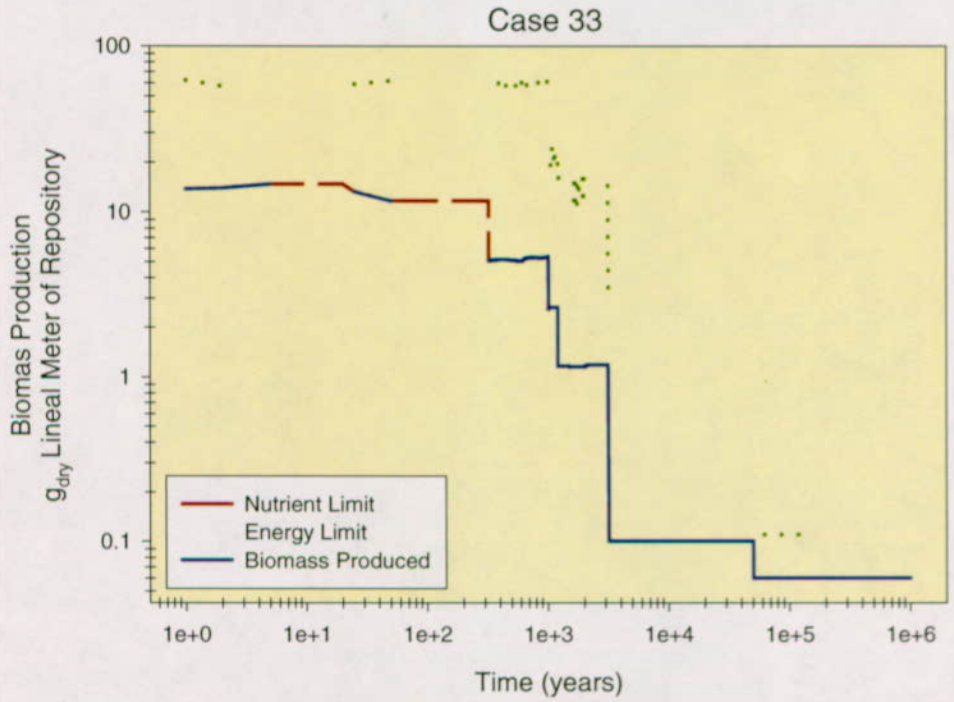

Figure VI-35. Case 33 Results.

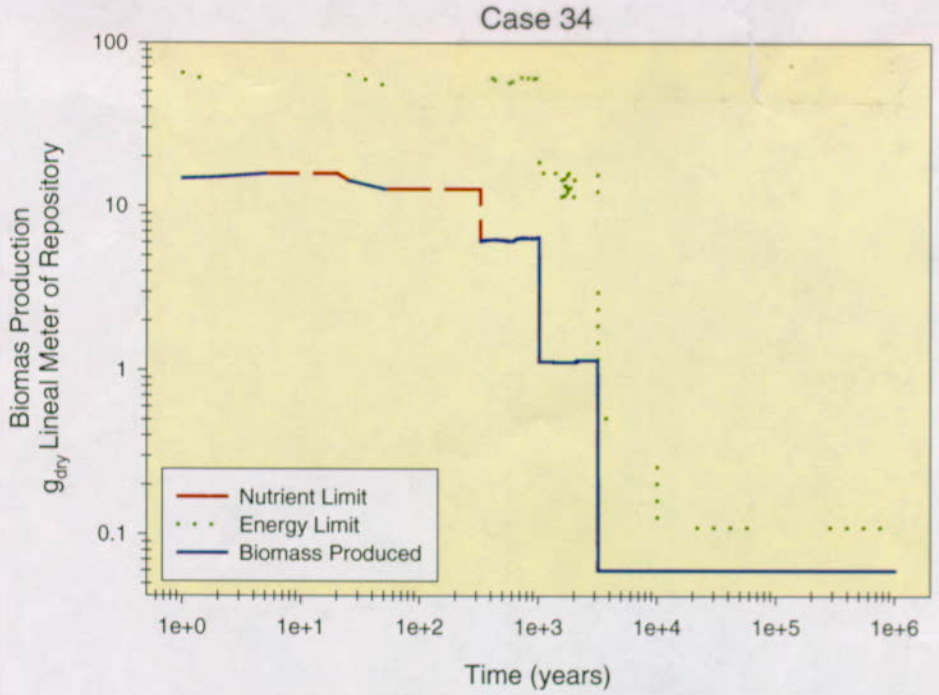

Figure VI-36. Case 34 Results.